DEVELOPMENT AND CHARACTERISATION OF BRAKE PADS FOR LIGHT TO HEAVY DUTY APPLICATIONS

A THESIS

Submitted in partial fulfilment of the requirements for the award of the degree of

DOCTOR OF PHILOSOPHY

in

METALLURGICAL AND MATERIALS ENGINEERING

by

ANIL KUMAR CHATURVEDI

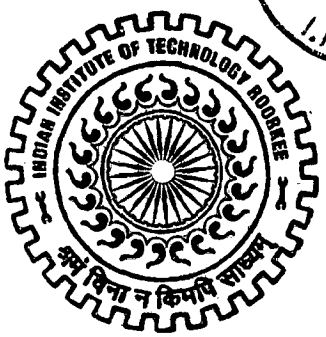

DEPARTMENT OF METALLURGICAL AND MATERIALS ENGINEERING
INDIAN INSTITUTE OF TECHNOLOGY ROORKEE
ROORKEE - 247 667 (INDIA)

JANUARY, 2010

INDIAN INSTITUTE OF TECHNOLOGY ROORKEE
ROORKEE

CANDIDATE'S DECLARATION

I hereby certify that the work which is being presented in this thesis, entitled **DEVELOPMENT AND CHARACTERISATION OF BRAKE PADS FOR LIGHT TO HEAVY DUTY APPLICATIONS** in partial fulfillment of the requirements for the award of the Degree of Doctor of Philosophy and submitted in the Department of Metallurgical and Materials Engineering of the Indian Institute of Technology Roorkee, Roorkee is an authentic record of my own work carried out during a period from July, 2006 to December, 2009 under the supervision of Dr. P.S. Misra, Professor and Dr. Kamlesh Chandra, Professor, Department of Metallurgical and Materials Engineering, Indian Institute of Technology Roorkee, Roorkee.

The matter embodied in this thesis has not been submitted by me for the award of any other degree of this or any other Institute.

Anil kumar Chaturvedi

(ANIL KUMAR CHATURVEDI)

This is to certify that the above statement made by the candidate is correct to the best of our knowledge.

(KAMLESH CHANDRA)
Professor

(P.S. MISRA)
Professor

Date: January 10, 2010

The PhD. Viva-Voice Examination of Mr. Anil Kumar Chaturvedi, Research Scholar, has been held on Aug. 13, 2010.

Signatures of Supervisors

Signature of External Examiner

Abstract

Friction materials are mainly employed in brakes, clutches and gear assemblies of automobiles, locomotive trains, commercial/fighter aircrafts, earth moving equipments, agricultural equipments, cranes, heavy presses and excavators. When the brakes are applied, the kinetic energy of the moving system transforms into heat due to friction between brake pads/discs/linings and rotor, which dissipates through brake assembly to the surroundings.

Three main categories of friction materials are normally available namely: organic based friction materials, metallic based friction materials and carbon-carbon friction materials.

Sintered metallic friction materials can be operated in either dry or wet conditions. Usually, copper based friction materials are used in wet conditions i.e. immersed in oil whereas iron based friction materials are operated in dry conditions only. The sintered copper-based friction materials are suitable for temperatures up to 600 °C whereas iron based sintered friction materials are suitable up to 1100 °C.

Al based brake friction element such as brake pad with built-in backing plate has not been develope until now as per letarature review. Present investigation is the first example of such type of friction materials.

The present work relates to the development of aluminium powder based brake pads/stators; which comprise of Al powder based friction and back plate materials. It is aimed to fabricate net-shape Al powder based brake pad in a single forming operation, employing a technology namely "Preform Hot Powder Forging". This is likely to provide alternative to resin based brake pads/stators for light/medium/heavy vehicles and Iron/Cu/Resin based brake pads for aircraft with appreciably low wear, low temperature rise, stable coefficient of friction, high recovery, low fade, light weight and low cost.

In this invention, thirty different formulations for friction layer designated as **FAl01 to FAl30** and **31st** formulation for back plate layer designated as **FAl31** were developed. The weight percentages of different constituents in aluminum matrix based friction material were varied in following ranges; Silicon carbide (coarse-200 μ) from 6.5 to 25 wt. % and graphite (fine ≈ 50μ and flake ≈ 350μ) from 4 to 12 wt.%. Other constituents are zinc, ceramic wool, coconut fiber, antimony tri sulphide, and barium sulphate in varying percentages. Silicon carbide (fine ≈ 50μ) about 30 wt. % is added in pure aluminium powder to develop a chemistry for back plate material. The metallic constituents provide strength, high temperature stability, oxidation resistance and high thermal conductivity. The coarse abrasive particles improve wear strength, coefficient of friction; fade resistance, whereas fine abrasive particles in back plate improve the strength of back plate material. Fine graphite is usually a solid lubricant and is introduced for

coating of hard SiC particles to improve their matching with the matrix whereas flaky graphite is a solid lubricant meant for smoother application of brakes and improvement of anti-seizure and anti-galling properties. Their simultaneous presence gives rise to parallel enhancement of tribo-performance of brake material.

The 'Preform Hot Powder Forging' method (described in Indian patent filed on Feb. 7, 2009) employs high rate of forming where the material undergoes severe plastic deformation under application of impact load. This method is a combination of cold compacting and hot forging processes. It involves three steps viz. i) powder blending/mixing; ii) cold compacting and iii) hot forging of the preform in open air. The mixing/blending of powders for preparation of homogeneous powder mixture is achieved by dry mixing of powders using attritor and pot mills in a particular sequence. Thereafter homogeneous powder mixture is cold compacted in a die to yield a green preform followed by hot forging of the preform at 450 °C in another die to obtain a net shaped product as brake pad of actual dimensions. This method enables to fabricate highly densified, net shaped aluminum powder based brake pads/stators with built in backing plate. It does not require inert/vacuum environment for processing and secondary processes like sintering, machining and homogenization. Such a product has been found to be suitable for light/medium/heavy duty automobiles and for AN-32 military transport aircraft where weight reduction in association with low coefficient of thermal expansion, higher thermal conductivity, stability of friction coefficient at high temperature, high recovery and low fade are prime considerations. The process as described above largely overcomes the limitations of presently practiced conventional P/M route based on compacting and sintering.

Detailed characterization of brake pad materials produced this way exhibit improved physical, tribological, mechanical, thermal and metallurgical properties. It has been completed in seven stages namely i) physical tests, ii) pin-on-disc test, iii) krauss rig test, reduced/full scale test, iv) subscale dynamometer test, v) mechanical tests, vi) thermal tests and vii) metallographic examination.

The physical tests have been conducted to measure the density and hardness of brake pad materials. The range of obtained green and forged densities is 2.26 to 2.69 gm/cc and 2.39 to 3.00 gm/cc respectively and hardness variation is from 56 to 80 BHN for composites from **FAl01** to **FAl 31**

The pin-on-disc wear tests have carried out at loads of 5 and 8 kg at a constant speed of 9 m/s for all the samples made in the present investigation to asses the tribological characteristics at the laboratory level. The chemistry developed are evaluated in terms of specific wear, coefficient of friction, and temperature rise and noise level. Results are compared to corresponding values of Fe based friction materials. Based on pin-on-disc tests, the

compositions; **FAI17, FAI21, FAI22, FAI23, FAI24, FAI25, FAI26, FAI28, FAI29 and FAI30** were selected for standard level tribo-characterization.

Krauss test: ECR R-90 standard regulation friction tests of selected Al based brake pads against cast iron disc have been carried out on near-to-actual field conditions to judge their suitability for heavy/medium/light automobile vehicles. Parameters evaluated are in terms of i) performance friction coefficient ($\mu_{Performance}$), ii) performance friction fade coefficient (μ_{Fade}), iii) performance recovery ($\mu_{Recovery}$), iv) fade (%), v) recovery (%), vi) disc temperature rise (DTR), vii) wear, and viii) fluctuation in coefficient of friction. This test has been completed in two phases. Reduced scale friction test: a non-standard test, which has been, carried out to asses the tribological characteristics at low brake pressures (0.5 to 0.7 MPa). Full-scale friction test: a standard test carried out at high brake pressures (1.0 to 1.3 MPa) to judge the suitability of developed brake pad materials in heavy/medium/light automobile vehicles. The developed Al based composites namely **FAI21, FAI23 FAI24 FAI25** and **FAI26** qualify the standard operating parameters and have been found suitable for light/medium/heavy duty automotive brake applications.

Subscale dynamometer tests has been performed for evaluation of brake pad characteristics on near-to-actual field conditions for AN32 aircraft in three phases. Initial subscale dynamometer tests under low and medium input kinetic energy have been carried out to assess the tribo-performance and develop a base for selection of composites for higher energy test. High kinetic energy subscale dynamometer standard test -TQ1 has been carried out to assess the tribological characteristics of brake pads materials for AN-32 aircraft. Based on overall performance and their evaluation in comparison to commercially used sintered iron based friction materials in AN32 aircraft, developed composites namely **FAI28, FAI29** and **FAI30** qualify the standard parameters and have been found suitable for AN32 aircraft brake application.

The thermal properties namely thermal diffusivity, specific heat, thermal conductivity, and thermal expansion coefficient at different temperature ranges have been measured using thermal dilatometer, flash thermometer, thermal calorimeter and differential calorimeter respectively. For the study of mechanical properties namely elastic modulus, yield and ultimate tensile strength, compressive strength, shear modulus and shear strength, the mechanical test of samples has been conducted using TPT-426 tensometer. The thermal properties like thermal diffusitivity, specific heat, thermal conductivity and thermal expansion coefficient vary with in a range from 4.10 to 7.23 (10^{-5} m^2 s^{-1}), from 830 to 876 ($Jkg^{-1}K^{-1}$), from 167 to 171 ($Wm^{-1}K^{-1}$) and from 7.10 to 10.3 (10^{-6}/ K) respectively and mechanical properties namely longitudinal young's modulus, transverse young's modulus, yield tensile strength, ultimate

tensile strength, yield compressive strength, shear modulus and shear strength vary with in a range from 228 to 247 GPa, from 100 to 105 GPa, from 310 to 323 MPa, from 347 to 366 MPa, from 253 to 268 MPa, 24 to 32 GPa and from 76 to 88 MPa respectively.

Optical microscopic, EDAX, X-ray mapping and SEM micro examinations have been performed to analyze the distribution of ingredients in matrix and their diffusion. The significant features recorded were i) distribution of ingredients in matrix is homogeneous, ii) few voids were noticed, iii) interface between friction layer and back plate material is not clearly defined due to mass diffusion of elements at the interface.

Analysis of results has been made to optimize the chemistry of friction materials and investigate their suitability for different applications. Results are evaluated quantitatively and qualitatively with published standards for specific applications.

Overall conclusions are i) Al based brake pad compositions are suitable and better than existing brake pad materials for light to heavy duty vehicles and also for AN-32 aircraft, ii) Preform Powder Forging' technology overcomes the limitations of sintering process and has been successfully adopted for brake pad with built-in back plate manufacture, iii) Friction layer with back plate layer (brake pad) can be fabricated in one operation alone, iv) Sintering, inert/vacuum environment and secondary process have been completely eliminated, v) For optimum tribo-performance of Al based friction composites, ingredients should be in the range from 22 to 25 wt.%, vii) New set of Al based friction materials have been prepared with simpler chemistry and superior characteristics for automobiles and aircrafts and viii) Significant mass reduction (40-60%) in friction elements has been achieved in case of aircrafts and automobiles with excellent recyclability and environmental sustainability.

Acknowledgements

I have great privilege and pride to express my sincere thanks and immense gratitude to **Dr. P.S Misra**, Professor and **Dr. Kamlesh Chandra**, Professor, Metallurgical and Materials Engineering Department (MMED), Indian Institute of Technology Roorkee, Roorkee for their valuable intellectual guidance, thought provoking discussions and untiring efforts throughout the tenure of this work. Their timely help, constructive criticism and painstaking efforts made the author possible to present the work contained in this thesis in its present form.

I am highly indebted to Dr. P.K. Ghosh, Head, MMED and Dr. S.K. Nath, Ex. Head, MMED for his co-operation in extending the necessary facilities and supports during my course of work. I wish to record my deep sense of gratitude to Head, Institute Instrumentation Centre (IIC), IIT- Roorkee for extending facilities.

I am highly thankful to Mr. S. Raghunathan, Ex-General Manager, F&F Division, Mr. Mohan Abraham, General Manager, Mr. V.N. Anil Kumar, Chief Manager, Powder Metallurgy Shop, Foundry and Forge Division, HAL Bangalore for their support in extending dynamometer test facility and constructive interaction.

I owe my sincere thanks to Mr. V. Saksena, Ex. President, Dr. A.K. Mathur, Ex.General Manager, Mr. V.S. Tomar, General Manager (R&D), Mr. Nitin Agrawal, Engineer, M/s Allied Nippon Ltd., Shaibabad for extending Krauss test facility and constructive interaction.

I wish to owe my sincere thanks to the technical and administrative staff, especially to Mr. R.K Sharma, Mr. H.K. Ahuja, Mr. S.M Giri, Mr. T. K. Sharma, Mr. Rajendar Sharma, Mr. B.D. Sharma, Mr. Dhan Prakash and Mr. Ashish Kush, who helped me in all possible ways with experimental work.

I would like to express my sincere thanks to Mr. S.D Sharma, IIC for carrying out SEM with EDAX analysis. Sincere thanks are conveyed to Mr. Narendra Kumar, Computer Lab, MMED.

I wish to thank my friends; Mr. Sidharth Jain, Mr. A.A.S.Ghazi, Mr.M.Asif, Ms.Deepika Sharama, Ms. Miti for their moral support and camaraderie.

I would like to express respect and great admiration for my father; Hari Narayan Chaturvedi, my mother; Sunana Chaturvedi, my wife Arachana Chaturvedi, my sons Atharva Chaturvedi and Ygyans Chaturvedi, for being the guiding and encouraging force.

I would like to humbly dedicate this thesis to my parents.

Anil Kumar Chaturvedi

(ANIL KUMAR CHATURVEDI)

Preface

The entire work carried out for this investigation has been presented into six chapters.

Chapter one begins with brief introduction of Al powder based friction materials, their development and scope etc.

Chapter two is a literature review for different materials and technologies relevant to current work. It also deals with application aspects of these materials their selection criteria, patented literature and market survey reports etc.

Chapter three consists of the formulation of the problem, it begins with the scope of the thesis, limitations of existing technology, methods proposed in present investigation leading to improvement in existing technology. Aims, detailed objectives and methodology have been suitably described.

Chapter four deals with the experimental work, which includes and explains the steps followed in carrying the present investigation based on 'Prefom Hot Powder Forging' technique and the characterization methods of friction materials so produced.

Chapter five consists of results and discussions; where the physical, tribological, mechanical, thermal and metallurgical characteristics of the friction materials are described.

Chapter six deals with conclusion and suggestions for future work.

Terminology	Symbol
Test code	T.C.
Part number	P. N.
Kinetic energy, kgfm	K. E.
Brake speed, rpm	N
Piston area, 10^{-4} m^2	A_p
Brake pad contact area	A_{pad}
Hydraulic pressure, 10^4 kgf m^2	p_h
Brake force, kgf	F_b
Brake torque, kgf m	M
Braking time, s	t_b
Interval time, s	t_i
Diameter of rotor inertia wheel, mm	D_r
Thickness of rotor inertia wheel, mm	T_r
Friction radius of rotor inertia wheel, mm	R_f

Contents

List of Tables

List of Figures

Chapter 1

INTRODUCTION

Initial friction materials (1878–1897) were based on fibrous structure like wood, hair or cotton. Automotive friction materials have been formulated for about 100 years. In the early 1920s, asbestos fiber was chosen as a friction material for automobiles, trucks, and all kinds of moving machinery. Because asbestos causes health problems, brake lining designers have been scrambling to find a replacement for it, using glass fibers, mineral fibers, metal fibers, and, more recently, carbon and synthetic fibers. Mixtures of chopped or powdered metal and other filler materials bound together with phenolic resin, known as semi-metallic brake pads, have been popular since the 1970s. Metal is mostly favored for heat transfer. Generally, steel wool and iron powder can be used for higher temperature applications. Thirty years ago, when disc brakes designs were introduced, the brake users were impressed by how long the linings could last. Unfortunately, most of the late model brake pads wore quickly. Therefore, the tendency is to design new friction materials with good wear resistance. Furthermore, most of the cars today are designed for high horsepower, which makes them to attain quick acceleration. As a result, manufacturers are investing heavily on new friction materials to get optimal performance from the brake pads. Good performance for brake pads is not the only concern for engineers designing them; the costs of their manufacturing and raw materials have to be taken into consideration **[188].**

An automotive brake provides a means of converting the kinetic energy of a moving vehicle into heat. The heat thus generated at the sliding interface of the rotor and friction material of the brake is dissipated primarily by conduction through various components of the brake, by convection to the atmosphere and by radiation to the atmosphere and adjacent components. It is also absorbed by chemical, metallurgical and wear processes occurring at the interface. In addition, some of the kinetic energy is absorbed by the engine, tires, windage and viscous drag of the mechanical components **[73].**

Generally speaking, there are two types of brakes available for motor vehicles (disc or drum) and they come in different sizes and configurations depending on the applications.

Generally speaking, there are two types of brakes available for motor vehicles (disc or drum) and they come in different sizes and configurations depending on the applications. The disc-drum rotor material typically is cast iron and aluminium metal matrix composites (AlMMCs) and the friction material is a complex composite consisting of a pheholic resin (or rubber and a combination of both) matrix, reinforcing fibers such as asbestos, glass, steel or

organic, and friction and wear modifiers of organic, inorganic and metallic compositions. For certain heavy duty applications, metallic matrix friction materials (called cermets or cerametalix) are being used. Depending on the service conditions of the vehicles, various classes of friction materials with specific types of performance characteristics, such as friction level, friction stability, wear resistance and noise behavior, in various temperature ranges are developed **[73].** Until the late 1960s, the U.S. passenger car and light truck automotive market used drum brakes on all four wheels and asbestos-fiber-reinforced brake linings. The improved braking requirements initiated in the late 1960s with stopping distance requirements and which culminated with the **Federal Motor Vehicle Safety Standard 105 [51,73,139]** in the mid-1970s, are responsible for the transition to the disc front-drum rear brake system. Two other new requirements are imposed in the mid-1970s: the conversion to asbestos-free friction materials and the conversion of the heavy passenger vehicles to more energy-efficient lighter and smaller front wheel drive vehicles. These changes necessitated the development of a new generation of automotive brake asbestos-free friction materials. The general characteristics of automotive friction materials are summarized as follows. The friction level must be adequate and stable over a wide range of operating speeds, application pressures and temperatures, regardless of the conditioning and age of the material. The particular interest is the fade-recovery characteristics, i.e. the ability to resist friction level deterioration when subjected to extreme elevated temperatures (the fade) and then to return to the pre-fade friction level on cooling (recovery). The friction material must also have good wear properties for long life, but it must also not cause excessive wear or grooving on the mating disc or drum. Excessive compressibility, noise and roughness (chatter, vibration and pulsation) must be avoided for comfort, and sensitivity to moisture or water must be minimized. The friction material must be capable of being manufactured with consistency at a reasonable cost **[73].**

Until now, however, many of the brake pads available in the market did not have good performance, causing the need for frequent replacement of the brake pads. For further brake design, the main consideration in the development of brake pads predominantly depends upon material constituents in the brake pads. Because the development of friction materials is a complex and interactive process, most formulations that are available in the market were designed by trial and error coupled with prior experience and testing expertise called one-variable-at-a-time experimentation (OVAT design). Dr. Peter Filip has reported that the average coefficient of friction (μ) of the commercial brake pads used in North America is around 0.35–0.45. This is lower than that of μ of pads (≈ 0.45) employed in Europe and Asia. It has been established that the μ value of commercial brake pad formulation (CFE) available in North America is around 0.357, but wear (%) (ratio of weight loss to initial weight of brake

pad) of the pads is too high (≈19.75 %) and it needs to be reduced for extending its life **[188].**

Friction materials for automotive brake systems typically contain metallic ingredients to improve their wear resistance, thermal conductivity, and strength. Various metals such as copper, steel, iron, brass, bronze, and aluminum have been used in the form of fibers or particles in the friction material, and it is known that the type, morphology, and hardness of the metallic ingredients can affect the friction and wear of friction materials. Currently, steel fibers are often used in the friction material industry since steel fibers provide good wear resistance and maintain friction effectiveness at elevated temperature (fade resistance with fast recovery). However, steel fibers can induce excessive disk wear and large disk thickness variation (DTV) which is the main cause of brake vibration or judder. The aggressiveness of steel fibers against a brake rotor appears due to their high hardness and the metallic adhesion between steel and gray cast iron (as rotor). Copper or copper alloys are mainly added to improve the thermal conductivity. Copper is also known to stabilize coefficient of friction (COF) at elevated temperatures by forming copper oxide at the friction interface. Therefore, copper or copper alloys are added to control the friction level while avoiding the aggressiveness against counter surface. Aluminum fibers are added to the friction material when aluminum metal matrix composite (Al-MMC) brake rotors are used. Information concerning the particular role of Al fibers on friction characteristics is seldom found in the literature **[61].**

The development of Al MMCs has been one of the major innovations in materials in the past 25 years. Particle-reinforced light metals are already attracting the attention of materials producers and end users because of their outstanding mechanical and physical properties. A major goal in manufacturing and utilizing MMCs is to achieve the highest possible strength-to-weight ratio, high thermal conductivity and stiffness to-weight ratio.

Aluminum powder possesses a number of mechanical and physical properties that make them attractive for automotive applications but they exhibit extremely poor resistance to seizure and galling **[12].** Reinforcement of aluminum alloys with solid lubricants, hard ceramic particles, short fibers and whiskers results in advanced metal matrix composites (MMCs) with precise balances of mechanical, physical and tribological characteristics. Brake rotors, pistons, connecting rods and integrally cast MMC engine blocks are some of the successful applications of AlMMCs in automotive industry.

On the other hand, there is an increasing demand to develop new friction materials, for brake lining to withstand the technological progress in industry, instead of the conventional. Friction materials used as brake linings and clutch facing are commonly made from asbestos or other inorganic fibers and ingredients which include metallic powders and mineral filler as well as

the binder in the form of a resin. Frictional materials containing conventional organic binding agents exhibit poor frictional stability. Therefore, AlMMCs are produced to overcome the poor thermal resistance and withstand higher thermal stresses as well as increasing wear resistance. The friction and wear of three uniaxial metal matrix composites **(graphite/Al, stainless steel/Al and $Al_2O_3/SiC_p/Al$)** are tested **[1].** It is found that, graphite/Al composite has a low friction and wear resistance because of spreading of the graphite at the sliding interface, while, stainless steel has a high friction and wear resistance. Composites of aluminium matrices with reinforcements of SiC and Al_2O_3 are potential candidates for advanced friction applications due to their increased strength and reduced density compared to conventional aluminium alloys **[90].** It is pointed out that, the wear resistance of the composite decreased with increasing the reinforcement above a certain level. Also, it is observed that, the wear rates increased with increasing reinforcement volume fraction in the sintered aluminium alloys. AlMMCs with SiC as reinforcement are investigated for rotors and drum fabrications and other automotive applications. It is reported that, the addition of SiC into aluminium improved the mechanical properties of the matrix including wear resistance. At 20 wt.% SiC, the level of wear resistance presents the possibility of lifetime rotors and drums for the first time. Al_2O_3 and Al_4C_3 are characterized by high level of physical and mechanical properties, e.g. high temperature strength, thermal cyclic resistance, wear resistance and low linear expansion coefficient **[1].** Therefore, the reinforced aluminium by the above mentioned materials have recently become the subject of many studies and widely used for brake pad friction materials as well as back plate materials to provide tough support to break element.

The principal attractions for the use of MMCs are i) reduction in mass, ii) improved wear resistance or lubrication characteristics and iii) low thermal-expansion coefficient.

The application of Al based composites in brake lining is limited by following major drawbacks.

i) poor binding during sintering, ii) tendency to galling and seizing with disc material, iii) poor machinability and iv) requirement of secondary processing.

Little work has been reported on tribological, mechanical and thermal behavior of Al based friction materials as brake rotor/disc (fabricated by casting route) **[61,123.US.P5372222]** but nothing is available on Al based friction and backing plate materials for stator brake pads possibly due to above mentioned drawbacks and complex chemistry associated. In this investigation, Al based brake pads (comprising of friction layer and backing plate) has been fabricated using 'Preform Hot Forging' and evaluate their tribological, thermo-mechanical behavior of brake pads for light/medium/heavy duty automobiles and also for AN-32 aircraft stator. The preform forging technique used for the first time for Al based brake pads in the

present investigation permits net-shape manufacturing and eliminates all the drawbacks mentioned earlier. Detailed processing and characterization of the brake pads for different applications have been carried out in this investigation. The matrix material as aluminium, is common for friction layer and back plate. Advantage of using same matrix in both is obvious, namely strong bonding between friction and back plate, high thermal conductivity at interface and better bonding at the interface. Furthermore, the brake pad material is possible to recycle to develop rotor by casting route.

In recent years, the potential of metal-matrix composites (MMCs) for significant improvement in performance over conventional alloys has been recognized widely. However, their manufacturing costs are still relatively high. There are several fabrication techniques available to manufacture the MMCs. Based on the choice of material and of the types of reinforcements involved, the fabrication technique may vary considerably. The processing methods used to manufacture particulate reinforced MMCs can be grouped as i) solid-phase fabrication methods: diffusion bonding, hot rolling, extrusion, drawing, explosive welding, P/M route and pneumatic impaction, ii) liquid-phase fabrication methods: liquid-metal infiltration, squeeze casting, compo-casting, pressure casting and stir casting and iii) two phase (solid/liquid) processes: which include rheocasting and spray atomization The main processing route available for Al metal matrix composites is casting only whereas for resin based friction materials, the available processing routes are dry, wet and impregnation. For metal powder based friction materials like Fe and Cu, the processing route is compacting and sintering. These fabrication processes are limited because processing is not possible in open environment and require designing, manufacturing and joining method for back plate to support the friction layer. On other hand, fabrication of aluminium base friction materials is not possible by above grouped fabrication methods due to the difficulty in sintering, wettability of ingredients, heat treatment and machining and shaping process (geometry of the brake pads). The difficulty in sintering of Al is a consequence of the surface oxide film. This oxide film is a barrier to sintering because it inhibits inter particle welding and the formation of effective inter particle bonds. The problem is particularly severe for aluminium because of the inherent thermodynamic stability of the oxide (Al_2O_3). Another problem is poor machinability of Al based composites. These problems are overcome in this work by a combination of chemistry formulation and adoption of 'Preform Hot Forging'.

First phase of development involved gradual optimization of Al powder based formulation for brake pad and backing plate based on expected characteristics as per literature survey.

In this invention, **thirty** different formulations for friction layers designated as **FAl01 to FAl30** and **31th** formulation for brake plate layer were developed. The weight percentages of different

constituents in friction material are varied in following ranges; Aluminium from 70 to 83 wt.%, silicon carbide (coarse) from 6.5 to 25 wt.% and graphite (fine ≈ 50μ and flake ≈ 350μ) from 4 to 12 wt.%. Other constituents are zinc, ceramic wool, coconut fiber, antimony tri sulphide, and barium sulphate in varying percentages. Silicon carbide (fine) about 30 wt.% is added in pure aluminium powder to develop a chemistry for back plate material.

'Preform Powder Forging' technique is a combination of cold compacting and hot forging. It involves three steps viz. i) powder blending/mixing; ii) cold compacting to fabricate green compact (perform) and iii) hot forging of the preform to achieve net shape open environment. The mixing/blending of powders for preparation of homogeneous powder mixture, was achieved by dry mixing of powders using attritor and pot mills in a particular sequence. Thereafter homogeneous powder mixture is cold compacted in die to yield preform and then hot forging of the preform at 450 °C in another die is carried out to obtain a net shape product as brake pad of actual dimensions.This method enables to fabricate highly densified aluminum powder based brake pads/stators with built in backing plate. Such a product has been found to be suitable for light/medium/heavy duty automobiles and for AN-32 aircraft rotor where weight reduction in association with low coefficient of thermal expansion, higher thermal conductivity, and better thermal capability, stability of friction coefficient with temperature, high recovery and low fade are of prime considerations.

The density variation of forged product is from 2.39 gm/cc to 3.00 gm/cc and hardness variation is from 56 to 71 BHN for composites from **FAl01** to **FAl30**. It can be inferred that these variations are very nominal and depend upon quality and quantity of different ingredients in the composites. Similar findings were observed by Aigbodion et. al. **[3]** while preparing Al-SiC binary composites by casting route.

The pin-on-disc wear tests were carried out under 5 and 8 kg loads at a constant speed of 9 m/s for all the samples made in the present investigation to evaluate the suitability of friction materials. The wear test performances were evaluated in terms of specific wear, coefficient of friction and temperature rise and noise level. Results were compared to corresponding values of Fe based friction materials (tested under identical input parameters) as reported by Singaravelu Lenin D **[157].**

The significant features recorded were i) Specific wear depends upon the applied load and material related factors, ii) Coefficient of friction of some composites is stable and lies in automotive industry standard range; 0.30 to 0.45 at lower as well as higher applied loads, iii) Temperature rise varies within a range from 40 to 200^{0}C. It is noticed that there is minor affect of changing the applied load on temperature rise. It is also noticed that the temperature

rise of Al based brake materials is 1.5 times lower than temperature rise in Fe based friction composites, iv) Noise levels of Al based composites are equivalent to Fe based composites.

Based on pin-on-disc tests, the compositions for candidates **FAl20, FAl21, FAl22, FAl23, FAl24, FAl25** and **FAl26** were selected for standard level tribo-characterization to develop brake pads for aircraft/heavy/medium/light duty automotive applications.

Krauss test: ECR R-90 standard regulation friction tests **[58]** of selected Al based brake pads against cast iron inertia wheel were carried out for characterization of the tribological properties, to judge their suitability for heavy/medium/light automobile vehicles. Parameters evaluated were in terms of i) performance friction coefficient ($\mu_{Performance}$), ii) performance friction fade coefficient (μ_{Fade}), iii) performance recovery ($\mu_{Recovery}$), iv) fade (%), v) recovery (%), vi) disc temperature rise (DTR), vii) wear, and viii) fluctuation in coefficient of friction.

Tribo-tests of developed Al based brake pads were carried out in three steps namely: ***i) Reduced scale tribo-test ii) Full scale tribo-test for light duty vehicles iii) Full scale tribo-test of for heavy duty vehicles.***

Reduced scale tests are not standard test, which have been conducted to assess the tribological characteristics at relatively low brake pressures. The light and heavy tests are ECR R-90 standard regulation friction tests, which have been conducted to assess the suitability of tribological characteristics at standard applied brake pressures for automobiles.

The significant features recorded were i) For heavy duty application, Al based brake pads in friction test run varies with in a range from 2.7 to 7.6 gm whereas for resin based, it varies with in range from 29 to 36 gm. The wear (%) for developed Al based composites varies with in a range from 2 to 5 % which is lower than optimum standard wear (%) of commercial brake pads ($\approx$ 6.36%) for heavy duty application as reported by Philip. ii) Coefficient of friction varies with in a range from 0.34 to 0.43. This range is optimum because it lies in a automotive industry standard range from 0.3 to 0.45, iii) Temperature rise varies with in range from 40 to 200^0C. It is 1.5 to 2.5 times lower than resin based brake pads. iv) Fluctuation in coefficient of friction for Al based brake pads varies with in range from 0.20 to 0.26 whereas for resin based, it varies with in range from 0.16 to 0.52 v) Fade (%) for Al based composites is 1.4 to 2.5 times lower than resin based friction composites, vi) Recovery (%) is about 120 which is higher than the recovery of resin based composites ($\approx$ 106).

The thermal properties like thermal diffusitivity, specific heat, thermal conductivity and thermal expansion coefficient vary with in a range from 4.10 to 7.23 (10^{-5} m^2 s^{-1}), from 830 to 876 (J kg^{-1} K^{-1}), from 167 to 171 (W $m^{-1}K^{-1}$) and from 7.10 to 10.3 (10^{-6}/ K) respectively and mechanical properties namely longitudinal young's modulus, transverse young's modulus, yield tensile strength, ultimate tensile strength, yield compressive strength,

shear modulus and shear strength vary with in a range from 228 to 247 GPa, from 100 to 105 GPa, from 310 to 323 MPa, from 347 to 366 MPa, from 253 to 268 MPa, 24 to 32 GPa and from 76 to 88 MPa respectively. These properties ranges lie in standard range of commercially used Al based composites, reported in literature.

The microstructures of optimized composites were studied using SEM and EDX method. The significant features recorded are i) Distribution of ingredients in matrix is homogeneous, ii) Few porosities are noticed in back plate materials, iii) There is no inclusions have been find out at interface between friction layer and back plate materials.

The subscale brake inertia dynamometer tribo-tests of selected Al-based friction composites against cast iron inertia wheel were carried out under low and medium energy levels to asses and evaluate the tribological characteristics for high energy standard test. After evaluation of tribological characteristics at low: TQ3 and medium: TQ2 energy levels, high energy level: TQ1 standard test for AN-32 is carried out under rejected-take-off (RTO) condition for composite **FAl26** to judge their suitability for AN-32 aircraft stator brake application. However, the composites **FAl27, FAl28, FAl29 and FAl30** are tested under high energy: TQ1 standard test for AN-32 (these samples are not tested under low and medium energy levels). The performance of samples were estimated in terms of wear, coefficient of friction, run down revolution, run down time, temperature rise and fluctuation in coefficient of friction.

The significant features recorded were i) The wear for Al based composites **FAl26, FAl28, FAl29 and FAl30** is 1.5 to 1.9 times lower than that of earlier developed Fe based composites for AN-32 aircraft, reported by Singaravelu Lenin D. However, for composites **FAl28** and **FAl30**, it is 6.5 and 8.5 gm respectively, which is two times lower than the aeronautic industry standard wear ($\approx$ 14 gm) for AN-32. For composite **FAl29**, it is equivalent to standard wear. It is also noticed that the wear of composites increases corresponding to increase the input energy, ii) Coefficient of friction and RD time for composites lie in standard range, iv) Maximum temperature rise is 2 to 3 times lower than sintered metallic brake pads, reported by Ho et. al. and v) Fluctuation in coefficient of friction for composites is 2 to 2.8 times lower than standard fluctuation in coefficient of friction for AN-32 aircraft.

Overall conclusions are i) Al based compositions are suitable and better than existing brake pad materials for light to heavy duty vehicles and also for AN-32 aircraft brake applications, ii) Preform Powder Forging' technology overcoming the limitations of sintering process has been successfully adopted, iii) Friction layer with back plate layer (brake pad) can be fabricated in one operation alone, iv) Sintering, inert/vacuum environment and secondary process have been completely eliminated, v) The combination of chemistry and fabrication technology completely eliminates the complex processing like designing, manufacturing and

joining of back plate material to support the friction layer, vi) For optimum tribo-performance of Al based friction composites, ingredients addition should be in the range from 22 to 25 wt.%. vii) New set of Al based friction materials have been prepared with simpler chemistry and superior application with regard to automobiles and aircrafts such as AN-32 viii) element distribution in matrix is homogeneous.

Investigations were carried out in detail in selective cases only where there is a scope for further exploitations towards application of friction elements developed in the present investigation for military aircrafts-AN-32 and light/medium/heavy duty road vehicles for which entire work of the thesis is concentrated.

Chapter 2

LITERATURE REVIEW

2.1 Friction materials

The literature review is carried out as a part of the thesis work to have an overview of composition and chemistry, fabrication method, physical, thermo-mechanical and tribological behavior of aluminium powder based friction composites for automotive brake pad/stator applications.

These friction materials are mainly employed in various brakes, clutches and gear assemblies of different kinds of automobiles, high speed trains and railways, commercial/fighter aircrafts, earth moving equipments, agricultural equipments, cranes and hoists, high way trucks, presses, excavators, machine tools, forging and pressing equipments, heavy lifting devices etc **[14,40,115,157]**.

The rotating counterparts in the friction assembly are usually made of cast iron because of its excellent friction and wear properties. Recently, new brake discs or counterparts based on aluminium matrix composites are also employed. However, cast iron is still practiced as the counterpart in variety of modern automobiles. The design of brake rotors are made into many groups like solid, vented, fin holed and many others types for faster heat dissipation, faster cooling rate, stable friction and wear properties etc **[34,157]**.

The choice of friction materials will depend upon vehicle load, speed, pressure, energy to be dissipated, counter face material etc. Wear resistance is one of the major factors influencing the choice of materials for friction pads **[49,50]**. The reduction of material losses due to wear require the development of a new class of materials and processes, and a new generation of thoroughly trained, knowledgeable tribologists in the coming decades **[97,120]**.

Pad materials for automotive braking usually are polymer matrix composites with a large number of constituents, which provide certain functionalities, like COF-stabilization, disc polishing or noise reduction. Though pad manufacturers know by experience how formulations must be changed in order to achieve certain properties, there is a lack of fundamental knowledge concerning the influence of pad materials on friction and wear properties. Certainly, features at the pad–disc-interface will control the latter properties, but it is difficult to find the appropriate length scale for the respective phenomenon. Though "Tribology at the Interface" was the topic of the 33rd *Leeds-Lyon Symposium* (Leeds, September 2006), there was no paper directly referring to brakes. During recent brake conferences, on the other hand,

the importance of surface films was mentioned several times, but experimental evidence has been rarely provided **[109].**

Friction brakes for ground vehicles require steady, repeatable and effective stopping behavior under a range of operating temperatures and environments. They must perform reliably under hot, dry, wet, or cold conditions. Vehicle owners also demand long life in the presence of varied driving conditions. In the United States, there are no federal standards for specifying the minimum acceptable wear rate or durability of brake materials despite the fact that commercial trucks can be removed from service if a routine highway inspection shows that the brakes are worn or damaged. Brake lining manufacturers commonly make claims as to the excellent wear of their original equipment or aftermarket products despite their long-standing aversion to guaranteeing a certain lining life or rarely publishing wear data from lining laboratory tests. There is a variety of bench-scale tests for lining wear, but most are criticized for not correlating very well with the kinds of wear lives that the materials experience in service. Industry sources report that the cost to run a single week-long, inertia-dynamometer wear test can cost more than US$ 10,000. Conducting multiple tests to establish repeatability of the results becomes cost prohibitive for many lining makers who are attempting to keep costs competitive in the open market **[118,120,138].**

Recent attention to the improvement of line-haul truck brake effectiveness is prompted by a need to compensate for improvements in truck and trailer aerodynamic drag and to increase road safety. While lower drag and improved rolling resistance impacts fuel economy, it also places more demands on the braking system. Therefore, the US Department of Energy has supported several projects aimed at the development of lightweight, high-performance brake materials for trucks. One of these projects, a portion of whose results are described here, examines the tribological response of non-traditional disc brake materials, including ceramic composites and intermetallic alloys. These materials tend to be lighter in weight and harder than the traditional cast iron brake drums and discs, and therefore they offer potential for reducing braking system weight and possibly, increasing the wear life of brake components as well. At this writing, ceramic composites and intermetallic alloy brake components have not been thoroughly evaluated functionally and economically to the extent that use in truck brakes is immanent. Functional evaluations include the measurement of frictional behavior under braking conditions, assessing wear resistance, and in the present case, examining the wear particles that are created during frictional contact. Brake wear debris is of interest from several points of view: i) to help better understand the processes of brake material wear, ii) to determine how material is redistributed, crushed, and consolidated in the sliding interface, and iii) to assess the environmental and health aspects of brake dust as a vehicle emission. When

brake surfaces slide against one another, transfer films tend to form on one or both. A number of studies have focused on the characterization of such transfer films. The films tend to have complex, heterogeneous microstructures since the friction materials from which they form may contain in excess of 15 different additives. While some of the wear debris arising from frictional braking may be expelled to the environment very quickly, some of it may become trapped for a time in a mechanically mixed, transfer film, eventually braking up into loose fragments **[15,119,120,138].**

2.2 Classification of friction materials

The friction materials that are used for brake applications are broadly classified into three sub-groups namely: organic, metallic and carbon based friction materials **[14,15].** In all three sub-groups the energy quantum, stopping distance/time, environmental issues like NVH (Noise-Vibration-Harshness) play a major role. For example in automobiles, NVH is a primary design parameter, whereas for aircrafts and railways it is a secondary parameter **[157].**

2.2.1. Organic friction materials

They were used in early days, in brakes and clutch systems. These consist of wood and leather **[156].** Asbestos fibers were used as reinforcing materials in brake pads as early as 1900's and employed till 1980's **[34].** Asbestos-based organic materials were widely used due to their better frictional stability up to 500°C. At this temperature, these materials disintegrated into hard silicates which stabilized friction, was more abrasive, durable with better thermal resilience. Asbestos fibers can lodge in lungs and induce adverse respiratory conditions found later by medical research and were therefore banned in 1986 by the Environmental Protection Agency (EPA). This led to development of non-asbestos alternatives by industry. However, asbestos-based brake products are still used in the aftermarket despite the fact that many people think asbestos was replaced by non-asbestos years ago; since asbestos is an economical fiber for low temperature brake applications **[RR1].** Now, Non Asbestos Organic (NAO) type friction materials are establishing in view of restrictions by EPA. NAO based materials consist of resin binders with low metallic and non-metallic constituents, different variety of fibers, various fillers and friction additives.

Semi-metallics are another kind of organic based material where 50% metallic constituents with a variety of fibrous materials present in the system were later developed. This type of friction material is mainly involved in racing cars and bikes due to their higher coefficient of friction requirements. NAO type friction materials comprise composites of binders, reinforcements, friction additives, fillers etc **[152,157,165,166].**

NAO materials include different fibers like chopped glass fiber, mineral wool, para-aramid (Kevlar), cellulosic and other organic forms. The binder resins used for organic friction material are usually thermosetting polymers, mainly phenolic type. The liquid and powder forms of resins are normally used **[14,34,157].**

Bijwe *et. al* **[24]** describes low metallic NAO based friction materials with SiC, SiO_2, ZrO_2, Al_2O_3 as abrasives and studied the influence of operating parameters by decision making approach. The author reported that abrasives cause significant effect on wear performance.

NAO type friction material with different ingredients including solid lubricants (graphite and Sb_2S_3) were evaluated for their frictional characteristics **[99].** Higher content of solid lubricants has shown positive effect on the fade characteristics. This is due to graphite oxidation and Sb_2S_3 decomposes into oxides at elevated temperatures and looses its effectiveness as solid lubricant. Thermal decomposition of the solid lubricants strongly affects the friction characteristics at elevated temperature **[36,37,38,157].** Therefore, role of solid lubricants should be carefully analyzed. The three different solid lubricants namely, Cu_2S, PbS and Sb_2S_3 of Non-Asbestos Organic friction materials are analyzed to evaluate their effects. Sb_2S_3 based formulations had the highest coefficient of friction and low wear as compared with other two lubricants **[99,154].** The effect of Sb_2S_3 as lubricant and $ZrSiO_4$ as abrasive on frictional characteristics was investigated by using a brake dynamometer under two different modes. Higher contents of Sb_2S_3 in the friction material improved the stability of friction coefficient at elevated temperatures. In general, solid lubricants are added to the friction material to build up a stable friction film (3^{rd} body layer) on the rotating counterpart and abrasives such as $ZrSiO_4$ are added to remove thermally decomposed layer of the friction film [37,38,61]. Therefore, it is established that Sb_2S_3 mainly improves friction stability and imparts better fading resistance in combination with abrasives **[117].**

NAO low metallic type friction materials with four different abrasive additions was examined to evaluate wear data using a regression model based on orthogonal array. The contribution of these abrasives towards wear rate had shown better influence on the various factors such as load, sliding speed and braking pressure **[25,157].** The influence of different metal fibers on frictional characteristics of NAO friction materials was also evaluated. Modified resins were also used for making friction materials **[RR1].** They improve frictional stability even at high temperature. Sometimes, resin modification may result in high wear rate and reduction in porosity **[34].** Five different modified resins with constant proportions of other ingredients were examined for mechanical and frictional performance. Considerable efforts were made [24] to correlate frictional characteristics of resin-based brakes including combinations of

different resins. However, it is concluded that no resin combination is available where frictional properties can be scientifically optimized.

Semimet linings are different from NAO linings because they have a restricted composition range, with unique friction and wear properties. Semimet linings comprise 50-60 wt % total metallic content, steel wool, graphite with a heat-resistant phenolic-type binder. The coefficient of friction of these materials is around 0.40 to 0.55. These materials are typically semi-metallics. When these pads are cold, they may be near impossible to deal with on the street because they do not reach the optimal carbonization temperature during normal driving. But, when they are warm, the braking performance of the vehicle is greatly improved. The effects of carbonization in the temperature range 400-800 °C were studied to improve the high-temperature performance of a copper/phenolic resin based semi-metallic friction materials. Low carbonization rate results in higher mechanical properties and fewer cracks. Increased carbonization temperature results in improved tribological properties. In general, carbonized samples exhibits better mechanical and tribological properties, better high-temperature heat/oxidation resistance etc. than non-carbonized samples. This is possibly due to formation of lubricant in the form of graphite during carbonization **[157,166].**

2.2.2 Carbon-carbon based friction materials

This was firstly developed in the period from 1960's to 1970's and were mainly developed for advanced military and commercial aircraft of multiple rotor and stator brake disks because of their greater mass reduction, lower wear, high temperature stability and a higher reliability under extreme braking conditions. Applications also include racing cars and other automobiles where weight reduction is of significance, performance is challenging, and cost is secondary **[14].** These are extensively used in braking devices of railways, tanks and other mechanical engineering products. Friction between rotating and stationary disks causes these composites to heat upto 1500°C (surface temperature can be as high as 3000°C), so good thermal shock resistance is required. In addition to requirements of friction materials mentioned in section 2.3, any braking material must be a good structural material, an efficient heat sink, and have excellent abrasion resistance. Carbon-carbon friction materials are made from carbon fiber (also called graphite fiber) that is bonded with amorphous carbon **[RR1, 14, 157].** The friction and wear of C/C materials is exerted by the value of elastic modulus of reinforcing fibers. Therefore, properties of reinforcing fibers and its type on the friction coefficient and wear are carefully noted **[120].** However, both COF and wear are practically independent of the material porosity over a relatively broad range of its values (upto 20-25%), while at a porosity level over 27%, wear increases. There are basically three methods that are being used for forming the carbon matrix. They are either thermal degradation of a thermosetting resin or a

thermoplastic pitch, and the chemical vapor infiltration (CVI) by depositing carbon into a fibrous preform and third is repeated cycles of CVI to achieve complete densification **[157].** Once desired density level is reached, the process of carbonization and graphitization are followed for the composites. Usually the density for aircraft C/C brakes is in the range of 1.7-1.9 gm/cm^3 **[14,157,190].** The advantages of using C/C fir disk brakes are excellent thermal conductivity, adequate and consistent friction coefficients independent of surface temperature(when dry), high thermal capacities, good strength, impact resistance, fatigue resistance, about 60% weight savings compared with metallic brake systems **[RR1].** Further, C/C composites are mainly employed in aircraft brakes for three basic reasons. First, the heat capacity of carbon is 2.5 times greater than steel, the kinetic energy from aircraft can be converted into heat and stored in the C/C brake heat sink, and this heat is dissipated slowly to prevent melting of nearby metal structures. Secondly, C/C can provide sufficient friction to bring the aircraft to a smooth, controlled stop under different K.E. conditions including normal and rejected takeoff (RTO). Third C/C composites have high mechanical strength, comparable to steel, at high temperatures, and carbon is nearly twice as strong **[157,190].**

Consider the demands made of a braking material in a Boeing 767 aircraft of about 170,000kg. Take-off velocity of about 320km/hr and the resultant kinetic energy at this take-off is 670MJ. Under these extreme braking conditions, this energy must be dissipated in about 30 seconds, by the eight brakes on the aircraft. An aborted take-off is, indeed, the worst case scenario, but then the braking material must be able to meet such requirements. Let us also consider the weight savings while replacing the conventional brakes by the of C/C brakes. In a large aircraft, a multiple stator and rotor arrangement (a sintered high-friction material sliding against a high-temperature steel) weighs about 1100 kg whereas C/C brakes (both the stator and rotor are made of carbon/carbon composite) weigh about 700kg, resulting in a weight savings of about 400kg.

The major disadvantages are oxidation behavior under higher temperatures; weight loss from oxidation is significant for non protected C/C friction elements. Oxidation may start at 450°C. However, in the modern aircrafts it may start beyond 800°C say from 850°C-1200°C. Hence, C/C friction materials are protected at those temperatures. Further, it involves costlier raw materials and as well as costly and complex materials processing. However, C/C friction materials are beyond the scope of the present investigation **[157,190].**

Organic and carbon-carbon friction materials discussed/included here are just for survey/review purposes and therefore they are beyond the scope of the present investigation. The present thesis is purely confined to aluminium based metallo-ceramic friction materials and literature pertaining to aluminium has therefore been investigated.

Xiong *et al.* **[185]** have reported that wear and temperature increases corresponding with increase in pressure however coefficient of friction decreases.

2.2.3 Metallic friction materials

These types of brake materials were introduced in the late 1930's and comprise of either copper or iron as matrix. Since these involve ceramics constituents, they are often called metallo-ceramic or cermet friction materials. The manufacturing technology for this type of friction material is conventional powder metallurgy based on compacting and sintering technology **[157].** Sintered friction materials contain metallic and nonmetallic constituents, in varying proportions. Variety of shapes can be produced, for various brake applications.

The components in these materials are divided in to three sub groups: metallic base (matrix) with alloying elements to provide load carrying capacity and thermal shock resistance, friction additives to raise coefficient of friction, and, anti-scuffing additions or solid lubricants which prevent seizure and sticking between rubbing parts, ensure even coefficient of friction and increase wear resistance **[82,87,162].** Metal matrix with different metallic constituents like tin, copper, ferro alloys, etc. (in the range about 50-80 wt.%), ceramics and non-metallics like Al_2O_3, SiO_2, ZrO_2, SiC, B_4C, WC, bentonite, asbestos, spoudumence, feldspar, kayanite etc. (in the range about 20-28 wt.%) and solid lubricants like graphite, MoS_2, Sb_2S_3, $CaSO_4$, $BaSO_4$, BN etc. (in the range about 5-25 wt.%) are blended/mixed either wet or dry mixed and then the powder mixture is cold compacted followed by pressure sintering with steel backing plates.

There are two principal types of applications or operating conditions for metallic friction materials: "wet" and "dry". Under wet conditions, the friction components, such as clutches in power shift, automatic transmissions and brakes are immersed in oil. Dry operating conditions involve direct contact of friction components with rotor such as in aircraft brakes **[14,50,81,157].**

Sintered metallic friction materials have been used as brake disks, especially for heavy-duty applications, because of their good braking performance and low wear rate at high temperatures **[48,157].** These have been developed for very high power input densities. For example, solid-state-sintered bronze and mullite linings are used in race car and high-speed railroad brakes. Sintered iron with graphite is used in some heavy-duty brakes in civilian/military aircrafts; both stator and rotor disk brakes, and as well as on a few production passenger car drum brakes **[18,157,182].** Multiple-disk brakes have alternating rotors and stators forced against adjacent members by hydraulic pressure. Metallic friction materials are

also used in other heavy-duty applications, such as clutch facings on tractors, trucks, earth-moving equipment, and heavy presses **[157].**

The most widely used metal matrices for heavy-duty friction materials are copper and bronze where service temperatures are less than 600°C. Iron matrices are used where service temperatures are likely to exceed 1100°C **[14,157].** Cu based materials are better at low to medium brake load conditions whereas Fe based are suitable for severe conditions. Fe based alloys are known for better frictional stability, while the Cu-based alloys display a "fade" phenomenon under higher load and speed conditions **[143,144,157].** Normally, the density of Fe based friction materials is in the range of 5-6.1gm/cc, its hardness 80-105 HRF, and a friction coefficient in combination with cast iron is 0.34–0.40, whereas Cu based friction materials have a density of 7.0–7.5 gm/cc, hardness 30–40 HB, and a friction coefficient of 0.28–0.30 in combination with chromium-plated steel **[81,110,157].**

Aluminum-based friction materials with a composition of (wt.%) 0-20 copper, 0.2-20 hard components (oxides, carbides, and/or nitrides of silicon, aluminum, and/or zirconium and also of solid solutions) and strengthening components (Mg, Si, Sn, Mn, Zn, Ni, Cr, Mo) have been proposed. The aluminum matrix significantly reduces the weight of the alloy. However, aluminum-base materials have not obtained wide use since the method of their production is very complex, sinterability of aluminium base materials is poor and they are expensive. These materials are used primarily in rubbing pairs for aerospace applications **[44,48,49,50,157].**

Investigations on Aluminium bronze type friction material of copper-tin matrix with higher contents of aluminium (10-15%), reveal that the wear resistance of these materials is maximum when their matrix has a single-phase structure (with the maximum aluminum concentration in α solid solution) or a two-phase structure ($\alpha + \gamma_2$) of minimum eutectoid content. The optimum combination of frictional characteristics and wear resistance under unlubricated friction conditions is exhibited by materials containing 11-14 wt.% Al. The structure of the matrix of these materials consist of a heterogeneous mixture of a ductile (α solid solution of aluminum in copper) and a brittle (the intermetallic compound Cu_2Al) component, the concentration of the latter being sufficiently low to produce no marked decrease in strength **[157].**

Ceramic-base (silicon carbide and nitride) **[157]** friction powder materials possess a unique combination of properties including low specific gravity and high strength, wear resistance, and chemical inertness, brittleness and poor machinability prevent broad use of ceramic base materials as friction materials **[44,157].**

Recently, wear resistant metal matrix composites (MMC) have been developed, which allow the selection of hard particles (HP) like carbides, borides, and nitrides and a metal matrix

(MM) independently of each other, and design microstructures of superior properties. In contrast to the solidification of castings in sand moulds close to phase equilibrium, the powder metallurgical (PM) production of MMC may stay away from this condition **[22].**

The process of damage by by particles cracking has been followed in a composite of A356 Al containing 20% by volume SiC. The probability of particles cracking is influenced by both particle size and aspect ratio and the results indicate that the relative importance of these factors depends on the Weibull modulus of the SiC particles **[31].**

The relative importance of the load bearing effect of the reinforcement compared to the matrix strengthening by the enhanced dislocation density in improving the yield strength of Metal Matrix Composites (MMCs) is studied. Nardone-Prewo's equation based on Modified Shear Lag theory is used for estimating the enhanced matrix strength but appropriately incorporating the effect of the matrix strengthening as well. The analytical estimation uses a Composite Sphere Model and involves the determination of the dislocation density of the matrix based on the effective plastic strain arising due to the thermal residual stresses. This presentation includes a systematic study of the dependence of the thermal residual stresses as well as the dislocation density on the volume fraction and the particle size of the second phase. The strength predicted in this study compares favorably with a few published experimental data **[129].**

Under dry conditions for a short sliding distance (less than 2 km), the wear resistance of Al-graphite (nickel-coated) composite increases with increasing graphite content. Babu *et al.* **[21]** have been characterized and to understand the dry wear properties of Al-graphite (synthetic, uncoated) composite at long (4-13 km) sliding distances. The study not only has relevance in terms of the industrial exploitation of the composite but also throws light on the mechanism controlling the wear of brittle materials. If other material parameters remain the same, the dry wear characteristics of graphitic aluminium may be considered to be principally influenced by the following two factors.

(i) The first factor is the action of graphite as a solid lubricant. Pai *et al.* have shown that graphite is transported from the bulk to the mating surface during sliding. If the synthetic graphite used in the present work does act as a solid lubricant, the composite can be expected to have wear characteristics superior to those of the base alloy.

(ii) The second factor is the plastic deformation of the subsurface. It has been reported by many researchers that the ability of subsurface material to undergo plastic deformation without fracture has a considerable influence on wear behavior. Particulate composites are brittle materials, the brittleness generally increasing with the weight percentage of particle addition. If the graphite particle has no independent tribological role under dry

wear conditions, with increasing loss of the strength and ductility of the present composite as a result of graphite addition the wear properties may be expected to deteriorate. This has been observed for Al-mica particulate composites.

Metal-matrix composites (MMCs) are a new class of materials that consists of a nonmetallic phase distributed in metallic matrix with properties that are superior to that of the constituents. According to many authors like Abouelmagd **[1]** and Ahlatci *et al.* **[2]** the most commonly used methods for manufacturing of MMCs are casting techniques and powder metallurgy (P/M) techniques. Aluminum matrix composites (AMCs) refer to the class of light weight high performance aluminum centric material systems. Aluminum-based alloys are usually reinforced with Al_2O_3, SiC, and graphite **[106,116]**. The major advantages of AMCs compared to unreinforced materials are: greater strength, improved stiffness, reduced density, good corrosion resistance, improved high-temperature properties, controlled thermal expansion coefficient, thermal/heat management, functionally graded macro-characteristics, improved wear resistance, and improved damping capabilities. Increased demand for light weight components, primarily driven by the need to reduce energy consumption in a variety of structural, automotive and recreational components, has led to increased use of aluminum. Additionally, the cost of fabrication coupled with a need to improve part recovery has generated significant growth in the net-shaped component manufacturing processes. Among the various methods to fabricate metal matrix composites, P/M method is one of the attractive production techniques for production of MMCs. Aluminum P/M offers components with exceptional mechanical and fatigue properties, low density, corrosion resistance, high thermal and electrical conductivity, excellent machinability, good response to a variety of finishing processes, and which are competitive on a cost per unit volume basis according to Torralba *et al.* **[168]**. *Eksi and Saritas* **[46]** found that aluminum P/M parts can be further processed to eliminate porosity and improve mechanical properties either by cold or hot working methods to obtain properties comparable to those of conventional cast aluminum products. Many applications of Al P/M in automotive industry include connecting rods, cams, and races for tapered roller bearing, valve seat etc. Reinforcement of aluminum alloys with Al_2O_3 or SiC has generally been observed to improve wear and abrasion resistance as described by many former researchers. *Sawla and Das* **[149]** studied the abrasive wear behavior of various Al matrices, such as Al–Mg, Al–Cu, and Al–Zn–Mg, which were reinforced with hard particles; they found that the wear rates of these hard particle composites are significantly lower than the wear rates of corresponding base alloys. *Das et al.* **[42]** found that wear resistance properties of Al–4.5 wt% Cu alloy improved significantly after addition of alumina and zircon particles. However, there is an increasing demand to develop new materials, for brake lining and clutch facing to

withstand the technological progress in industry. Friction materials used as brake linings and clutch facing are commonly made from asbestos or other inorganic fibers and ingredients, which include metallic powders and mineral filler as well as the binder in the form of a resin. Frictional materials containing conventional organic binding agents exhibit poor frictional stability. P/M parts of Al MMCs are produced to overcome the poor thermal resistance and withstand higher thermal stresses as well as increasing wear resistance **[1,35]**. The addition of small quantities of magnesium to Al/SiC composite system is recommended in order to improve the wettability and bonding strength between metal matrix and reinforcement particles, as well as to reduce the porosity volume fraction in the produced components **[2,35]**. The strengthening of aluminium alloys with a dispersion of fine ceramic particulates has dramatically increased their potential for wear resistant applications. One of these applications is the development of AMC brake discs, favored primarily over cast iron for their high thermal conductivity and low density. Consideration of frictional properties is of paramount importance in the design of automobile braking systems and Rhee found the frictional force in braking systems to be a power function of the applied normal load and sliding speed at a fixed local contact temperature **[64,135,172]**. In equation form:

$F = \mu\,(T)\, P^{a(T)}\, V^{b(T)}$

where

F = frictional force, $\mu(T)$ = coefficient of friction at temperature T, P = applied load, V= sliding velocity, a(T) = load factor at temperature T and b(T) = velocity factor at temperature T. In common braking systems a(T) ranges between 0.8 and 1.25, while b(T) ranges between -0.25 and +0.25.

μ= coefficient of friction = $\dfrac{M}{A\, i\, R_m\, q}$ **[5]**

where

M= braking torque, A= area of single face sintered disc, i = no of friction surfaces, R_m = mean radious of friction of discs, q = pressure on the disc

The dimensionless quantity known as the friction coefficient, or coefficient of friction as it is sometimes called, evolved from the work of many philosophers, scientists and engineers; in particular, daVinci, Amontons and Coulomb. These thinkers attempted to rationalize the sliding resistance between solid bodies with a universal law that explained observations of their day. In early work with simple machines and macro-scale tribometers, it was observed that the proportionality of the force opposing relative motion to the force holding the bodies together seemed to be constant over a range of conditions. Amontons, for example, is remembered for his two laws of friction:

i) The force of friction is directly proportional to the applied load.

ii) The force of friction is independent of the apparent area of contact.

Dowson calls our attention to Semen Kirilovich Kotelnikov (1723–1806), a former student of the famous mathematician Euler, who is credited for the use of the Greek mu (μ) to represent the friction coefficient. Kotelnikov conducted some of the earliest Russian studies of friction in the late 1700s. In his book on mechanics, he wrote If we denote the friction content F and the applied force P as unknowns, in the ratio μ: 1, then friction $F = \mu P$ **[117].**

Thus, from Rhee's analysis, the frictional force varies with temperature. A decrease in frictional force (braking capacity) with an increase in temperature is referred to as brake fade and it is the goal of braking system engineers to design friction couples for which μ, a and b are independent of rotor temperatures, the ideal values of a and b being 1 and 0, respectively. Further disadvantages of braking systems operating at high temperatures include; i)greater probability of brake fluid boiling, ii)increased pad wear, iii) increased tendency for rotor scoring, iv) higher stresses in the rotor due to thermal gradients which can in turn cause rotor cracking and warping **[64].**

It has been found that the maximum brake rotor temperature for a specified heat flux and braking time decreases as an inverse function of the square root of the thermal conductivity, specific heat and density **[64].** Thus, a rotor of high thermal conductivity will have a significant advantage over a rotor of low thermal conductivity provided the product of the specific heat and density remain constant. A rotor of high thermal conductivity efficiently conducts heat away from the hot points on the outer rim of the rotor to the hub of the rotor, which acts as a heat sink. Temperature gradients in the rotor are thus minimized decreasing the probability of rotor cracking through thermally induced stresses. **Table 2.1** shows thermal conductivity K ($Wm^{-1} K^{-1}$ at 25 °C), specific heat C, ($Jkg^{-1} K^{-1}$ at 25 °C), density ρ (gcm^{-3}) and the product of the specific heat and density Cp ($JK^{-1}cm^{-3}$) for a pearlitic grey cast iron commonly used in automobile brake rotors and an AMC rotor developed by Duralcan USA for its use as a brake rotor material. During light braking the product of the specific heat and density more significantly affect the peak rotor temperature than thermal conductivity, but during moderate to heavy braking, thermal conductivity plays a predominant role in determining peak rotor temperatures **[64].** It follows from Table 2.1 that, during light breaking, cast iron rotors will run cooler than AMC rotors but as the applied pressure increases, AMC rotors with their high thermal conductivity will run cooler and should show superior frictional stability over cast iron rotors. The thermal conductivity and expansion of MMC rotors can be tailored by adjusting the level and distribution of particulate reinforcement **[52,141].**

AMC brake discs are now in production with properties of both the disc material and friction lining material being refined to meet friction, wear and fabrication criteria **[42,124].** Friction

and wear performance are, however, the most important considerations in the design of MMC brake rotors and it is the investigation of the interdependence of these two properties that comprise the bulk of this paper. Standard procedures exist for the testing of automobile braking systems SAE (Society of Automotive Engineers) J661a **[64].** Testing of materials in this research has strictly followed these standard testing procedures. Current research has focused on the development of aluminium based metal matrix composites (AMC's) for brake pads/stators; develop an understanding of tribo-mechanisms occurring at the friction interface when MMCs are worn against a variety of automobile friction materials. These tribo-mechanisms determine the wear, frictional and thermal behavior of the sliding couple (brake pad/stator and rotor). By observing friction traces generated for each sliding velocity and contact pressure combination and then correlating this information with worn surface, insight is gained into the prevalent wear mechanisms for the specific velocity-pressure combinations. Literature on wear mechanisms occurring at the interface of MMC rotors sliding against automobile friction materials is extremely limited, if not unavailable, largely patented by manufacturers. Much research has, however, been conducted with respect to wear mechanisms involved with sliding MMCs against ferrous alloys **[7,8,11,101,125,126,140,178].** Usually, during standard brake testing, wear rate and frictional performance trends are established without investigating the wear mechanisms responsible for these trends. This has been the norm for recent testing of modern friction materials specifically formulated for use against AMC rotors **[64].** An improvement in the materials' durability and braking efficiency can only be facilitated once a thorough understanding of these wear mechanisms has evolved. Wear testing of materials has been conducted in two phases. The first phase is an investigation of a common aluminium alloy incorporated with varying ingredients (wt.% SiC particulates, alumina, graphite, antimony tri sulphide, ceramic fiber, coconut fiber, barium sulphate and mica) worn against two classes of commonly used brake discs (En-32 and cast iron) (pin-on-disc). In this phase, the evolution of transfer layers at the wear surface and their effect on friction and wear is investigated. Temperature rise and noise level are also investigated. This phase can be considered an introduction to the second phase where an AMC specifically designed for its use as a brake pad/stator material is worn against a commercial brake rotor/drum/disc materials used in light, medium and heavy vehicles and also for racing vehicles. In this phase the standard wear test, identification through optical and electron microscopy, of microstructure, role of third body (tribolayer), deformation and fracture wear mechanisms on the MMC wear surface is emphasized. The influence of transfer layers on friction and wear is again investigated in this testing phase.

Table 2.1 Properties of a pearlitic grey cast iron commonly used in automobile brake rotors and aluminium MMC (developed by Duralcan USA for its use as a brake rotor material [64])

Material	K ($Wm^{-1}K^{-1}$ at 25 °C)	C_p ($Jkg^{-1}K^{-1}$ at 25 °C)	ρ(gcm-3)	C_p ($J K^{-1} cm^{-3}$)
Cast Iron	42	511	6.9	3.53
AMC	182	840	2.8	2.35

2.3 Friction material ingredients

The combined effects of ingredient A and C in A + B + C systems where A and C are Al_2O_3, graphite, MoS_2, steel wool and Twaron (aramid pulp), and B is a binder (benzoxazine) on friction performance were studied. Ray design with Golden Section was used for the formulated A + B + C ternary composites. Two combined factors, morphological combinations including fiber/fiber, fiber/filler and filler/filler and combinations by means of material nature including abrasive/abrasive, abrasive/lubricant and lubricant/lubricant, and their composition dependence were considered. Synergetic effects, defined as a minimum wear in wear-composition relationships, were found in morphological combinations of fiber/filler (steel wool/Al_2O_3/B and Twaron/Graphite/B systems). Synergetic effects producing maximum values in friction coefficient (μ)-composition curves were not found in all combinations. All combinations of lubricant/lubricant and abrasive/abrasive reduce μand the effects of the combinations of abrasive/lubricant are dependent upon their abrasive or lubricant efficiency. Strong abrasive (Al_2O_3) plays an important role on the formation of friction layer that the transferred iron from disc to friction materials in combinations of Al_2O_3/lubricant/B systems, and there is no such a transfer of iron from disc to friction materials on the surface of lubricant/lubricant combinations. The S type friction transition was observed in MoS_2/steel wool/B and graphite/steel wool/B systems and was caused by adhesion friction mechanism **[189].**

2.3.1 Abrasives:

Abrasives improve the friction performance to a desired level, and they are added in various sizes and concentrations to create and as well as to increase friction/surface film which is formed when the brakes are applied. This will also induce low wear and frictional stability thus improving braking efficiency over variety of applications. The abrasives are described in **Table 2.2.**

Table 2.2 Abrasives [RR1]

S. No.	Material	Description / comment
1.	Aluminium oxide	Very hard and most in abrasive form either in hydrated form or anhydrous form is used.
2.	Iron oxides	Hematite (Fe_2O_3) and magnetite (Fe_3O_4) act as a mild abrasives
3.	Quartz	Crushed mineral particles (SiO_2)
4.	Silica	May be natural or synthetically-produced (SiO_2)
5.	Zirconium silicate/oxide	($ZrSiO_4$) or (ZrO_2)
6.	SiC	Very hard abrasive for severe conditions are used.

2.3.2 Friction producers/modifiers

These are responsible for control of coefficient of friction or the type of wear. They may form interfacial films and may act as lubricant. Solid lubricants are used to stabilize the coefficient of friction, primarily at elevated temperatures. The friction producers/modifiers are described in **Table 2.3**.

Table 2.3 Friction producers/modifiers [RR1,34,38,50,54,61,157]

S. No.	Material	Description / comment
1.	Antimony trisulfide	Solid lubricant added to enhance frictional stability; lubricates >450°C, is potentially toxic
2.	Brass	Typically 62%Cu – 38% Zn; sometimes used as chips or machine shop cutting swarf, said to improve wet friction and recovery, common additive.
3.	Carbon (graphite)	Cheap and widely-used solid lubrucant; many forms are available; synthetic or natural crystalline type used; burns in air at >700°C, friction level is affected by moisture and structure.
4.	Ceramic 'microspheres'	Special product consisting of alumina-silica with minor iron or titanium oxides, low-density filler; reduce rotor wear and control friction
5.	Coke	Cheap solid lubricant, improves friction performance
6.	Copper	Uses as a powder to control heat transport; improves thermal conductivity; can causes excessive cast iron wear
7.	Friction dust	Processed cashew resin, may have a rubber base; to reduce spontaneous combustion or help particle dispersion.

S. No.	Material	Description / comment
8.	Friction powder	Sponge Fe, e.g for semi-metallic brake pads a number of different particle grades (sizes) are available depending on requirements for surface area, light-medium-heavy duty vehicle applications.
9.	Lead oxide	PbO as friction modifiers; toxic in nature
10.	Metals – fluxing compounds	Pb, Sb, Bi, Mo as fluxing compounds serve as oxygen getters to stabilize friction induced films and promoting thick films.
11.	Metals oxides – various	Magnetite (Fe_3O_4) improves cold friction; ZnO lubricates but can cause drum polishing; Cr_2O_3 raises friction
12.	Metals sulfides – various	Cu_2S, Sb_2S_3, PbS are modifies and stabilize the friction coefficient; Sb_2S_3 has highest COF; PbS - soft solid lubricant additive which reduce noise, pad & rotor wear; MoS_2 – a typical layer-lattice-type lubricant and adheres more readily to metal surfaces than graphite; ZnS is a low cost solid lubricant for high loads and temperatures

2.3.3 Reinforcements/fillers

Reinforcements provide mechanical strength. Fibers of metal, carbon, glass and rarely mineral and ceramic fibers are used. Fillers are principally used to make the material less expensive and/or improve processing. Some reinforcements, fillers and others ingredients may also affect friction characteristics of the material **[157].** The reinforcements, fillers and others ingredients are described in **Table 2.4.**

Table 2.4 Reinforcements, fillers and others ingredients [RR1,34,61,76, 157]

S.No.	Material	Description / cmment
1.	Anti-oxidants	Graphite – common anti-oxidant in metallo-ceramic composite brakes; maintains proper oxide film thickness on aircraft brakes; thicker oxide film leads to unstable friction and can wear off.
2.	Aramid	Good stiffness to weight ratio; excellent thermal resilience; good wear resistance
3.	Asbestos	Most common filler in early brake materials
4.	Bariumsulfate (barytes)	($BaSO_4$) basically inert; increases density and wear resistance, stable at high temperature.
5.	Calcium carbonate	$CaCO_3$ is a lower cost alternative to braytes, but not quite as stable at high temperatures
6.	Calcium hydroxide	$Ca(OH)_2$ a cheap filler
7.	Cashew nut shell oil	Improves resilience in the binder system and reduces brake noise
8.	Cotton	Reinforcing fiber for the matrix

S.No.	Material	Description / comment
9.	Fibers – mixed oxide	Reinforcement fibers; produced from a base slag mineral wool; contains mixture of silica (40-50wt%), alumina (5-15wt%), calcia (34-42wt%), magnesia (3-10wt%), and other inorganics (0-7wt%); controls fade and increase braking.
10.	Glass	Sufficient thermal resilience; brittle
11.	Iron	Cheap filler, better high temperature characteristics, In semi-metallic type higher contents are used.
12.	Lime	$Ca(OH)_2$ is used to avoid corrosion in Fe-additives, helps in processing, raises fade temperatures
13.	Magnesium oxide	MgO promotes curing of binder
14.	Metal fibers	Cu fiber, Steel fiber, Al Fiber
15.	Polyacrylonitrile	PAN fiber is used as reinforcement
16.	Potassium titanate	Inert filler material; very hard and good wear resistance; thermally resilient
17.	Rock wool	Fibrous material
18.	Rubber – diene, nitrile	As stabilizers to promote cross-linking and increase wear resistance; rubber modifies the compressibility (modulus/stiffness)
19.	Rubber scrap	Ground up tires ('tire peels'), decreases cost, must not contain road dirt
20.	Sea coal	General low-cost particulate filler, may contain harmful ash; not good for high temperatures
21.	Steel wool	Used as reinforcement
22.	Styrene-butadiene rubber	(SBR) used as toughening agent for the binder
23.	Vermiculite	Expanded type is used

2.3.4 Binders

Binders are matrix for organic type friction material that hold the other components together, form thermally stable matrix and preserve their structural integrity under mechanical and thermal stresses, which are developed during braking. **Table 2.5** below shows common binders for friction material application **[157].**

Optimization of friction material formulation were carried based on Taguchi design, multiple regression analysis coupled with genetic algorithms, chemometrics, and golden section principle in combination with relational grade analysis to develop friction material of better triboligical performance aimed with higher wear resistance and moderate or high coefficient of friction (COF) **[25,157,188].**

Automotive brake squeal can be described as an irritating sound with a main frequency between 1 to 20 kHz, generated by the components. This noise generation needs to be suppressed for better or efficient brake design and manufacture. The article clearly states the important factors for noise level generation were vibration and waves, brake rotors designs, contact pressure and temperature. Also, experimental studies on brake squeal of different brake

friction materials, eliminations of brake squeal problem, friction laws, contact geometry asperities, modeling of brake squeal are carried. Squealing in brakes is mostly due to the contact between brake pad and disc (counterpart). The sizes of contact plateaus at the different brake pressures and higher temperatures evolved during friction affects the generation of brake squeals [**157**].

Table 2.5 Binder materials [RR1, 34,37]

S. No.	Material	Description / Comment
1.	Phenolic resin	Common binder; too little quantity leads to material weakness; if too much is used, there is a friction drop-off at higher temperatures; cheap and easy to produce; brittle, highly toxic.
2.	COPNA resin	High bonding strength with graphite; better wear resistance; decomposes at relatively low temperatures (450-500°C)
3.	Cyanate ester resin	High heat resistance; chemically inert; vibration dampener, brittle
4.	Thermoplastic polyimide resin	Abrasion resistant; does not exhibit thermal fade; lower thermal conductivity
5.	Modified resins	A variety of modifications includes phenolic, cresol, epoxy, cashew nut shell liquid (CNSL), PVB, rubber, alkylbenzene, linseed oil and boron are used to alter bonding characteristics and temperature resistance.

Binding agents present in the conventional organic friction materials exhibit poor frictional stability under varying temperature conditions. Higher temperatures generation during braking causes binders to disintegrate. Thermal degradation of binders results in inferior frictional characteristics, giving rise to fade and often resulting in increased wear. Furthermore, organic materials, particularly resins, tend to have a short shelf life, and are not always easy to reproduce **[157,167].** To overcome these deleterious effects of poor thermal resistance in an organic friction material, sintered metallo-ceramic friction materials, which withstand considerably higher thermal stresses have been developed and are described below. These brake materials are known for better frictional and wear performance under heavy duty applications. High mechanical strength, better thermal conductivity and thermal capacity, high heat resistance are some of the main attributes of metallo-cermic brakes and are therefore much superior in performance than organic brake materials.

2.4 Automotive friction materials

The existing automotive friction materials are classified in two categories as given below:

i) Automobile brake rotor materials [67, 64]

ii) Automobile disc brake friction linings/brake pads [64]

2.4.1 Automobile brake rotor materials

The metal matrix friction materials for brake rotors can be divided into five categories. These include:

(i) Pearlitic grey cast iron rotors used in modern light sedan. This material was supplied by BMW (South Africa) and was machined into test samples from the brake rotor itself. This cast iron has a type B size four (ASTM designation A257) rosette graphitic flake distribution.

(ii) An A357 cast magnesium/silicon aluminium alloy reinforced with 20 vol. % SiC particulates. This material was supplied by Hulett Aluminium (South Africa) in ready cast solid cylinders and was tested without prior heat treatment.

(iii) Unreinforced A357, being the matrix of the reinforced composite above, supplied in ready cast solid cylinders by Hulett Aluminium (South Africa) and tested without prior heat treatment.

(iv) An A359 cast magnesium/silicon aluminium alloy reinforced with 20 vol.% SiC particulates supplied by Duralcan USA. This is a precision cast composite specifically designed for its application in brake rotor materials. This material was heat treated according to the Duralcan T 71 heat-treating procedure which involves solutionizing the alloy at 538 °C for 15 h, quenching in hot water and artificial ageing at 246 °C for 3 hrs. This heat treatment places the composite in an over aged temper.

(v) An unreinforced magnesium/silicon A359 cast aluminium alloy supplied by Hulett Aluminium (South Africa), tested without prior heat treatment. This material is the matrix of the composite above. **Table 2.6** shows the actual percentage (weight) chemical composition and Vickers bulk hardness of the five rotor materials-note that the lighter elements are not represented.

Table 2.6 Brake rotor materials (wt. %) [64]

Material	Si	Fe	Cu	Mg	Ti	Al	SiC	$Hv_{20\ kgf}$
Cast iron	3.2	93.2	-	-	-	1.20	0	200
A357	6.2	0.42	-	0.24	-	93.14	0	61
A357-MMC	6.0	0.45	-	0.23	-	73.32	20	116
A359	9.35	0.06	0.12	0.42	0.04	69.99	0	65
A359-MMC	6.67	0.16	0.16	.51	0.16	70.32	20	125

2.4.2 Automobile disc brake friction linings/brake pads

Automotive friction linings usually consist of several ingredients bound into a composite. These ingredients can be classified as fibrous reinforcement, binder, filler and friction modifier. Accordingly, modern friction materials may be classified into three categories viz:

metallic linings (consisting of metal only), semi-metallic linings containing metal chips and organic fibres bound together with resins, and finally, organic linings are containing organic constituents. Of the above three lining categories only the latter two were considered for testing. Three makes of friction lining materials were tested against the rotor materials in the following order.

2.4.2.1 Organic pad

This friction lining is currently used in the disc brake systems of heavier vehicles and has been developed for use against cast iron rotors. It is composed of organic fibers, rubber, graphite and internal lubricant, bound together with phenolic resins. It must be noted that this friction lining contains a small percentage of copper (0.6 wt.%) which is added to improve the lining's thermal conductivity. Although, by definition, this friction lining is semi-metallic, it will be referred to as organic to provide clear distinction from friction linings with high metallic constituents.

2.4.2.2 Semi-metallic pad A

This friction lining material is used in the front disc brake system of medium sized sedans and has also been developed for use against pearlitic grey cast iron rotors. It is a complex composite containing copper, aluminium and iron metallic chips or fibers in addition to rubber and graphite fillers all held together with phenolic resin binder.

2.4.2.3 Semi-metallic pad B

This friction lining has been specifically developed for its use against aluminium MMC rotors. It has copper as its metal constituent embedded in a matrix of compressed paper. This pad also has an internal lubricant and contains no graphite nor rubber fillers, but does contain a small percentage of alumina. **Table 2.7** details approximate composition, density and hardness values for the three friction lining materials.

Table 2.7 Brake lining materials (wt. %) [64]

Lining	Cu	Fe	Al	Organic binder	Graphite	Rubber	Paper	Alumina	Organic	Other	ρ (gm/cc)
Organic	0.6	-	-	43	15	2	15	-	20	4.4	2.49
Semi-met A	15	43	3	25	7	5	-	-	-	2	3.12
Semi-met B	15	3	2	16	4	-	52	5	-	3	2.36

The wear resistance of AMCs sliding against organic pads is greatly enhanced by the formation of a solid lubricant graphitic layer at the wear interface. The SiC particulates in the AMC constrain the matrix, thus preventing strain to fracture. Slivers of unreinforced aluminium, which would otherwise be present at the interface, do not, therefore, disturb the formation and

maintenance of this solid lubricant graphitic tribo-layer. Wear rates are low and friction is constant for this rotor-pad combination. When AMCs are worn against semimetallic pads formulated for use against cast iron rotors, the loose/fractured SiC particles trapped at the wear interface, the hard metallic particles in the pad and the hard unfractured AMC surface perpetuate wear through a process of three body abrasions. This abrasion leads to subsurface delamination in the AMC and early melt wear. When AMCs are worn against a semimetallic pad specifically formulated for use against AMC rotors, friction traces are found to be highly irregular. Fracture of the SiC reinforcing particulates occurs at the lowest load and sliding velocity. This fracture is induced by the hard alumina particles within the pad. At higher loads and sliding velocities, melt wear occurs in the AMC and the cohesiveness of materials within the pad is poor. Wear rates at low loads for this rotor-pad combination are low, but at higher loads and sliding velocities, the wear rate of the A359 AMC is extremely high, sometimes higher than the wear rate of its unreinforced matrix. If the structure and composition of friction linings are arranged correctly, the wear resistance and frictional performance of AMC brake rotors are superior to those of cast iron brake rotors. In addition, the lower density of AMCs gives them an economic advantage over cast iron with respect to efficient use of fuel and fabrication expenses.

Rawa let al. **[130]** has been reported that composite materials with their high specific stiffness and low coefficient of thermal expansion (CTE), provide the necessary characteristics to produce lightweight and dimensionally stable structures. Therefore, both organic-matrix and metal matrix composites (MMCs) have been developed for space applications.

Discontinuously reinforced aluminum matrix composites (DRA) have been attracting attention because of their amenability to undergo deformation processing by conventional metalworking techniques **[28].** The dry sliding wear performance of discontinuously reinforced aluminum (DRA) as investigated by numerous studies during the last two decades is reviewed and discussed. In general, DRAs feature substantially better wear resistance than their respective unreinforced matrices. However, under particular conditions and wear mechanisms, the wear performance of the overall DRA-metal couple is similar to or lower than its respective unreinforced alloy-metal couple. Furthermore, conflicting results regarding the effect of the different tribological parameters on the wear performance of DRAs are noted among the reviewed studies, thereby increasing the difficulty in achieving the optimization of DRA-metal couples. It is shown that parameter interactions exist and are responsible for these conflicting results. The development of a general framework identifying groups of interactive parameters and assessing wear material performance through investigating these groups of parameter is therefore presented. It is suggested that material loss can be rationalized from the

understanding and description of the three wear precursors that delineate these groups of parameters, the wear precursors being surface, subsurface and third body behavior. It is proposed that optimization of a tribo-system can be done through optimizing the three behaviors independently, thus allowing consideration of a reduced number of parameters while providing a higher degree of practical extrapolation.

Discontinuously reinforced metal matrix composites (DRMMC) **[146],** of high-strength metallic alloys reinforced with ceramic particulates or whiskers, are advanced materials that have emerged from the perpetual need of lighter-weight, higher-performance components in the aerospace, aircraft **[53,54,127,128]** and more recently the automotive industries **[68].** Indeed, these "new" materials offer promising perspectives in assisting automotive engineers to achieve improvement in vehicle fuel efficiency. Their distinctive properties of high stiffness, high strength and low density have promoted an increasing number of applications for these materials. Several of these applications require enhanced friction and wear performances, for example brake rotors, engine blocks and cylinder liners, connecting rod and piston, gears, valves, pulleys, suspension components, etc. **[146].**

The principal tribological parameters that control the friction and wear performance of discontinuously reinforced aluminum (DRA) composites can be classified into two categories **[146]:**

(i) Mechanical and physical factors (extrinsic to the material undergoing surface interaction), e.g. the effect of load normal to the tribo-contact **[6,11,12,27,33,63,122],** the sliding velocity **[75,98,134,148,178],** the sliding distance (transient and steady state period) **[7,98,112,134,178],** the reinforcement orientation for non equiaxed particulates **[78,98,112,175],** the environment and temperature **[101,146],** the surface finish **[43]** and the counterpart **[43,46].**

(ii) Material factors (intrinsic to the material undergoing surface interaction), e.g. the reinforcement type **[16,27,63,146],** the reinforcement size **[10,27,63,75,146,148,159]** and size distribution **[145,146,174,176],** the reinforcement shape **[146,175,178],** the matrix microstructure **[111,146,177]** and finally the reinforcement volume fraction **[10,98,146].**

While DRA composites generally exhibit enhanced wear performance when contrasted with unreinforced aluminum alloys **[146],** some investigators, e.g. **[6,11,12,33]** have shown that under specified conditions DRA composites display a wear resistance comparable with their unreinforced alloys; indeed under these conditions use of DRA is no longer justified. In consequence, careful identification of these conditions through analysis and understanding of tribological parameters is a major issue for material selection and development. Moreover,

contradictory results regarding the influence of the different tribological parameters on the DRA's wear performance can be found among previous investigations **[146].** This demonstrates that significant interactions exist among the tribological parameters and consequently assessing these parameters independently can be misleading. On the other hand, it is obvious that conducting an experimental investigation or deriving a formal model including all tribological parameters is currently out of reach.

2.5 Factors affecting the tribo-properties of friction materials

Engineering experience shows that there is a direct impact of influencing factors like interface pressure, sliding speed or temperature on friction and wear in friction mechanisms.

The Factors affecting the tribo-properties of friction materials can be classified in two categories:

2.5.1 Extrinsic factors

2.5.1.1 Sliding distance

An initial unstable non-linear period followed by a steady state period, during which the wear rate increased linearly with increasing sliding distance, was observed by Wang and Rack **[178].** Wear mechanisms changed as sliding distance increased; it was found that abrasion was the predominant wear mechanism for both DRA pin and steel counterpart during the initial run-in period. While abrasion was still the wear mechanism for the steel counterpart, adhesion induced tribo-fracture occurred in the 2124 Al-SiC, during steady state sliding. Alpas and Embury **[7]** noted a very short initial run-in period with the friction coefficient increasing from 0.35 during the run-in to 0.6 for the steady-state period after only a sliding distance of 10 m. They attributed this to generation of loose debris that transformed wear into a three body abrasive wear during the first ten meters. They also reported that the predominant wear mechanism for the DRA was delamination of subsurface layers generating loose debris and giving turbulent friction behavior, in agreement with Sannino and Rack **[146].** Alpas and Embury **[7]** finally concluded that subsurface cracks nucleated at interfaces between SiC particulates and Al matrix, and the size of the debris was related to size of the SiC particulates. In contrast to the previous observations, Pan *et al.* **[112]** did not identify any run-in stage for higher normal load **52 N [112]** vs. 14.2 N **[178,146]** and 9.35 N **[7].** However, they did not perform wear loss measurements below 300 m and a possible run-in period ending at lower sliding distance may have gone undetected.

2.5.1.2 Normal load

Cao *et al.* **[33]** observed a transition load for all the materials tested, above which the wear rate increased dramatically, the wear mechanism changing from oxidation assisted flaking to

adhesion-induced tribo-fracture. Below the transition load, unreinforced material and composites showed similar wear rates while significant improvement of wear resistance by SiC addition was observed above the transition load. Moreover, the transition load increased with increasing SiC whisker content; addition of 20 vol.% reinforcements, acting as load-bearing elements, increased the transition load by more than 60%. In contrast, Alpas and Zhang **[6,11]** noted three regions when considering the effect of load on the wear rate. In the first load region (0.9-15 N) a tenfold increase in the wear resistance of the composites with respect to the unreinforced material was observed. They explained this phenomenon as the consequence of the load-bearing capacity of the SiC, reinforcement. Oxidative microgrooving was reported to be the main operative mechanism. For higher loads (15-98 N), where stresses were greater than the fracture strength of the SiC particulates, the reinforcement loses its capacity to support the load and similar wear rates for unreinforced A356 and A356-SiC 20 vol.% composites were reported, in agreement with Jokinen and Anderson **[75],** who reported similar wear rates for 6061 Al and 6061Al/ 20 vol.% SiC, composites at high (39.2 vs. 10 N) loads. Stable crack growth and delamination of the matrix became the main process of debris formation and the fracture toughness, rather than the hardness, of the composites controlled the wear rates. Finally above 98 N, the wear rates of the aluminum alloy were increased by two orders of magnitude. In this load region the unreinforced materials exhibited severe loss of material by adhesion-induced tribofracture and generation of plate-like press-slide flattened debris, while subsurface cracking continued to be the dominant wear mechanism for the composite material with wear rates being similar to those observed at lower loads. It was finally suggested that the thermal stability and the enhanced high temperature strength of the SiC reinforced aluminum alloy was responsible for the composites' better wear and seizure resistance at high load. The same investigators **[I2]** also reported three differing load dependent regions in 6061Al reinforced with 20 vol.% alumina particulates. They noted however that in the third region (high load) the reinforcement did not suppress the transition to sever wear, but rather delayed it (180 N vs.98 N). Under other experimental conditions, Hosking *et al.* **[63]** observed that the wear rate under dry-sliding conditions monotonically increased with applied load up to 10 N for all tested materials. However, they did note that the wear mechanism in 2124 Al 20 wt.% SiC and Al_2O_3, particulate changed from adhesion to pure abrasion with increasing load. Similarly, Pramila Bai *et al.* **[122]** reported that A356 SiC, 20 vol.% composites exhibited better wear resistance over the entire range of loads investigated (6-75 N). Scanning electron microscopy examination of surfaces and subsurfaces showed that the SiC, presence increased the wear resistance through a decrease in the tendency of material flow at the surface. No significant change of mechanisms, delamination and oxidative abrasion, was noted as load

increased. Summarizing, the effect of load on wear behavior when dealing with sufficiently wide ranges of loads is best represented by three differing load dependent regions, the extent of these regions being dependent upon many other parameters **[146].**

The incorporation of ceramic particles in an Al-alloy increases its load-bearing capacity and hence the load and sliding speed range within which dry sliding wear is mild. This has been investigated in detail by many researchers and opens new opportunities for the employment of Al-based metal-matrix-composites (Al-MMCs) in applications where sliding resistance is of concern. Some investigations have also analyzed the wear behavior of Al-MMCs in the case of external heating, in the temperature range up to 200 °C or 500 °C. It has been found that wear increases as temperature is increased, because of the thermal softening of the composite, and becomes severe at a critical temperature. Friction coefficient was also observed to increase and this was attributed to an increase in the adhesion forces. Most experimental investigations were carried out using hard steel as a counter face. The investigation of the friction and wear behavior of Al-MMCs against friction materials is receiving particular attention, because of the possibility of using these materials for disc brakes in automotive applications. With respect to the traditional cast iron, Al-MMCs disk offers promising advantages, such as lower density and higher thermal conductivity. Howell and Ball, for example, investigated the friction and wear behavior of two Al-MMCs against organic as well as semi-metallic friction materials. Wear rate was found to be lower against the organic friction material, because of the formation of a graphite-rich transfer layer, and higher against the semi-metallic friction materials, because of the abrasive action of the metallic chips or fibers present in the friction material. A detailed investigation on the surface damage and on the properties of the transfer layer was carried out by Sallit *et al.* Understanding the nature of the tribological contacts is very important in order to explain the observed friction and wear behavior in discs/pad couplings, as demonstrated in recent investigations **[161].**

2.5.1.3 Sliding velocity

Cao et al. **[33]** observed that the transition load was dependant on the sliding velocity, a transition load of 110, 80 and 50 N for the unreinforced 6061Al being observed at sliding velocities of 1, 1.5 and 2 m/s respectively, and 110 and 80 N for 20 vol.% SiC, 6061 composites, sliding velocities of 1.5 and 2 m/s, respectively. Sato and Mehrabian **[148],** observed that the wear rate of aluminum alloy unreinforced and reinforced with 10 vol.% SiC, 15 vol.% SiC, 30 vol.% SiO_2 glass and 20 vol.% SiO_2 tended to increase with increasing sliding velocity, whereas for 15 vol.% Al_2O_3,15 vol.% TiC and 10 vol.% S and N, reinforced composites wear rates seemed to be unaffected by sliding velocity. Wang and Rack **[178].** reported that below 1.2 m/s, where the main operative mechanism is microcracking, SiC,

reinforcement did not improve the wear resistance, in agreement with Lee *et al.* **[88]** who, however, observed the transition speed at 0.37 instead of 1.2 m/s for their experimental conditions, and attributed the low DRA wear resistance to higher friction coefficient and third body abrasion at low speed. From 1.2 m s-l to 3.6 m/s, Wang and Rack **[178]** noted a change of mechanism; adhesion and abrasion assisted by microcracking controlled debris generation. Also, improvement of wear resistance by SiC was more significant in this velocity region, in agreement with Lee *et al.* **[88]** for the range of 0.37-2 m/s. Furthermore, sliding velocity increased the initial and steady state wear rate for the unreinforced material, whereas for all composites, the initial-state wear rate was increased and the steady state wear rate decreased as sliding velocity increases **[178].** These three investigations are complementary, however, counterpart type and load discrepancies, probably leading to the conflicting results between [148] and **[134,148,178],** making it impossible to establish a general sliding velocity- DRA wear behavior relationship in the total range of 0.05- 3.6 m /s. Maps predicting wear severity and mechanism during dry sliding wear as a function sliding velocity and normal load were developed by Lim and Ashby **[92]** for steel-steel tribo-system. However, such maps would not be valid for DRA-steel systems since, as it will be shown later, other parameters (e.g. intrinsic factors such as reinforcement volume fraction size and shape) interact.

2.5.1.4 Reinforcement orientation

According to Wang and Rack **[178],** the run-in period wear rate of the composites depends upon the reinforcement orientation, the highest rates being observed with the perpendicularly oriented SiC, composite. However, the steady state wear rates were generally independent of the reinforcement geometry (particulates vs. whiskers) and orientation (perpendicular vs. parallel) with the exception of sliding wear at 3.6 m s-l were the parallel-oriented SiC, was superior, the applied load being fixed at 14.2 N. At a much higher normal load, 52 N, Pan *et al.* **[112]** concluded that the sliding wear rate of SiC, composite varied twofold in magnitude depending on orientation. The higher wear rate was found for the perpendicular-oriented SiC, whereas the highest performance was for the parallel orientation which has the largest areal fraction of whiskers These two investigations show that the reinforcement orientation becomes a more significant parameter as the normal load increases and the contribution to wear resistance of the reinforcement as load bearing agents is influenced by both applied load and reinforcement orientation.

2.5.1.5 Extend temperature

Only limited investigations of external temperature on DRA wear behavior has been reported. Li *at al.* **[93]** studied the effect of $A1_2O_3$ reinforcement on the wear resistance of an aluminum alloy at high temperature (150 and 250 ^{0}C) during fretting. They reported that Al_2O_3 was more

efficient in improving the composite wear resistance at high environmental temperature than at room temperature **[146]**. They attributed this phenomenon to the improvement of the thermal stability, the seizure resistance and the high temperature strength aluminum alloy by the presence of refractory Al_2O_3. Martinez *et al.* **[101]** observed two distinct wear behaviors for eutectic Al-Si and Al-Si-SiC, composites, depending upon the test temperature. At low temperature the wear behavior is controlled by the Si or SiC particulates, whereas at high temperature wear in the former system was rather controlled by the matrix tribological properties. Moreover they observed, similarly to Li *et al.*, that the thermal stability was improved by the reinforcement and noted that the transition temperature between low temperature and high temperature wear behavior was increased by SiC, addition (110 ^{O}C for the unreinforced material and 150 ^{O}C for composites materials).

2.5.1.6 Surface finish

Wang and Rack **[176]** reported that the reduction of the surface roughness of the sliding surfaces decreased initial wear rates in both composite and unreinforced counterpart surfaces, but had no effect on the steady-state behavior of either the part or the counterpart.

2.5.2 Intrinsic factors

2.5.2.1 Reinforcement type

Composites containing hard SiC, TiC, Si_3N_4, Al_2O_3, and SiO_2 exhibited lower (four to ten times lower, depending on the velocity and the reinforcement type combination) wear rate than the unreinforced matrix alloy **[148,169]**, obvious superiority among these reinforcement types was detected throughout the velocity range under investigation.

In contrast, composites containing soft particulates, MgO and BN, displayed wear rate four to five times higher than the unreinforced matrix alloy. However, Hosking *et al.* **[63]** reported that, at low load (0.5 N) and other experimental conditions, SiC particulate are more effective than Al_2O_3 particulates in resisting wear. They attributed this discrepancy to the difference in wear performance and hardness (1800 vs. 2600 VHN for Al_2O_3 and SiC, respectively) of the reinforcements themselves. Long *et al.* **[96]** reported that, at a given reinforcement volume fraction, the best improvement in wear resistance was obtained by an hybrid composition of SiC whiskers and Al_2O_3 fibers followed by SiC whiskers, the least efficient being Al_2O_3 fibers. This phenomenon was attributed to the barrier effect of the SiC whiskers against the slip of Al_2O_3 fibers during the flow of the matrix. Optimization by combining two reinforcement types (alumina/aluminosilicate) was also observed in lubricated sliding **[74]**. Roy *et al.* **[137]** found significant improvement of the 6061 aluminum alloy wear performance by addition of SiC, TiB_2, B_4C and TiC. Similar wear performance and friction coefficient were reached by the various reinforcement types except for the TiC who exhibited slightly higher wear rate.

Subsurface cracking and delamination mechanisms were common to the composites; however, the crack zone for the Al-TiC extended to a larger depth as compared with the others (160 against 70 μm). Furthermore, the wear resistance of TiC ceramic was lower than these of SiC, TiB, and B_4C **[26]**. These two factors were proposed to be the cause of lower wear resistance 6061-TiC composite with respect to the other composites investigated. Alternatively, orientation and fracture toughness of particulates may be a predominant factor of wear severity for non-equiaxed particulates **[146]** and for other mechanisms such as abrasion or adhesion. From these observations, SiC, TiB, and B_4C appear to be the best candidates for improving the wear performance of DRA; however, a choice among these reinforcement depends also on the reinforcement size and shape, and requires prediction or knowledge of the operative wear mechanisms.

2.5.2.2 Reinforcement size

Al_2O_3, reinforcements at low load (0.5 N) were reported to give decreasing wear rate with increasing reinforcement size within the size range studied (1-142 μm) **[63]**. However, *Hosking et al.* **[63]** did not mention the influence of particulate size on the operative wear mechanisms. Jokinen and Anderson **[75]** also observed a slight DRA wear rate decrease with increasing SiC, size for heavy (39.2 N) load, while at lower (10 N) load, the DRA wear rate abruptly decreased from 5 to 13 μm and slightly increased from 13 to 29 μm, in agreement with Alpas and Zhang **[10]** who observed a consequential improvement of DRA wear performance though reinforcement size at low load. These investigators **[10,75]** explained this phenomenon to be due to a better protection from large reinforcements against adhesion wear, this mechanism being predominant at low load. In contrast, Sato and Mehrabian **[148]** observed for 15 vol.% SiC, for a load of 3N, that below 0.3 m s^{-1} larger size (46 μm) composites wear more as compared with lower size (20 μm), the opposite results occurring above 0.3 m/s. An explanation of this phenomenon was not provided. Sannino and Rack **[146]** concluded that adhesion was a common wear mechanism for all 2009-SiC,-17/4 PH tribo-systems, with increasing reinforcement size resulting in higher DRA wear rate, in agreement with Skolianos and Kattamis **[159]**, who observed a continuous DRA wear rate increase with SiC size increase from 10.7 to 29 μm. This increase was observed by Sannino and Rack to be due to transition of predominant mechanism from microcutting, plowing and wedge formation to particulate cracking induced delamination. From these results, the effect of particulate size is related to the normal load and the sliding velocity. Indeed, both sliding velocity-induced temperature rise and load may contribute to a change of mechanisms, the particulates playing a distinct role in different mechanisms such as oxidative abrasion, oxidation-assisted flaking, adhesion, delamination **[6,11,12,33,98,178]**. This suggests that increasing particulate size can

be both beneficial and detrimental according to the operative mechanisms and a simple rule dealing with the reinforcement size effect on the DRA wear performance cannot be inferred.

The effects of sintered porosity, volume fraction and particle size of silicon carbide particles (SiC_p) on the abrasive wear resistance of powder metallurgy (P/M) aluminium alloy 6061 matrix composites have been studied. Aluminium alloy 6061 manufactured following the same route was also included for direct comparison. The results show that the beneficial effect of hard SiC_p addition on wear resistance far surpassed that of the sintered porosity in the P/M composites. Tremendous improvements in the wear resistance of aluminium alloy can be expected by adding the SiC_p reinforcements **[89].**

Axen *et al.* **[20]** have reported that the fiber reinforcement increases the wear resistance in milder abrasive situations, i.e. small and soft abrasives and low loads. However, in tougher abrasive situations, meaning coarse and hard abrasives and high loads, the wear resistance of the composites is equal to or, in some cases, even lower than that of the unreinforced material. It is also shown that the coefficient of friction decreases with increasing fiber content and matrix hardness of the composites.

2.5.2.3 Reinforcement shape

For DRAs undergoing high strain deformation, void and crack nucleation generally occurs at either the reinforcement matrix interface due to inhomogeneous plastic deformation **[17,66,146],** or by fracture of cylindrical or plate-like particulates. Particulate shape can control the DRA wear performance through their ability (a) either to undergo rotation, e.g. Refs. **[6,11,33]** or to bear the applied load **[6,11,12,63],** to enhance the composites' seizure resistance and thermal stability **[75,146],** and above all to provide preferential sites for stress concentration **[69,94,146]** and subsurface delamination **[146].** In the case of SiC particulate vs. whiskers, Wang and Rack **[178]** concluded that the steady state wear rate was dependent on reinforcement geometry and strength, and sliding velocity. They reported that at low velocities particulates were more efficient (i.e. wear rate of 3.23 vs. 3.64 X 10^3 mm^3/ m for parallel oriented whiskers), while at high velocity the opposite was observed (i.e. wear rate of 1.63 vs. 1.11 X 10^3 mm^3m^{-1}). For the initial run-in period, parallel oriented whiskers were more efficient than particulates, especially at high velocity (i.e. wear rate of 28.1 vs. 13.2 X 10^3 mm^3m^{-1}). From these results, it is clear that the effect of reinforcement shape is affected by sliding velocity. Again we may expect other parameter interactions besides sliding velocity such as load and reinforcement size. Since the latter has been shown to govern the predominant wear mechanism and therefore the wear rate **[6,10,11,12,33, 98,178]** a simple rule dealing with the individual effect of the reinforcement shape on the DRA wear performance cannot be formulated. Lewandowski *et. al* **[91]** have reported the effects of matrix microstructure and

particle distribution on the fracture of an aluminum alloy metal matrix composite containing 20% by volume SiC particulate. The matrix microstructure was systematically varied by heat treating to either an under- or over-aged condition of equivalent strength, and was characterized using a combination of techniques. It is shown that the micro-mechanisms of fracture are significantly affected by the details of the matrix microstructure, interface character, and degree of clustering in the material.

2.5.2.4 Effects of solid lubricant: Graphite

Some papers on aluminium/graphite composites have reported significant improvements on tribological behavior related to wear and seizure resistance of these materials as reported by Lin *et al.* (1998), Harrison and Perry (1998), Pai *et al.* (1974), Krishnan *et al.* (1981) and Surappa and Rohatgi (1978). Proportion of particles content in aluminium-graphite composite dispersed from pellets method had significant effect on wear behavior, so that if pellets contain too much graphite particles then they become crumble able, on the other hand if the composite contains above 8 wt%content in graphite, become brittle (Lin *et al.*, 1998). By this way, a good wear behavior performance expected from an aluminium-graphite composite is not a direct proportion of graphite content.Distribution of particles inside the composites ingot and size of particles entrapped could have a suitable tribological effects on the wear behavior leading the anti-seizure and sliding of surfaces (Lin *et al., 1998;* Krishnan *et al.,* 1981). Some aluminium alloys such as Al-Zn and Al-Cu have a kind of affinity to graphite reinforcement that could accept greater amount of graphite than Al-Si alloys (Terry and Jones, 1990). At the same time, shape of particles has an important effect on the graphite content to be incorporated in the alloys, in such a way, low volumetric fraction less than 0.9 wt% content of graphite in shape flakes, has been observed as permissible amount to be incorporated into an aluminium alloy making difficult in increasing the weight content with graphite as reported by Rohatgi *et al.* (1986). Samples of aluminium/graphite composites analyzed in this paper contained much more graphite flakes particles as 4.5 wt% entrapped by desegregation of pellets, casting and cooling. For casting process is still difficult to reach a uniform reinforcement particles distribution into the ingots, segregation problems due to differences in specific gravity and lack of wettability of constituents, agglomeration of particles and others factors, make the particles distribution be heterogeneous. In aluminium/ graphite composites, good performance in wear behavior is expected to be reached as a result of self-lubricant of graphite property while friction and sliding of surfaces that turn out to be reduced the loosing of mass during the relative movement into a tribological system (Harrison and Perry, 1998). However, the physical presence of a layer of graphite while sliding aluminium/ graphite composite ould alter the frictional properties of the interface, in the same way, the chemical composition at the

interface could influence the modes of energy dissipation, so that, it could take lace some tribo-chemical reaction induced by the mechanical interaction of two sliding tribo-elements. Graphite is chemically stable, its low thermal expansion could allow the clamping effect due to the radial compressive stress of the aluminium matrix against the graphite particle (*Silvain et al.*, 2000) **[55,65,79,164,170].**

The researchers have found the active lubrication mechanism of phosphorus and doil compounds containing additives with aluminium. They have reported that phosphorus is not beneficial to reducing the wear of aluminium **[179,180]**.

The wear behavior of the composite aluminium alloy/graphite particles were improved as the particles size of the graphite was smaller and the volume distribution better as compared to insolated graphite particles. The particles size distribution of graphite could be controlled by cooling condition during solidification of molten of the aluminium alloy 356, which allowed the entrapment of the graphite particles sizes in their corresponding dendrite arm spaces size frozen during the structure growing. The unidirectional cooling during casting process had an effective entrapment of graphite particles even in the shape flakes **[55].**

This paper reports the dry sliding wear behavior of AA7075 aluminium/SiC_p composites fabricated by powder metallurgy technique. Five factors, five levels, central composite, ratable design matrix is used to optimize the required number of experiments. The wear test has been conducted in a pin-on-roller wear testing machine, under constant sliding distance of 1 km. An attempt has been made to develop a mathematical model by response surface method (RSM). Analysis of variance (ANOVA) technique is applied to check the validity of the developed model. Student's *t*-test is utilized to find out the significance of factors. The effects of volume percentage of reinforcement, particle size of reinforcement, applied load, sliding speed and hardness of counter part materials on dry sliding wear behaviour of AA7075 aluminium/SiC_p have been analyzed in detail **[83].**

Lo *et al.* **[95]** have reported that the Zinc-aluminium (Zn-Al) based alloys have found considerable industrial used. This is primarily due to their excellent fluidity, castability and good mechanical properties. The effects of systematic changes in matrix microstructure on crack initiation and growth toughness were determined on an A1-Zn-Mg-Cu alloy containing 0.15, 20% by volume of SiC particulates. Materials were heat treated to underaged (UA) and overaged (OA) conditions of equivalent matrix microhardness and flow stress. Although both the fracture initiation and growth toughness, as measured by J_{Ic} and tearing modulus, were similar for the unreinforced materials in the UA and OA conditions, significant effects of microstructure on both J_{Ic} and tearing modulus were observed in the composites. SEM and

TEM observations of fracture in the two conditions used to rationalize these observations in light of existing theories of ductile fracture propagation **[100,153,164].**

2.5.2.5 DRA heat treatment

Wang and Rack **[177],** reported that the abrasive wear performance of overaged 2124 Al-SiC, composites were slightly higher than for underaged composites, the hardness for over and underaged composites being the same. They ascribed this difference to the relaxation of the tensile stresses in the matrix and compressive stresses in the reinforcement induced by solution heat treatment during aging, the overaged state providing more effective stress relaxation than the under aged. Pan *et al.* **[111]** reported the same results during lubricated sliding. They attributed the better resistance of the overaged 2124 Al-SiC, composite to fewer dislodges of SiC particulates. The latter was proposed to be due to the change of the fracture path from the matrix-particulate interface in the peak and underaged composites to the alloy grain boundary in the overaged composite, which is in agreement with Wang and Rack's observations **[177].** Moreover embrittlement of the reinforcement-matrix interface through increased S'/S precipitation at the vicinity of the reinforcement has been observed to counterbalance the effect of stress relaxation and cause overaging to decrease the 2009-SiC, composite wear resistance **[146,184].** Therefore the effect of heat treatment and overaging on the 2xxx aluminum composite wear performance is governed by the competition of two mechanisms engineered by aging time increase, i.e. stress relaxation leading to better wear performance and reinforcement-matrix embrittelment leading to lower wear performance.

Matejka **[103]** has reported the effect of silicon carbide (SiC) on friction–wear properties of semi-metallic friction composites (FC). Semi-metallic FC with increasing content of silicon carbide (SiC: 0, 3.4, 5.6, 9 and 14.6 vol.%) were prepared and slide against cast iron disc and their friction–wear properties were evaluated. The friction coefficient (μ) was observed to increase with SiC content, nonetheless the highest content (14.6 vol.% of SiC) did not significantly increase its value. The volume wear rate (V) of tested friction composites slightly increases with SiC content and temperature. The character of friction layer was analyzed using scanning electron microscopy (SEM) with energy dispersive X-ray microanalysis (EDX) and the topography of friction surface was studied using atomic force microscopy (AFM). Two types of films assigned as film I and film II appearing on the friction surfaces of samples after friction test were observed. Film I originate on the friction surface of sample without SiC and is composed of debris of iron, iron oxide, stibnite and carbon. Film II is formed on the friction surface of composites containing SiC and in contrast to film I contain additional debris of SiC. They have also reported that the addition of SiC to formulation improves the volume wear rate

stability up to temperature 250 °C. Above this temperature the volume wear rate increases what can be attributed to loosing of the binding ability of phenolic resin and its easier abrasion.

Delamination of material layers adjacent to the worn surfaces is a commonly observed form of wear in unlubricated or poorly lubricated surfaces. In ductile materials, the delamination process usually involves large plastic deformation and subsurface damage. In this study, metallographic techniques have been used to determine the extent of plastic deformation and strain localization events during the sliding wear of annealed OFHC copper samples. Tests were performed using a block-on-ring type wear machine under constant load and constant velocity conditions. Subsurface displacement and microhardness gradients were measured as a function of sliding distance **[9].**

The effects of silicon carbide (SiC) particles on the as-cast microstructure and properties of Al–Si–Fe alloy composites produced by double stir-casting method have been studied. A total of 5–25 wt% silicon carbide particles were added. The microstructure of the alloy particulate composites produced was examined, the physical and mechanical properties measured include: densities, porosity, ultimate tensile strength, yield strength, hardness values and impact energy.. The results revealed that, addition of silicon carbide reinforcement, increased the hardness values and apparent porosity by 75 and 39%, respectively, and decreased the density and impact energy by 1.08 and 15%, respectively, as the weight percent of silicon carbide increases in the alloy. The yield strength and ultimate tensile strength increased by 26.25 and 25% up to a maximum of 20% silicon carbide addition, respectively. These increases in strength and hardness values are attributed to the distribution of hard and brittle ceramic phases in the ductile metal matrix. The microstructure obtained reveals a dark ceramic and white metal phases, which resulted into increase in the dislocation density at the particles–matrix interfaces. These results show that better properties are achievable by addition of silicon carbide to Al–Si–Fe alloy **[3,170].**

According to Abachi *et al.* **[4],** the wear resistance of the matrix alloy could be increased by incorporation of SiC particles. However, in some cases, decrease of the wear resistance has been experienced. The wear resistance does not increase monotonically with increasing the particle content. The increase of sliding distance causes more weight loss at a constant rate. The application of higher loads induces more wear on specimens. The sliding velocity increment has same effect on wear behavior of specimens. The sharp shape reinforcing particles are more easily pull out and machined away from the composites with high particles content. According to observations, in various sliding test conditions, the abrasive, oxidation and delamination are mostly operated in combination.

Akhlaghi *et al.* **[19]** found that an increase in flake graphite content reduced the coefficient of friction for both dry and oil impregnated sliding, but this effect was more pronounced in dry sliding. Hardness and fracture toughness of composites decreased with increasing flake graphite content. In dry sliding, a marked transition from mild to severe wear was identified for the base alloy and composites. The transition load increased with flake graphite content due to the increased amount of released flake graphite detected on the wear surfaces. The wear rates for both dry and oil impregnated sliding were dependent upon flake graphite content in the alloy. In both cases, Al/Gr composites containing 5 wt.% flake graphite exhibited superior wear properties over the base alloy, whereas at higher graphite addition levels a complete reversal in the wear behavior was observed.

2.5.2.6 Reinforcement volume fraction and spatial distribution

It has been recognized that an increase of hard ceramic reinforcement volume fraction improves the DRA wear performance during abrasion, fretting and sliding up to approximately 20 vol.% **[136,146],** except under some conditions in which the wear rate for reinforced and unreinforced are similar (e.g. for a certain range of applied normal load **[6,11,12,33,80]** and sliding velocity **[98,158,160,178].** For the case of dry sliding wear, Anand and Kishore **[13],** reported a wear performance improvement by natural alumina incorporation in Al-10 wt.% Zn up to 30 wt.% alloy, the wear rate increasing above 35 wt.% Zn. They proposed that the deterioration of wear resistance above this level was due to the reinforce metal-matrix interfacial area, which is the region of weaker cohesion and large stress concentration, which became excessive above 35 wt.% of reinforcement, optimum reinforcement content value being in the range of 25-35 wt.%.

It has been found a decreasing friction coefficient owing to reinforcement in an (Al-l.5 Mg)-SiC, with a friction coefficient of 0.63 for the unreinforced, 0.45 for the 12.5 vol.% SiC composite and 0.25 for the 15 vol.% SiC **[146].** However, the reduction of the friction coefficient by the reinforcement presence seems to be controlled by the sliding velocity; indeed, Martinez **[101]** reported higher friction coefficient for a 7091 Al-SiC, 20 vol.% (0.42) than in unreinforced Al 7091 (0.35) at low, 0.36 m s-l, velocity and they observed the opposite at high, 3.6 m s^{-1} velocity where the friction coefficient was of 0.5 for the Al 7091 alloy and of 0.35 for the Al 7091-SiC, composite. In the latter investigation, the authors observed a decreasing tendency of mass transfer and an increasing severity of grooving on the unreinforced counterpart disc surface with increasing SiC, volume fraction. They concluded that the operative wear mechanism changes from adhesion to abrasion owing to the presence of reinforcement. The same investigators noticed that increasing reinforcement volume fraction improved the DRA wear performance while increasing the unreinforced wear rate thereby

limiting the overall tribological performance of the DRA-steel couple. Studies on the microstructural aspects of friction and wear of DRA **[174,176]** indicated that the rule of mixtures or phenomenological wear laws such as Archard's law **[16]** cannot successfully predict the wear behavior of DRA and its metal counterpart because of the complexity of wear mechanism, occasioned by the introduction of hard dispersed phase in the system. Wang and Rack **[174]** proposed a statistical wear model which is based upon the fact that the reinforcement distribution is not perfectly homogeneous. Using the theory of random clumping **[145,146],** they proposed a statistical approach to model the wear rate of a single-phase metal sliding against a composite. This model predicts that the wear rate of the metal counterpart increases with increasing reinforcement volume fraction and is influenced by the degree of reinforcement clustering, in the case of unique particulate **[174]** and distributed particulate size. The degree of clustering is also expected to influence the DRA wear performance by providing preferential sites for crack nucleation **[17,66,69,94,145,146,181]** however, extensive investigation is needed to clarify this effect.

2.6 Wear

Wear is not a material property; however, it is a systems response. The wear rate of a material can vary from 10^{-3} to 10^{-10} mm^3/N-m depending on contact conditions, such as the counterpart material, contact pressure, sliding velocity, contact shape, environment and the lubricant . The wear rate changes through the repeated contact process under constant load and velocity **[77].**

Wear of metals is probably the most important yet at least understood aspects of tribology. It is certainly the youngest of the trio of topics, friction, lubrication and wear. To attract scientific attention, although its practical significance has been recognized throughout the ages, the findings of Guillaume Amontons in 1699 establishing scientific studies of friction are almost of 300 years age, while Petrov *et al.* brought enlightenment to the subject of lubrication a century ago in the hectic 1880s. Substantial Studies of wear can be associated only with the five decades that have elapsed since *R. Holm*, who explored the fundamental aspects of surface interactions encountered in electrical contacts. One third of our global energy consumption is consumed wastefully in friction. In addition to this primary saving of energy, very significant additional economics can be made by the reduction of the cost involved in the manufacture and replacement of prematurely worn out components. The dissipation of energy by wear impairs strongly the national economy and the lifestyle of most people. So, the effective decrease and control of wear of metals is always desired **[77,142].**Wear causes an enormous annual expenditure by industry and consumers. Most of this is in replacing or repairing equipment that has worn to the extent that it no longer performs a useful function. For many machine

components this occurs after a very small percentage of the total volume has worn away. For some industries, such as agriculture, 40% of the components replaced have failed by abrasive wear. Other major sources of expenditure are losses in production, consequential upon lower efficiency and plant shutdown. Estimates of direct cost of abrasive wear to industrial nations vary from 1 to 4 % of gross national product and Rigney has estimated that about 10% of all energy generated by man is dissipated in various friction processes. Wear is not an intrinsic material property but characteristics of the engineering system which depend on load, speed, temperature, hardness, presence of foreign material and the environmental condition. Widely varied wearing conditions cause wear of materials. It may be due to surface damage or removal of material from one or both of two solid surfaces in a sliding, rolling or impact motion relative to one another. In most cases, wear occurs through surface interactions at asperities. During relative motion, material on contacting surface may be removed, resulting in the transfer to the mating surface, or may dislodge as a wear particle. The wear resistance of materials is related to their microstructure, transformation may take place during wear process, and hence, it seems that in wear research emphasis is placed on microstructure **[169].** Wear of metals depends on many variables, so wear research programs must be planned systematically. Therefore, researchers have normalized some of the data to make them more useful. The wear map proposed by Lim and Ashby **[92]** is very useful in this regard to understand the wear mechanism in sliding wear, with or without lubrication.

2.6.1 Recent trends in metal wear

Much of the wear research carried out in the 1940's and 1950's were conducted by mechanical engineers and metallurgists to generate data for the construction of motor drive, trains, brakes, bearings, bushings and other types of moving mechanical assemblies **[113].** It became apparent during the survey that wear of metals was a prominent topic in a large number of the responses regarding some future priorities for research in tribology. Some 22 experienced technologists in this field, who attended the 1983 'Wear of Materials Conference' in Reston, prepared a ranking list **[113].** Their proposals with top priority were further investigations of the mechanism of wear and this no doubt reflects the judgments that particular effects of wear should be studied against a background of the basic physical and chemical processes involved in surface interactions. The list proposed is shown in **Table 2.8.**

Table 2.8 Priority in wear research [113,114]

Ranking	Topics
1	Mechanism of wear
2	Surface Coatings and treatments
3	Abrasive, adhesive, flow and fatigue wear
4	ceramic wear
5	Metallic wear: sliding wear
6	Wear with lubrication
7	Piston ring-cylinder liner wear
8	Corrosive wear
9	Wear in other internal combustion engines

Peterson **[114]** reviewed the development and use of tribo-materials and concluded that metals and their alloys are the most common engineering materials used in wear applications. Grey cast iron for example has been used as early as 1388. Much of the wear research conducted over the past 50 years is in ceramics, polymers, composite materials and coatings.

Wear of metals encountered in industrial situations can be grouped into categories shown in **Table 2.9.** Though there are situations where one type changes to another or where two or more mechanism plays together.

Table 2.9 Types of wear in industry [113, 114]

Type of wear in Industry	Approximate percentage involved
Abrasive	50
Adhesive	15
Erosion	8
Fretting	8
Chemical	5

2.6.2 Theory of wear

Adhesive wear with low to moderate wear rates usually predominates at lower sliding speeds and forces; opposing asperities bond together and later break at different spots, generating tiny wear particles. If conditions intensify, more severe wear can be activated. With abrasive wear, hard particles from earlier wear events and/or the environment become entrapped within the sliding interface and cut or plow the surfaces. Large loads at high speeds may induce thermal mounds, wherein heat generated by friction and electric currents (if present) elevate local temperatures and bulge material near the contact spots. Faster growing bulges separate less dominant neighbors, transferring and further concentrating loads. Temperatures, stresses, and thermal expansions increase, promoting loss of large particles **[32].**

Wear testing is a time consuming process, as the test has to be repeated with different sliding distance until a steady state wear condition is achieved. Furthermore, it may also be difficult to

judge correctly whether a steady-state wear condition has actually been attained. The wear volume versus distance curve can generally be divided into two regimes, the transient wear regime and the steady-state wear regime. The standard wear coefficient value obtained from a volume loss versus distance curve is a function of the sliding distance. Due to the higher initial running-in wear rates, it has a higher value initially and will reach a stead state value when the wear rate becomes constant.. This is because the standard method to calculate the wear coefficient is to make use of the total volume loss and the total sliding distance covered. However, it is obvious that the standard wear coefficient value obtained would be higher if the sliding distance covered remains within the transient wear regime. On the other hand, excessive distance would also damage the wear track to give a higher wear coefficient. Hence, it is no surprising that wear coefficient values obtained from different investigators have been found to vary significantly up to a deviation of 1000%. As there is a lack of a standard test method available for the determination of the wear coefficient of a wearing pair, it is high time to look into it. Standard testing practice tends to perform the wear test only in the so-called "steady-state" region without knowing exactly where the steady-state regime is located. Hence, under-tested condition or over-tested conditions are often used **[186].**

2.6.3 Wear mechanisms

Wear mechanisms may be briefly classified by mechanical, chemical and thermal wear whose wear modes are further classified into seven subtypes. Some of them have mathematical expressions of wear rate, but many of them lack satisfactory wear models and wear equations for reliable predictions **[71,77,86,104,105,173].**

2.6.3.1 Classifications of wear mechanisms

Rolling wear, sliding wear, fretting wear and impact wear are terms often used in practice and in papers. They are useful to describe the type of friction required to generate wear; however, they do not describe possible wear mechanisms. Mechanical wear, chemical wear and thermal wear are terms used to describe wear mechanisms briefly with scientific expressions.

2.6.3.1.1 Mechanical wear, chemical wear and thermal wear

Mechanical wear

Mechanical wear describes wear mainly governed by the processes of deformation and fracturing. The deformation process has a substantial role in the overall wear process of ductile materials, and the fracturing process has a major role in the wear process of brittle materials.

Chemical wear

Chemical wear describes wear governed mainly by the growth rate of a chemical reaction film. The growth rate of the film is accelerated mechanically by friction. Therefore, chemical wear is also called tribo-chemical wear.

Thermal wear

Thermal wear describes wear governed mainly by local surface melting due to frictional heating. Diffusive wear is also included in the term thermal wear, since it becomes noticeable only at high temperature. The wear of brittle materials caused by thermal shocks, and fractures, may also be included in thermal wear.

These three descriptions of wear are necessary to characterize wear broadly; however, they are not sufficient to develop wear models for wear rate predictions.

2.6.3.1.2 Abrasive, adhesive, flow, fatigue, corrosive and melt wear

Abrasive, adhesive, flow and fatigue wear are more descriptive expressions for mechanical wear, and their wear processes are shown in fig. 2.1a, 2.1b, 2.1c and 2.1d respectively.

Abrasive

The abrasive wear of ductile materials is shown in fig. 2.1a **[77]**. Three-dimensional wear models of scratching against a hard asperity have been proposed and confirmed through quantitative agreements between experimental results and theoretical predictions. The wear volume V is given by

$$V = \alpha\beta \frac{WL}{H}$$

where W is the load, L the sliding distance, H is the hardness, α the shape factor of an asperity and β the degree of wear at one abrasive asperity. Experimentally, α takes a value of about 0.1 and β varies between 0 and 1.0, depending on the value of the degree of penetration of an abrasive asperity, the shear strength at the contact interface and the mechanical properties of the wearing material.

Adhesive wear

As for the adhesive wear of ductile materials, shown by Fig. 2.1(b) **[77,187]**, no predictive theories have been quantitatively confirmed by experiments. Assumptions have been made dealing with the unit volume of wear particles removed from the unit contact region, but they do not agree well enough with experimental data to give a basis for a quantitative theory. Wear equations for adhesive wear are given by the following equation, which are similar to equation (1):

$$V = w_s W L \qquad (1)$$

Where specific wear rate, $w_s = \alpha\beta H_v$

Experimental results for adhesive wear show that the wear volume increases almost linearly with the load and sliding distance. However, useful physical models were not found to explain the observed values of w_s and K, where w_s varied from 10^{-2} to 10^{-10} $mm^3/N\text{-}m$.

Flow wear

As for flow wear, as shown by fig. 2.1(c) **[77,113,114],** experimental observations of steel are explained well by a theoretical model, called 'ratchetting', and the wear coefficient, K is given as a function of the plasticity index, surface roughness and friction coefficient. Although the mechanism of flow wear is similar to that of low cycle fatigue, crack initiation and propagation are not necessary to produce wear particles, and plastic flow is the major part of wear generation. The question of whether the wear of butter -like tribofilm covering a hard substrate could be treated as another form of flow wear still remains unanswered.

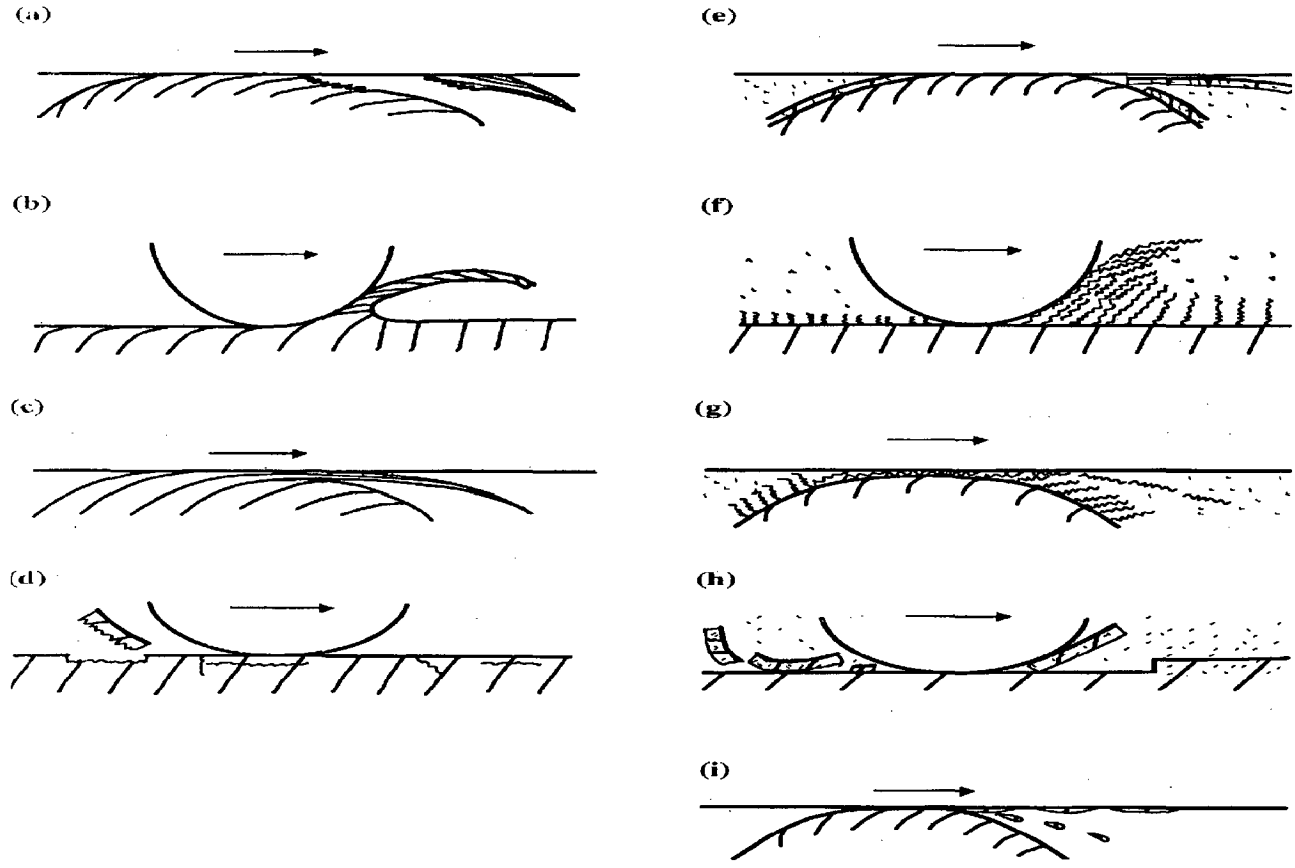

Fig. 2.1 Schematic wear modes: 2.1a) adhesive wear by adhesive shear and transfer, 2.1b) abrasive wear by microcutting of ductile bulk surface, 2.1c) flow wear by accumulated plastic shear flow, 2.1d) fatigue wear by crack initiation and propagation, 2.1e) corrosive wear by shear fracture of ductile tribofilm, 2.1f) corrosive wear by shaving of soft tribofilm, 2.1g) corrosive wear by accumulated plastic shear flow of soft tribo film, 2.1h) corrosive wear by delamination of brittle tribo film, 2.1i) melt wear by local melting and transfer or scattering [77].

Fatigue wear

In the case of fatigue wear, predictions of high cycle fatigue wear were first made. It is generated by crack initiation and propagation as shown in fig. 2.1d, in a repeated contact stress

cycle. Stress conditions are assumed to be either elastic or elasto-plastic. Wear particle shape or unit wear volume is decided, therefore, by the path of crack propagation. The critical number N_f of rolling cycles for surface spalling by high cycle fatigue in a steel ball bearing is experimentally given by the following equation:

$N_f = bW^{-n}$ where

W is the load and b and n are experimental constants **[77].** The value of n is 3 for ball bearings. Its basic premise is that spalling can be treated as a statistical fracture phenomenon following the theory of Weibull.

Corrosive wear

In the situation of corrosive wear, thin films are assumed to form through a tribochemical reaction between contact surface materials and the surrounding media, such as air or a liquid lubricant. A hard tribo-film such as an iron oxide film on steel and a soft tribo film such as a silica gel film on Si_3N_4 in water or a ZDDP reaction film in oil are expected to be worn by the forms of figs. 2.1e) and 2.1f) for the former and by figs. 2.1g) and 2.1h) for the latter **[77].**

Melt wear

The evidence that melt wear, fig. 2.1i), exists is obtained by observing spherical wear particles of unique surface morphology and by observing a wear surface partially covered by droplets or a film on the smooth surface. This wear mode is not considered as a dominant steady wear mode in general tribo-elements; however, it is generated by unexpected contact conditions, such as hard inclusions at the contact interface or a sudden overloading due to vibration.

High wear resistance is an attribute frequently ascribed to metal matrix composites and is of clear importance to the designer is considering both the use of these materials in some applications and in selecting the machining processes which can be employed to fabricate components. Sliding wear of metal matrix composites is important wherever there is relative motion, either deliberate or unintentional. If hard particles are present in the system, for example, as contamination in a lubricant or intentionally in abrasive machining, then the abrasion resistance of the material may be relevant **[70,72].**

2.7 Requirements and characteristics of friction materials

The basic requirements of friction materials which are used in brakes of different vehicles are similar i.e. they should posses high coefficient of friction (COF), stable COF under wide ranges of speed, pressure and temperature, low wear rate, good thermal conductivity to dissipate heat, good strength to withstand high pressure and temperature rise during braking, negligible wear of the opposing member, fabricabilty and low cost **[18,81,157].** Therefore, these essential requirements of friction materials are briefly discussed below.

(i) Coefficient of friction is essential for efficient braking. Higher value is desirable.

(ii) The coefficient of friction may vary with rise in temperature, speed and applied pressure of the moving surface and remain constant under different climatic conditions encountered in service. Stability of the coefficient of friction over the temperature range is known as fade resistance and hence brake fade should as minimum as possible.

(iii) Good thermal conductivity results in better resistance to heat flow and hence it solves problems at higher temperature at the braking surface; conduction of the heat towards the interior tends to minimize warpage of pressure plates, or other parts of the assembly. This may results in faster heat dissipation.

(iv) Good strength levels; where the friction materials are subjected to complex state of stresses in which compressive, shear, tensile, fatigue, centrifugal forces or any other stresses encountered during service. Hence, the friction materials should have good mechanical strength to withstand these stresses.

(v) Good wear resistance: This decides the life of the component. It is in this attribute that powder metallurgy products have excelled over other materials.

(vi) Further, friction materials should also possess other properties like resistance to score, gall & ablation, proper energy capacity, proper engagement characteristics, good thermal properties, high heat capacity, adequate durability, fabricability or formability, negligible wear of the opposing member and safe use.

(vii) Environmentally sustainable and

(viii) Minimum cost.

2.8 Selection and applications of friction materials

Selecting the perfect brake lining for a heavy-duty brake application is very important to ensure that the vehicle can be stopped. The perfect brake lining will need to have an appropriate coefficient of friction that will remain constant for the life of the vehicle under all operating conditions of speed, braking pressure, vehicle load, temperature, and humidity. The perfect lining would not score or wear the drum, should not be subject to vibration and noise, should wear slowly, and should not have an offensive odor while operation. The selection of lining is a balance of all these factors and will depend on the service that the brake will be subjected to during its useful life [SAE, Brake Bible, **196**].

Lining fade is the inability of friction material to maintain its normal effectiveness when it is forced to work at elevated temperatures. This is called "heat fade" and is the result of reduced coefficient of friction as the brake temperatures increases. Fade resistance is another feature of high performance pads. Brake fade can be caused by the out-gassing of the pad that creates a

boundary layer of gases between the pad and rotor. Recovery is the rate at which the lining returns to its original friction level after having been exposed to a fade condition.

Recovery is typed as normal recovery, slow recovery, or over recovery. Most desired is normal recovery in that it will return to its pre-fade friction level with very little temperature reduction.

Speed Sensitivity is the measure of a lining's ability to maintain its coefficient of friction at different rubbing speeds. The friction level of most friction materials is reduced with increasing speed.

Brake Noise is a vibration in the brake system whose frequency is in the normal hearing range. Low noise levels leads to better engagement characteristics.

Brake wear is a cost of operation consideration. The best lining will have minimum wear at low to normal operating temperatures and only a modest increase in wear rate at elevated operating temperatures. All of these mentioned terms are to be considered for selection and type of application in automobiles or aircrafts **[132,133].**

2.9 Manufacturing technologies for friction materials

Conventional manufacturing technology of making composite friction materials are briefly described here. However, methods pertaining to its modifications, alterations, improvements etc. from the existing technique and the new solutions or production techniques for making such materials are not included / covered here.

2.9.1 Manufacturing technique for organic type friction material [157]

Steps involved are as follows

i) Dry mixing

ii) Hot pressing

iii) Post curing

iv) Finishing

Dry Mixing: Mixing is carried in plough shear-type mixer to ensure macroscopic homogeneity at a chopper speed of 3000rpm. The mixing sequence involves feeding of all the powdered ingredients, then the metallic additives, inorganic and organic fibers. Glass fibers are added last to minimize fiber damage and to open up the strands to provide mechanical isotropy to the mixture. The mixing duration will vary according to powder characteristics, type, size etc. but here it is 5min.

Hot pressing: The mixture is then placed into a four-cavity mould supported by adhesive-coated back plates. Each cavity is filled with constant quantity of the mixture and then heat cured in a compression-moulding machine at different temperatures under a pressure of 0.5-15 MPa for 10-12 min at 150 °C-250 °C for 10-30 minutes. The temperature, time and pressure

vary according to materials (or ingredients) added, its bonding and other characteristics and are carefully chosen.

Post curing: There intermittent breathings are also allowed during the initiation of curing to expel volatiles. The pads are then removed and post-cured in an oven at 100 °C-350 °C for 1-10 hrs. to relieve the residual stresses.

Finishing: Finally, finishing operation is done by grinding, sizing etc. Thus surfaces of the pads are polished with a grinding wheel to attain the desired thickness and to remove the resinous skin **[34, 61].**

The above said four steps are same for NAO type whereas for semi-metallic type friction materials only hot pressing & curing temperature and time are slightly varied.

2.9.2 Manufacturing techniques for sintered friction materials [157,183]

The metal powders namely matrix which provide the basic strength, must possess a high degree of sinterability. Because addition of non metallic (ceramic/organic) ingredients tends to reduce the sinterability of the powdered mixture. They should also form a sufficiently stable structure. For this reason spongy and dendirtic powders with particle size below 150um are preferred since they have high surface area. Spongy iron powders which are produced by reduction of oxides are mainly used for Iron based friction materials. For copper based material electrolytic powder is used. Further, copper alloys like brass, bronze are also used since they form transient liquid phase during sintering. Mixing should be done carefully.

Friction materials are composite materials consisting of metallic and nonmetallic constituents. Their manufacturing is not possible by the conventional liquid metallurgy/P/M route in which miscibility plays the dominant role. This limitation can be overcome by using powder metallurgy technique in which different powders can be mixed irrespective of their miscibility limitations. The composition and final properties can be controlled by powder metallurgy route as different metallic and nonmetallic constituents otherwise immiscible can be properly blended in powder form to develop properties desired.

In sintering technique, following are the basic steps for production of friction components:

(i) Preparation of powders,

(ii) Blending of the components,

(iii) Compaction of the performs of friction components,

(iv) Sintering the compacts under pressure in a protective atmosphere and

(v) Finishing operations (polishing, groove cutting etc.) **[18]**

The finishing operation will be same for the elements either prepared by sintering technique or hot forging technique.

All powders are screened through a sieve of required mesh size before mixing since many of the powders tend to agglomerate and this is most undesirable. Mostly fine size powders are preferred to achieve uniformly distributed microstructures. Mixing can be carried out in many ways. Generally this is carried out in conventional equipment such as double cone or V- cone blenders or ribbon type mixers. But using pot mill mixer is very much beneficial because in mixing itself we can achieve homogeneous distribution of different elements at room temperature, without need of protective/inert atmospheres.

Mechanical alloying (MA) is a powder metallurgy processing technique involving cold welding, fracturing, and re-welding of powder particles in a high-energy ball mill and has now become an established commercial technique to produce oxide dispersion strengthened (ODS) nickel and iron-based materials. MA is also capable of synthesizing a variety of metastable phases, and in this respect, the capabilities of MA are similar to those of another important non-equilibrium processing technique, viz., rapid solidification processing (RSP). However, the "science" of MA is being investigated only during the past 10 years or so. The technique of mechano-chemistry, on the other hand, has had a long history and the materials produced in this way have found a number of technological applications, e.g., in areas such as hydrogen storage materials, heaters, gas absorbers, fertilizers, catalysts, cosmetics, and waste management **[163].**

Compaction is done in a large hydraulic press. Iron based materials are compacted in the pressure range of 400 to 800 MPa. Copper based materials are compacted in the pressure range of 150 to 300 MPa.

The porosity is effectively removed when the total strain equals the net compressive strain. The strain profiles that develop in the truncated cones are largely independent of the processing temperature and the strain rate although the strain required for pore closure increases as the forging temperature is reduced. This suggests that the microstructure and the strain rate sensitivity may also be important factors controlling pore behavior **[41].**

Aleksandrova *et al.* **[5]** have reported that certain combination os sintering conditions (temperature, pressure, and duration of holding during sintering) enable specimens of MK-5 friction material to be produced having the same density and strength characteristics with different matrix structures.

Sintering is carried out in a number of ways like pressure-less sintering, sintering under pressure, liquid phase sintering, electric discharge, electric arc sintering, microwave sintering, double sintering with intermediate repressing, sintering in conjunction with supplementary heat

treatment, etc. The backing plate can be joined with friction element either by brazing or welding, or by sintering the two components together under pressure.

The sintering temperature of the copper based components is usually in the 650 °C to 900 °C range and in the case of the iron based ones; it is the 1030 °C to 1070 °C. The sintering time of the friction components depends on the chemical composition of the material and the required final density. In the case of the copper-based components it varies from 15 to 20 minutes up to 4 hrs, and in case of iron based components, it amounts to 3 to 4 hrs. Sometimes, raising the sintering time and temperature increases the wear of iron-phosphorous base materials and slight increment in friction; pressure applied during sintering has no effect upon the wear of the material but results in higher coefficient of friction **[80,118].**

During sintering, the stack of disc is subjected to a load using hydraulic, pneumatic, or mechanical devices. For copper base products, the pressure amounts to 0.5 to 1.0 MPa and for iron-base components it amounts to 1.0 to 1.5MPa. The sintering operation is carried out in a protective atmosphere under pressure in conveyer furnaces or in special continuous furnaces in which the shaft is positioned vertically so that the pressure can be applied on the pile of discs.. Iron base materials can be heat treated for improving the properties of the layer. Annealing is carried out at 900 °C for decreasing the hardness of the friction layer. Quench hardening is conducted at a temperature 900 °C to 950 °C in oil or hot water followed by tempering at 500 °C.

Figs. 2.2 and 2.3 are the illustrative flowcharts for manufacture of copper and iron based brake pads respectively, employing sintering technology.

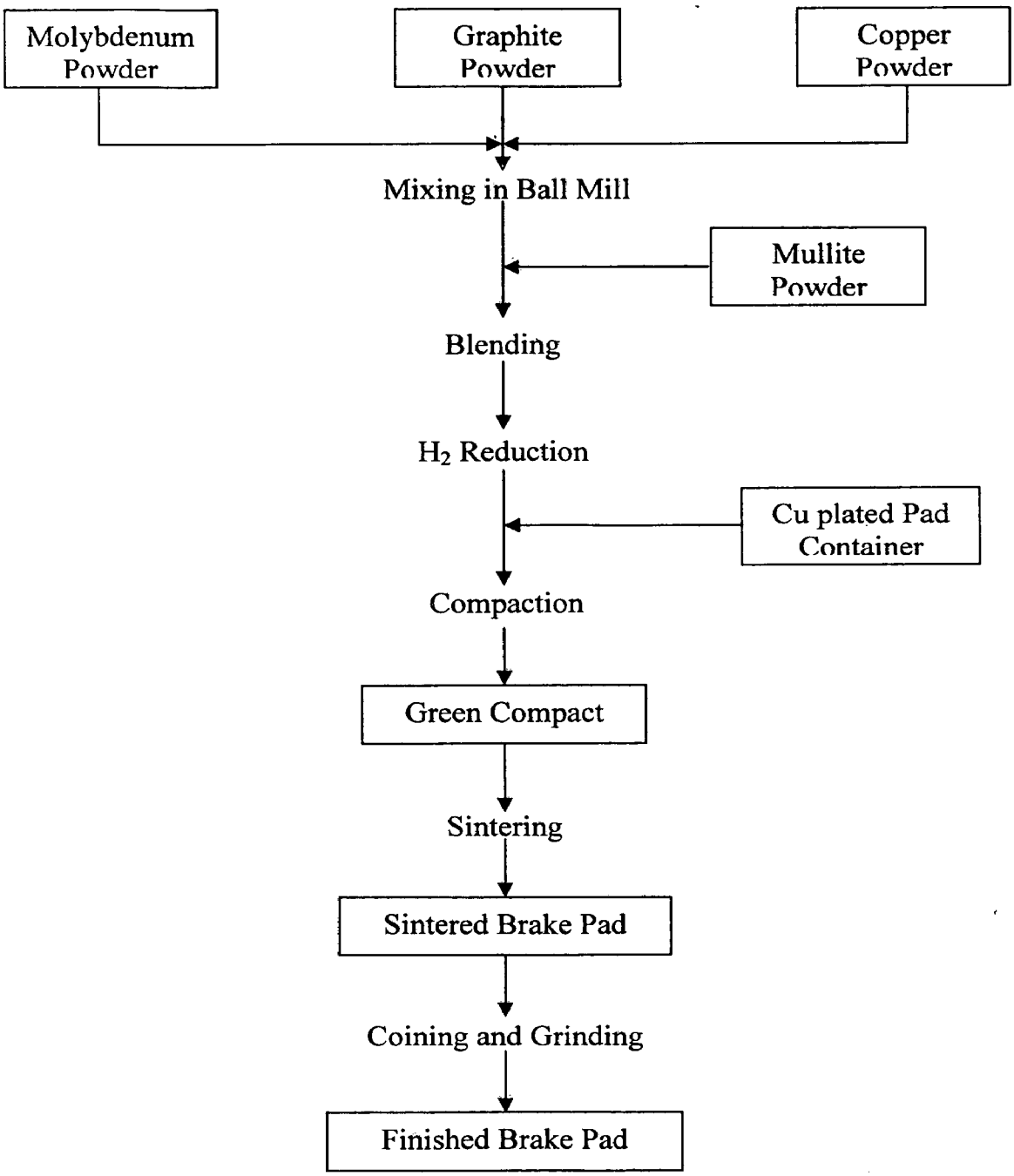

Fig. 2.2 P/M process for the manufacture of copper based brake pads **[113, 157]**

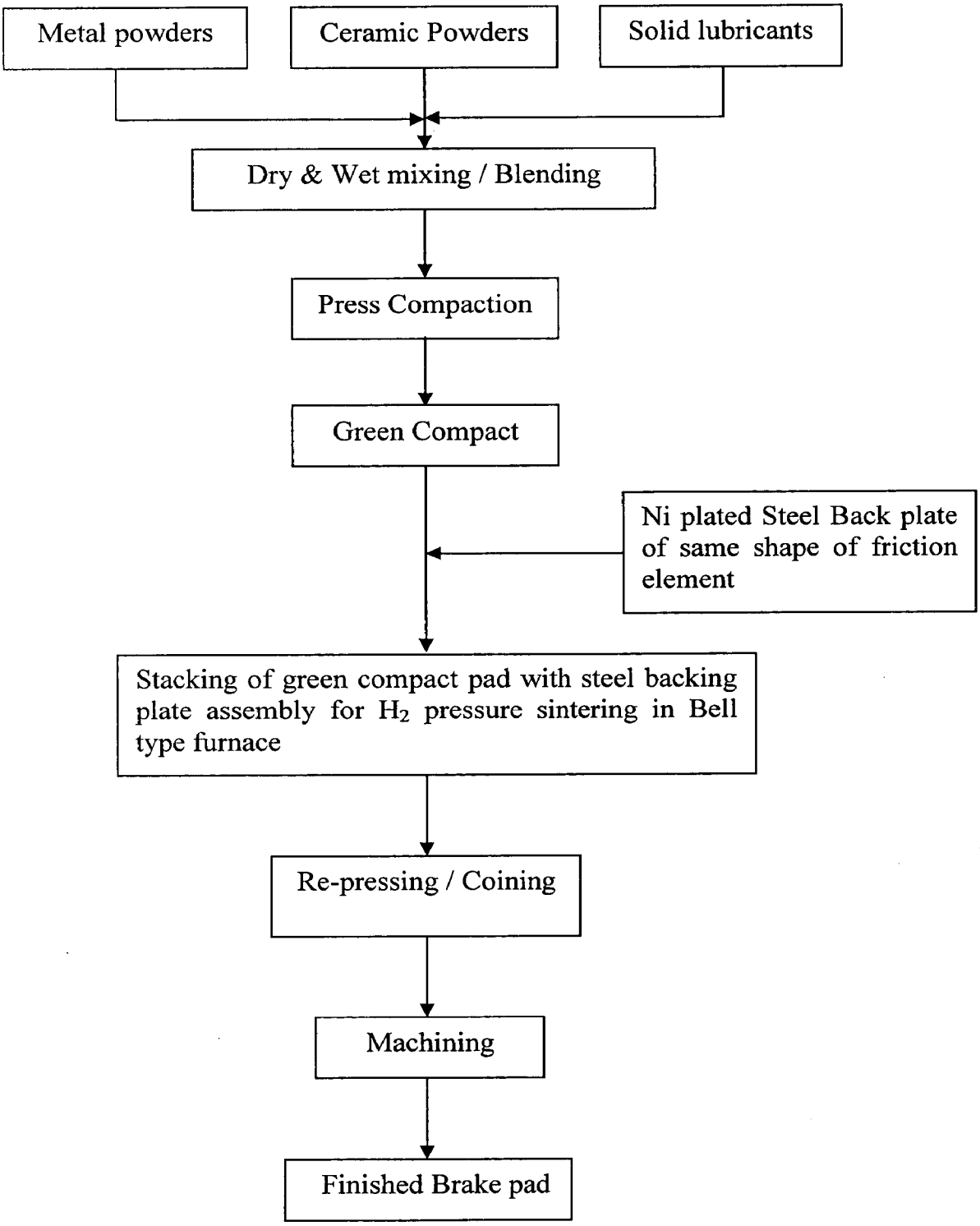

Fig. 2.3 P/M process for the manufacture of iron based brake pads **[113,157]**

2.9.3 Manufacturing technique for Carbon/Carbon friction materials

These materials are also produced by compacting and sintering route but containing predominantly graphite based powder. The friction and mating part both are graphite based and are essentially lubricating type of materials with very low coefficient of friction. These are excellent friction materials for heavy duty applications due to high temperature stability of

ceramic graphite. However, this type of friction materials is beyond the scope of the present investigation **[RR1].**

2.10 Characterization of friction materials

The different characteristics of friction materials namely physical, frictional, metallurgical and thermal properties are briefly described below.

2.10.1 Physical properties

The physical properties and microstructures of grey cast iron and AMCs are mentioned below (shown in **Table 2.10**, figs.2.4(a) and fig.2.4(b) where graphite flakes in former and composite phase in latter are visible **[61,67,157].**

Table 2.10 Physical properties of gray cast iron and AMCs [157]

Physical properties	Grey Cast Iron	A 356 Al alloy + 30% SiC
Density ($\times 10^3$ kg/m^3)	7.2	2.85
Specific heat (J/g K)	0.498	1.027
Thermal conductivity (W/m-K)	47.3	148.1
Coefficient of thermal expansion at 50–100°C (10^{-6} K^{-1})	12.6	17.4
Hardness (kg/mm^2)	80 ± 10	98.4 ± 2.4

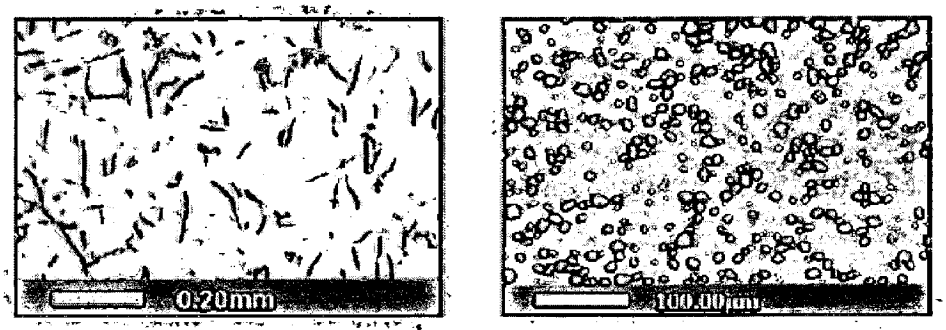

Fig.2.4. Microstructures of two counter discs: 2.4a) Gray cast iron 2.4b) Al-MMC.

2.10.2 Thermo-mechanical properties

Conventional heat conducting materials for base plates (Cu, Al) do not meet the requirement of having a sufficiently low coefficient of thermal expansion. The limitations of conventional materials have led to tailoring of the properties by development metal matrix composites (MMCs), particularly, Al matrix composites containing high volume fractions of SiC-particles (Al/SiC). Al/SiC metal matrix composites exhibit thermal expansion coefficients between 6 and 10 ppm/K, the Young's modulus is 160–210 GPa and the thermal conductivity varies between 180 and 210 W/mK, all depending on the matrix alloy, the volume fraction of SiC, and the temperature **[68].**

2.10.3 Metallurgical properties [68]

Figs. 2.5 (a) and 2.5(b) are optical micrographs of composite 1 and composite 2, respectively, with isolated SiC particles of different particle size classes. The SiC particles in composite 1 are not distributed uniformly owing to particle pushing during solidification. They are found embedded into the Al–Si-eutectic between the dendritic arms of the α-Al phase. The SiC-particles as well as the eutectic Si seem uniformly distributed in composite 2. In composite 3 and 4 (figs. 2.5(c), 2.5(d)), SiC particles of tri-modal size distribution are densely packed. A volume fraction of voids in the range of 1–2 vol% was found in the densely packed composites 3 and 4. The porosity has been determined by image analysis of inverse backscattered electron SEM images. The same value was determined from the difference in composite density (measured by Archimedes' principle) and the calculated density by the rule of mixtures with the determined reinforcement volume fraction. Such porosity has been visualized by high resolution synchrotron computed tomography.

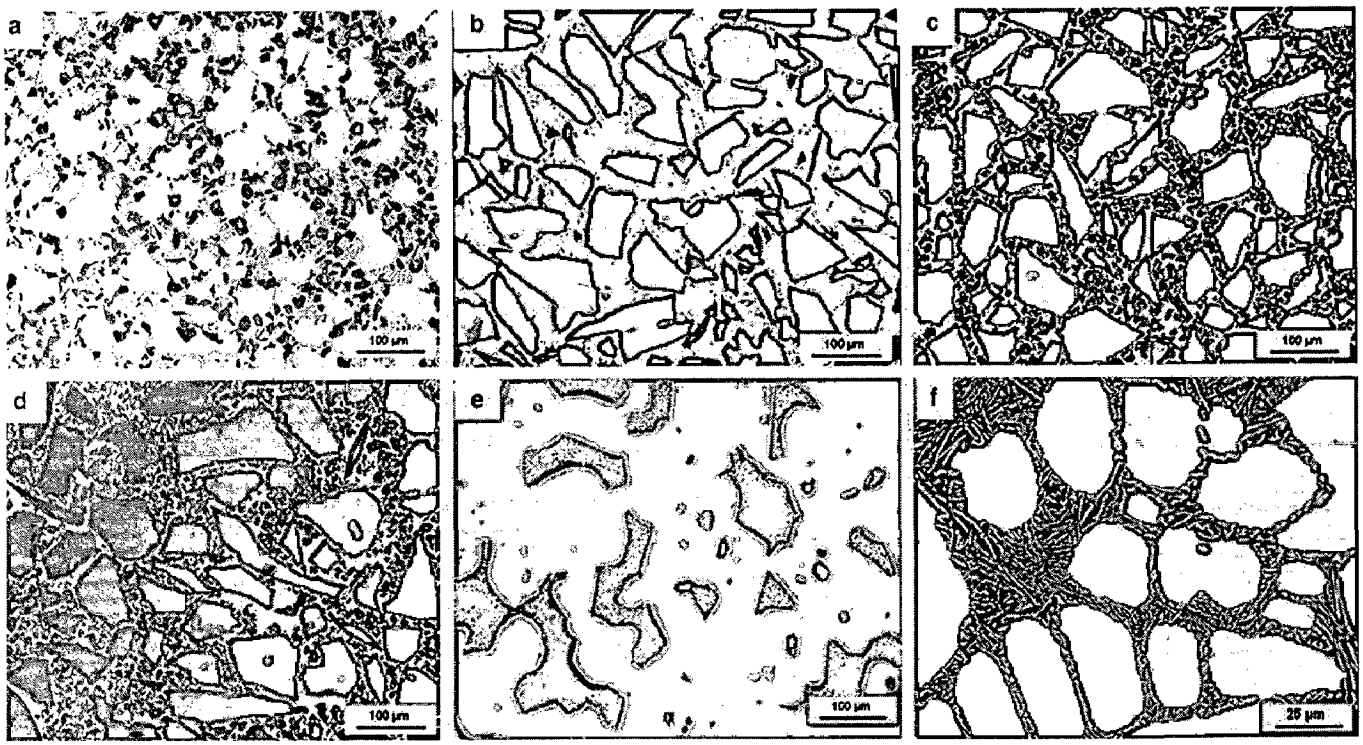

Fig. 2.5 Optical micrographs of Al/SiC composites: 2.5a) composite1-A359/SiC/10p, 2.5b) composite2-AlSi7Mg/SiC/55p 2.5c) composite3-AlSi7Mg/SiC/70p 2.5d) composite4 -Al99.5/SiC/70p, 2.5e) composite5-AlSi7Mg/R-SiC/85 and 2.5f) SEM image of AlSi7Mg showing the bright Si in the Al–Si eutectic **[68].**

The micrograph of composite 5 (fig. 2.5(e)) shows the sintered SiC structure (85 vol% SiC), the open pores of which are infiltrated with AlSi7Mg. Closed pores within the SiC structure remain empty. Fig. 2.5(f) depicts the hypoeutectic microstructure of the AlSi7Mg alloy imaged by SEM. Close inspection of optical micrographs of Al/SiC with an AlSi7Mg alloy matrix

(composite 3, fig. 2.5(c)) reveals Si segregations (little darker than Al) between the SiC particles. After the dendritic solidification of the α -Al-phase of the matrix alloy, the remaining eutectic liquid (containing 12.6 mass % Si) tends to freeze around the particles .The SEM micrograph of composite 3 in fig. 2.5, where the α -Al-phase has been removed by deep etching, visualizes the ''Si-bridges'' between the SiC particles forming a percolating ''SiC–Si-network''. Of course, such Si bridges do not exist in composite 4 formed by pure Al matrix.

2.10.4 Recycled automotive components

Aluminium has been recycled since the days it was first commercially produced and today recycled aluminium accounts for one-third of global aluminium consumption worldwide. Recycling is an essential part of the aluminium industry and makes sense economically, technically and ecologically. Currently, aluminium is used for structural, automotive components and aerospace fuselage. The others main markets are engineering, packaging and building. The use of aluminium in transportation sector especially for automotive applications is expected to grow in Malaysia for the future years. There is a possibility remelting recycled aluminium from automotive component and combined with reinforcement to produce aluminium matrix composite with better desired mechanical properties. Aluminium matrix composites reinforced with ceramic particulate are well known for their higher specific modulus, strength and wear resistance as compared with conventional alloys. One of the major driving forces for the technological development of aluminium matrix composites reinforced with ceramic particles is a result of these composites posses superior wear resistance and is hence potential candidate materials for a number of tribological applications. Applications in which materials are subjected to mechanical wear include pistons and cylinder liners in car engines and automotive disk brakes in vehicles. Aluminium based metal composites offer a very useful combination of properties for brake system applications in replacement of cast iron. Specifically, the wear resistance and high thermal conductivity of aluminum metal composites enable substitution in disk brake discs and brake drums, with a significant weight savings on the order of 50 to 60%. The weight reduction will reduce the inertial forces thus providing an additional benefit in fuel economy. In addition, lightweight metal composite brake discs provide increased acceleration and reduced braking distance. It is reported that, based on brake dynamometer testing, metal composite reduce brake noise and wear, and have more uniform friction over the entire testing sequence compared to conventional commercial cast iron brake disc. A number of automobiles now use MMC brake components. The Lotus Elise used four discontinuously reinforced aluminium brake discs per vehicle from 1996 to 1998, and the specialty Plymouth Prowler has used DRA in the rear wheels since production started in 1997. Discontinuously reinforced aluminum brake discs are particularly attractive in lightweight

automobiles and are featured in the Volkswagen Lupo 3L and the Audi A2 **[102].** In addition, a number of electric and hybrid vehicles, such as the Toyota RAV4, Ford Prodigy, and the General Motors Precept, are reported to use MMC brake components. Previous researches related to the recycled aluminium composites were such as recycled aluminium matrix composites reinforced with Inconel 601 fibres, recycled of AlSiMg–SiCp composite, recycling of aluminium alloy and aluminium composite chips AA6061/Al2O3 and recycled aluminum-alloy scrap with Saffil ceramic fibers. There is no research concerning aluminium composite from the combination of recycled engine block and SiC particle. The objective of this research is to fabricate the aluminium composite brake disc by using the recycled aluminium engine blocks with the addition of commercial SiC particles **[102].**

2.10.5 Frictional properties

The coefficient of friction is probably the most important single property of a facing material, but its application to the design of working assemblies requires careful interpretation. The data quoted in the **Table 2.11** below are determined under standardized conditions. A new specially designed equipment for evaluating tribological performance of ceramic-based composites for braking applications were developed. As the conclusion from the author, if the speed increases wear rate of the sintered iron increases **[157].**

Table 2.11 Properties of some sintered friction materials

Type	Grade No	Coefficient of friction				Permissible facing pressure		Typical applications
		Dynamic		Static				
		Oil	Dry	Oil	Dry	Oil, psi	Dry, lb/in^2	
Bronze	Durasint S1	0.08	0.31	0.16	0.29	75-600	50-300	Main drive, steering & powdershift clutches
Bronze-ceramic	Durasint S14	-	0.35	-	0.48	-	50-250	Heavy duty dry industrial clutches
Bronze-graphite	Durasint S73	-	0.21	-	0.23	-	30-300	Torque limiting and safety clutches (dry)
Bronze	Ferodo SM1	0.07	0.31	0.11	0.37	100-500	50-300	Main drive, steering & powdershift clutches
Bronze	Ferodo SM6	0.09	-	0.11	-	100-500	-	Automatic transmission, power and steering clutches in oil
Iron-ceramic	Durasint S92	-	0.39	-	0.45	-	30-500	Disc brakes and dry main drive clutches
Iron-graphite	Durasint S210	-	0.30	-	0.30	-	25-150	Dry main drive and steering clutches

2.11 Calculations for sub-scale dynamometer test parameters

2.11.1 Input parameters [147, 157]

Energy absorbed per brake stop (E_s):

The kinetic energy absorbed per stop (E_s) and the resulting heat produced in the friction material is the major factor influencing brake service life.

i) The following formulae are used to calculate the kinetic energy absorbed by the brake per stop (Es).

ii) For a caliper brake, the kinetic energy absorbed by the brake per stop is given by, $Es= WR^2N^2 / 5872$, where E_s = energy absorbed per stop, ft. lb (N.m); W = weight of body stopped,R =radius of gyration, ft (m);N = number of turns to stop

iii) The kinetic energy absorbed is also calculated by, $Es=½ I \omega^2$,where I = inertia, (provided by the machine builder),ω = angular velocity = $2\pi N/60$

iv) Kinetic Energy = CWV^2, ftlb, according to [MIL W 5013],where C = 0.032 for nose wheel of aeroplanes and for all helicopters, C = 0.026 for tail wheel airplanes, W = weight of aircraft in pounds under the loading conditions, V = power-off stalling speed of the aircraft in mph at the weight W(a speed of 40 mph shall be used for helicopters, unless otherwise specified).

v) The rotational speed of tire is the same as that of the brake where it is fitted. Thus, the speed (rpm) can be estimated from the vehicle speed at the time of application of brakes. For example, if the landing speed of aircraft is 280km/hr, brakes are applied say at 240km/hr, correspondingly the speed in rpm is ((240x1000)/60)/πD, where D is wheel diameter for the vehicle.

vi) Brake force / brake pressure is strongly dependent on vehicle design specifications; the number of brake cylinders, stroke length, and diameter of piston will determine the brake force/pressures.

The kinetic energy, rotational speed, brake force/pressure as estimated above, are set as the testing input parameters for sub scale inertia dynamometer test of the brake pad material/element **[157].**

2.11.2 Output parameters [147, 157]

i) The brake torque,T = 5250 PK /s, lb.ft (N. m),where, T = brake torque which the brake handles,P = hp absorbed (kw),K = a safety factor between 1.5 and 5 as the duty cycle of the brake increases,s = brake rotation speed, rpm; i.e. P= 5kw, K=5, s=3600rpm then T = 5250 (5) (5) /3600 = 36.46 lb.ft (49.4 N.m)

ii) The average brake torque required to stop the vehicle load, $T_a = Wk^2n / (308t)$, lb ft, where, T_a = average torque required to stop the load, Wk^2 = Inertia, load including brake rotating member, lb.ft^2 (kgm^2), W = weight of body stopped, lb (kg), k = radius of gyration, ft (m), n = shaft speed prior to braking, rpm, t = required or desired stopping time, s, i.e. example, T_a = (200) (1800) / [308 (40)] = 29.2 lb.ft. or 351 lb.in (39.7 Nm).

A service factor varying from 1.0 to 4.0 is usually applied to the average torque to ensure that the brake is of sufficient size for the load. Applying a service factor of 1.5 for this brake yields the required capacity = 526 in.lb. (59.4 N.m)

iii) No. of Revolutions prior to stopping, run down revolutions $R_s = (tXn) / 120$, where, R_s = number of revolutions prior to stopping; other symbols as given above; for example, R_s = (40) (1800) / 120 = 600 r.

iv) Stopping distance, t = (2) (π) (k) (R_s), t and k both are either m or in ft.

v) The heat the brake must dissipate, $H = 1.7FWk^2 (n / 100)^2$, ft.lb / min, Where, H = heat generated at friction surfaces, ft.lb / min, F = number of duty cycles per minute, Other symbols are as described earlier,i.e., $H = 1.7 (1) (200) (1800/100)^2 = 110200$ ft.lb/min. (2490.2 N.m/s)

vi) Required radiating area of the brake, A = 42.4 hpF / K, where, A = required brake radiating area, in^2, hp = power absorbed by the brakes, F_l = brake load factor = operating portion of use cycle, K = constant = Ct_r, where C = radiating factor (a value for different temperature rise); t_r = brake temperature rise, °F; Assume C = 0.00083 for t_r = 300°F; i.e., A = 42.4 (20) (0.5) / [(0.00083) (300)] = 1702 in^2 (10980.6 cm^2)

vii) Heat produced in the brake; The heat produced in the brake by the energy absorbed is found from $H = E_s / 778.3$, Where H = heat absorbed per stop, Btu (kJ). The temperature rise of the brake is $T_r = H / 0.12W$, where T_r = temperature rise per stop, °F (°C)

viii) Average disk temperature per stop, $T_d = HT_a / 2.25A$, where T_d = disk temperature per stop °F (°C); T_a = average disk temperature ; A = disk surface area, ft^2 (m^2). In this expression the factor 2.25 is the cooling index used when the disk is stationary during cooling- the usual condition following an emergency stop. However, if the disk rotates during cooling, a factor of 4.5 should be used instead.

ix) The peak temperature of the brake, $T_p = T_d + 0.5T_r$; Where, the temperatures are in either °F or (°C).

x) The brake service life (L), in number of stops for a brake, L = (1.98 x 106)ZY / E_s, where the service factor, Z, is found from standard curves available from brake manufacturers and friction-material suppliers; Y = total friction material volume, in^3 (cm^3)

2.12 Characteristics of brakes for domestic Russian aircraft [39]

One of the main indicators governing the operability of aircraft take-off and landing devices is the loading of the aircraft wheel brakes, the ability to absorb rapidly the aircraft's kinetic energy during landing by accumulating the friction heat in a limited volume of the frictional elements of the brakes. Frictional polymeric materials operate satisfactorily in aircraft brakes up to loading of 300 kJ/kg and frictional baked powder materials upto 500 kJ/kg. Carbon frictional composite materials (CFCM) provide multi-disc brakes with a significantly larger specific mass power capacity (up to 1100 kJ/kg) and service life of over one thousand takeoffs and landings, corresponding to the best world indicators. Application of CFCM in aircraft braking devices reduces their weight by 800 kg in the IL-96T/M and by 500 kg in the TU-204, in addition to extending the service life of the brake disks by 2.5 times. **Table 2.12** provides information on a number of domestic-produced aircraft with brakes in which CFCM of various grades are advisable.

2.12 Operating parameters of brakes for domestic Russian aircraft [39]

Aircraft code	Number and dimensions of disks, mm		Operational loading		Operational braking moment, kgf m
	Rotating	Stationary	Total, 10^5kgf m	Specific, 10^5kgf m	
KT 166,An-124	5 (505–340)×20.3	6 (480–286)×20.3	31.0	152	2700
KT 191, Tu-160	5 (490–320)×18.9	6 (456–286)×18.9	26.5	160	2200
KT 196M, Tu-04/214	5 (439–292)×18.9	6 (410–263)×18.9	18.0	148	1800
KT 213, Su-27	5 (448–290)×20.3	6 (415–259)×20.3	19.0	137	1500
KT 240, Su-80	2 (318–203)×18.2	3 (290–177)×18.2	2.9	98	265
KT 251, Yak-130	2 (318–203)×18.2	3 (290–177)×18.2	4.2	167	365
KT263A, An-148	3 (414–273)×22.0	4 (382–242)×22.0	11.0	167	1100
KT 240M, Il-96M	6 (502–342)×23.5	7 (476–312)×23.5	38.2	198	3200

2.12.1 Mechanical properties

Table 2.13 lists the results of determination of the mechanical properties of the CFCM tested. It is apparent that the mechanical characteristics of the studied carbon materials vary within a broad range. This factor allows us to compare the results of full-scale tests with the properties of materials and to choose depending on the test results the range of the characteristics responsible for their operability in brakes and the specific values of these characteristics that ensure operability. A number of characteristics, such as the limits of strength in bending and tension, as well as the impact viscosity, are sufficiently well-correlated with each other to allow us to reduce the number of strength characteristics to be taken into account when

comparing the test results and to select for future optimization the characteristics that are easiest to determine, namely, the limits of strength in tension and compression. The strength limit of all the materials in compression exceeds 100 MPa. The materials reinforced with discrete fibers (Termar-DF and Termar-ADF) and continuous fibers as a cloth with the orthogonal arrangement of fibers (Termar-TD and Termar-FMM) are stronger. The latter material is the strongest because it contains cloth based on high-strength polyacrylonitrile fibers UKN-5000. The materials reinforced with spiral radial braiding of continuous fibers (Termar-DNV and Termar-CTD) have a somewhat inferior strength in compression. The opposite is observed when analyzing the strength in bending. This characteristic is considerably more sensitive to the nature of material reinforcement. The material Termar-DF-P, with discrete fibers strongly powdered as a result of intensive mixing in the process of blank preparation, has a very poor strength. Introduction of a low-strength viscose-based cloth (Termar-TD) into the material with the powdered fibers fails to significantly enhance the strength in bending, while high-strength polyacrylonitrile-based cloth in the Termar-FMM material is able to solve the problem. A high enough strength is achieved if the aerodynamic method is used to produce the fibrous skeleton in the Termar-ADF material while the long discrete fibers remain preserved. This material has the optimum combination of strength characteristics when two ways of loading of the specimens are used.

Table 2.13 Mechanical properties of the studied CFCM

Material grade	Density, g/cm^3	Strength limit, MPa				Impact viscosity, kJ/m^2
		in bending	in compression	in tension	in shear	
Termar-DF	1.75-1.78	70-80	80-100	20-22	12-15	3-5
Termar-DNV	1.66-1.68	140-180	110-120	28-30	6-8	-
Termar-TD	1.65-1.66	75-90	85-110	22-24	5-8	7-8
Termar-STD, nongraphitic cloth, heat treatment at 1500 ^0C	1.65-1.69	150-180	120-140	32-34	6-8	23-26
Termar-STD, nongraphitic cloth, heat treatment at 1750^0C	1.66-1.69	140-170	100-110	26-30	5-8	-
Termar-STD, nongraphitic cloth, heat treatment at 2000^0C	1.80-1.85	130-160	100-110	25-28	5-7	-
Termar-FMM	1.75-1.82	140-170	120-130	34-40	10-12	19-22
Termar-ADF*, NEF fibers unglazed	1.80-1.85	85-95	100-110	22-25	9-13	4-7
Termar-ADF* CEF fibers	1.75-1.78	100-120	120-150	32-35	8-10	10-14
Argolon-TH	1.70-1.78	60-90	130-200	35-50	-	-
Carbenix-4000	1.69-1.73	110-120	130-140	-	-	-

2.12.2 Thermo-physical properties

The specific heat capacity, coefficient of heat conductivity, and coefficient of thermal expansion are among the most essential CFCM thermophysical characteristics. The carbon heat capacity is determined by its chemical nature; it is independent of its state or origin (whether it is in the form of fibers or monolithic graphite, if it is from pitch, tar, or gaseous hydrocarbons), or of the degree of perfection of the crystallographic structure. It follows from the data in Table **2.14** that the heat capacity drops as temperature rises. Structure and production factors leads to the conclusion that the only way to make the material denser is by increasing the CFCM heat capacity, and together with it the kinetic energy share absorbed by the stack of frictional disks at its constant volume; this method will be considered below. Unlike the heat capacity, the carbon heat conductivity depends very much on the crystalline lattice perfection For carbon-to-carbon composite materials containing at least two components differing significantly in their method of production and structure, namely, the fibers and the matrix, the heat conductivity is a function of complex nature, depending on such parameters as the conditions of treatment of the components, their quantitative and dimensional relations, the reinforcement type, the pattern of distribution of fibers in the matrix, etc. This fact is confirmed by the results of measurement of the heat conductivity coefficient of various CFCM previously used in brakes, tested on Unitrib 2168UMT and IM-58 friction machines and on a special testing apparatus at Rubin Corporation **(Table 2.13).**

Table 2.14 Heat capacity of carbon and steel in response to temperature

Temperature, ^0C	Specific heat capacity (mass), kJ/kg		Specific heat capacity (volume), kJ/dm^3	
	Carbon	Steel	Carbon	Steel
27	0.678	-	1.187	-
127	1.002	0.494	1.754	3.853
227	1.223	0.528	2.214	4.118
327	1.397	0.565	2.445	4.407
427	-	0.611	-	4.766
527	1.534	0.682	2.685	5.320
627	-	-	-	-
727	1.800	-	3.150	-
827	-	-	-	-
927	1.907	-	3.337	-
1027	-	-	-	-
1127	1.982	-	3.469	-

Table 2.15 also presents the coefficients of CFCM thermal expansion. This value has a substantial anisotropy as well. In addition, it is much less vulnerable to changes than the heat

conductivity because of different production processes and material structure. Thus, optimization of the coefficient of thermal expansion seems a less urgent problem.

Table 2.15 CFCM thermophysical properties after standard tests

Material grade	Heat capacity, W/m K, relative to the working surface		
	Parallel	Perpendicular	Parallel
Termar-DF	33-45	12-15	0.8
Termar-DNV	25-30	10-12	-
Termar-TD	20-25	8-10	-
Termar-STD, nongraphitic cloth, heat treatment at 1500 ^{0}C	15-18	6-8	0.9
Termar-STD, nongraphitic cloth, heat treatment at 1750^{0}C	18-22	8-12	-
Termar-STD, nongraphitic cloth, heat treatment at 2000^{0}C	45-60	18-22	-
Termar-FMM	50-55	15-20	0.2
Termar-ADF*, NEF fibers unglazed	60-65	20-25	-
Termar-ADF* CEF fibers	60-65	20-25	0.5
Argolon-TH	35-40	10-15	-
Carbenix-4000	30-35	15-20	-

2.12.3 Friction and wear characteristics

Table 2.16 presents the results of tests with the thermopulse method using an IM-58 friction machine following the above conditions in a number of main CFCM that were in operation at different times or underwent full-scale stand tests. It proves the sensitivity of the friction and wear characteristics determined with the thermopulse method to the structure of the carbon material, i.e., the matrix nature of the reinforcing fibers and the reinforcement type. The values of all the characteristics in Table 2.15 vary within broad limits.

The materials reinforced with cloth treated at comparatively low temperatures (Termar-TD, Termar-CTD, Termar- FMM), and the materials based on the pyrocarbon matrix (Argolon-TH, Carbenix-4000) have high friction coefficient and wear; they are characterized by low stability of the friction coefficient **(Table 2.16).** The materials reinforced with discrete highly graphitized fibers feature high wear resistance, but the friction coefficient is somewhat inferior to that of the above materials.

Table 2.16 Friction and wear characteristics of the tested UFCM

Material grade	Friction coefficient	Linear wear, μm/braking
Termar-DF	0.20-0.25	05-1.0
Termar-DNV	0.28-0.312	1.8-2.5
Termar-TD	0.33-0.38	2.5-7.0
Termar-STD, nongraphitic cloth, heat treatment at 1500 ^{0}C	0.24-0.26	1.5-3.0
Termar-STD, nongraphitic cloth, heat treatment at 1750^{0}C	0.27-0.28	2.1-3.3
Termar-STD, nongraphitic cloth, heat treatment at 2000^{0}C	0.22-0.25	1.2-2.0
Termar-FMM	0.32-0.40	1.5-2.0
Termar-ADF* CEF fibers	0.27-0.43	0.8-1.5
Argolon-TH	0.34-0.40	1.9-5.2
Carbenix-4000	0.40-0.45	2.3-5.5

2.13 Review of patented literature on friction materials

This review on patents purely confines to Alumunium base friction composites/materials for brake rotors only. However, in the present investigation, Al based brake pads for motor bike and AN32 aircraft are first time developed using Preform Hot Forging Process and patented literature is not available. The investigated inventions relate to friction materials and in particular friction materials for use in brake pads.

US Patent 3844800 is related to friction materials and particularly to friction materials used in braking loads having ranges of kinetic energy from zero to those generated by today's aircraft during maximum energy braking at rejected take-off (RTO) where speed and load are greatest and available stopping distance is minimal. The general class of friction materials presently in use for such high energy applications is those friction materials which comprise a metallic base or matrix. That is, the friction material constituents are bonded together by a metal matrix. In addition to the metal matrix, such materials may also include friction producers such as ceramics, anti-oxidants such as graphite, friction modifiers such as boron nitride or molybdenum disulfide, and various reinforcement additives such as steel fibers. The friction material presently in use in aircraft brakes possesses three characteristics which are interrelated to the point that the end product will often possess an unhappy comprise of these characteristics. The first of these is the size (weight) which the friction article components of aircraft brakes must have in order to achieve the required useful life in order to be accepted by the aircraft manufacturers; the second is efficiency (friction level) achieved by the system and the third is cost. In order to achieve maximum useful life for a given weight requirement, certain additions are made to the base or matrix metal, usually copper and commonly iron, in

order to achieve a specific friction level or braking efficiency, with other additions being made to improve wear characteristics. These additions, which fall within one or more of the broad classes referred to above, provide various chemical effects and controls as described herein below. These additions are usually offsetting so that often a third, a fourth, a fifth addition, and sometimes more, must be made before an acceptable friction material is achieved. The seemingly never-ending adding process causes the cost of the friction material to increase as the additions become more exotic and the development time increases. Furthermore, as the percentage of additions increases, the percentage of base material decreases so that the matrix strength of the friction article is reduced. It is often the case that the matrix strength is reduced to the point that further additions are not possible, even though the wear characteristic or the efficiency of the friction article is not completely satisfactory.

US Patent 5856278 describes friction material for use with Al/SiC alloy brake rotors containing 15 to 80% of finely powdered alumina abrasive (1-10 μm), 5 to 40% of cured organic binder, less than 5% metal in particulate form and less than 5% particulate carbon and/or graphite, from 1 to 40% of organic fiber the balance being particulate inert filler and optionally, a non-graphitic lubricant, all percentages being by volume. The composition was press moulded into pads and the rubber/resin binder was thereafter cured, to produce a final product.

On testing in a conventional dynamometer rig fitted with an Al/SiC alloy rotor, the behavior of the pads was excellent, despite the highly abrasive nature of the silicon carbide toughened rotor. Pad wear was good; the coefficient of friction was stable at about 0.35, a satisfactory value.

US Patent 6439353 cited aircraft wheeling segments of stator brake disks and rotor brake disks. The pads are made of sintered metal and the rotor brake disks are made of ceramic or ceramic composite. This patent mainly describes brake design aspects rather the technique of producing the friction material.

US Patent 6918970 describes high strength Al-Si alloy suitable for high temperature applications for cast components such as brake calipers and brake rotors. Most prior alloys are not suitable for high temperature applications because their mechanical properties, such as tensile strength and fatigue strength, are not as high as desired in the temperature range of 500-700^0 F. A large mismatch in lattice coherency contributes to an undesirable microstructure that can not maintain excellent mechanical properties at elevated temperatures.

US patent 2004/0175544 describes a non-asbestos based friction material for rotors and brake drums of Al alloy for automobiles or the like, which exhibits lower counter surface attack and excellent wear resistance, produced by forming and then curing a non asbestos based friction

material composition, comprising of a fibrous base, binder and filler as the major ingredients, wherein the filler is incorporated with 1 to 10% of abrasive particles having an average size of 0.5 to 10 μm and 4 to 20 % of un-vulcanized rubber, all percentages by volume based on the whole friction material.

US patent 6382368 describes a support member of a disc brake and backing plate of a drum brake formed integrally, and a pair of pin supported portions for supporting a pair of caliper slide pins passed through on the radially outward side of rotor portion.

US Patent 4415363 discloses a method for manufacturing an aluminum-based composite plate. The billet production step includes reducing, by magnesium nitride, an oxide-based ceramic as a porous molded body. The reduced oxide-based ceramic has improved wettability. An aluminum alloy is then caused to infiltrate into porous sections of the reduced oxide-based ceramic to thereby provide the aluminum-based composite billet. The billet is extrusion molded into a flat plate form which plates of desired shapes are punched and molded by a press.

US Patent 4391641 claims of an iron base sintered powder metal friction material for railroad braking use, formed by solid phase sintering and consisting essentially of, by volume, 10-70% carbon in the form of coke or graphite; 0-2.5% sulfur, 0-10% alumina; 9-40% of a metal powder additive of copper, manganese, ferrochrome and chrome carbide compounds. Two dynamometer test procedures UIC (European) and AAR (USA) are used for determination of friction characteristics. The technology and the materials so developed exhibit low metal pickup. Here, the application is narrow and only suitable for railways and also bonding between friction materials and backing plate is not provided.

US Patent 5902943 relates to the development of an Al alloy powder blend which can be used for the manufacture of sintered components. The sintered component can be subjected to secondary processing operations. Specifically, this invention is concerned with the composition of the alloy and the powder size distribution, particularly that of the alloying additions, which optimize the sintering process. The powder is based on the precipitation hardenable 7000 series Al-Zn-Mg-Cu alloys with trace additions of lead or tin. The powder blend comprises 2-12 wt. % zinc, 1-5 wt. % magnesium, 0.1-5.6 wt. % copper, 0.01-0.3 wt. % lead or tin..

This patent also describes the difficulty in sintering of metal powders as a consequence of the surface oxide film which is present on all metals. This oxide film is a barrier to sintering because it inhibits inter particle welding and the formation of effective inter particle bonds. The problem is particularly severe in aluminium because of the inherent thermodynamic stability of (Al_2O_3).

This patent relates the effect of zinc in Al based composites. Zinc is the principle alloying addition. Its melting point is below the sintering temperature and it forms a number of binary and ternary eutectic phases. This should enhance sintering. However, zinc is highly soluble in aluminium and this is an impediment to its use as a sintering agent. When small zinc particles are used, the entire zinc addition is quickly absorbed by the aluminium and little or no liquid phase is formed, which hinders sintering. This has limited its previous application. In contrast, when large zinc particles are used, the aluminium adjacent to a zinc particle becomes locally saturated and elemental zinc persists long enough for enhanced liquid phase sintering to occur. The amount of liquid phase formed is therefore a function of the zinc particle size. Because the thermodynamic driving force is inversely proportional to the particle size and the smaller particle sizes aids particle packing, the zinc particle size needs to be optimized. This size effect is also dependent on other process variables such as heating rate and compaction pressure. A similar particle size effect occurs in other systems where there is some solid solubility of the additive in the base element and where there is a diffusive flow from the additive to the base. Examples include copper in aluminium and copper in iron.

US Patent 4311524 discloses sintered iron based friction materials and limits the application in friction devices operating under liquid lubrication conditions at medium performance modes; listed compositions of the friction material fade at severe energy levels and are not suitable for heavy duty applications. The patent does not describe the materials for use in dry operating conditions. It also does not discuss about the bonding between friction elements and backing plate.

US Patent 5925837 describes a manufacturing method for production of metallic friction materials by 1. preparing powder materials, 2. mixing copper as a base with proper proportion of iron powder or steel wool, aluminum powder, zinc or tin or lead powder, graphite powder and alumina or silicon dioxide powder, 3. pressing mixed materials into green bodies under 375~625 MPa at room temperature, 4. pre-heat treating the green bodies in an air furnace with temperature raised to 100~300° C. for 1~3 hours, 5. sintering the green bodies into test samples under 350~750 MPa for 24~60 hours to gain sintered friction materials having an oxidized layer of less than 1 mm thick, 6. processing and grinding the sintered test samples with grinders to remove the oxidized layer, 7. washing the outer surface of the sintered test samples ground into finished products. The method of the invention may reduce complexity in manufacturing and investment and production cost. Products according to the invention have friction coefficient within the standard value, low wear loss and good thermal stability. This patent also describes metallic friction materials based on copper or iron alloys, as disclosed in U.S. Pat. Nos. : 3,981,398, 4,311,524, 4,391,641, 4,415,363, 5,370,725. It is evident that the

manufacture of copper-base or iron-base friction materials according to powder metallurgy utilizes sintering in vacuum or under controlled protective atmospheres. The manufacturing processes used in these disclosures have the following disadvantages, reducing their commercial applicability to a large extent.

i) A high temperature vacuum or controlled atmosphere furnace is necessary, resulting in an extremely high investment.

ii) Sintering needs a temperature as high as 800-1200° C, under a proper protective atmosphere (preventing oxidization), evidently increases difficulty in manufacture.

iii) Sintering powder materials at high temperatures in vacuum or atmosphere-controlled furnaces slows the speed of production, and requires higher energy, resulting in high cost.

US Patent 5841042 is related to brake lining material for a heavy-duty braking. The present invention is to provide a novel brake lining material which can have extended useful life under heavy-load conditions, can retain stable coefficients of friction, can have appropriate wear resistance and can reduce the wear of its opponent material significantly. In accordance with the present invention, the novel brake lining material is composed of copper-base metal powder, refractory material powder and graphite powder, the metal powder containing iron powder and titanium powder and being used as a matrix, the refractory material powder and the graphite powder being sintered together with this matrix in a uniformly distributed state. For example, a brake lining material for a heavy-load braking device comprises of (a) 10 to 20 wt % of refractory material powder;(b) 15 to 25 wt % a graphite powder, and (c) as its remainder, a copper-based metal powder comprising powders of copper-based metal, iron and titanium wherein a total weight of said iron powder and said titanium powder is 0.2 to 0.4 of a total weight of said metal powder and a remainder of said metal powder comprising copper-base metal which consists of copper powder, copper alloy powder or a mixture of said copper powder and said copper alloy powder and in which said refractory material powder and said graphite powder are sintered together with said metal powder in a uniformly distributed state in the said metal powder. Although a conventional organic lining material for such a heavy-load braking device which is bound by a phenolic resin binder is not so costly, its mechanical strength is relatively low and it wears away steeply under heavy load conditions, which causes the abrupt decrease of its coefficient of friction. Particularly, when the temperature of the lining material reaches 300° C or higher due to frictional heat, the phenolic resin binder carbonizes or decomposes and, because of this, the coefficient of friction of the lining material decreases rapidly and its wear resistance deteriorates substantially. As for a conventional metallic lining material, when this lining material is put under a heavy load condition, its temperature can rise steeply and may seize up with an opponent material to be braked. As a

result of this, both the metallic lining material and the opponent material may wear away severely under such a heavy-load condition. Thus, a conventional brake lining material needs to be replaced frequently because the usable period during which its coefficient of friction remains stable is limited.

US Patent 4203936 describes a process for producing an organic friction article from a composition of materials in a dust free environment. Water is mixed with the composition of organic materials to produce slurry. A fixed volume of the slurry is communicated into a mold. The slurry in the first mold is compressed to remove up to 95% by weight of the water to form a briquette. The briquette is conveyed to a force air oven or dielectric heater where the water is further reduced to about 1% of the weight of the briquette. This dry briquette is then placed in a second mold and pressed into the shape of a friction pad. The pressed friction pad is placed in an oven and heated to cure the resin in the composition of materials to complete the manufacture of the organic friction pad.

In the manufacture of organic friction pads it has been considered essential that all water be removed from the composition of materials before curing the resin binder contained therein. If the water content is greater than 2% by weight of the composition of materials, the heat required to cure the resin in the composition of materials in evaporating the water can cause bubble marks and/or voids adjacent to the surface of the friction pad. Therefore, all the ingredients in the composition of materials are dried before being mixed together to form a friction pad. However, the density of the dry asbestos as compared to the other ingredients in the composition of materials requires substantial mixing before a uniform composition of materials is obtained. Unfortunately, such mixing causes a portion of the asbestos to become airborne and pollute the surrounding environment. Often the amount of such airborne asbestos exceeds the allowable limits set in the United States by the Occupation Safety and Health Act of 1970. In an effort to maintain the quality of air within the allowable limits, most manufacturers have discovered that extensive air filtration systems are required in existing structures.

US Patent 5830309 is related a friction material and process of forming a friction material embodies slurry of aramid, acrylic and carbon fibers, together with kaolin clay and aluminum oxide used as fillers in a phenolic resin binder. The matrix formed by the fibers entraps a relatively large quantity of carbon particles. The carbon particles comprise more than forty or fifty percent of the weight of the material. During the process of formation, the slurry is de-watered to reduce moisture content to the order of two percent before the resin binder is cured under heat and pressure.

Paper-based friction materials are subject to significant limitations. A most important limitation relates to the customary inclusion of cellulose fibers, which tend to char and/or burn readily at the temperatures frequently encountered in the operation of friction engagement devices. As a direct result of this charring and burning characteristic, the coefficient of friction of paper-based friction materials tends to decline dramatically under heavy-use conditions. Any decline in the coefficient of friction of a friction material in a transmission-like device can have an undesirable adverse effect on the overall performance of the device. In certain instances, decline of the coefficient of friction can render the device entirely inoperative, with consequent serious if not catastrophic consequences.

Carbon-based friction materials similarly are known to be acceptable for certain applications. Forms of such materials are disclosed in U.S. Pat. Nos.4,700,393, 4,639,392 and 5,083,650. However, the use of carbon-based materials is subject to significant drawbacks as they are relatively expensive and difficult to manufacture. Sprayed molybdenum coatings have been used as friction materials, also. However, molybdenum has been found to have an energy limit above which it does not function effectively in such applications. Further, it is very expensive to manufacture. Environmental concerns impose further limits on the use of molybdenum

US Patent 5712029 is related to friction elements such as brake or clutch and includes a rotor formed from an aluminum alloy, hardened with a ceramic reinforcing material, a component such as a brake pad having a friction surface which incorporates a hard inorganic material which is an oxide, carbide, or nitride in an amount of 0.5 to 15% by volume. The reinforcing agent in the aluminum alloy and the hardening materials are selected to be compatible in accordance with intended applications.

US Patent 5620791 relates to metal and ceramic matrix composite brake rotors comprising an interconnected matrix, embedding at least one filler material about 26% by volume of the brake rotor for most applications, and at least about 20% by volume for applications involving passenger cars and trucks. In a preferred embodiment of the present invention, the metal matrix composite brake rotor comprises an interconnected metal matrix containing at least about 28% by volume of a particulate filler material and more preferably at least about 30% by volume. Moreover, the composite rotors of the present invention exhibit a maximum operating temperature of at least about 900° F and preferably at least about 950° F and even more preferably at least about 975° F and higher. Traditionally, automotive brake rotors have been made from cast iron which provides good wear resistance and excellent high temperature properties. However, cast iron is dense relative to other candidate materials and, therefore, a cast iron brake rotor is relatively heavy. A heavy brake rotor is considered to be undesirable for at least three reasons. The first reason is that a heavy brake rotor contributes to the overall

weight of the vehicle and thus reduces its fuel efficiency and correspondingly increases its emissions levels. The second reason (relevant mainly to passenger cars and trucks) is that a brake rotor is part of the "unsprung" weight of a vehicle (i.e., the weight of a vehicle that is below the springs) and, as such, contributes to the noise, vibration and harshness (commonly known in the automobile industry as "NVH") associated with the operation of the vehicle. When the unsprung weight of a vehicle is reduced, the NVH properties are usually improved. The third reason is that a brake rotor is a part of a vehicle that requires rotation during use and, accordingly, a heavier brake rotor requires the use of additional energy to increase and decrease the rotational speed of the rotor. In addition, the ability of a heavier brake rotor to cause undesirable vibration during rotation is greater than that associated with a lighter brake rotor.

US Patent 5620042 describes an annular rotor insert formed by casting a metal matrix composite. The rotor insert includes a pair of brake friction plates which are disposed in mutually spaced apart relationship. The brake friction plates include inner surfaces and generally parallel outer surfaces. At least one of the inner surfaces of the brake friction plates is provided with a plurality of spacing elements for engagement with the inner surface of the other brake friction plates for maintaining the plates in predetermined spaced apart relationship. The rotor insert is placed in a rotor mold. A hat-shaped rotor body is cast around the rotor mold whereby the spacing elements are effective to maintain the plates in a predetermined spaced apart relationship.

To produce a lightweight rotor, it has been suggested to cast the rotor from an aluminum alloy, such as 319 or 356 aluminum. However, while aluminum alloy rotors possess satisfactory thermal properties, they do not possess adequate mechanical properties of high temperature strength, hardness, and wear resistance, which are typically required for disc brake applications. In order to satisfy these mechanical properties and still produce a lightweight rotor, it is known to cast the rotor from an aluminum based metal matrix composite (AMC) containing silicon carbide particulate reinforcement. Such an AMC is commercially available under the name DURALCAN; a registered trademark of Alcan Aluminum Limited of San Diego, California, USA. The AMC provides the finished rotor with sufficient mechanical and thermal properties to satisfy the requirements of brake rotor designs at a significantly reduced weight. For example, it has been found that a weight reduction of approximately 60% over a comparable grey cast iron rotor can be achieved by casting the rotor from the AMC.

One disadvantage to castings made with the AMC is that they are rather expensive compared to the costs of castings made from grey cast iron and conventional aluminum alloys. Another disadvantage is that the very hard particulate reinforcement makes the AMC castings more

difficult to machine compared to grey iron and conventional aluminum castings. U.S. Pat. No. 5,183,632 to Kiuchi *et al.* discloses a method for producing an aluminum "composite" disc brake rotor in which only the friction plate portions are formed of a reinforced aluminum alloy, while the remainder of the rotor is an aluminum alloy. According to this method, an aluminum alloy is first cast or press molded to form a rough-shaped disc brake rotor body. Next, an annular recessed portion (corresponding to the friction plate portions) is formed in each rotor face by machining. A separate reinforced aluminum alloy powder preform or a mixture of an aluminum alloy powder and reinforcing particles is then placed in each of the recessed portions of the rotor. The rotor body including the preform or mixture is heated to mushy state temperature, and then molded under pressure to secure the preform or mixture to the rotor body and produces a rough-shaped disc brake rotor.

US Patent 5595266 describes a friction brake subassembly which is provided with a metallic backing plate element and with a friction material brake lining element integrally adhered to the backing plate element, the brake lining element and friction material composition comprising friction material particles and an epoxy resin binder preferably in the approximate range of from 10% to 40% of the friction material composition total weight. Methods are disclosed for integrally bonding the brake lining element to the backing plate element.

It has been a common industrial practice in the United States to manufacture friction brakes subassemblies such as the friction brake shoes and friction brake pads typically utilized in automotive vehicle brake systems to first form a friction material particulate mixture having an included phenolic resin binder into a cured brake lining in shape of specific configuration and afterwards join the cured brake lining shape to a cooperating brake member backing plate by mechanical fasteners such as rivets or by a suitable adhesive such as a cured phenolic resin, a cured elastomeric rubber, or a like adhesive. The friction material particulate mixture cured brake lining shape is typically constituted of inorganic compound particles, organic compound particles, metallic particles, reinforcing fibers, and sometimes carbon particles, in addition to the phenolic resin binder. Another form of conventional friction brake member, sometimes referred to as an integrally molded brake shoe or integrally molded brake pad, is manufactured using a method wherein the required adhesive material is applied to the brake subassembly backing plate element in its uncured condition and the friction material brake lining with phenolic resin binder is placed in contact with the applied uncured adhesive. The adhesive material is subsequently cured simultaneously with the necessary curing of the brake lining friction material particulate composition mixture.

US Patent 5538104 describes a brake pad assembly comprising of a backplate, a friction lining secured to one side of the backplate and a planar dampening sheet secured to the other side of

the backplate. The dampening sheet has at least one embossed projection extending from the one side thereof and the backplate has at least one recess in the side thereof secured to the dampening sheet and which is of generally the same configuration as the projection in the dampening sheet to receive the projection. The projection is partially outlined by at least one cut in the dampening sheet forming a cut edge on the projection which extends outside the plane of the dampening sheet to abut against the wall of the recess and compensate for excessive shearing forces caused between the dampening sheet and the back plate during a braking operation.

US Patent 5407035 describes a method of making and the resulting product for a disk brake rotor with a self-lubricating, thermally conductive coating thereon, that enhances the friction-wear life of a disk brake assembly within which it is used, comprising: (a) controllably toughening at least the outside braking surfaces of a lightweight metal disk brake rotor, said roughening being carried out to promote mechanical adhesion of coatings applied thereover; (b) thermally spraying one or more coatings onto the roughened outside braking surface, the exposed coating being electric arc sprayed using a codeposit of iron-based material and powdered graphite to form an iron matrix composite coating; and (c) surface heat treating essentially the exposed coating to dissolve and precipitate graphite and form a simulated cast iron and also to densify the coating and remove residual stresses resulting from the deposition. To inhibit heat transfer, the method may further comprise forming the lightweight metal rotor to have a pair of annular ring walls supported by a hub, the ring walls being separated by a plurality of vanes for inducing air cooling as the rotor rotates, and interposing a thermally sprayed metallic-based heat barrier coating between the rotor and exposed coating. The barrier coating may be a nickel-based material which preferably includes graphite codeposited therewith. The cooling vanes and intermediate coating cooperate to protect the rotor against extreme heated conditions.

US Patent 5384087 discloses a process for making an aluminum silicon carbide composite material in strip form. The process comprises blending a powdered aluminum matrix material and a powdered silicon carbide material, roll compacting the blended powdered materials in an inert atmosphere to form a green strip having a first thickness, and directly hot working the blended and roll compacted materials to bond the aluminum matrix material particles and the silicon carbide particles and to form a thin strip material having a desired thickness.

US Patent 5372222 describes lightweight and high thermal conductivity brake rotor. The rotor has a hub with a plurality of openings therein for attachment to an axle which rotates with a wheel of the vehicle. The hub has spokes which radially extend from the hub to an integral annular head member. The head member has parallel first and second friction surfaces thereon

for engagement with brake pads on actuation during a brake application. The rotor which is made from a composition consisting essentially of 50-85 percent by volume of silicon carbide and 50-15 percent by volume of copper and from 0-15 percent by volume of graphite fiber, develops a thermal conductivity at room temperature of from 0.16-0.74 cal/cm sec °C (50-310 W/m-°K). In an effort to increase the overall fuel efficiency, the overall weight of vehicles has been decreasing for a period of time. One of the ways that the weight can be reduced is to replace a typical cast iron brake rotor with a brake rotor made from aluminum or other light weight metal. Unfortunately, aluminum is not normally resistant to abrasion, and as a result, when aluminum is used, a wear resistant surface coating of the type disclosed in U.S. Pat. No. 4,290,510 must be applied to the friction engagement surfaces or a friction material retained in a backing plate is attached to a rotor such as disclosed in United Kingdom Patent No. 1,052,636 or as recently disclosed in U.S. Pat. No. 5,103,942, wherein layers of friction material are attached to a rotor. This type of protection for aluminum rotors is adequate for most applications as long as the thermal energy generated during a brake application is below 482° C. (900° F.). However, in instances where the thermal energy generated approaches the melting point of aluminum, the structural rigidity decreases as the rotors actually soften and in some instances where the thermal energy exceeds the melting point of aluminum, the rotors can fail. Therefore, it was imperative to develop a rotor having the capability of conducting thermal energy away from a wear surface while maintaining good mechanical properties such as hardness and strength at high temperatures during a brake application.

A performance satisfactory rotor made from a copper chromium alloy has been developed which has exhibited a thermal conductivity of approximately seven times greater than cast iron. Unfortunately, the density of rotors made from copper chromium alloys would also be more than similar cast iron rotors and as a result an increase in the overall weight of a vehicle would not improve the desired fuel efficiency.

After evaluating many compositions, copper alloy-silicon carbide composites were developed for use as a brake rotor which has high thermal conductivity, a relative density of approximately three-fourths of cast iron and sustained structural strength at temperatures above 450° C (842° F). Particular families of such composites has been evaluated with from 50-15 percent by volume of copper and from 50-85 percent by volume of silicon carbide and under some circumstances from 0-15 percent by volume of graphite fiber have been added to modify the resulting mechanical properties. Typically, in the manufacture of such a rotor silicon carbide powder is packed into a mold and copper is infiltrated into the packed volume of silicon carbide powder as the temperature of the mold is raised to approximately 1200° C. (2192° F) to form a unitary brake rotor. The brake rotor has a hub with a plurality of openings

therein for attachment to an axle of a vehicle which rotates with the wheel spokes or disc which radially extend from the hub to an annular head portion. The head portion has first and second friction surfaces thereon for engagement with brake pads during a brake actuation. The brake rotor has a density of 4.0 to 6.0 g/cm^3 and a resultant thermal conductivity at room temperature 20° C (68° F) of 0.16-0.74 cal/cm-sec-°C (50-310 W/m-°K).

US Patent 5325941 is directed towards a combination of composite brake rotors or clutches and a brake pad where the composite rotor or clutch is composed of a low density metal and particles of a nonmetallic material. Specifically the rotors or clutches are of a metal matrix comprising aluminum or magnesium or alloys thereof homogenously mixed with a refractory ceramic, such as silicon carbide, silicon nitride, boron nitride or aluminum oxide among others. The composite brake rotors and clutches are very durable and have greatly increased thermal conductivities which improve brake and clutch performance. The rotors or clutches are manufactured by casting, followed by diamond cutting and finally followed by surface burnishing to smooth and condition the surface of the rotor or clutch. The brake pad may be composed of cupric oxide, antimony sulfide, silicon alumina alloy, barium sulfate, kevlar, zinc sulfide, coke, and graphite.

A further object of this invention is to provide a composite brake rotor or clutch, characterized by high structural stability and strength, which minimizes adverse effects due to galling and enhances the thermal conductivity of the rotor, in order to allow more efficient thermal heat dissipation. The low density metals useful in the present application can be selected from the representative and illustrative group consisting of aluminum, aluminum alloys, magnesium, magnesium alloys and a mixture thereof. Preferably, the low density metal is an aluminum alloy while the nonmetallic material is a refractory ceramic which can be selected from the representative and illustrative group consisting of a metal oxide, metal nitride, metal carbide, metal silicides and mixtures thereof. Preferably, the nonmetallic material is selected from the group consisting of silicon carbide, aluminum oxide, boron carbide, silicon nitride, and boron nitride. In particular, the nonmetallic material is selected from the group consisting of silicon carbide and aluminum oxide. The composition is characterized by high strength and high heat conductivity which allows fast and efficient removal of heat away from the contact surface between the brake rotor and the brake pad. Improving the conduction of heat away from the contact surface is thought to increase the brake pad longevity and reduce brake pad operating temperature during braking. The reduced brake pad temperature is also thought to reduce brake fluid boiling problems in the brake lines connected to the braking assembly. Such heating is thought to result in brake fading as well as failure, after long and sustained brake operation. These improvements are especially critical in race car and airplane braking systems. The same

improvements also improve clutch behavior and durability. The heat conductivity of the present composite is about four times than typically found for cast iron rotors or clutches. The composition is extremely durable and requires cutting of the rotor or clutch surface using a diamond cutting tool.

An additional interesting property of such composite materials is their higher thermal conductivity. For example, the above material exhibits a thermal conductivity that is of the order of four times greater than thermal conductivity of cast iron. Generally, the thermal conductivity, that is the ability of the material to conduct heat away from the point of heat generation, is such that heat dissipation from the object is limited by the ability of the heat to be conducted through the material. For example, plain carbon steel has a thermal conductivity of 30 Btu/hr-ft-°F.; stainless steel 304 has a thermal conductivity of 10 Btu/hr-ft-°F.; ductile cast iron ASTM A339, A395 has a thermal conductivity of 10 Btu/hr-ft-°F.; aluminum alloy 3003 ASTM B221 has a thermal conductivity of 90 Btu/hr-ft-°F.; and aluminum alloy 2017 (annealed) ASTM B221 has a thermal conductivity of 95 Btu/hr-ft-°F.

US Patent 5028494 describes an aluminum composite material as a brake disk material for railroad vehicles obtained by dispersing and mixing reinforcement particles of alumina, silicon carbide or the like into an aluminum alloy. The reinforcement particles are 5 to 100 μm in diameter, and are dispersed uniformly in the alloy in an amount of 1 to 25% by weight. An extremely excellent brake disk material for railroad vehicles is thus provided which is light in weight and has high strength, good thermal conductivity and high wear resistance. The superiority or inferiority of friction-wear characteristics of a brake disk material for high-speed vehicles is evaluated based on the propriety of average coefficient of friction in braking, the stability of instantaneous coefficient of friction and the wear resistance of the brake disk and the mating material. Though aluminum alloys are generally deemed low in resistance to wear, it is possible to provide an aluminum alloy with an extremely high wear resistance by adding and dispersing hard reinforcement particles uniformly in the aluminum matrix. Besides, a brake disk material is required to have sufficient strength under the centrifugal force generated by the high-speed rotation of the brake disk and the thermal stress generated by the heat load at the time of braking, and the reinforcement particle dispersion type aluminum alloy is superior to the cast iron in strength and thermal conductivity. Namely, the reinforcement particle dispersion type aluminum alloy as a brake disk material is superior also in resistance to heat cracking at the sliding surface of the brake disk under high-frequency (service braking) or high-load (emergency braking) frictional conditions. Moreover, the specific gravity of the aluminum alloy, 2.7, is as low as about one-third of the specific gravity of cast iron, 7.2-7.3;

thus, by use of the aluminum alloy it is possible to markedly improve the lightness in weight, which is essential to the high-speed vehicles, on a material basis.

US Patent 4865806 describes a method for preparing cast composite materials of nonmetallic carbide particles in a metallic matrix, wherein the particles are roasted and then mixed into a molten metallic alloy, and the particles and metal are sheared past each other to promote wetting of the particles by the metal. The particles are roasted in air or other source of oxygen to remove the carbon from the near-surface region of the particles and to produce an oxide surface diffusion barrier, resulting in a reduction of carbide formation at the interface. The mixing occurs while minimizing the introduction of gas into the mixture, and while minimizing the retention of gas at the particle-liquid interface. Mixing is done at a maximum temperature where the particles do not substantially chemically degrade in the molten metal during the time required for processing, and casting is done at a temperature sufficiently high such that there is no solid metal present in the melt.

US Patent 4661154 describes a process for the production by power metallurgy of a material based on an aluminum alloy, a solid lubricant and at least one ceramic is disclosed. The process is characterized by using a ceramic in powder form with a granulometry of between 1 and 10 μm. This invention finds application in the manufacture of components which are subjected to friction, in particular under hot condition, such as engine liners. These components provide an optimum compromise between coefficient of friction and resistance to seizure and wear.

US Patent 4409298 describes metal composites comprising a metallic matrix and discrete, non-metallic solid particles as useful friction materials, and may be die-cast to form friction elements. The preferred metallic matrix components are alloys containing aluminum such as aluminum-silicon and aluminum-silicon-zinc alloys. The disclosed invention is a metal composite friction material comprising a metallic matrix and discrete non-metallic components and a method for the preparation thereof. Unlike the sintered composites, the friction materials of this invention comprise a continuous metallic matrix which imparts a substantial improvement in mechanical strength to the resulting friction element, thus avoiding the need for added strengthening means. Although the metal composite friction materials of this invention may be formulated from any of a variety of metals or metal alloys, the use of low density metals or metal alloys will permit a substantial reduction in weight over the prior art sintered composites.

US Patent 4173681 describes a disc brake pad which comprises an organic friction material layer and an organic backplate layer. Both layers are formed of pulverulent materials compacted into "green" preforms at a pressure of 80-150 bars, which are then placed in a mold

where heat and pressure are applied to create the integral disc brake pad. Both layers use the same resin and they may even be of identical composition. Conventional disc brake pads are composed of two very distinct materials, i.e., the friction material and the metallic backplate. A metal backplate has several well-defined functions which include giving a general rigidity to the friction material, transmitting the braking torque and mounting the pad in the caliper. However, pads with metal backplates have certain disadvantages. During brake application, the pad vibrates relative to the disc at high frequencies and, because of which, the pressure applied by the piston, causes a "squeal". This results from the stress of steel-on-steel contact between the metal backplate and the piston. This noise is quite objectionable. Also during long braking application and under high braking pressures, the friction material can reach temperatures from 600° to 800° C. The metal backplate conducts heat well and transmits this heat to the metal caliper piston which causes the brake fluid to boil and turn to vapor. This phenomenon is very serious, because braking pressure declines dramatically. Automobile disc brakes are quite exposed and are frequently wetted during rainy weather and when traversing puddles of water. The metal back plates, although they are usually protected with different coatings, often become oxidized or corroded. This oxidation often occurs between the friction material and the backplate and can, in some cases, cause separation or delamination of the lining. Automotive friction materials are usually composed of a high percentage (20-60%) of asbestos, which has good heat resistance and also good mechanical strength. However, environmentalists and others are demanding a reduction or elimination of asbestos in wear parts such as friction materials. There has been a great effort to develop friction materials using substitutes for asbestos. Some substitutes used are metallic fibers, carbon fibers, iron powder, cast iron powder. But these products are very heat conductive and do not have the insulating ability of asbestos; this accentuates the phenomenon of oil boiling in the brake cylinder. In order to eliminate the disadvantage of metallic backplates, organic backplates have been developed which comprise layers of cloth bonded by a resin, as shown in **French Pat. No.1,347,812**. These laminated backplates are then bonded to the friction material and have the advantage of decreasing the weight of the pads since the specific gravity of the organic material forming the backplate is only 2. These brake pads are somewhat difficult and expensive to manufacture, since the back plate must first be completely formed and then be trimmed to size before bonding to the friction material.

A method is provided for pressing and forging hot metal powder directly in one operation into a high density metal article of a finished worked shape. The method uses a simple shaped, readily deformable container with loose metal powder therein and substantially closed to allow the powder to evolve its own protective atmosphere during preheat while permitting some

gases to escape. The powder-filled container is pressed and forged in one operation in a preheated die cavity resulting in a high density article of a homogeneous composition. The invention is also well suited for cladding powder forged articles and producing composite articles from multiple powder alloys. The invention is particularly useful with powders of aluminum and its alloys.

US Patent 4069042 describes, in accordance with the present invention, an improved method for forging metal parts from metal powder, eliminating any need of degassing a closed metal container with metal powder therein, of compacting and repressing into an intermediate shape, and of removing the deformed metal container after forging. The invention generally includes placing in a metal container of light gauge metal foil loose metal powder. The container, of the general simple shape related to the article to be forged, is substantially closed with a cover during heating to contain the powder and to shield the powder from contamination. The cover also permits the powder to generate its own protective atmosphere during preheating while permitting some gases to escape from the container. The amount of metal powder put into the container is in excess of the metal needed to forge the article to a predetermined density and is heated to a uniform temperature to facilitate metallurgical bonding. Forging of the powder-filled container into an article of at least 0.99 relative densities is done within closed dies having limited relief for flash. Such an uncomplicated method provides a forged article having a homogeneous composition when the container and powder are of the same composition. Cladded forged articles from metal powders are obtained when the metal container and cover are of an alloy that is different from the metal powder but is compatible as it bonds with the forged metal powder to form a composite product. Composite forged articles are also obtained by placing multiple powder alloys in the metal container. Thus the method facilitates forging metal powder without the need for complex multi-action tools or intricately shaped containers and provides forged powder metallurgy parts having improved mechanical properties and/or metallurgical characteristics over conventionally forged powder metal parts.

US Patent 6093482 describes a carbon--carbon composite for friction products comprising of an outer frictional part and a load bearing structural part supporting the frictional part. The frictional part contains a mixture of carbon fibers, pitch powder and graphite powder, whereas the structural part is comprised of a pack of alternating layers of the mixture and layers of one member selected from the group consisting of carbon fabrics, carbon-based prepregs and carbon-based, segmented prepregs. The carbon--carbon composite is formed by way of alternating piles of layers of a mixture of carbon fibers, pitch powder and graphite powder and layers of one member selected from the group consisting of carbon fabrics, carbon-based prepregs and carbon-based, segmented prepregs one above the other to provide a preform,

heating and pressing the preform within a mold to obtain a green body, carbonizing the green body to prepare a carbonized body, impregnating the carbonized body with pitch powder and recarbonizing the impregnated body, and subjecting the impregnated and recarbonized body to chemical vapor infiltration with hydrocarbon gas.

US Patent 4946647 discloses a process for the manufacture of aluminium-graphite particulate composite using uncoated graphite particles for automobile and engineering applications. In the process the aluminium-alloy melt is treated with a reactive metal to increase the wettability of the alloy and the graphite particles. Further treatment of the melt and gradual addition of activated graphite powder and stirring at about 500 to about 600 r.p.m. at a temperature of about 700° to about 720° C. results in the composite.

EP0539011 relates a light metal alloy composite having a nickel coated graphite or carbon with a nickel-containing intermetallic phase within a portion of a casting. A mold is provided to cast a light metal into a predetermined shape. A nickel coated carbon phase structure is placed into a portion of the mold. The light metal is cast into the mold around the carbon structure to wet an interface between the light metal and the nickel coated carbon structure. A nickel-containing intermetallic phase is formed in the light metal proximate to the nickel coated carbon to provide increased wear resistance. The light metal is then solidified to form the metal matrix composite.

EP0567284 describes an aluminum-base composite material. The aluminum-base material contains a uniform distribution of carbide particles and lubricating phase particles such as carbon or graphite. The carbide particles increase hardness for improved wear resistance. The lubricating phase particles provide improved wear resistance and especially improve unlubricated wear resistance under increased loads. Finally, a dispersoid of nickel aluminide intermetallic phase may also be used to provide additional hardness and wear resistance. The composite is formed by introducing carbide particles and lubricating phase such as graphite into a molten aluminium alloy to neutralize buoyancy and to form an aluminum-base mixture. Stirring the aluminum-base mixture to uniformly distribute carbide and carbon particles throughout the molten aluminium. Carbide and carbon particles counteract each other to remain uniformly distributed throughout the aluminum-base alloy despite prolonged holding or cooling times.

2.13.1 Business survey reports

2.13.1.1 BCC research: AVM028C reports highlight 'The friction products and material - market'

The North American friction products and materials market was worth $6.9 billion in 2006. By the end of 2007, the market will be worth slightly less, taking a dip to $6.8 billion. By the end of 2012, the market will be worth 7.7 billion with a compound annual growth rate (CAGR) of 2.6%.Ground transportation will maintain the highest share of the market throughout the forecast period. By the end of 2006 the market was worth $3.9 billion, 57.3% of the market. By 2012, this share will drop slightly to 55.8%.The aircraft and aerospace sectors of the market remain the fastest growing, with a 4.5% CAGR throughout the forecast period.

2.13.1.2 BCC research: AVM028D reports highlight 'The friction products and material market'

Provides in-depth analysis of the North American market for friction products and materials in light vehicles, medium- and heavy-duty trucks, aircraft and other industrial applications. Forecasts trends and sales in the North American market for friction products and materials though 2014, broken down by ground transportation, aircraft/aerospace and industrial sectors. Assesses the underlying economic issues driving the friction products and materials business. Analyzes social, political and regulatory issues influencing the industry. Discusses new and potential products. Profiles top players within the industry.

2.13.1.3 Bharat Book Bureau: ISBN000046784G provides report on '2009 World market friction material and articles thereof'

This report was created for strategic planners, international marketing executives and export managers whose primary concern is the world market for friction material and articles thereof. With the globalization of this market, managers can no longer be contented with a local view. Nor can managers be contented with out-of-date statistics that appear several years after the fact. I have developed a methodology, based on macroeconomic and trade models, to estimate the market for friction material and articles thereof for those firms serving the world via exports and foreign direct investment. It does so for the current year based on a variety of key historical indicators and econometric models. In what follows, this report begins by summarizing the world exporter's market for friction material and articles thereof. The total level of exports on a worldwide basis is based on a model that aggregates across over 150 key country markets and projects these to the current year. From there, each country represents a percent of the world market. This market is served from a number of competitive countries of origin. Based on supply-side dynamics, market shares by country of origin are then calculated

across each country market. These shares lead to a volume of import values for each country and are aggregated to regional and world totals. In doing so, we are able to obtain maximum likelihood estimates of both the value of each market and the shares that competitors (countries serving that market) are likely to receive this year. From these figures, world rankings are calculated to allow managers to prioritize markets. In this way, all the figures provided in this report are forecasts that can be combined with internal information for strategic planning purposes. Of the 150 countries considered, if a country is not reported here it is therefore estimated to have only a negligible level of trade in friction material and articles thereof (i.e. their market shares are close or equal to zero percent). "Friction Material and Articles Thereof" as a category is defined in this report following the definition given by the United Nations Statistics Division Classification Registry using the Standard International Trade Classification, Revision 3 (SITC, Rev. 3). The SITC code that defined "friction material and articles thereof" is 66382 .This report is updated on an annual basis.

2.14 Applications

The application of metal matrix composites (MMCs) in many engineering components has generally increased over the last few years, particularly in the automobile industry. It is mainly due to the ever-increasing restrictions on the fuel consumption and pollutant emission which have forced the automotive manufacturers to look for new light weight materials for automobile components suitable for saving fuel. Among the various manufacturing processes available for MMCs production, liquid metallurgy technique is the most economical one and allows fabrication of very large sized components required for automobile parts. The amount of scraps (feed heads, runners and rejected components) generated during manufacturing MMC products by liquid state process will increase as the world consumption increases. According to Business Communications Company (BCC) market survey 1999, the world market for MMCs reached 2.5 million kg valued at $102.7 million. BCC projects a rise of 4.9 million kg valued at $173.3 million during the next five years corresponding to a 14.1% AAGR (average annual growth rate) from 1999 through 2004 **[131,153]**.

Chapter 3

FORMULATION OF PROBLEM

Friction materials which are being used in brake linings/ brake shoes/brake discs/ clutches are meant for deceleration or stopping a vehicle or a mechanical device. Early friction materials contained asbestos, which has been found harmful for the human health and their use has been gradually prohibited. Therefore, these friction materials are replaced with non-asbestos organic friction materials, semi-metallic and metallic friction materials that are asbestos free. In the recent decade powder metallurgy has been developed greatly, however only a few commercialized P/M (Powder/Metallurgical) components namely sintered and heat treated automotive components such as cam shaft pulleys, cam shaft and crank shaft gears, cam shaft lobes, oil pump gears, transmission components including synchronizing rings, water pump impellers, bearing caps, battery terminal clamps, sintered and heat treatment components for business machines, computer equipment such as pulleys and gears, powder forged components for high cyclic stress environments such as connecting rods in internal combustion engines, automotive suspension ,brake components, recording heads in video and audio tape recorders and disk drive components in computers and related equipment are found in the market **[US.P5902943].**

The present work relates to the first time development of aluminium powder- based metallic friction and back plate materials for brake pads/stators employing cold compacting and hot powder forging. Such pads are expected to have improved performances than resin bonded ones which are being commercially used in light/medium/heavy duty vehicles and these might also substitute iron based AN-32 aircraft rotor brake pads.

3.1 Features and limitations of existing friction materials

There are following types of available friction materials:

i) Sintered metallic friction materials (Fe and Cu based)

ii) Resin bonded friction materials

iii) Carbon-Carbon (C/C) friction materials

iv) Aluminium based friction composites for brake rotors/counterface.

It may be noted that Al-based friction pads for stators have not been made owing to the limitations of processing of such materials which have been highlighted in **section 3.2.1, pp. 97.**

3.1.1 Sintered metallic friction materials (Fe and Cu based) [34,48,RR1,US.P5841042]

These types of brake materials were introduced in late 1930's and comprise of either iron or copper matrix. They are also often called metallo-ceramic or cermet friction materials since they involve ceramics constituents. Iron and copper based metallic friction materials are manufactured though conventional powder metallurgy process using compacting and sintering **[34,48,157,RR1,US.P4415363,US.P5841042].** Sintered friction materials contain metallic and nonmetallic constituents in varying proportions. Variety of shapes can be produced, for various kinds of brake applications. The constituents in these materials are divided into three sub groups: i) metallic base (matrix) with alloying elements to provide load carrying capacity and thermal shock resistance; ii) friction additives to raise coefficient of friction and, iii) anti-scuffing additions or solid lubricants which prevent seizure and sticking b/w rubbing parts to ensure even friction and wear resistance **[82,87,162].** Different metallic constituents such as Tin, Copper, Ferro alloys etc. (in the range 50-80 wt.%) constitute the metal matrix; ceramics and non-metallics like Al_2O_3, SiO_2, ZrO_2, SiC, B_4C, WC, Bentonite, Asbestos, Spoudumence, Feldspar, Kayaniteand etc. (in the range 20-28 wt.%); and solid lubricants like graphite, MoS_2, Sb_2S_3, $CaSO_4$, $BaSO_4$, BN etc. (in the range 5-25 wt.%) are blended/mixed either wet or dry. The powder mixture is cold compacted followed by pressure sintering with steel backing plates. There are two principal types of applications or operating conditions for metallic friction materials namely "wet" and "dry". Under wet conditions, the friction components, such as clutch in power shift, automatic transmissions and brakes are immersed in oil. Dry operating conditions involve direct contact of friction components with brake rotor/counterface such as in aircraft brakes **[14,50,81,157].** Sintered metallic friction materials have been used as brake disks, especially for heavy-duty applications, because of their good braking performance and low wear rate under high temperatures **[48,157].**These have been developed for very high power input densities. For example, solid-state-sintered bronze and mullite linings are used in racing cars and high-speed railroad brakes. Sintered iron with graphite is used in some of the heavy-duty brakes in civilian/military aircrafts and as well as in few drum brakes of passenger cars drum brakes **[18,182].** Multiple-disk brakes have alternating rotors and stators forced against adjacent members by hydraulic pressure. Metallic friction materials are also used in other heavy-duty applications, such as clutch facings in tractors, trucks, earth-moving equipments and heavy presses.

The most widely used metal matrices for heavy-duty friction materials are copper and bronze where service temperatures are less than 600 °C. Iron matrices are used where service temperatures are likely to exceed 1100 °C **[14,157].** Cu based materials are better at low to

medium brake load conditions whereas Fe base are suitable for severe conditions. Fe-based alloys are known for low wear loss and better frictional stability, while Cu-based alloys display a "fade" phenomenon under higher load and speed conditions **[143,144,157].** Normally, the density of Fe based friction materials is in the range of 5-6.1 gm/cc, hardness lies in between 80-105 HRF, and a friction coefficient in combination with cast iron is 0.34–0.40; whereas Cu based friction material has density of 7.0–7.5 gm/cc, hardness 30–40 HB, and a friction coefficient of 0.28–0.30 in combination with chromium-plated steel **[81,157].**

3.1.1.1 Features of Fe based sintered friction materials

Iron matrix based friction materials are considered due to its stability at higher temperature (900 °C) and their use under heavy dry operating conditions because of high melting point and other improved properties such as strength, hardness, ductility and heat resistance **[US.P4311524,US.P4391641,57,157].** There is wide spread use of sintered iron-based friction materials intended to operate under both dry friction and liquid lubrication conditions **[US.P4311524,57].**

(i) Sintered (porous) friction materials consist of metallic and non-metallic components. Metallic components endow the material with strength, whereas non-metallic components enhance the coefficient of friction and decrease the jamming tendency and provide smooth engagement, increase wear resistance**[57,157,US.P.4311524].**

(ii) A thin tribolayer is formed over the sintered friction material during engagement process. The plasticity and viscosity of such a layer depends upon its constituents. This layer is plastic at room temperature and also at elevated temperature in comparison to the bulk of the friction material. It provides a uniform gradient of mechanical properties and prevents over deformation **[US.P4311524,36,56,57,157]**

(iii) Friction materials based on iron are intended mainly for transmission and braking devices of machines and systems that operating under "dry" friction condition. These are suitable at higher temperatures than copper based friction materials **[157].**

(iv) Heat resistance is higher, so it retains their tribological properties on heating up to 1100 °C **[157].**

(v) With limited thermal conductivity, but high temperature stability, it is suitable for heavy duty braking applications **[US.P5841042].**

(vi) It has higher coefficient of friction range: 0.30-0.60 **[157].**

(iv) Strength /weight ratio is excellent **[US.P5620791]**.

3.1.1.1.1 Limitations of Fe based sintered friction materials

(i) With a poor adhesion of the hard particles and the base material, these harder particles, may crumble out at high sliding speeds, and when engrossed in the friction zone, can result in an increased wear **[US.P5841042,157].**

(ii) Chemical reactivity amongst friction constituents at high temperature is increased.

(iii) Processing is not possible in normal environment under elevated temperature range due to formation of oxides of low melting point ingredients and their chemical reaction with matrix materials. It requires inert or reducing gas to generate a special environment during sintering/forging at higher temperatures **[47,48,157].**

(v) Repetitive heating and cooling during engagement and disengagement of brake and rotor/counterface, resulting change in the microstructure of contact surface and then transforms into hot spot and brittle martensitic layer. At high speed, it separates from friction material and automatically loses the tribological property (fading) **[US.P5841042,115].**

(vi) Distribution of ingredients in matrix material is heterogeneous due to different flow characteristics of individual constituents consisting of powder particles **[157].**

(vii) Requires homogenization and or annealing, repressing at higher temperature to adjust its density**[157].**

(viii) Processing is lengthy and complex leading to increased cost of fabricated product **[US.P4069042].**

(ix) Friction layer is joined with wrought steel plate (backing plate) by two stage pressure sintering. The joint is often poor and may be separate in actual operation **[US.P4350530, US.P4391641,157].**

(x) Constituents of the backing plate and friction layer are so different that during brake application, the layers might separate due to differing thermal properties. Heat transfer across backing plate is poor leading to excessive temperature rise in friction layer which might deteriorate tribological properties of friction layer.

(xii) While grey cast iron rotors generally possess sufficient mechanical and thermal properties to satisfy requirements of disc brake systems, they are relatively heavy and for passenger car and light truck applications, can each weigh upto approximately 30 pounds. Since rotors are considered rotating mass and unsprung mass as well as being part of the total mass of the vehicle, the weight of the rotor adversely affects the performance and fuel economy of a vehicle **[US.P5620042].**

(xiii) Limited thermal conductivity of matrix metal leads to poor heat transfer capability of brakes.

3.1.1.2 Features of Cu based sintered friction materials

(i) Copper-based alloys are selected for use as a medium duty friction/bearing material according to conditions such as oil lubricating conditions, sliding speed and sliding contact surface pressure. These are also known for improved properties such as strength, hardness, ductility and heat conductivity **[US.P7087318, 157].**

(ii) Higher thermal conductivity of copper based friction material improves heat transfer rate from friction material to backing plate. It accordingly improves heat stability and stabilizes coefficient of friction **[US.P6068094].**

(iii) It does not lose the tribological properties on heating up to 600 °C during brake application **[157].**

(iv) These materials also resist corrosion under sulfur environment **[US.P5824923].**

(v) It exhibits a much higher stability to oil additives **[US.P5824923].**

(vi) It can stably maintain a high coefficient of friction exceeding about 0.2 under wet type sliding and exceeding 0.4 under dry type sliding, which has a difference between the coefficient of static friction and the coefficient of the dynamic friction of at most 0.1, and which can solve the problem of vibration, chattering, creaky noise or the like at the time of sliding can be obtained in a highly economical manner **[US.P5824923].**

(vii) These materials are more suitable for heavy duty clutch plates due to their good wear resistance and precise adjustment of coefficient of friction Better properties of friction material have been obtained due to partial substitution of the main matrix component (copper powder) with copper coated graphite fibers (copper coating is done by an electrochemical method) **[US.P5824923].**

(viii) Good seizure resistance, wear resistance and heat resistance **[US.P7087318].**

(ix) Cu based sintered friction material exhibits a coefficient of friction of 0.3 with thermal stability and without seizure when it slides against titanium or titanium alloy in the atmosphere **[US.P6068094].**

3.1.1.2.1 Limitations of Cu based sintered friction materials

(i) It is conceivable that the frequent occurrence of galling accompanied by abnormal abrasion under high speed and high surface pressure sliding conditions is attributable to occurrence of agglutination/adhesion and its rapid growth caused by contact between the metals in boundary lubrication**[US.P7087318].**

(ii) It is used in combination with a brake rotor which is made of titanium or titanium alloy only **[US.P6068094].**

(iv) The brake pad of copper based friction materials for a rotor of cast iron, steel or stainless steel can not be used for an untreated surface of a disc rotor of titanium or titanium alloy, because heat resistance and abrasion resistance are insufficient **[US.P6068094].**

(v) The copper based sintered friction materials exhibit a lower coefficient of friction range: 0.25-0.35 **[157].**

(vi) In a condition where, among others, sliding speed is high, or where acceleration and deceleration are repeated with changes in the rotating (sliding) direction so that sliding speed greatly changes, or where the mating material has high surface roughness, wear resistance will rapidly increase and as a result, sufficient durability cannot be ensured for long use **[US.P7087318].**

(vii) To achieve high density and strength, repeated (two times) compacting/ shaping/ sintering is recommended, that increases wear and abrasion resistance **[US.P6068094].**

(viii) It can be used use as a bearing material **[US.P7087318].**

(ix) In copper based sintered friction material, the hard particles or the friction adjusting agent become loose and fall out from the grain boundaries of the sintered material (especially from the triple point of grain boundaries) at the time of friction sliding, and thus form an abraded powder, which powder attacks the counterpart or the sintered friction material itself, causing seizure or damage due to wear **[US.P5824923].**

(x) The hard particles or the friction adjusting agent do not have an appropriate grain diameter, and are not dispersed uniformly in the copper based matrix. Therefore, it is difficult to realize a stable coefficient of friction of at least 0.2 under wet type sliding and at least 0.4 under dry type sliding, which values are required of the high performance friction material **[US.P5824923].**

(xi) Graphite does not react to a bronze based or lead bronze based sintered material, markedly restrains the sinterability of the sintered compact, weakens the strength of the sintered material, and is hardly wet by Sn rich and Pb rich liquid phases which are generated during sintering. Therefore, addition of graphite presents the problem that sweating becomes significant during sintering, producing a number of melt-off pores. In addition, boundary lubrication is promoted by the facts that as the amount of residual graphite increases, it becomes more difficult to compact the sintered layer and that graphite is a porous substance. In consequence, sliding properties under high-speed oil lubricated conditions cannot be improved as much as expected **[US.P7087318].**

(xii) Poor wettability of copper based friction material with steel backing plate, resulting improper joining which often causes for debonding during operation.

3.1.1.3 Features of resin bonded friction materials

(i) The resin bonded friction material based brake pads with stable coefficient of friction are used in heavy/medium/light and clutch facings.

(ii) Preferably phenolic resin is used in friction materials because of good combination of thermal and mechanical properties and low cost **[29]**.

(iii) Phenolic resin-based friction materials are widely used in automobile and aviation industries, due to their high specific strength, low density, and good cost-effectiveness of raw materials. Various reinforcing and filling constituents such as fibers, abrasives, binders, and friction modifiers (solid lubricants) are also incorporated in phenolic resin-based friction composites for the purpose of increasing the stability and wear resistance.

(iv) It has an average coefficient of friction range: 0.34 to 0.48 **[150].**

(v) It maintains a constant coefficient of friction and lower wear in a narrow range of operating temperature: 125 to 225 °C.

(vi) It can be used satisfactorily in relatively large-scale and high-powered power transmission assemblies due to good frictional behavior.

(vii) It has good specific heat capacity: 0.85-1.5 kJ/(kg K) **[150].**

(viii) Thermal expansion coefficient is lower: $7X10^{-6}$/K than sintered friction material (P/M): $10\text{-}14X10^{-6}$/K **[150].**

(ix) Porosity of resin bonded friction material (<1 %) is less than porosity of sintered friction material (7-8 %) **[150].**

(x) It can absorb a substantial amount of frictional energy while maintaining a substantially constant coefficient of friction.

(xi) It is not subject to significant charring or burning within the narrow operating temperature range.

(xii) Noise level is relatively lower than metallo-ceramic pads.

(xiii) Product cost is low and R/M are easily available.

3.1.1.3.1 Limitations of resin bonded friction materials

(i) Poor stability of resin based friction materials under moisture-based environment is a serious concern, which limits their applications. During manufacture of organic based friction materials, it is essential that all water should be removing from the composition of materials before curing the resin binder contained therein. If the water content is greater than 2 wt.% of the composition of materials, the heat required to cure the resin in the composition of materials by evaporating the water can cause bubble marks and/or voids adjacent to the surface of the friction materials **[US.P4203936].**

(ii) Resin-based friction materials are subject to significant limitations. A most important limitation relates to the customary inclusion of cellulose fibers, which tend to char and/or burn readily at the temperatures frequently encountered in the operation of friction engagement devices. As a direct result of this charring and burning characteristic, the coefficient of friction of friction materials tends to decline dramatically under heavy-use conditions **[US.P5830309].**

(iii) The tribological application of resin-based friction materials is usually limited owing to the relatively poor stability and wear resistance **[189,190].**

(iv) It shows frictional and wear stability up to 225°C only. There is a drastic increment in coefficient of friction and wear loss with rising temperature up to 325 °C, followed by a sharp decrease in coefficient of friction at 425 °C, leading to a severe thermal fade.

(v) Strength/weight ratio is low.

(vi) Thermal conductivity is lower: 1-2 W/ (mK) than sintered friction material (P/M): 3-15W/ (mK) **[150].**

(vii) Resin bonded materials have poor mechanical characteristics in comparison to metallo-ceramic pads.

(viii) These are also likely to crack during severe applications **[60].**

(ix) These have very poor recovery and higher levels of fading **[29].**

(x) An adhesive chemical is used for joining resin bonded friction material to metal base back plate, which impairs the heat transfer characteristics.

(xi) Density of the dry asbestos as compared to the other ingredients in the composition of materials requires substantial mixing before a uniform composition of materials is obtained. Unfortunately, such mixing causes a portion of the asbestos to become airborne and pollute the surrounding environment. Often the amount of such airborne asbestos exceeds the allowable limits set in the United States by the Occupation Safety and Health Act of 1970. In an effort to maintain the quality of air within the allowable limits, most manufacturers have discovered that extensive air filtration systems are required in existing structures **[US.P4203936].**

(xii) Incompatibility of friction layer with back plate owing to different class of materials employed **[US.P4173681].**

(xiii) These brake materials have poor shelf life owing to degradation of phenolic resin **[29].**

(xiv) Average coefficient of friction is limited to 0.35 only which is lower than international standard set for Asian region about >0.45.

(xv) Pads have poor performance under moisture owing to swelling and degradation **[121].**

Although a conventional organic lining material for such a heavy-load braking device, which is bound by a phenolic resin binder, is not so costly, its mechanical strength is relatively low and it wears away steeply under heavy load conditions, which causes the abrupt decrease of its coefficient of friction. Particularly, when the temperature of the lining material reaches 300 °C or higher due to frictional heat, the phenolic resin binder carbonizes or decomposes and because of this, the coefficient of friction of the lining material decreases rapidly and its wear resistance deteriorates substantially **[US.P. 5841042].**

(xvi) Resin based brake pads have poor performance under moisture owing to swelling and degradation **[30].**

3.1.1.4 Features of carbon-carbon (C/C) friction materials

(i) Carbon/carbon friction material is used in heavy duty applications such as in military/commercial aircrafts and racing cars. They are light in weight; possess lower wear, high temperature stability and a higher reliability under extreme braking conditions **[157].**

(ii) They can be used in other vehicles (aeroplane plane) where significant reduction in weight, desired performance is challenging, and cost is secondary **[14,US.P 6093482].**

(iii) Usually the density of C/C friction materials is in the range of 1.7 - 1.9 gm/cc **[14,157].**

(iv) It has excellent thermal conductivity **[US.P 6093482].**

(v) It has much higher temperature strength, chemical strength and somatological aptability **[US.P 6093482].**

(vi) Heat capacity of carbon is 2.5 times greater than steel, the kinetic energy from aircraft can be converted into heat and stored in the C/C brake heat sink, and this heat is dissipated slowly to prevent melting of nearby metal structure **[157].**

(vii) It has high mechanical strength comparable to steel at high temperatures **[157].**

(viii) It can be used at temperatures more than 3000 °C under an inert gas environment **[US.P 6093482].**

(ix) Elemental carbon in general and carbon particles in particular are known to provide desirable frictional characteristics, good burn resistance, high energy capacity, and a satisfactory coefficient of friction value.

(x) Due to their inherent property of lightweight, high strength and increased heat conductivity, the carbonic composites are spotlighted in a frontier industry, which often requires a new material of highly enhanced property **[US.P 6093482].**

3.1.1.4.1 Limitations of carbon-carbon (C/C) friction materials

(i) The major disadvantages are oxidation behavior under high temperatures. There is no fundamental understanding of oxidation kinetics of the C/C composites **[157].**

(ii) During application, cracks are formed due to lower thermal expansion.

(iii) Porosity is around 13% **[157].**

(iv) Weight loss is higher due to wear and oxidation.

(v) Environmental concerns imposed further limits on the use of molybdenum **[US.P 5830309].**

(vi) It involves costlier raw materials as well as costly and complex material processing.

(vii) It is acceptable for certain specialized applications only because it is relatively expensive and difficult to manufacture **[US.P 5830309].**

(ix) Carbon-Carbon and C/SiC aircraft brakes suffer from 'morning sickness', a condition of low friction after standing overnight in damp conditions **[30].**

3.2 Features of Aluminium based friction materials

(i) Aluminium alloy/pure aluminium powders are mixed homogeneously with refractory ceramic material. It provides a composite, which is non-degradable and has improved thermal conductivity **[US.P5372222, US.P4409298]**.

(ii) Aluminium based castable friction material composites have an average dynamic coefficient of friction greater than 0.2 and have utility in low and high load applications **[US.P4409298].**

(iii) Aluminium based composites are suitable for brake rotors or clutches, characterized by high structural stability, high strength, minimum adverse effects due to galling and high temperature stability **[US.P6918970, US.P5028494].**

(iv) It provides a composite brake rotor which is substantially lighter in weight than conventional rotors; weight reduces from 15 to 42 and has a positive effect on fuel economy when utilized on motorized vehicles **US.P5372222, US.P5620042, 108]**.

(v) Strength/weight ratio is excellent **[US.P5620791, US.P4946647].**

(vi) Al based friction material is adequate for most a applications as long as the thermal energy generated during brake application is below 482 ^{0}C **[US.P5372222, US.P5339931].**

(viii) Temperature rise at contact surface during braking is low due to high thermal conductivity (k_{al} = 4 to 7 k_{fe}) **[US.P5372222,US.P5325941]**.

(ix) It results in stable contact surface, which improves the brake performance **[US.P5372222]**.

(viii) The reduced brake pad temperature is also thought to reduce brake fluid boiling and disintegration **[US.P5325941, US.P4173681]**.

(ix) The characteristics of aluminium based composites are especially suitable for racing car and aero plane braking systems **[US.P4946647]**.

(x) It reduces the noise, vibration and harshness (NVH) **[US.P5620791].**

(xi) Aluminium and its alloys are extensively used in a large number of industrial applications due to their excellent combination of properties, e.g. high strength to weight ratio, good corrosion resistance, better thermal conductivity, easy to deform etc. Casting is easy due to low melting point of aluminium matrix **[US.P4946647, 192]**.

(xiii) It is easy to recycle.

(xiv) Effective cost is low.

(xv) It shows self-lubricating properties.

(xvi) It provides coefficient of friction about 0.38-0.42 when an operational temperature of 40° to 450° C

3.2.1 Challenges in development of Al-based brake pads

Recent efforts to improve the fuel economy and emissions levels of air and ground vehicles have created a need for new materials which can provide weight savings to the vehicle without sacrificing performance levels. The immediate desirability of such materials is enhanced when the weight savings can be achieved by directly substituting the materials for current materials in existing designs. Moreover, the long-term desirability of such materials is maximized when the unique properties of the materials provide the possibility of improved designs and performance for vehicle components. There is no ideal material for friction elements that can successfully perform under all the conditions. Furthermore, there is no single material chemistry, which can be selected for such varying situations. The only solution is therefore to design friction elements based on composites where each constituent while retaining its basic features is able to perform quantitatively and qualitatively under varying conditions imposed by environment and mechanical device. In the present chapter, we have attempted to cover the features including limitations of existing friction materials and thereby tried to evolve the scope of present investigation.

The main challenges in the development of Al-based brake pads are as follows:

(i) It is not considered for use as brake pads/stators due to inferior tribological properties such as softness, unacceptable wear of the braking surface material that is brought to bear against the brake lining or disc brake pads, thermal distortion due to high heat transfer and poor anti seizure resistance and bonding **[US.P5407035,US.P5712029]**

(ii) Poor wetting between aluminum-base alloys and graphite prevents formation of adequate graphite/aluminum bonding. Furthermore, graphite particles, having a density of 1.8 g/cm ^{3} , have a tendency to "float" in the molten aluminum (density 2.7 g/cm ^{3}). Badia et. al, in U.S. Patent No. 3,753,694, disclosed a method of subjecting nickel coated graphite to a vortex in an aluminum bath in an attempt to overcome casting problems. When using the method of Badia et. al, continued mixing in combination with solidification prior to dissolution of the nickel coating is required to limit flotation of graphite particles. In fact, the main reason the vortex method has never received widespread use is that during casting, the nickel coatings quickly and completely dissolve leaving uncoated graphite particles that float in the melt. The castings resulting from the vortex method have a distinct heterogeneous and unworkable distribution of graphite particles **[EP0567284].**

(iii) Alternative substitutes for metal coatings such as copper and nickel that provide wetting with aluminum have been attempted. Rohatgi *et al.*, in U.S. patent No. 4,946,647 and Komura et. al, in U.S. patent No. 4,383,970 disclose use of additives to promote wetting of carbon particulate with aluminum. However, the methods have not achieved commercial acceptance due to the graphite density in relation to the aluminum alloy remaining a problem. Despite the improved wetting achieved by addition of additives, graphite particles continue to float during casting and solidification **[EP0567284].**

iv) Aluminum-silicon carbide composites have been proposed for use in several automotive and aerospace applications. The problem with casting aluminum-silicon carbide composites is that silicon carbide tends to settle to the bottom of the melt during holding of the melt or during prolonged solidification. The settling of silicon carbide particles in aluminum-base alloys tends to limit holding times of molten metals. Furthermore, the settling of silicon carbide limits the maximum cross-section that may be cast for aluminum-base silicon carbide composites **[EP0567284].**

(v) Skibo *et al.*, in U.S. Pat. No. 4,865,806, teach oxidizing of silicon carbide particles surfaces prior to mixing the oxidized particles in an aluminum alloy to promote wetting of the silicon carbide partides by the alloy. Certain alloy additions which promote the wetting of silicon carbide particles are also preferred. Stepped alloying has also been proposed by Skibo et. al in U.S. Pat. No. 5,083,602. Badia et. al, in U.S. Pat. No. 3,885,959, also produced silicon carbide particulate reinforced melts by mixing nickel coated silicon carbide with molten aluminum. In the Skibo case the surface oxidation and the alloying elements in the melt did not materially alter the 3.2 g/cm ^{3} density of the silicon carbide particles or the density of the aluminum melt. Likewise in the Badia

method, the nickel dissolves off the SiC in to the melt and silicon carbide particle specific gravity remains unchanged. Having an opposite effect in comparison to graphite particles in Al alloys, silicon carbide particles (density 3.2 g/cm^3) tend to settle during casting and solidification of aluminum composite alloys **[EP0567284].**

(vi) Many powder metallurgy routes have also been used to make hybrid composite materials. For example, A. Shibata in U.S. Pat. No. 3,782,930, proposes a partially molten reactive sintering process wherein TiC and graphite are formed. Also, Hagiwara et. al, in U.S. Pat. No. 4,959,276, disclose Al_2O_3 + graphite particulate aluminum matrix composites formed by blending powders of the three constituents and hot extruding or pressing. While these powder methods may form a desirable end product, they are prohibitively expensive to produce **[EP0567284].**

(vii) Welding or casting of aluminium based friction materials with steel back plate is not possible, that limits its application as dry friction materials in brake pads/stators.

(ix) It loses mechanical properties at high temperature **[US.P5620042].**

(x) Machining is difficult **[US.P4661154].**

(xi) Due to fast heat transfer and repeated heating and cooling under braking application, contact surface become brittle with formation of aluminium carbide/oxide. The aluminium carbide/oxide thin film separates in form of coarse particles during braking and enhancing sticking, galling and seizing.

(xi) Sintering of Al powder based materials leads to negative densification parameter (i.e. sintered density is lower than green density) and in presence of porosity in the final product, problems as high lighted under (ii), (vi), (viii) and (x) as above aggravate. The difficulty in sintering metal powders is a consequence of the surface oxide film over the surface of Al powder particles. This oxide film is a barrier to sintering because it inhibits inter particle welding and the formation of effective inter particle bonds. The problem is particularly severe in aluminium because of the inherent thermodynamic stability of the oxide (Al_2O_3) and impractical for making sound failure proof brake pads out of Al-based materials **[US.P5902943].**

(x) Casings made with the Al MMCs is expensive compared to the costs of castings made from grey cast iron **[US.P5902943].**

(xi) Al powder degassing is essential to control residual porosity in the product. According to the conventional practice, the green compacts are enclosed in welded cans and degassed. At the completion of the degassing treatment, the cans are sealed to retain the vacuum and then subjected to a combination of high temperature and pressure (hot working). Such type of process is obviously complicated: in addition to the fact

that it is time consuming and costly. Furthermore, it is difficult to obtain net shape in a single forming operation.

(xii) The disc brake rotors constructed of aluminium powder have not been introduced commercially because of poor wear resistance. Such wear often promotes unpredictable braking characteristics.

(xiii) Welding or casting of aluminium based friction materials with steel back plate is not possible, that limits their applications as dry friction materials in brake pads/stators.

3.3 Objectives of the present study

Iron based or Cu-based metallic brake pads are manufactured using compaction and sintering of powder mix. However, Al powder-based brake pads, which are also metallic, still remain unexplored due to the difficulties being faced in Al-powder compaction and sintering.

To develop Al-based brake pads, the objectives of the present study are:

1 To adopt the 'Preform Powder Forging' technique in manufacturing the Al Powder based friction materials to overcome the difficulties of Al powder compaction and sintering.

2 To obtain new set of aluminium powder-based friction materials.

3 To improve upon the anti seizure resistance, hardness and strength of existing aluminium based composites, so as to make them usable in brake pads.

4 To avoid the formation of oxide layer and sticking of powder with die during processing using coarse powder (>200 mesh) of irregular morphology, incorporation of coarse SiC powder and flaky graphite powder in bulk with matrix material.

5 To avoid the requirement of special environment such as inert/vacuum during compacting and sintering to achieve the desired densification using 'Preform Powder Forging' technique and incorporation of selective ingredients.

6 To eliminate the requirement of heat treatment of products after hot forging.

7 To improve the wear rate with high densification of product during cold compacting and hot forging.

8 To avoid the brittleness at contact surface due to fast heat transfer and repeated heating and cooling under braking application by incorporation of ingredients.

9 Sintering of aluminium powder is overcome by selection of size of matrix powder and ingredients.

10 To produce brake elements in desired shape and size to replace the existing and commercially used resin bonded brake pads/stators from light/medium/heavy vehicles and iron based rotor from AN-32 aircraft.

11 To produce brake pad with in built backing plate with adequate adherence to eliminate the problem of joining of backing plate with braking pad material by use of same matrix material for back plate.

12 To allow the use of economical powders as compared to powders required in existing technology.

13 To reduce ceramic content without sacrificing end properties, in turn resulting in and simplification of chemistry.

14 To improve thermal conductivity of the product thus extending life of the friction elements.

15 To reduce brake fading and improve recovery characteristics of brake pad materials at high temperature.

16 To characterize the brake pad materials and compare their performance with resin bonded brake pad materials.

17 To improve upon the quality of product as produced by sintering technique.

18 To reduce failure rate of the product due to breakage and warpage of the product.

19 To economize processing with improved product performance.

20 To avoid use of sophisticated and costly custom built equipments.

21 To develop low cost processing technique.

22 To eliminate machining process.

3.4 Work plan

To fulfill the above objectives, the detailed plan is as follows.

(i) **Procurement of raw materials**: to begin with, the study the following raw materials are required:

a) ~~electrolytic~~ Automized grade of Al powder,

b) abrasive powders such as SiC powders, Alumina powders and ceramic wool,

c) solid lubricants such as graphite flakes and antimony tri sulphide powder,

d) filler- barium sulphate and coconut fibers etc.

(ii) **Formulation of chemistries:** Keeping Al powder as the base material, the ingredients and their proportion for forming the friction material and the backing plate will be decided based on expected characteristics as per literature survey. Further, the chemistry is expected to alter based on friction tests and intended applications.

(iii)**Mixing/blending of powders:** For preparation of homogeneous powder mixture, it is thought to adopt dry mixing of powders using attritor and pot mills.

(iv)**Preform powder forging:** Two sets of dies, one for forming 'Preform' from the powder mix and other for 'Hot forging' of perform will be used. The perform die will be filled with powder mix for making back plate to some height (compactiong ratio ≈ 3) and then it will be filled with powder mix for making friction material. Preform will be prepared by compacting powder mix in perform die. The heated preform will then be transferred to ' hot powder forging' die for forging using friction screw press of 100 tone capacity.

(v) **Characterization of brake material and optimization of the chemistry**: Following equipments will be used for characterization of the material with subsequent alteration of the chemistry:

a) Pin-on-disc friction test equipment for initial friction characteristics of the material.

b) Krauss friction test rig for characterization of the component (brake pad).

c) Subscale dynamometer test for evaluation of brake pad characteristics on near to actual field conditions of brake application.

(vi) **Thermal tests, mechanical tests and microstructure analysis**:

It is thought to measure the thermal diffusivity, specific heat, thermal conductivity, and thermal expansion coefficient at different temperature ranges using thermal dilatometer, flash thermometer, thermal calorimeter and differential calorimeter respectively.

For the study of mechanical properties, the test samples for TPT-426 tensometer will be prepared and elastic modulus, yield and ultimate tensile strength, compressive strength, shear modulus and shear strength will be estimated.

Optical microscopic, EDAX and SEM micro analyses are planned.

vii) **Analysis of results, optimization of chemistry and suitability of material:**

Observations are to be made starting from the compaction to form preform and hot forging of performs. The results of friction test studies, thermal, mechanical, microstructural analysis will be analyzed and compared with that of standard friction materials which are being presently used in automobiles (resin bonded) and AN32 aircraft (Fe based) rotor brake pads.

Work plan has been summarized in fig. 3.1.

WORK FLOW

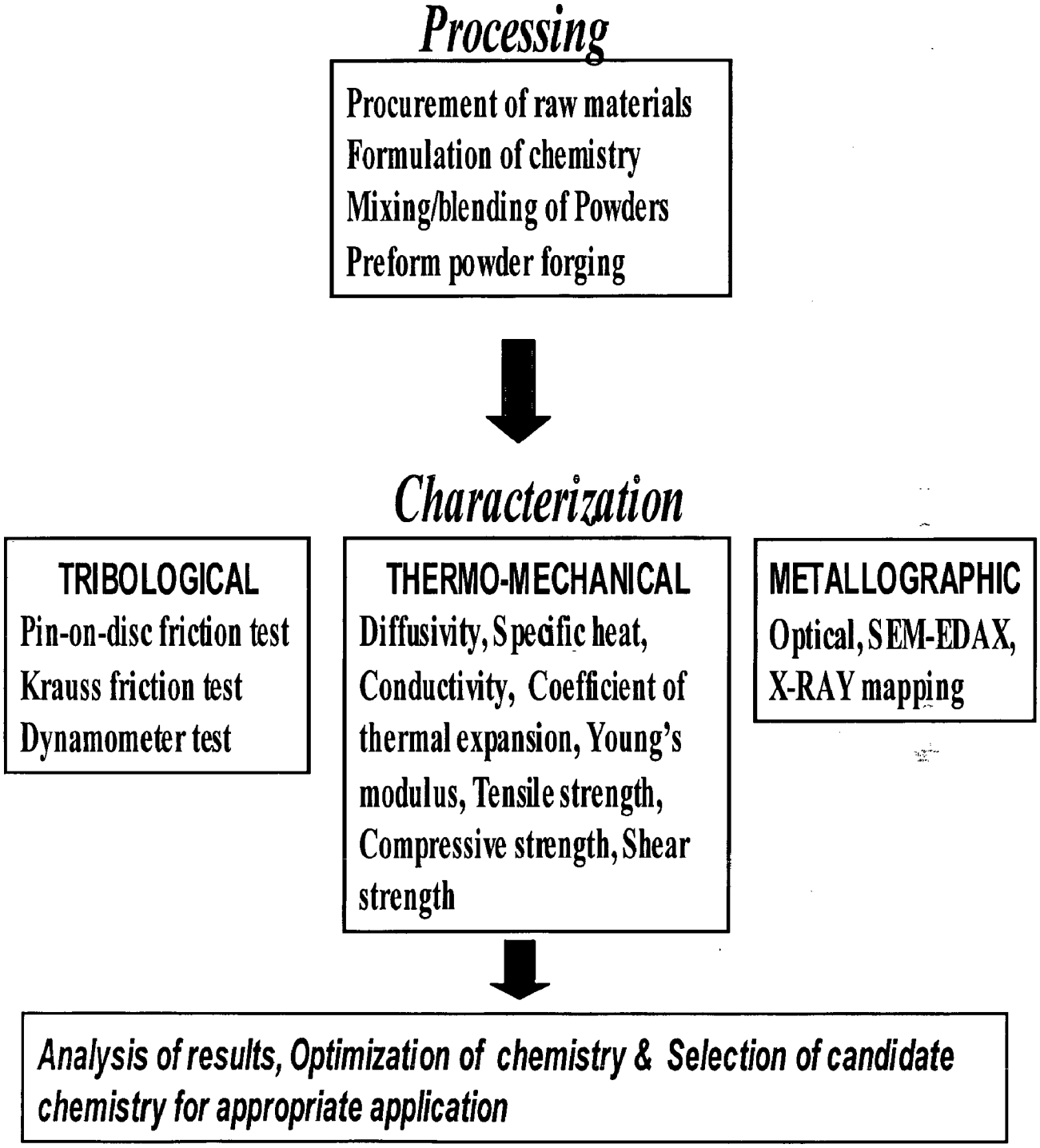

Fig. 3.1 Work flow

Chapter 4

EXPERIMENTAL PROCEDURE

Friction materials are very complex multiphase composites. Friction and backing plate materials investigated in this work are non-asbestos metallo-ceramic type containing pure aluminium powder as matrix. Abrasive powders such as SiC, Al_2O_3, ceramic wool; solid lubricants as graphite/antimony tri sulphide and fillers such as barium sulphate and coconut fiber are incorporated in the aluminium matrix. The brake pad comprising friction and backing plate materials are fabricated using 'Preform Powder Forging' technology. There are two principle requirements of proposed aluminium based brake pads, one to achieve improved wear resistance with stable coefficient of friction under low as well as high applied loads and second to maintain lower temperature at contact surface during braking. Another requirement is low noise during braking.

4.1 Raw materials specifications

Aluminium

Commercially pure aluminium powder of IE–07 grades from Metal Powder ***Company Limited, Madurai***- Tamil Nadu, India is used for experimental purpose. The composition is presented in **Table-4.1.**

Table 4.1 Pure aluminium powder

Si	Fe	Ti	V	Cu	Mn	Al
0.08	*0.15*	*0.001*	*0.007*	*0.001*	*0.003*	*99.76*

Ingredients

Commercial ingredients of different grades from respective sources are collected and are used for experimental purpose. The general details are presented in **Table-4.2.**

Table 4.2 Ingredients

S. No.	Size		Density gm/cc	Source
	Nature	(μm)		
Al	Fine	100	2.70-2.72	Metal Powder Company Limited, Madurai-Tamil Nadu, India
SiC	Coarse	200	2.94-3.16	Metal Powder Company Limited, Madurai-Tamil Nadu, India
	Fine	50	3.21-3.26	
Gr	Flakes	350	2.26-2.36	Graphite India Ltd. 31, Chowringhee Road Kolkata – 700016, India
	Fine	45	2.09 -2.23	
Sb_2S_3	Fine	40	6.68-6.98	Chemico Chemicals Private Limited 341, Functional Industrial Area, Patparganj, New Delhi - 110 092, India
$BaSO_4$	Fine	40	3.51-3.55	Barium Sulphate Sree Rayalaseema Alkalies & Allied Chemicals Ltd.-Delhi, India
Zinc	Fine	75	7.14-7.21	Hindustan Zinc Ltd., Yashad Bhawan Udaipur Rajasthan - 313004 Tel: 2420813-15

4.1.1 Brake pad materials

The criterion for the selection of different powder materials/constituents is based on their wear characteristics, frictional stability, thermal conductivity and strength. The thirty different chemistry for friction composites designated as **FAl01 to FAl30** with different ingredients in each are formulated **(Table 4.3, pp.106)** where as chemistry 31th is for backing plate. In this nomenclature, the first character 'F' indicates that these compositions belongs to 'friction materials'; second and third characters A & l stands for 'Al base'; these characters are followed by numerical digits corresponding to detailed chemistry of that material as given in **Table 4.1, pp.104.** The aluminium powder as a matrix varies within a range of 70 to 80 wt.% in these friction materials. Other constituents (total ranging from 20-30 wt.%) are silicon carbide powder, graphite, antimony tri sulphide, barium sulphate, ceramic wool, coconut fiber and zinc powder.

The constituents (wt.%) of these composites along with its nomenclature/designation, density and hardness are given in **Table 4.3, pp.106.**

Table 4.3 Nomenclature and chemistry alongwith density and hardness

Nomenclature/ Designation	Constituents (wt.%)						Density (gm/cc)		Hardness (BHN)
	Al.	SiC	Graphite	Sb_2S_3	$BaSo_4$	Others	Green	Forged	
FAl01	80	20	-	-	-		2.45	2.78	67
FAl02	78	22	-	-	-		2.65	2.74	71
FAl03	75	25	-	-	-		2.41	2.67	75
FAl04	74.8	18.2	4	1	2		2.40	2.62	65
FAl05	70	20	5	1	2	Ceramic wool -2	2.56	2.73	64
FAl06	70	20	5	1	2	Coconut fiber -2	2.49	2.70	66
FAl07	70	20	5	2	3		2.46	2.67	64
FAl08	71.5	18	6.5	1.5	2.5		2.39	2.61	63
FAl09	78	15	4	2	1		2.41	2.46	56
FAl10	76	15	6	2	1		2.26	2.39	60
FAl11	74	15	4	2	4		2.41	2.71	70
FAl12	83	15	6	2	4		2.39	2.68	65
FAl13	81	15	8	2	4		2.54	2.73	67
FAl14	79	10	4	2	4		2.62	2.72	69
FAl15	78	10	6	2	4		2.61	2.87	65
FAl16	76	10	8	2	4		2.52	2.80	66
FAl17	78	15	4	2	4		2.37	2.80	66
FAl18	77	15	6	2	4		2.62	2.89	69
FAl19	78	10	6	2	4		2.51	2.82	64
FAl20	76	10	8	2	4		2.43	2.80	69
FAl21	75	8.45	9.54	2	3	Zinc-2	2.67	3.00	67
FAl22	75	-	9.54	2	3	Zinc-2	2.48	2.71	70
FAl23	75	8.45	11.54	2	3	-	2.39	2.86	70
FAl24	75	6.45	9.54	2	3	Zinc-4	2.45	2.80	67
FAl25	77	8.45	7.54	2	3	Zinc-2	2.58	2.89	65
FAl26	77.55	7.45	8	2	3	Zinc-2	2.57	2.84	66
FAl27	75.55	7.45	8	2	3	Zinc-4	2.67	2.85	70
FAl28	77	8.5	9.5	2	3	-	2.69	3.00	75
FAl29	75	6.45	9.54	2	3	Zinc-3	2. 6	2.80	70
FAl30	77	8.45	7.54	2	3	Zinc-3	2.5	2.89	70
Back plate (31^{th})	70	30	-	-	-	-	-	-	85

Notes: Forging temperature 450 °C; Soaking time 1 hr. at 450 °C. Backing plate of powder mixture (Al-30 wt.% fine SiC) is incorporated from sample no. from FAl16 to FAl27 at cold compaction stage.

4.2 Preparation of powder preform and forging

'Preform Powder Forging' technique is combined form of cold compacting of powder mixture and hot forging of the resulting perform. It involves three steps viz. i) powder blending/mixing; ii) cold compacting and iii) hot forging of preform in open air. However, the conventional compacting and sintering process consists of four steps such as powder mixing, cold compacting using heavy presses, pressure sintering under controlled atmosphere and finishing (grinding, coining, etc), with 'Preform Powder Forging', more dense products are obtained.

4.2.1 Blending/mixing of powders

Powders mix for backing plate material and friction materials are separately prepared as described below.

4.2.1.1 Blending/mixing of powder mixture for back plate

70 wt% Al powder (100μm) and 30% fine SiC (50 μm) powder are thoroughly blended (manually) and then this powder mix is mechanically alloyed in a pot mill for about 2-3 hrs using ceramic balls (10 mm dia.) in the ratio of 1:5 (weight of powder mixture / weight of ceramic ball).

4.2.1.2 Blending/mixing of powder mixture for friction material

Mixing of the various ingredients is done in three steps. Firstly, the total amount of ceramic SiC (coarse: 200 μm) powder, total amount of filler $BaSO_4$ (40μm), total amount of Sb_2S_3 (40μm) (solid lubricant) and $1/3^{rd}$ amount of graphite powder (45 μm) are mixed manually for one hr. and then this mixture is mechanically alloyed in pot mill for 6 hrs. using hardened steel balls (dia.- 4.5mm) in the ratio of 1:5 (weight of powder mixture / weight of steel balls).

Secondly, $1/3^{rd}$ of the total metallic (Al) powder and $1/3^{rd}$ of graphite powder (45 μm) are separately mixed in another pot mill using hardened steel balls for 6 hours similar to mixing as in step one.

In third and the last step, balance of Al and graphite powder (350 μm) are taken and then mixed manually with powder mixtures obtained in first and second steps. Then this complete powder mix is again blended in pot mill without using hardened steel balls for two hours. In some of the friction materials Zn powder (75 μm) as required is also added at this stage of mixing. This entire procedure of mixing ensures the uniform coating of graphite over SiC particles and uniform distribution of constituents. Now this powder mix is ready for preparation of green compacts.

4.2.2 Tool design (die & punch) for cold compacting and hot forging of powder mix

The powder mix is converted into net shape braking product (brake pad), followed by cold compacting (preparation of perform) and hot forging (forging of perform). These processes are done in dies namely cold compacting die and hot forging die. The hot forging die is of actual dimension of brake pad where as the dimension of cold compacting die is relatively less about 1.5 mm. due to consideration of variation in thermal characteristic (thermal stain) of brake pad material at forging temperature. The hot forging die is similar to cold compacting die except in dimension change. The details of tool design (die-punch), compacting process and products are shown in figs. 4.1, 4.2 and 4.3.

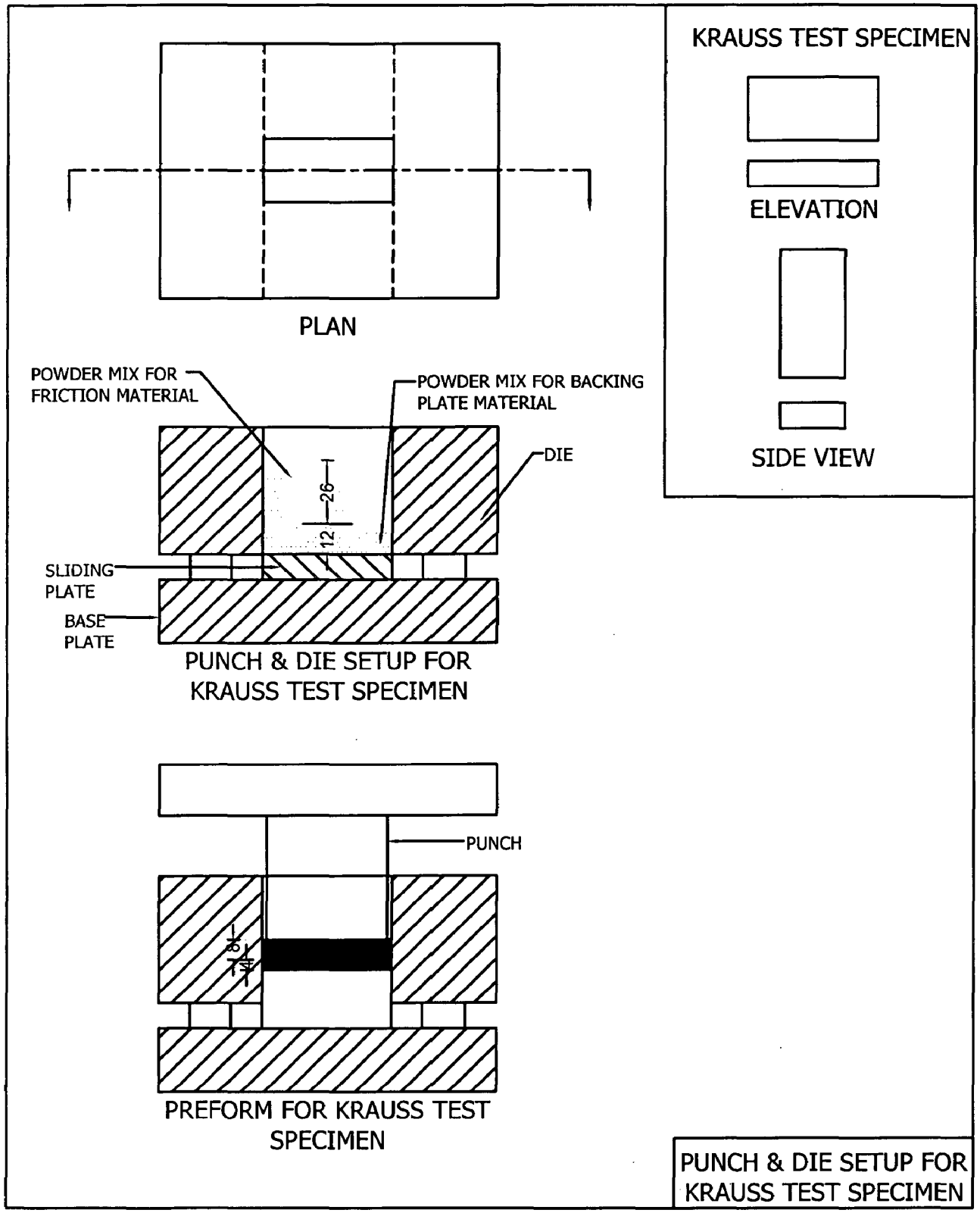

Fig.4.1 Punch & die setup for Krauss test specimen

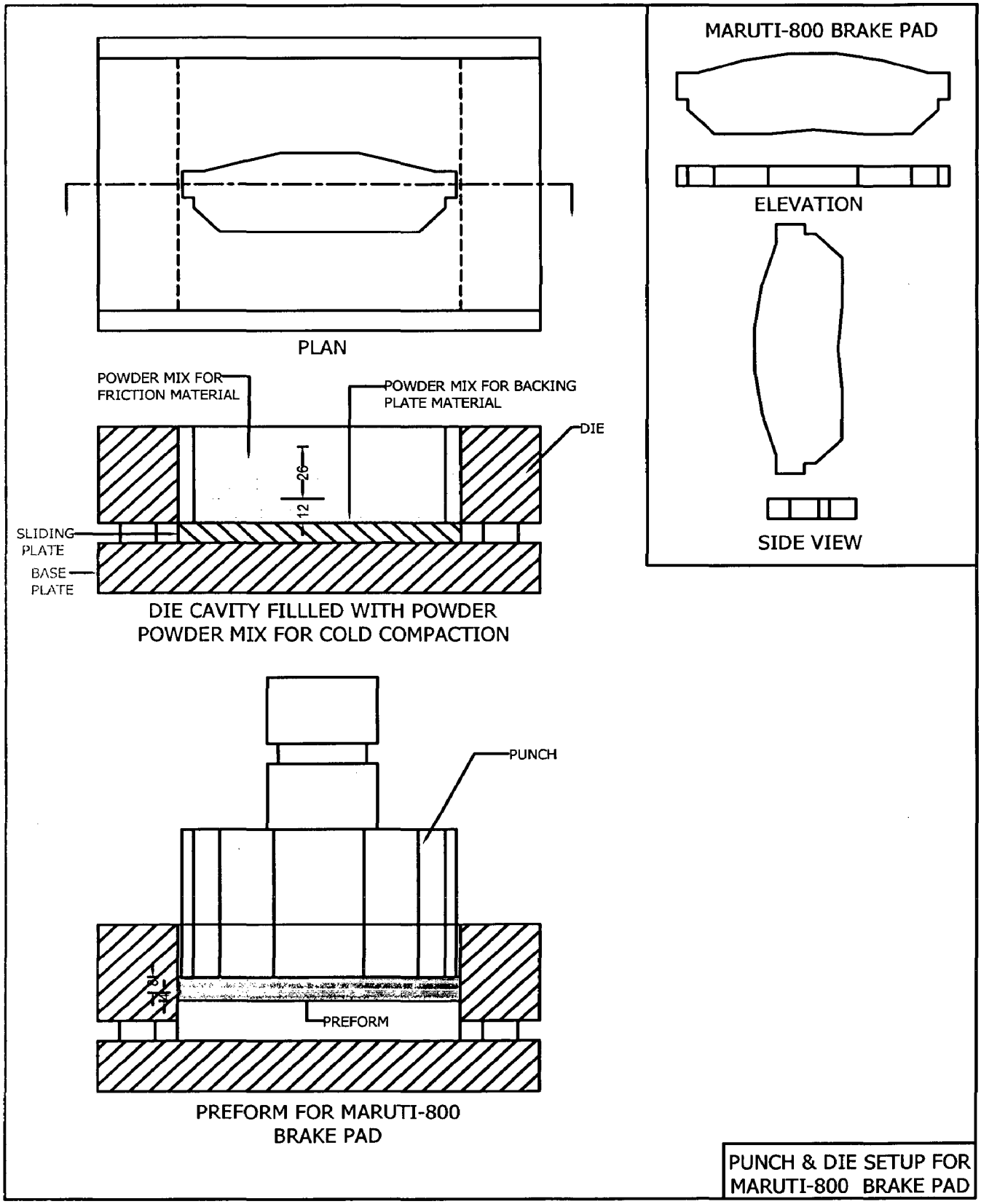

Fig. 4.2 Punch & die setup for Maruti-800 brake pad

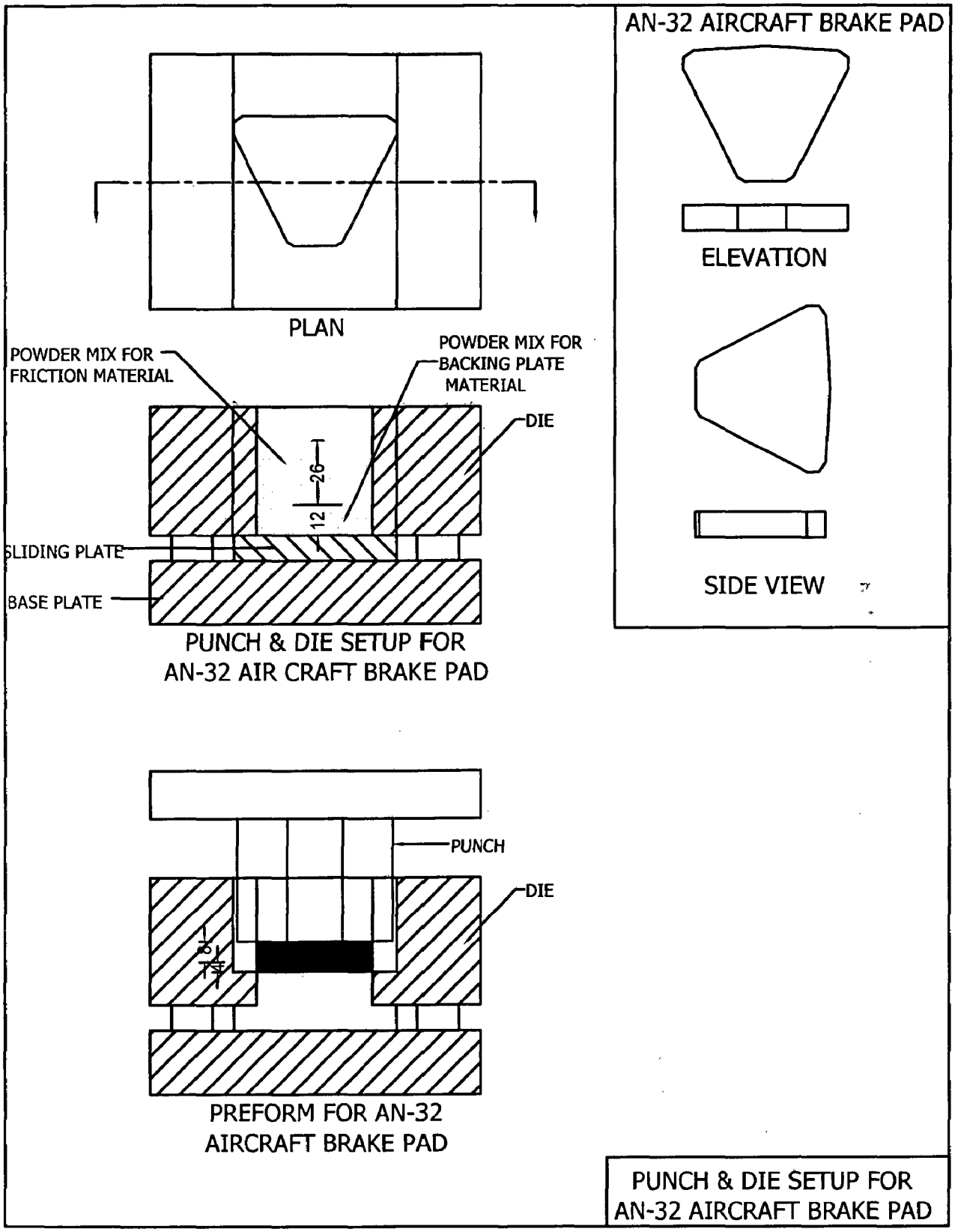

Fig. 4.3 Punch & die setup for AN-32 aircraft brake pad

4.2.3 Cold compacting (preform forming)

Preform is prepared from the above stated powder mix by cold compacting which consists of i) Powder filling in the die, ii) Compacting of powder using friction screw press and iii) Ejection of the preform.

To avoid the rubbing between die and punch during compaction and easy withdrawal of the preform, the die and punch surfaces are coated with suspension of fine graphite (45 μm) and ethanol. This makes it possible to produce a net-shaped preform and eliminate the probability of die-punch damaging.

Firstly, powder mix for back plate is filled in to the die cavity (50 mm length X 25 mm width X 38 mm depth) to about $1/3^{rd}$ depth and leveled mechanically to get a uniform powder layer of about 15 mm thickness. Further, mix of friction powders for development of friction layer is delivered over the back plate mix layer into the die cavity and leveled again to get a uniform powder layer of about 24 mm thickness. Then the backing plate powder layer and the friction material layer are compacted together by using a friction screw press of 100 ton capacity in a single stroke of the punch, keeping the die stationary, causing a single-ended compaction (SEC). The compaction pressure lies in between 700 and 800 MPa. During compaction, the powder mixtures are compressed inside the die, where powder particles experience intensive deformation and the powder undergoes large densification. The relative density increases by a factor of ≈ 3 during compaction.

According to the movement of the upper punch, the compaction process can be divided into two phases: compression and decompression. During compression, as the upper punch moves towards the die, the powder bed experiences intensive densification: the powder particles come together to form aggregates with appreciable cohesive strength due to Vander Waals forces and mechanical interlocking and formation of solid bridges. Decompression takes place once the punch moves away from the die, the compaction pressure drops quickly and some of the elastic strain induced during compression recovers.

It is generally anticipated that the elastic recovery rate during decompression is one of the main factors responsible for occurrence of defects, such as cracks and fracture of powder compacts, faster elastic recovery is more likely to cause failure. Some researchers have also speculated that the failure of compacts during compacting is due to the entrapment of air that prevents strong bonding between particles from being established during the compaction. Both the theories appear reasonable, however very little conclusive evidence supporting either hypothesis has been reported so far. Based upon a combination of theoretical and experimental investigation, it has been found that the failure (in particular the phenomenon of capping) is associated with an intensive shear band formed during the decompression stage.

A logical question that follows from this is therefore how to avoid capping. Therefore the objective of this process is to explore possible approaches to alleviate the propensity for capping, based on the fundamental understanding of the mechanical behavior of powders during compaction.

In the present process, capping is successfully eliminated through two approaches. First approach is to fillet the sharp edge corners of the punch face into rounded edges and the second approach is to alter the material properties, i.e. changing the elasticity of the materials (by using matrix powder of coarse and irregular shape). It is also apparent that effective lubrication provided by graphite coating of the die cavity as well as large amount of the graphite powder mixed in the friction layer also helps reducing this phenomenon.

4.2.4 Hot forging of preform

The final process is hot powder preform forging, which is capable of producing the finished product of substantially reduced porosity, high strength and high toughness.

Green compact (powder preform) is heated to 450 °C and held at this temperature for one hour in muffle furnace (soaking), and then it is transferred into a stationary die and hot forged at this temperature by a movable punch. Light impact is given on the preform in the first stroke by carefully controlling the speed of movement of the punch, so that the bonding of powder particles advances preferentially prior to the densification of the preform. The second stroke is applied which results in substantial densification of the green compact and the bondability of the powder particles.

For lubrication of die and easy withdrawal of the product, the die and punch, surfaces are coated with suspension of graphite (45μm) and ethanol. This makes it possible to produce a net-shaped forged product having high density and high strength.

The process flow chart of 'Powder preform hot forging' is shown in fig. 4.4.

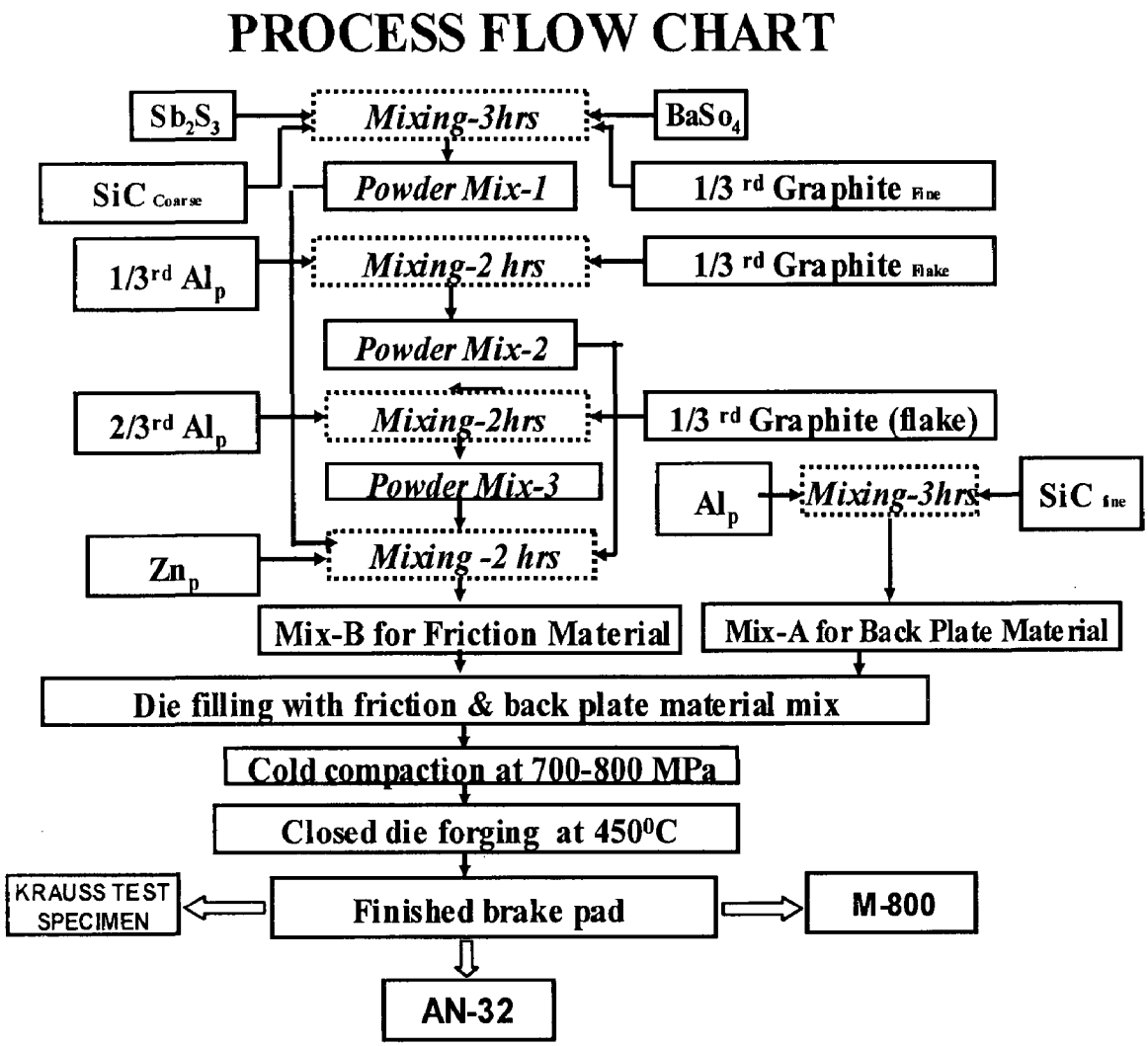

Fig. 4.4 Process flow chart

4.3 Characterization of brake pad materials

The brake pad materials with built-in backing plates are characterized to obtain densities, hardness, wear loss, coefficient of friction, temperature rise, noise level, mechanical properties, thermal properties and microstructures. The different tests being conducted to obtain the above characteristics are: Archimedes' method (density measurement), Brinell hardness test, pin-on disc dry wear test, Krauss rig friction test (:reduced/full scale inertia test), sub-scale dynamometer inertia test, mechanical tests, thermal tests, optical metallography and SEM with EDAX.

4.3.1 Density and hardness measurement

The basic method of determining the density of materials by measuring the ratio of mass and volume of the specimen is used. The volume of the specimen of the material is measured by water displacement method based on Archimedes principle and its weight in air using a chemical balance.

Brinell hardness test method consists of indenting the test material with a 10 mm diameter hardened steel ball subjected to a load of 15.25 kg applied for 10 to 15 seconds. The diameter of the indentation mark on the test material is measured at two right angles and the average diameter of the impression is determined. Brinell hardness number corresponding to the average diameter of the impression was noted.

4.3.2 Pin-on-disc wear test [23]

To analyze the tribological characteristics of frictional materials at laboratory level, pin-on-disc wear test is performed under different set of parameters like applied load, sliding speed, and sliding time/distance according to ASTM-G99 standard test procedure. In this test, test pin of friction material with dimension about 30mmx7mmx7mm machined from brake pad is used against a mating counterface of cast iron disc. The specifications of cast iron disc are given in **Table 5.1, pp.126.** To ensure proper contact between test pin and disc, test pin adjusting screw is provided. Slotted weights are used for normal loading on the test piece, which are placed on a pan. This load is transferred on to the specimen holder through a lever. Electric motor is directly connected to the steel disc and the speed of the disc can be controlled by variable speed regulator.

The surface of the test pin which comes in contact with the disc, is rubbed on emery papers of 1/0, 2/0, 3/0, 4/0 grades before clamping it on the pin-on-disc wear testing rig. The applied loads are 5kg and 8kg with specific pressure of 1.02 MPa and 1.63 MPa respectively. Sliding speed of 9m/s (1140±10 rpm at a track radius of 75mm) is kept constant during the test. Sliding time is 90 minutes. The wear loss and the frictional force generated at every 1 minute is recorded.

The noise generated during the wear test is also continuously recorded by means of special microphone based noise level meter placed 50 mm away from rubbing surface in decibels (dB).

The rise in temperature of the wear surface is a function of time. The temperature rise measurement during wear test is carried out using a chormal-alumel thermocouple placed at 5mm away from the wearing surface by making a hole of 2mm diameter with 3mm depth approximately. The rise in temperature is recorded till the temperature at the wear surface

becomes stable. Simultaneous measurement of coefficient of friction and temperature rise during the test provide brake fading characteristics of friction material. The schematic view of the pin-on-disc apparatus used in this study is shown in fig. 4.5.

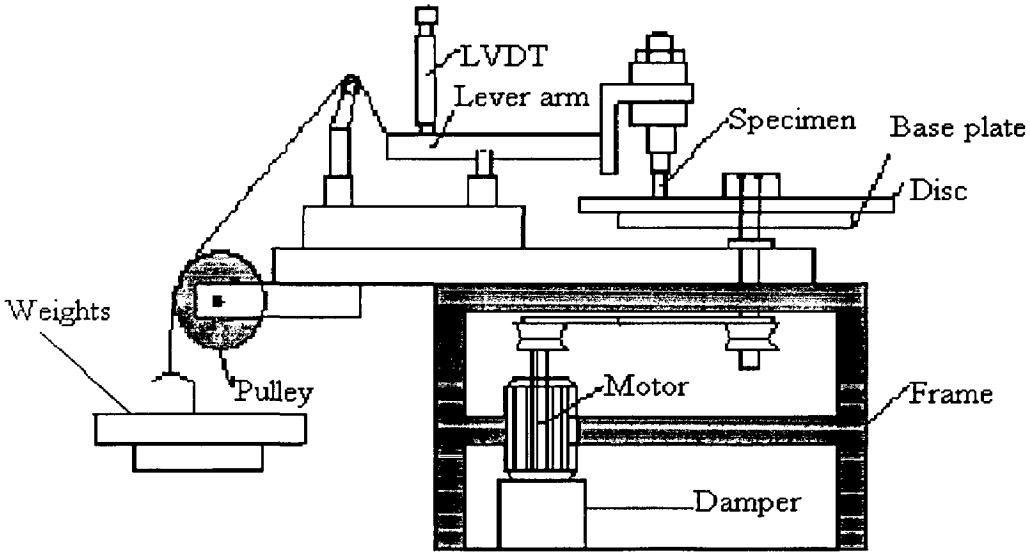

Fig. 4.5 Schematic view of the pin-on-disc apparatus used in this study **[23]**

4.3.3 Krauss: ECR R-90 standard regulation test

The performance evaluation tests are conducted on a Krauss type RWDC 100C (450 V/50 Hz) machine conforming to ECR R-90 standard regulation test **[58].** A schematic diagram of Krauss machine is shown in fig. 4.6 pp.118. The Krauss machine is computer-controlled and has data acquisition capabilities. The cast iron disc with radius of 0.12 m with Brinell hardness number (BHN) of 183-212 is fitted as the mating counterface. The disc is connected through an interchangeable flange to a shaft that generates a mass moment of inertia of 2.5 kgm^2. The disc rotation is kept fixed at 660 rpm as per ECE R-90 standard test.The surface temperature of the pad and disc is measured with the help of a thermocouple touching across the disc. A couple of brake pads with respective contact areas of 29.1 cm^2 (full-scale test) and 18.5 cm^2 (reduced-scale test) are push fitted in sliding caliper assembly connected to a pressure actuator against the opposite sides of the rotor disc with a friction radius of 101 mm. The load on the pads is adjusted to keep the applied contact pressure at 1.82 MPa. A load cell linked to the frame carrying the caliper pad assembly measures the friction force. A standard regulation test ECE R-90 described in 'uniform provisions concerning the approval of replacement brake lining assemblies for power driven vehicles and their trailers' by UN is followed for the evaluation of cold friction-fade. The braking pressure of 1.82 MPa is manipulated following the regulation in accordance with the pad surface area. Before the pads are actually subjected to the seven- stepped friction assessment tests consisting of one cold

friction run, five fade runs, and one recovery run, they are allowed to bed-in for 30 braking applications in such a manner that the temperature of the disc does not exceed 280^{0}C. The disc is allowed to cool down to 100°C intermittently in the case of temperature rise exceeding 280 ^{0}C. The braking duration and the interval between two successive braking is kept at 5 seconds each. The uniform contact of the friction surface is assured through 30 cycles of initial bedding-in operation under a bedding load of 2 MPa and at a speed of 660 rpm on the disc. The disc and pad surfaces are allowed to cool down to a temperature of <100 ^{0}C as the temperature rise reaches above 280 ^{0}C during the course of bedding to ensure a controlled friction-induced thermal history. After completing the bedding cycle, the cold friction cycle is initiated, consisting of 10 braking, where the initial temperature is maintained at 45 ^{0}C with the help of the air blower to dissipate the excessive frictional heat. After this the subsequent five cycles of fade, termed as first, second, third , fourth, and fifth fade runs are followed. Thus, the fade cycle consists of five fade runs each of 10 braking (total 5x10=50 braking in one fade cycle), where the initial braking is at 100^{0}C further allowing the friction-induced temperature to rise uninterruptedly until the completion of all the 10 brakings. The subsequent fade run begins after the disc is cooled down to a temperature about 100 °C in a way similar to the first fade run (FFR). The sequence is repeated till all the five fade runs are completed. Finally after completion of the fifth fade run, the disc is cooled to a temperature of 100 °C and with air blowers on, the recovery run is carried out. Recovery run is the seventh and last cycle of ECR R-90 standard test. The frictional force and temperature rise of the disc surface is recorded after every cycle of braking operation in a synchronized manner. The loss in braking effectiveness at elevated temperatures because of reduction in friction coefficient (μ) and the revival of the same at lower temperatures is referred as fade and recovery respectively. The wear is calculated in terms of weight and volume losses.

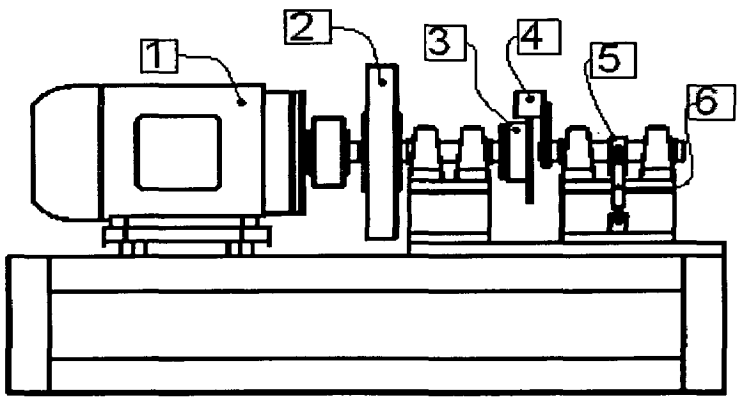

Fig. 4.6 (i) Krauss type RWDC 100C (450 V/50 Hz) machine **[58]**

The Krauss test: reduced-scale test (under test code A, B, C and D) and full-scale inertia test (as described in appendix B) are conducted for selected samples (FAl20 to FAl26) which have better tribological characteristics at laboratory level.

Krauss type RWDC 100C machine consists of the following main elements are as shown in fig. 4.6 (i) 1. Motor 2.Interchangeable flywheels 3.Brake disk 4. Calliper and adapter 4. Power transfer axle 5. Load bearing arm and loadcell. Fig. 4.6(ii) shows a typical automobile brake assembly.

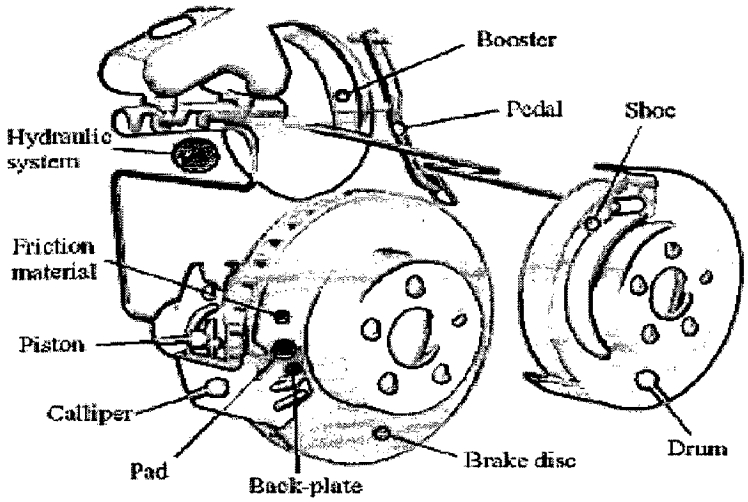

Fig. 4.6 (ii) Typical automobile brake assembly

Note: The disc cooling process (blower-on-process) is applied for resin based brake pad testing, because the temperature rise during brake applied exceeds 280 °C. The maximum temperature rise during Al powder based brake pads testing is 200 °C, so that disc cooling process is not required (blower-off-process).

4.3.4.1 Sub-scale dynamometer test of brake pad materials for AN32 aircraft rotor application [157]

The sub-scale brake inertia dynamometer tests are carried to characterize the tribological properties of Al powder based brake pad materials namely FAl20 to FAl26 to judge their suitability for AN32 aircraft rotor application. The Al based brake pads from FAl20 to FAl26 friction materials are prepared according to AN32 aircraft rotor design using suitable 'preform compacting' and 'preform forging' dies for this component. A pair of brake pads for each composition is taken for testing on sub-scale dynamometer and subjected to repeated cycles of real time brake performance tests simulating the actual aircraft brake energy conditions. The tests are conducted in the range of 8000-17300 kgfm kinetic energy, 687-1000 rpm brake speed and 7.5-18kgf/cm^2 brake pressure. A pair of our brake pads is mounted in the subscale dynamometer using caliper brake assembly and the machine is set to run on selected K. E., brake speed and brake pressure. On reaching the speed of brake disc at the required level,

brakes are applied with pressure (as defined in the input parameters) and thus the disc is stopped. The output parameters such as run down revolutions (revolutions prior to stopping), run down time (stopping time), brake torque (mean and peak), drag force (mean and peak), COF, temperature of brake pad/disc are recorded for each cycle. The brake applied is 50 times in each test run.

For an aircraft, the brakes are applied in three different situations namely i) normal landing, ii) rejected take off (RTO), iii) overload conditions. First, normal landing condition.which refers to the aircraft landing on the runway (normal landing). Second, rejected take off (RTO) condition which refers to emergency landing when the aircraft takes off from the runway, due to technical fault or some other reasons. In such cases, higher pressures are applied to stop the aircraft in short distance within runway. Third, overload condition, which refers to braking for stopping the aircraft under over loading condition. In all of these conditions, the input parameters of dynamometer tests are varied and new calculations are made and fixed.

In the present investigation, sub-scale dynamometer tests are carried under RTO brake energy conditions and the specifications of dynamometer are as follows.

1. Make : Dynaspede Integrated Systems Pvt. Ltd.
2. Inertia :14-54 Kg.m2 (Stepless by electrical simulation)
3. Maximum energy : 1.2 Laks kgfm = 1.18 MJ
4. Speed : 100-2000 rpm
5. Braking force : 50-1000 Kgs
6. No of disc : 2 (alloy cast iron and alloy steel)
7. Disc diameter : 500mm
8. Maximum no. of cycles : 200
9. Acceleration time : 30sec
10. Noise level : 85 dB

The sub-scale brake inertia dynamometer tests under low energy (codes: TQ2 and TQ3) and high energy test (code: TQ1) are conducted for some of the selected test samples which have better tribological characteristics at laboratory level pin-on-disc test (Chapter 5).

4.3.5 Estimation of mechanical properties

In this work, mechanical testing is performed in metro railway testing laboratories- DMRC, Delhi, India in accordance with ASTM E8-93 using a crosshead speed of 1.3 mm min^{-1}. The test specimens are held at 350^{0}C and at 575 ^{0}C for 10 min prior to testing and mechanical properties are estimated on these two temperatures. To monitor strain, a "T" gauge rosette is bonded to the gauge section of each specimen using AE-10 adhesive. Mechanical properties are computed from the engineering stress-strain curves. Yield stress is determined at 0.2%

offset. Elastic modulus is determined by the slope of the chord of the stress-strain curve between 70 and 175 MPa (ASTM E111-8). Poisson's ratio (υ) is determined as the absolute ratio of transverse to axial strain at 70 MPa.

The cylindrical shape specimens with 10 mm diameter and 30 mm length are used in mechanical testing.

4.3.6 Estimation of thermal properties

The thermal testing of brake pad materials is performed in metro railway testing laboratories, DMRC, Delhi, India. Dissipation of the braking energy as a heat and optimization of friction materials for low wear and stable friction coefficient during braking are the main considerations in the design of friction materials. Two different strategies are currently under study: i) the use of ceramic materials that offer good frictional performances (such as low run down time and low wear rate) and ii) the recourse to use the materials with high thermal diffusivity, high specific heat, high thermal conductivity and low thermal expansion coefficient, which bring about a reduction in the temperature of sliding, hot spot formation and the probability of brake pad and disc cracking through thermally induced stresses.

The thermal test of Al based brake pad materials is carried out to measure the thermal properties such as thermal expansion coefficient, thermal diffusivity, specific heat and thermal conductivity using different thermal measuring devices. The details are separately explained here.

4.3.6.1 Estimation of coefficient of thermal expansion

In this study, the measurement of coefficient of thermal expansion (CTE) to know the thermal strain behavior of the friction materials is carried out using 'Dilatometer' at different temperature ranges: 20^0C(RT) -.350^0C and 350 -.575^0C. The dilatometer measures the length or the volume changes of the sample, when the sample follows a temperature cycle and submits a small force (push rod contact pressure is adjusted between 15 and 50 N). In dilatometer, the change in length of the sample is detected by an inductive displacement transducer. Calibration and corrections of measurements are done by using various standards and comparison with materials of known expansion. The present dilatometer can measure the coefficient of thermal expansion in the temperature range from -150°C to 1500°C within an error of 3-5%.under various conditions (air, inert gas or vacuum).

The schematic setup for the measurement of coefficient of thermal expansion by dilatometer is shown in fig 4.7.

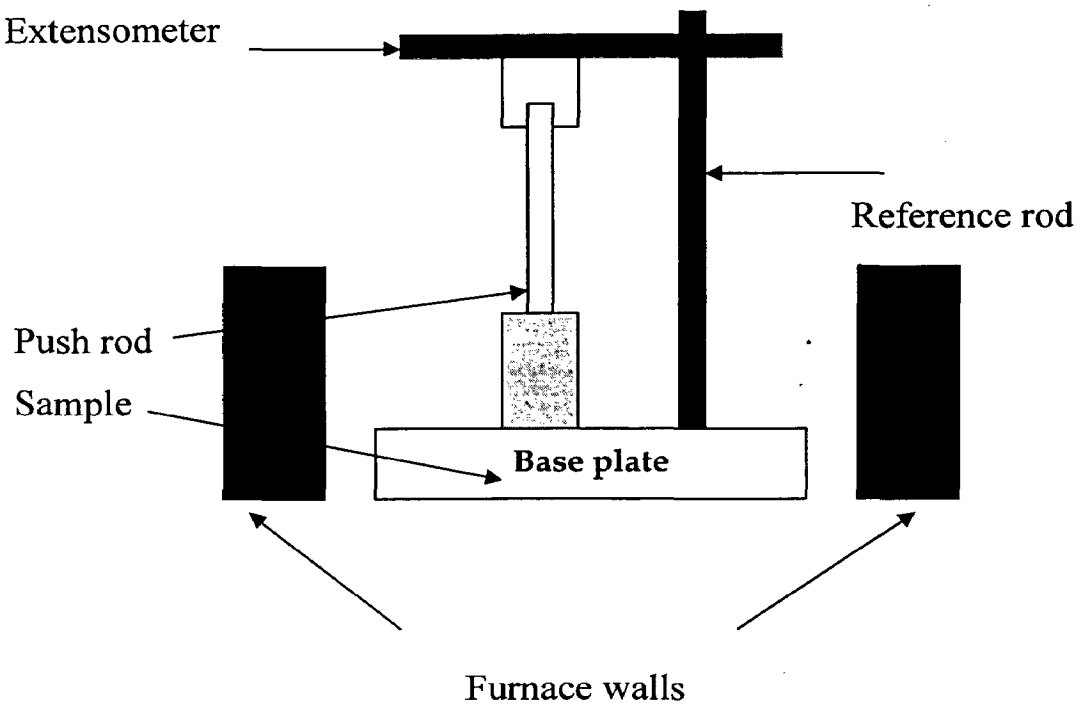

Fig. 4.7 Schematic setup for estimation of coefficient of thermal expansion by dilatometer

4.3.6.2 Estimation of thermal diffusivity

The measurement of thermal diffusivity of aluminium based brake pad materials is carried out using 'Laser flash method'. The schematic setup of the laser flash method is shown in fig. 4.8.

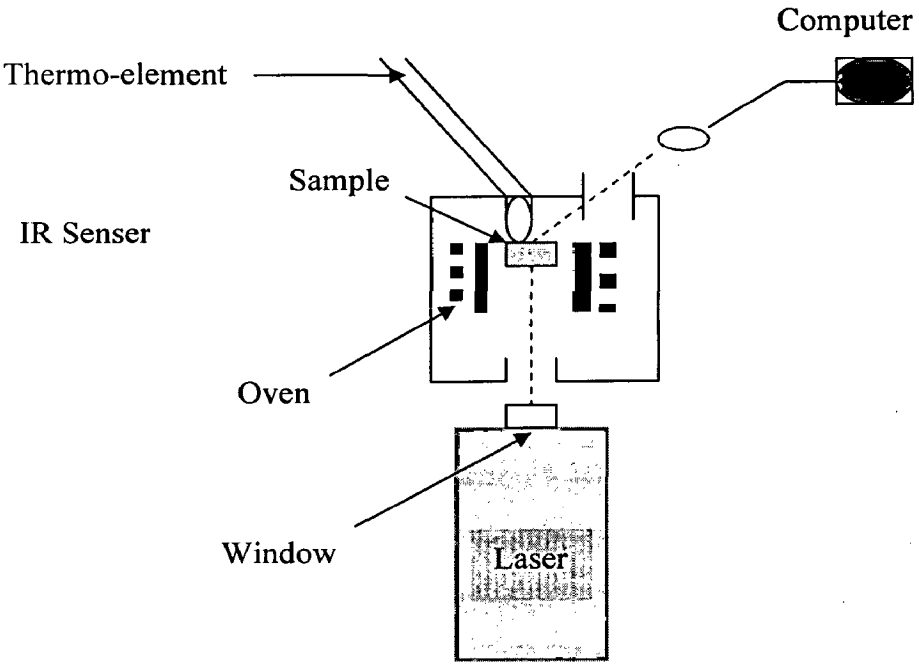

Fig. 4.8 Schematic setup of thermal diffusivity estimation by laser flash method

The laser fires a pulse at the sample's front surface and the infrared detector measures the temperature rise of the sample's back surface. The software uses literature-based analysis routines to match a theoretical curve to the experimental temperature rise curve. The thermal

diffusivity value is associated with the selected theoretical curve. These measurements can be performed very rapidly with an accuracy of about ± 5 %.

4.3.6.3 Estimation of specific heat

The specific heat of Al based brake pad materials is measured using 'Differential Scanning Calorimetry', at two different temperature ranges: 20^0C (RT) -.350^0C and 350 -.575^0C.

The differential scanning calorimetry (DSC) is a thermo-analytical method, which determines the specific heat of composites by measuring the temperature difference between the sample and a reference sample. Specific heat is determined by a quantitative measurement of the heat flow difference for the test sample and the reference sample subjected to the same temperature program. Measurements of specific heat (Cp) is done in inert gas (argon) however, it can also be performed in air, or vacuum with a possible error less than 3%.

4.3.6.4 Estimation of thermal conductivity

Thermal conductivity (λ) is expressed mathematically as given below and its value can be theoretically calculated. $\lambda = \alpha \rho c_p$

λ = Thermal Conductivity, W/mK

α = Thermal Diffusivity, m^2 /s

ρ = Density, kg/m^3

c_p = Specific Heat, J/kgK

However, in the present study it is experimentally determined by using 'Furnace/hot-wire method -TCT 426', which is an absolute method based on the measurement of the temperature increase of a linear heat source/hot wire (cross-wire technique) or at a specific distance from a linear heat source (parallel-wire technique). The hotwire and thermocouple are embedded between two test pieces, which makes the actual test assembly. The time-dependent temperature increase after the heating current is switched on is a measure of the thermal conductivity of the material being tested. Thermal conductivity measurements up to 1000°C with an error <2% are possible with this method. Dimension of solid samples have a diameter <= 10 mm and a length of 22 mm.

4.3.7 Metallographic examination: Optical/scanning electron microscopy of fracture surfaces/EDAX

The microscopic examination of some of the selected Al based friction composites are carried out using optical and scanning electron microscope (SEM) with energy dispersive X-ray analysis (EDAX). Microstructures of backing plate, interface layer and friction element have been studied. The distribution of graphite flakes and SiC rich phase with the aluminium matrix are analyzed. Specimens (about 15x15mm surface area) having cross section of backing plate

Chapter 5

RESULTS AND DISCUSSIONS

In the present investigation, thirty one compositions were developed. These are based on aluminum as the main constituent known as matrix metal. Thirty compositions are for friction material and remaining one is for the back plate. The weight percentages of different constituents in friction material are varied in following ranges; Aluminium from 70 to 83 wt. %, silicon carbide (coarse) from 6.5 to 25 % and graphite (fine and flake) from 4 to 12 %. Other constituents are zinc, ceramic wool, coconut fiber, antimony tri sulphide, and barium sulphate in varying percentages. Silicon carbide (fine) about 30 wt. % is added with pure aluminium powder to develop chemistry for back plate material. These materials are being developed for the first time in this investigation as there is no literature available to provide any guideline for designing them. The compositions were gradually developed in different phases **(Annexure C1 to C2)** and tested to fulfill the requirements of braking for light, medium and heavy duty applications. **The table 4.3 (pp.106)** gives details of the compositions. This table also gives an idea about density and hardness of green and hot forged products. Based on the compositions and processing parameters, symbols have also been assigned to each type thereof. The details of processing brake pads through these powder mixtures are given in chapter 3.

Following tests were conducted to characterize the friction materials developed in the present investigation.

i) Density and hardness tests.

ii) Pin-on disc wear test under different loads at constant sliding speed (9m/s) against heat treated cast iron counterface disc having hardness of 45 Rc.

iii) Sub-scale inertia dynamometer test under varying; low, medium and high kinetic energy.

iv) Krauss rig reduced and full-scale tests under varying brake pressure

v) Thermal test: Measurement of thermal diffusitivity, specific heat, thermal conductivity and coefficient of thermal expansion at different temperature ranges.

vi) Mechanical test: Measurement of elastic modulus, shear modulus, yield tensile strength, ultimate tensile strength compressive strength and shear strength.

vii)Optical microscopy to identify the distribution of different constituents in friction/backplate/interface layers.

viii) EDAX analysis to confirm distribution of different constituents.

ix) Bend test to asses the joining of friction material and backing plate.

5.1 Density and hardness

Density and hardness of friction materials are reported in **Table 4.3(pp.106)**. Both parameters depend upon cold compacting of powder mix and hot forging of preform. They also indirectly depend upon the chemistry of friction materials and uniformity of distribution of ingredients in metal matrix. The density and hardness are the dominating parameters to decide the suitability of friction elements for various braking applications.

Figs. 5.1 (i) and (ii) show the variation of density and hardness of composites FAl01 to FAl 27 respectively.

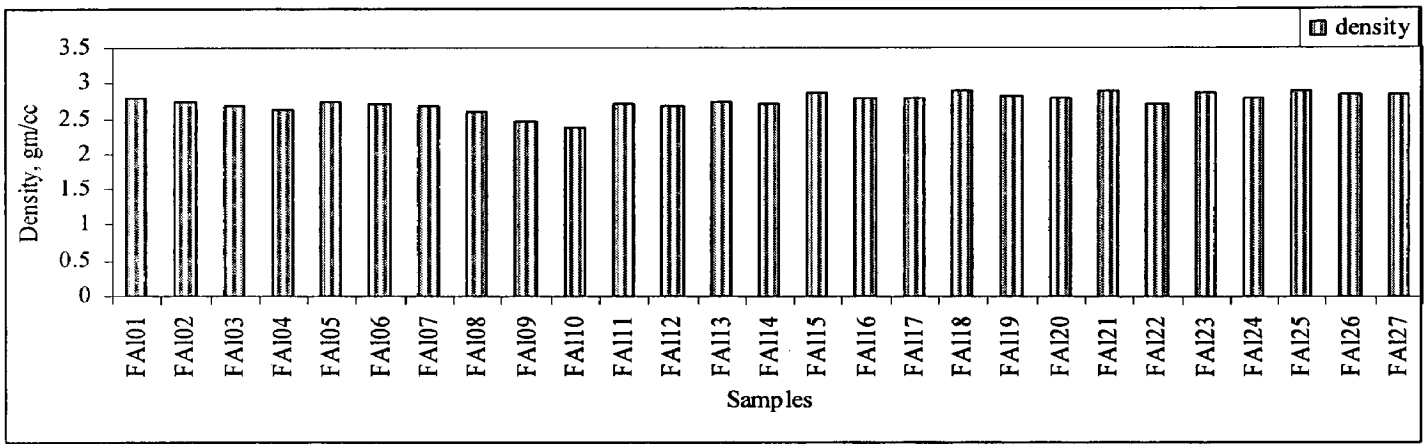

Fig. 5.1 (i)

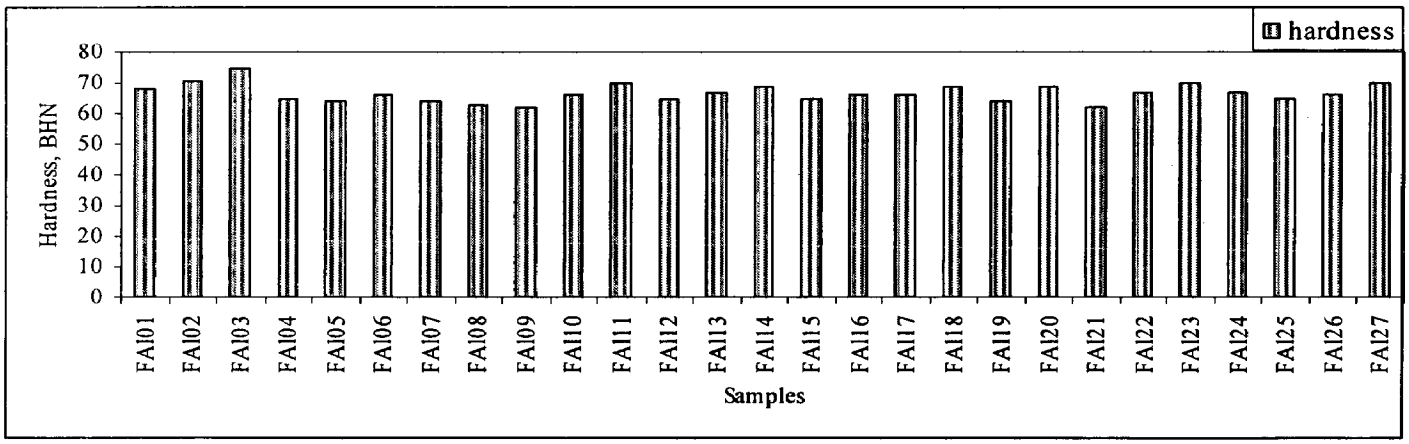

Fig. 5.1 (ii)

Fig. 5.1 Variation of i) density and ii) hardness of developed Al-based composites

The density variation is from FAl01 to FAl 27 and hardness variation is from FAl01 to FAl 27. It can be inferred that these variations are very nominal and depend upon quality and quantity of different ingredients in the composites.

5.2 Pin-on-disc wear test

Pin-on-disc wear tests were carried out for all the samples/composites made in the present investigation for preliminary assessment to evaluate the suitability of friction materials for different applications. On the basis of better tribo-performance during laboratory level tests, few samples were selected for standard friction test namely Krauss rig test, sub-scale dynamometer test, thermal test, mechanical and for microscopic examinations.

Tables 5.1a and 5.1b show specifications of cast iron disc and the pin-on-disc friction test input parameters respectively. The tribo-test is carried out under different test parameters which are shown in table as test codes (PD1 and PD2).

Table 5.1(a) Specification of grey cast iron counterface disc [157]

D_r (mm)	t_r (mm)	R_f (mm)	Hardness (BHN)	Constituents, (wt.%)		Heat treatment
215	10.5	95.5	163-217	C	3.5	Soaked at 550 °C for 3hrs. followed by furnace cooling
				Si	2.0	
				Mn	0.8	
				C_r	0.3	
				Mo	0.35	
				Ni	1.1	
				S	0.1	
				P	0.3	

Table 5.1 (b) Pin-on-disc friction test input parameters

Sliding speed-9m/s

Test codes	Test period, min	Contact area of pin (mm^2)	Load applied (kg)	Pressure (MPa)	RPM	Disc material*
PD1	90	49	5	1.02	1140	Cast iron
PD2	90	49	8	1.63	1140	Cast iron

* Specifications of compositions of cast iron disc as per Table 5.1a

5.2.1 Wear studies at lower load: Test code PD1

The wear test results of twenty seven Al powder based samples (tested under test code- PD1) are summarized in **Table 5.2**. It includes wear, coefficient of friction, and temperature rise and noise level.

Note: The parameters (load/speed) fixed for pin-on-disc test, were chosen to enable correlation with full/reduced-scale tests, and performed in later part of the investigation.

Table 5.2 Pin-on-disc friction test performance: PD1

Contact area of pin: 7×7 mm^2

Samples	Wear		Coefficient of friction			Peak temp. rise.		Noise level, (dB)	
	Cumulative wear (gm)	Specific wear, (gm-cm^2/HP-hr)	Max	Min	Avg	T °C	t*(s)	Max	Min
FAl01	4.9	4.41	0.54	0.44	0.49	144	1020	27	24
FAl02	4.3	3.87	0.65	0.61	0.63	123	360	29	26
FAl03	4.3	3.87	0.54	0.48	0.51	148	600	35	29
FAl04	4.1	3.69	0.57	0.47	0.52	163	580	32	30
FAl05	4.0	3.60	0.54	0.46	0.50	154	490	32	28
FAl06	5.9	5.31	0.67	0.56	0.62	139	1100	43	37
FAl07	4.2	3.68	0.57	0.45	0.51	147	1600	29	25
FAl08	5.1	4.59	0.55	0.49	0.52	123	1540	23	21
FAl09	4.1	3.69	0.43	0.39	0.41	122	1340	32	29
FAl10	3.9	3.51	0.47	0.39	0.43	127	960	30	27
FAl11	3.6	3.24	0.32	0.29	0.30	120	900	25	22
FAl12	3.5	3.15	0.34	0.30	0.32	123	1600	24	20
FAl13	4.1	3.69	0.31	0.25	0.28	118	1500	25	23
FAl14	3.1	2.79	0.54	0.49	0.44	148	1460	36	32
FAl15	2.6	2.34	0.46	0.40	0.43	145	800	34	29
FAl16	2.0	1.80	0.42	0.38	0.40	146	900	31	27
FAl17	1.8	1.62	0.44	0.41	0.44	150	660	32	29
FAl18	2.2	1.98	0.52	0.40	0.46	140	330	29	24
FAl19	2.4	2.16	0.45	0.37	0.41	142	720	35	26
FAl20	2.7	2.43	0.53	0.33	0.43	141	1200	37	29
FAl21	1.2	1.08	0.47	0.37	0.42	126	590	30	26
FAl22	1.6	1.44	0.46	0.36	0.41	138	1460	34	26
FAl23	1.4	1.26	0.46	0.40	0.39	136	1320	30	27
FAl24	1.7	1.53	0.52	0.38	0.41	134	1500	31	26
FAl25	1.4	1.26	0.41	0.33	0.37	139	1820	30	24
FAl26	1.3	1.17	0.44	0.26	0.35	128	1020	35	32
FAl27	3.1	2.79	0.29	0.23	0.26	122	1920	32	26

* Time period to attain peak temperature.

Specific Wear: It is observed that specific wear is higher for the composites FAl01 to FAl014 and FAl27. The specific wear varies in a broad range from 2.79 to 5.31 gm-cm^2/HP-hr. whereas for other composites FAl15 to FAl26, it varies in a short range from 1.08 to 2.34 gm-cm^2/HP-hr. The specific wear is maximum about 5.31 gm-cm^2/HP-hr for sample FAl06 and minimum about 1.1gm-cm^2/HP-hr for composite FAl21.

A highest increment in specific wear is recorded for composite FAl06. This composite contains coconut fiber (2 wt.%) which has poor matching with metal matrix.

It is marked that relative adjustment of wt.% of SiC and graphite with in a range from 15 to 20 wt. % in composition of composites reduce the specific wear of composites to about 44%. It is also reduced up to minimum value when 1% of $BaSO_4$ is replaced by 2 % of zinc.

Prasad **[123]** has reported a similar effect that addition of zinc powder in composition improves wear resistance.

Preferences of composites on the basis of low specific wear are in following order starting from the best.

FAl21> FAl26> FAl25≈FAl23> FAl22> FAl24> FAl17> FAl16

Coefficient of friction: Coefficient of friction is higher for composites FAl01 to FAl08. The range of coefficient of friction for these composites varies within a range of 0.49 to 0.63. This range is larger than the ***automotive industry standard range of 0.3 to 0.45*** **[155].** Coefficient of friction range for other composites FAl09(0.41) to FAl26(0.35) lies in automotive industry standard range. It is noticed that the composites which have better combination of solid lubricants (9.54 wt.% of graphite and 2 wt.% of Sb_2S_3) with addition of 2 wt.% of zinc and 8.45 wt.% of SiC showed better overall performance. It may be concluded that frictional characteristics can be improved with addition of solid lubricants in bulk amount but on the other hand, it is excessive amount weakens their stiffness resulting in cracks during testing.

Preferences of composites in the decreasing order on the basis of automotive industry standard range of 0.3 to 0.45 **[155]** are in following order:

FAl27> FAl26> FAl25> FAl23> FAl16> FAl24≈ FAl22≈FAl19> FAl21

Temperature rise: For all the friction materials developed in the present investigation, temperature rise is lower due to high thermal conductivity of matrix material. The temperature rise ranges from 118 to 163 ^{0}C. It is noticed that higher wt. % of metallic matrix improves heat transfer rate (due to higher thermal conductivity), resulting lower temperature rise. For composite FAl13 (81 wt. % Al), temperature rise is minimum (118°C).

Preferences of composites on the basis of low temperature rise are in following order:

FAl13>FAl27> FAl21> FAl26> FAl24> FAl23> FAl22> FAl25> FAl18

Noise Level: Noise level is also lower than Fe powder based samples **[157].**

Preferences of composites on the basis of lower fluctuation (max-min) in noise level are in following order:

FAl26>FAl23 > FAl17> FAl25> FAl17> FAl24

5.2.2 Wear studies at higher load: Test code PD2

Table 5.3 shows the wear test results of twenty seven Al powder based samples (under test code: PD2). It includes wear, coefficient of friction, temperature rise and noise level.

Specific Wear: The specific wear increases with increasing the load from 5 to 8 kg. It is observed that specific wear varies in broad range from 1.35 to 5.67 gm-cm^2/HP-hr for the composites FAl01 to FAl014. It is maximum for composite FAl05 and minimum for composite FAl23.

Preferences of composites on the basis of low specific wear are in following order:

FAl23> FAl25≈ FAl22>FAl24> FAl22≈ FAl16> FAl21> FAl26

Coefficient of friction: Coefficient of friction decreases with increasing load. Coefficient of friction is higher for composites namely FAl01 to FAl10. The range of coefficient of friction for these composites is from 0.64 to 0.48. This range is above than automotive industry standard range of 0.3 to 0.45 **[155].** The range for coefficient of friction for **FAl11-FAl126** composites is 0.44 to 0.30, which is within the automotive industry standard range.

Preferences of composites on the basis of automotive industry standard range of 0.3 to 0.45 **[155]** are in following order:

FAl25> FAl26> FAl24> FAl15> FAl21> FAl22> FAl23

Temperature rise: For all Al-based samples, temperature rise is lower due to high thermal conductivity of matrix material. Temperature rise for composites increases with increasing the load from 5 to 8 kg. Temperature rise is obviously the function of load **[123].** For all Al powder based samples, temperature rise is lower than iron based samples **[157].**

It is noticed that temperature rise is increased about 1.9 times with increasing the applied load from 5 kg to 8 kg for composites FAl09 and . FAl10. For other composites, it increased 1.2 times. Temperature rise is almost stabilized with slight variation at low as well as high applied load.

Preferences of composites on the basis of low temperature rise are in following order:

FAl27> FAl26> FAl26≈ FAl25> FAl24> FAl19> FAl22> FAl21

Noise level: Noise level of Al based composites is lower than Fe powder based samples **[157].**

Preferences of composites on the basis of lower fluctuation in noise level are in following order:

FAl27> FAl25> FAl26>FAl24>FAl15>FAl19> FAl22> FAl21

Table 5.3 Pin-on-disc friction test performance: PD2

Contact area of pin: 7×7 mm^2

Samples	Wear test		Coefficient f friction			Peak tem. rise		Noise level, (dB)	
	Cumulative wear (gm)	Specific wear, (gm-cm^2/H.P-hr)	Max	Min	Avg	T °C	t*(s)	Max	Min
FAl01	5.6	4.94	0.57	0.49	0.53	178	920	32	30
FAl02	4.8	4.32	0.68	0.58	0.63	145	900	29	27
FAl03	5.0	4.50	0.61	0.53	0.57	169	600	30	28
FAl04	6.0	5.40	0.56	0.50	0.53	171	360	36	32
FAl05	6.3	5.67	0.47	0.39	0.43	167	540	32	28
FAl06	6.1	5.49	0.57	0.47	0.52	180	300	31	27
FAl07	6.0	5.40	0.52	0.44	0.48	112	240	34	31
FAl08	5.7	5.13	0.56	0.46	0.51	151	300	34	31
FAl09	4.1	3.69	068	0.56	0.62	232	720	24	22
FAl10	4.6	4.14	0.68	0.60	0.64	235	540	24	22
FAl11	5.1	4.59	0.34	0.30	0.32	145	540	25	21
FAl12	4.3	3.87	0.38	0.32	0.35	148	720	26	23
FAl13	4.6	4.14	0.37	0.29	0.33	151	600	26	24
FAl14	4.9	4.41	0.44	0.34	0.39	147	360	36	31
FAl15	2.3	2.07	0.39	0.31	0.35	150	720	32	29
FAl16	2.0	1.80	0.46	0.40	0.43	157	540	44	42
FAl17	2.5	2.25	0.46	0.42	0.44	148	270	33	31
FAl18	3.4	3.06	0.45	0.33	0.39	152	600	27	23
FAl19	3.1	2.79	0.43	0.35	0.39	146	590	29	25
FAl20	3.4	3.06	0.44	0.36	0.40	149	470	27	25
FAl21	2.1	1.89	0.40	0.34	0.37	148	550	23	20
FAl22	1.9	1.71	0.42	0.38	0.40	148	640	28	26
FAl23	1.5	1.35	0.46	0.36	0.41	150	854	25	21
FAl24	2.0	1.80	0.38	0.30	0.34	145	662	32	28
FAl25	1.9	1.71	0.33	0.25	0.29	139	820	35	30
FAl26	2.2	1.98	0.38	0.24	0.31	134	970	33	30
FAl27	3.4	3.06	0.24	0.20	0.22	129	980	36	31

* Time period to attain peak temperature

5.3 Comparison of selected developed Al-based composites with Fe-based composites

Table 5.4 and 5.5 show the pin-on-disc test results of earlier developed iron based composites **[157]**. It provides the details about specific wear, coefficient of friction, temperature at contact area and noise level.

Table 5.4 Pin-on-disc friction test performance for iron based brake pads [157]

Test code- PD1, pin area 7x7 mm^2

Samples	Cumulative wear loss(gm)	Specific wear, (gm-cm^2/HP-hr)	Coefficient of friction			Peak temperature rise		Noise level (dB)	
			Max	Min	Avg	°C	t** (s)	Max	Min
MIG-21*	-	2.03	0.54	0.48	0.51	286	270	29	96.1
FM08N	1.60	0.66	0.54	0.48	0.51	186	820	30	95.8
FM09N	0.61	0.24	0.48	0.40	0.44	193	970	23	92.6
FM10N	0.82	0.26	0.54	0.40	0.47	186	980	32	92.5
FM11N	0.59	0.21	0.54	0.48	0.51	184	920	22	89.4

Table 5.5 Pin-on-disc friction test performance for iron based brake pads [157]

Test code- PD2

Samples	Cumulative wear loss (gm)	Specific wear (gm-cm^2/HP-hr)	Coefficient of friction			Peak temperature rise		Noise level (dB)	
			Max	Min	Avg	°C	t** (s)	Max	Min
MIG 21*	-	4.86	0.54	0.46	0.51	235	390	27	95.8
FM08N	2.5	1.53	0.38	0.29	0.34	156	800	37	102
FM09N	1.4	0.41	0.33	0.24	0.29	120	700	30	96.2
FM10N	2.0	3.16	0.46	0.33	0.39	111	750	40	95.5
FM11N	2.2	0.68	0.42	0.33	0.38	141	700	34	94.5

*It is fabricated through sintering route and commercially used as brake pad in MIG21 fighter aircraft.

** Time taken to attain peak temperature.

The output parameters of pin-on-disc test results of thirteen selected Al powder based composites from FAl15 to FAl27 are compared with corresponding values of Fe based composites under identical input parameters **(Tables 5.4 and 5.5) [157].**

The comparison of specific wear, coefficients of friction (COF), temperature rise and noise levels of aluminium and iron based brake pads is as follows:-

Specific wear

At lower applied load, it is observed from fig. 5.2 that specific wear of Al based samples from FAl15 to FAl27 is higher in comparison to Fe based samples FM08N, FM09N, FM10N and FM11N. But specific wear of few Al powder based samples: FAl21 to FAl226 is lower than the specific wear of Fe powder based sample: MIG21.

Preferences of samples are in following order (on the basis of lower specific wear)

FAl21> FAl23> FAl25 ≈ FAl22> FAl22> FAl24 ≈ FAl16>FAl26

At higher applied load, it is observed that the specific wear of Al based composites increases with increasing the normal applied load from 5 (PD1) to 8 kg (PD2) (fig.5.1). Similarly, specific wear of Fe based composites increases with increasing the load. At higher applied load, drastic increment in specific wear of sample MIG21 and FM10N has been recorded. It is noticed that variation in specific wear of composite FAl15 decreases and for composite FAl16 is constant when load is increased from 5 to 8 kg.

Specific wear of Al based composites is lower in comparison to Fe based composites MIG-21 and FM10N.

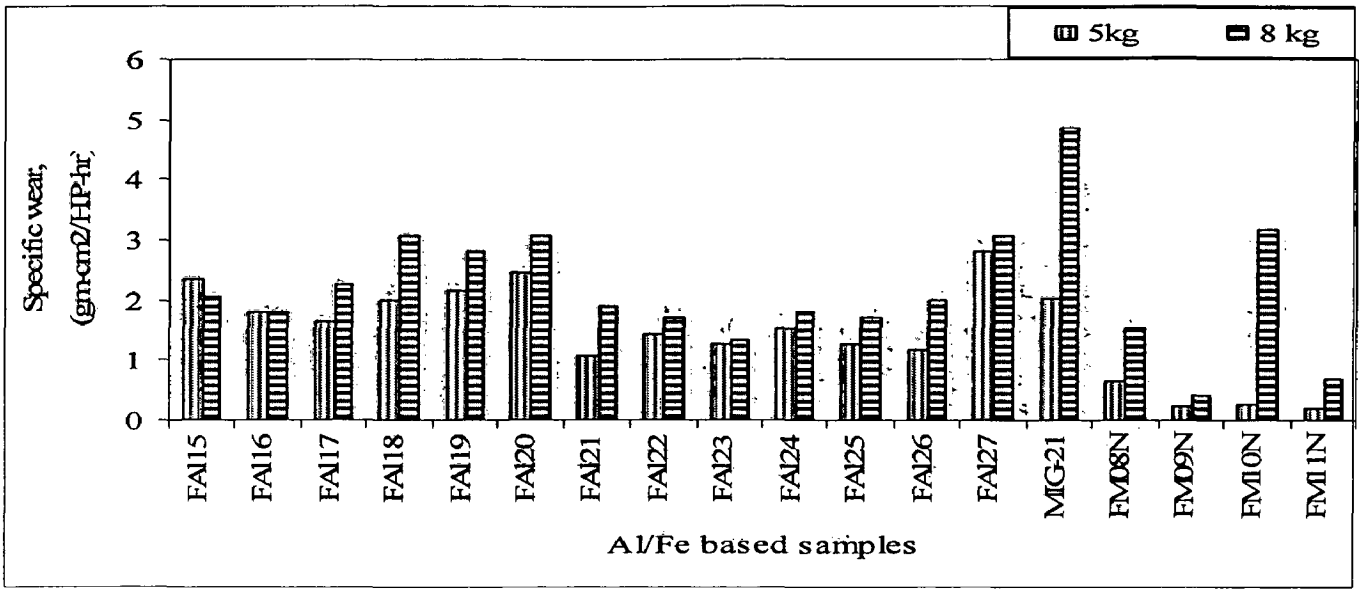

Fig. 5.2 Comparison of specific wear at 5 and 8 kg loads

The preferences of samples on the basis of lower specific wear are given below.

FA23> FA122≈ FA125 >FA116≈ FA124> FA121>FA126 ≈ FA115

Coefficient of friction

At lower applied load (PD1), coefficient of friction of Al powder based samples from FA115 to FA126 is lower in comparison to Fe based samples and lies within industry standard range of 0.3 to 0.45 for automotive brake systems (fig. 5.3) **[155].** The range for coefficient of friction of Fe based samples: MIG21, FM08N, FM10N and FM11N is higher (0.44-0.51) and does not lie in the automotive industry standard range. Whereas the coefficient of friction of composite: FM09N (0.44) is within standard range.

At higher applied load (PD2), coefficient of friction of composites FA115 to FA126 reduces with increasing the load from 5 to 8 kg. Similar effects have been noticed for Fe based composites. It increases with increasing the load for composite FA116. It is also noticed that there is no effect of load variation on coefficient of friction for composite: FA117 (stable COF). The coefficient of friction for Al based composites is lower than Fe based composite MIG-21 and slightly higher than FM09N. However, coefficient of friction in Al-based samples can be increased to match iron based samples by adjusting different constituents in it.

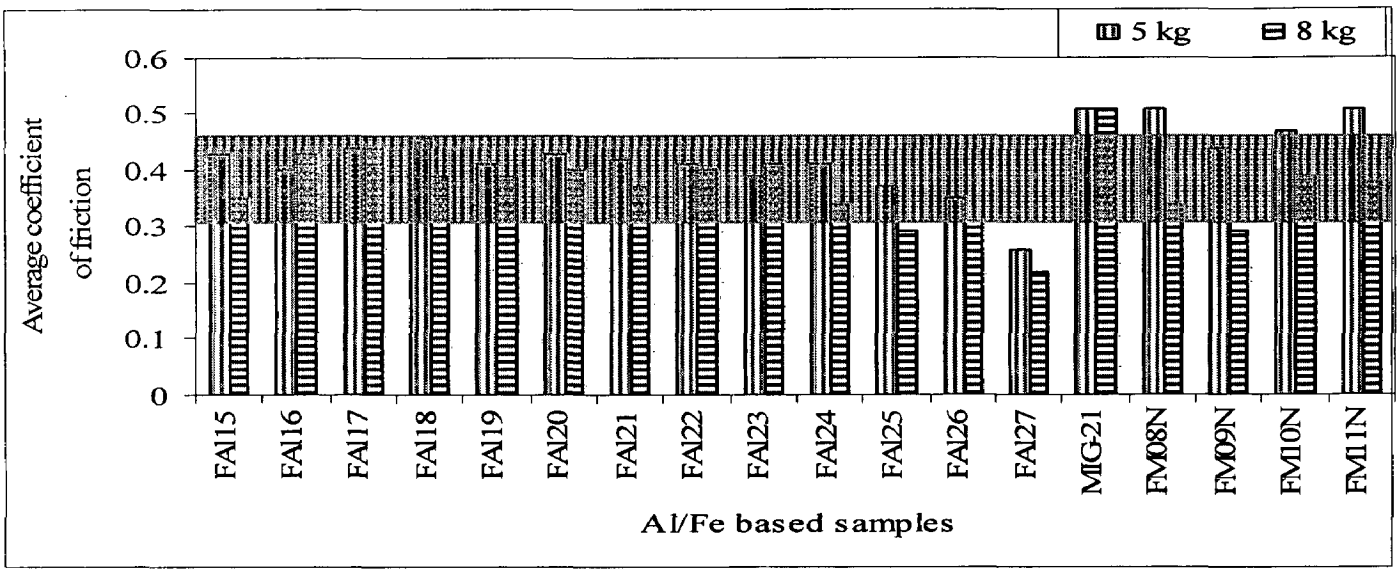

Fig. 5.3 Comparison of average coefficient of friction at 5 and 8 kg loads

The preferences of samples on the basis of industry standard range (0.3-0.45) presented by shaded region in fig. 5.3 are given below.

FAl20 ≈FAl22 > FAl23>FAl18 ≈ FAl19>FAl21>FAl15>FAl24> FAl26>FAl25

Temperature rise (ΔT)

At low as well as high applied load, temperature rise of aluminium based samples is lower in comparison to iron based samples (fig.5.4).Temperature rise for all Al based samples increases corresponding to increase in applied load from 5 to 8 kg. It noticed that there is minor change in temperature rise for Al–based samples corresponding to change in load from 5 to 8 kg whereas for iron based samples, it rises about 1.5 times.

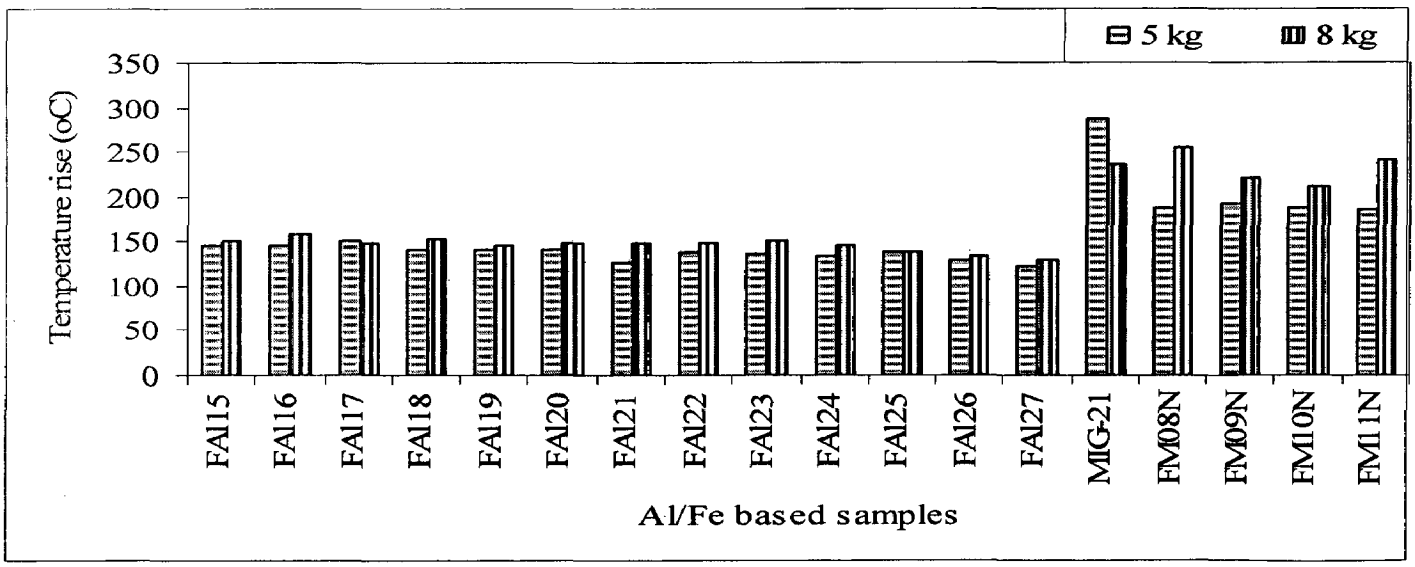

Fig 5.4 Comparison of temperature rise at 5 and 8 kg loads

The preference of samples for fabrication of brake pads is given below:

FAl27>FAl21 > FAl26>FAl24> FAl23>FAl22>FAl25>FAl18> FAl20

Noise level (dB)

According the graph (fig 5.5), it is observed that noise level of Al-based samples during tribo-test is higher than Fe-based samples at lower applied load. At higher applied load, the noise levels are higher for samples FAl16, FAl27, FM08N and FM10M whereas for remaining samples noise level are of similar range.

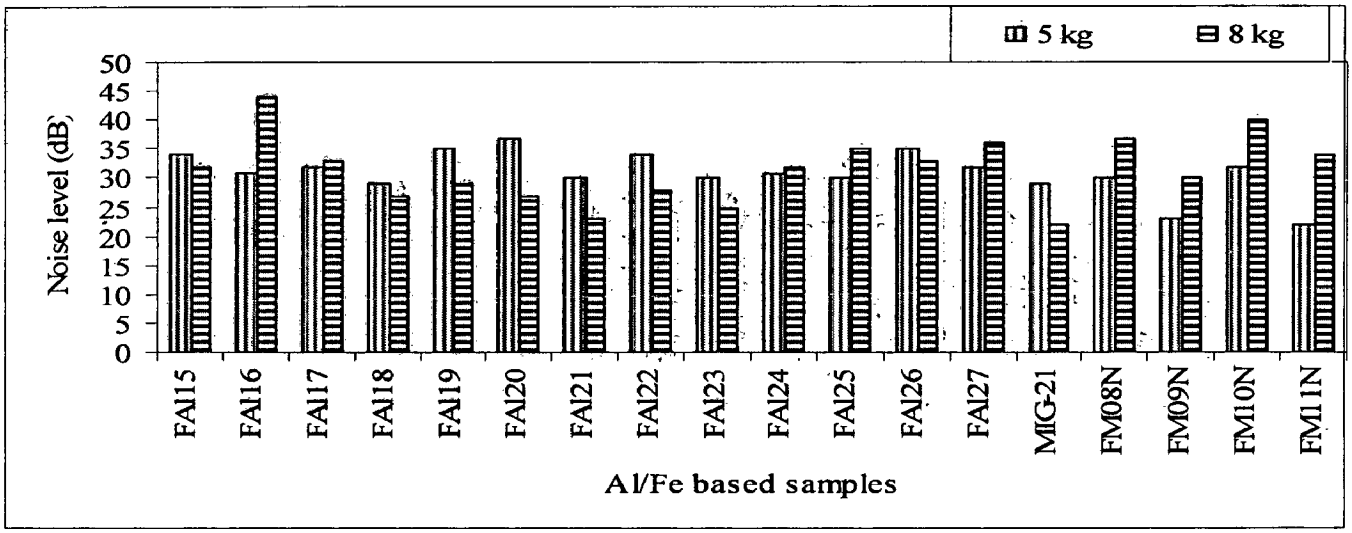

Fig. 5.5 Comparison of noise level at 5 and 8 kg loads

It is observed from tribo-evaluation of Al based composites at laboratory level that solid lubricants with ceramic play crucial role in building and maintaining the friction film at the friction interface. The main function of friction film is to lower the wear loss, provide stable coefficient of friction at low as well as high temperature and reduce the noise level. The effectiveness of the solid lubricants is strongly affected by temperatures, pressure, speed and environmental condition. Therefore two solid lubricants namely graphite and antimony tri sulphide have been effectively utilized in developing Al-based brake pads. Kim *et. al.* **[151]** have reported that the brake linings containing a single solid lubricant either graphite or antimony tri sulphide showed large change of COF with pressure. On the other hand, brake linings containing both solid lubricants showed smaller changes of the COF with pressure variation. In particular, the brake lining 6G3S (6 wt.% graphite and 3 wt.% antimony tri sulphide) containing higher contents of graphite exhibited the best friction stability among different brake linings. The developed Al based friction composites which have better performance contains graphite range from 8 to 11 wt.% with addition of antimony tri sulphide about 2 wt.%.

The composites, which are added with ingredients exhibit stable coefficient of friction, better load carrying capacity and reduce enhancement of micro-cracking characteristics of various micro- constituents **[123].**

From aforementioned tribo-evaluation of Al based composites and their performance, the following conclusions are made

(i) Specific wear depends upon the external (load) as well as internal factors (characteristics of incorporating ingredients and its uniform distribution in matrix). It is proportional to the power function of load and followed the theoretical equation (proposed by Rhee) for the wear of lining material **[107].**

(ii) Coefficient of friction of selected composites is stable and lies in standard industries range at lower as well as higher applied load.

(iii) Temperature rise is low. There is minor affect of higher applied load on temperature rise.

(iv) Sound levels of Al based composites are equivalent to Fe based composites.

(v) For optimum tribo-performance of Al based friction composites, ingredients addition should be lie in range from 22 to 25 wt. %.

(vi) Summation of wt. % of main ingredients like graphite and SiC in matrix should be in the range from 15 to 20 and other ingredients should be in the range from 7 to 9 wt.%.

Optimized Chemistry for development of friction materials

Based on the Pin-on-disc tests results, following composition were selected for high level characterization to develop brake pads for aircraft/heavy/medium/light duty automotive applications.

FAl26, FAl25, FAl24, FAl23, FAl22, FAl21, FAl20

5.4 Krauss rig tribo-tests for light and heavy vehicles

Krauss rig tribo-tests against cast iron inertia wheel were carried out at Allied Nippon Ltd., Ghaziabad, U.P. INDIA for characterization of the tribological properties of developed Al-based brake pad materials namely **FAl20** to **FAl26**, to judge their suitability for heavy/medium/light automobile vehicles. Friction test data sheets namely **ANL21** to **ANL26** corresponding to our samples are available in **Annexure-A1-A21.** In this stion, following points are covered:

i) tribo-tests like friction/wear test and recovery and fade test of developed Al based friction composites under applied brake pressures with in a range from 0.5 to 1.3 MPa at constant speed: 660 rpm for pad areas 18.86 and 29.1 cm^2, ii) effects of brake pressures, iii) effects of pad areas, iv) comparison of output parameters of developed Al based brake pad materials to corresponding output parameters of existing brake pad materials like resin/sintered iron based

in different applications namely road vehicles, railway and high speed vehicles, v) standard evaluations and vi) suitability of developed brake pads in different applications.

Note: No effort has been made to assess the tribological characteristics of inertia wheels.

The input parameters for reduced and full scale friction tests for light and heavy duty applications on Krauss test rig are shown in **Tables 5.6 and 5.7** respectively, as test codes (**RS5** and **RS7** test codes for reduced scale test and **AN700/ADB-0130**, **NAO-507/ADB-256**, **JBNH/ADB-0130** and **LCVHY/ADB-0130** test codes for full-scale/product test).

Reduced scale tests are non standard tests which have been carried out to asses the tribological characteristics at low applied pressures with in a range from 0.5 to 0.7 MPa whereas ***full scale/product tests*** are standard tests which have been carried out under high pressures with in a range from 1.0 to 1.3 MPa to judge the suitability of developed brake pad materials in heavy/medium/light automobile vehicles.

Note: Under these employing input parameters; friction test and recovery and fade test were conducted for selected composites; from **FAI21** to **FAI26**. The test responses were recorded on ANL data sheet in graphic and numeric term. It incorporates the test specifications, performances like coefficient of friction (μ), performance friction coefficient, recovery friction coefficient; fade friction coefficient, recovery (%), fade (%) and temperature rise corresponding to applied brake pressures.

Table 5.6 Krauss rig test: Reduced scale friction test input parameters

Pad area = 18.5 cm^2

Test code	K.E.(kgfm)	N (rpm)	p_b (MPa)	M (kgfm)	t_b (s)	t_i (s)
RS5	6000	660	0.5	50	5	10
RS7	6000	660	0.7	50	5	10

Table 5.7 Krauss Test: Full scale friction test input parameters

Applications in Heavy / light duty	Designated test codes under ECR R-90 standard test	Test parameters							
		K.E(kgfm)	N (rpm)	F_b (kgf)	P_b (MPa)	A_{pad} (cm^2)	M (kgfm)	t_b(s)	t_i(s)
Heavy	*AN700/ADB-0130	6000	660	377.2	1.3	29.1	50	5	10
Heavy	*NAO-507/ADB-256	6000	660	377.2	0.8	48.5	50	5	10
Light	*JBNH/ADB-0130	6000	660	188.6	1.0	18.5	50	5	10
Light	*LCVHY/ADB-0130	6000	660	188.6	1.0	18.5	50	5	10

* ***These test codes are designated by Allied Nippon Ltd., Ghaziabad, U.P. INDIA on the basis of type of vehicles under ECR R-90 standard test [147].***

The description of the performance parameters as obtained from Krauss rig tribo-tests are as follows **[147].**

Performance friction coefficient ($\mu_{Performance}$): It is the average friction coefficient of all the braking operations irrespective of the nature of the run i.e., cold cycle, fade cycle and recovery cycle.

Performance friction fade coefficient (μ_{Fade}): It is calculated on the basis of the difference between the performance friction coefficient and the friction coefficient at the maximum disc temperature rise for every fade cycle run which is normalized against the number of fade cycle runs (5 in this case). The fade is higher, poorer the performance.

Performance recovery coefficient ($\mu_{Recovery}$): It is the revival of braking efficiency in terms of attaining the same performance after the friction material is cooled down to a lower temperature.

Fade (%): It is the ratio of Performance Friction Fade (μ_{Fade}) to Performance Friction ($\mu_{Performance}$). It is one of the performance evaluation factors to evaluate the performance of friction materials at high temperature.

Fade (%) = μ_{Fade} / $\mu_{Performance}$

Recovery (%): It is the ratio of Performance Recovery ($\mu_{Recovery}$) to Performance Friction ($\mu_{Performance}$).

Recovery (%) = $\mu_{Recovery}$ / $\mu_{Performance}$

It is one of the performance evaluation factors to evaluate the performance of friction materials when it is cooled after brake application. It shows the recovering properties of friction material when it is cooled because at temperature it looses some part of frictional characteristics

Disc temperature rise (DTR): It is the frictional temperature rise of the rotor disc due to the friction braking irrespective of all the runs. The lower the temperature rise, better the performance as the thermal distortion and friction undulations will be lower.

Wear loss: It is progressive removal of the material from the surface due to thermo-mechanical stresses caused by the frictional interactions. It is measured in both pads thickness (mm) and weight loss (gram).

Judder and vibration: Judder and vibration are the main cause of jerk during braking. It is directly related to fluctuation in coefficient of friction. It is lower when fluctuation in coefficient of friction is lower, resulting lower jerk experienced by driver during brake applied **[132,133].**

Tribo-tests of developed brake pad materials are completed in three steps namely: **i) Reduced scale tribo-test ii) full scale tribo-tests for light duty vehicles iii) full scale tribo-tests for heavy duty vehicles**

5.4.1 Reduced scale test

Reduced scale tribo-tests were carried out under test codes RS5 and RS7 to evaluate the tribo performances of selected composites FAI21 to FAI26. The purpose of this test is to asses the variation in tribological characteristics of Al based composite under low applied brake pressures and provide a base for selection of composites for full scale tribo-tests. Tribo-test performances are measured in terms of **i) wear (gm) and wear in pad thickness(mm), ii) avg. coefficient of friction (μ), iii) fluctuation in coefficient of friction ($\Delta\mu = \mu_{max}-\mu_{min}$), iv) temperature rise, v) performance friction coefficient ($\mu_{Performance}$), v) performance recovery coefficient ($\mu_{Recovery}$), vi) performance friction fade coefficient (μ_{Fade}), vii) fade (%), and viii) recovery (%).**

Reduced tribo-test performances are shown in **Table 5.8 (a)** and **5.8 (b).**

Table 5.8 (a) Reduced scale friction test performance

Samples	Test codes	Tem. rise		Coefficient of friction				Wear					
								Pad thicknes (mm)		Wt.(gm)		Avg. wear	
		T_{min}, ^0C	T_{max}, ^0C	μ_{min}	μ_{max}	$\mu_{av.}$	$\Delta\mu = \mu_{max}-\mu_{min}$	Pad1	Pad2	Pad1	Pad2	Thick. (mm)	wt.(gm)
FAI21	RS5	40	170	0.27	0.40	0.35	0.13	0.23	0.19	1.8	1.8	0.20	1.8
FAI23	RS5	40	170	0.31	0.41	0.41	0.15	0.19	0.25	2.0	2.3	0.20	2.2
FAI24	RS5	40	170	0.35	0.54	0.43	0.19	0.07	0.23	0.6	0.9	0.15	0.8
FAI21	RS7	40	200	0.34	0.43	0.40	0.09	0.02	0.03	1.2	1.7	0.14	1.5
FAI23	RS7	40	200	0.35	0.41	0.42	0.10	0.01	0.09	1.1	1.3	0.10	1.2
FAI24	RS7	40	170	0.34	0.50	0.41	0.17	0.04	0.18	0.3	0.6	0.10	0.5

Note: Friction test performances for composites FAI25 and FAI26 are not recorded at 0.5 and 0.7 MPa

Wear (gm): It is observed from **Table 5.8(a)** that the wear of developed friction composites decreases corresponding to increase in applied brake pressure from 0.5 to 0.7 MPa. It is inferred that loss in wear (%) (wear % = ratio of wear at 0.7 MPa to ratio of wear at 0.5 MPa) is about 83, 55 and 62 % for composites **FAI21, FAI23** and **FAI24** respectively. For composite **FAI23**, the lower loss in wear (%) shows the better tribological effect of more solid lubricant like graphite (11.54 wt. %) in chemistry of composite at applied brake pressure 0.7 MPa. The minimum wear for composite **FAI24** (0.5 gm) shows the additional effect of incorporation of zinc (4 wt. %) with graphite (9.54 wt.%) in composition at applied brake pressure 0.7 MPa.

The preference of composites on the basis of wear is:

FAI24>FAI23>FAI21 (0.7 MPa) FAI24>FAI21>FAI23 (0.5 MPa)

Wear (mm): Table 5.8(a) shows the wear in pad thickness, mm of developed friction composites. The wear ratio is about 67, 50 and 67 % corresponding to composites **FAI21, FAI23** and **FAI24** under increase in applied brake pressure from 0.5 to 0.7 MPa. The preferences of composites on the basis of wear is

FAI23≈FAI24>FAI21 (0.7 MPa) FAI24>FAI23≈FAI21 (0.5 MPa)

Avg. coefficient of friction (μ)

Table **5.8(a)** shows that the coefficient of friction increases for composites **FAI21** and **FAI23** and decreases for composite **FAI24** corresponding to increase in applied brake pressure from 0.5 to 0.7 MPa. It is inferred that the coefficient of friction for Al based friction composites varies with in range from 0.35 to 0.43; lies in standard automotive range ≈0.3 to 0.45 **[155].** Preference of composites on the basis of μ_{avg} is

FAI21>FAI23>FAI24 (0.7 MPa) FAI24>FAI23>FAI21 (0.5 MPa)

Fluctuation in coefficient of friction ($\Delta\mu = \mu_{max} - \mu_{min}$): It is inferred that the fluctuation in coefficient of friction decreases corresponding to increase in pressure from 0.5 to 0.7 MPa **(Table 5.8(a)).** It is decreased about 31, 33 and 11% for composites **FAI21, FAI23** and **FAI24** respectively. It may be concluded that for friction composite **FAI21,** lower judder and vibration will be generate during braking because fluctuation in coefficient of friction is minimum. Preference of composites on the basis of lower amplitude of frictional fluctuation at applied brake pressures is

FAI21>FAI23>FAI24 (0.7 MPa) FAI21>FAI23>FAI24 (0.5 MPa)

Interdependence of $\mu_{Performance}$, $\mu_{Recovery}$, μ_{Fade} and temperature rise

Table **5.8(b)** shows the recovery and fade test performance namely performance friction coefficient ($\mu_{Performance}$), performance recovery coefficient ($\mu_{Recovery}$), performance friction fade coefficient (μ_{Fade}), recovery (%) and fade (%) corresponding to increase in applied brake pressures with in a range from 0.5 to 0.7 MPa. The interdependence of performance, fade and recovery is poorly understood. One of the reasons for the inadequate understanding of the mechanistic details of such a vicious cycle of interdependent performance criteria of friction materials lies in the fact that the ingredients of these multi-component composition-based materials are of disparate nature.

Fade is conceptually a phenomenon directly dependent on the temperature rise of a friction material individually. However, in a series of composites based on the incorporation of

ingredients in sequence, the fade performance seems to be dependent on the adiabatic potential and other thermal characteristics of the ingredients.

Table 5.8(b) Reduced scale fade and recovery test performance

Test parameter	Al based friction composites					
	FAl21		**FAl23**		**FAl24**	
	RS7	RS5	RS7	RS5	RS7	RS5
$\mu_{performance}$	0.383	0.424	0.412	0.433	0.400	0.478
$\mu_{recovery}$	0.433	0.538	0.442	0.452	0.506	0.539
μ_{fade}	0.349	0.376	0.364	-	0.341	0.431
Fade (%)	9	11	12	-	15	10
Recovery (%)	113	128	107	104	127	113
Wear (cm^3)	0.51	0.41	0.42	0.77	0.18	0.27
Disc. temp.(^{0}C)	40 -170	40-200	40- 170	40-200	40 - 170	40-200

Performance friction coefficient ($\mu_{Performance}$): Table 5.8(b) shows the performance coefficient of friction ($\mu_{Performance}$) for composites decreases corresponding to increase in brake pressure from 0.5 to 0.7 MPa. It is inferred that the $\mu_{Performance}$ for composite **FAl23** is stable at lower as well as high applied brake pressure.

Preference of composites on the basis of $\mu_{Performance}$ at applied pressures

FAl23>FAl24>FAl21 (0.7 MPa) FAl24>FAl23>FAl21 (0.5 MPa)

Performance recovery coefficient ($\mu_{Recovery}$): Table 5.8(b) shows that the performance recovery coefficient ($\mu_{Recovery}$) for composites **FAl21, FAl23** and **FAl24** decreases corresponding to increase in brake pressure from 0.5 to 0.7 MPa. It is decreased about 20, 12 and 6% for composites FAl21, FAl23 and FAl24 respectively corresponding to increase the applied brake pressure from 0.5 to 0.7 MPa. It is inferred that loss in $\mu_{Recovery}$ is lower for composite FAl24 shows better frictional characteristic at lower as well as high applied brake pressure.

Preference of composites on the basis of $\mu_{Recovery}$ at applied pressures

FAl24>FAl23>FAl21 (0.7 MPa) FAl24>FAl21>FAl23 (0.5 MPa)

Performance friction fade coefficient (μ_{Fade}): Table 5.8(b) shows the performance friction fade coefficient decreases corresponding to increase in brake pressure from from 0.5 to 0.7 MPa. It is inferred that loss in performance friction fade coefficient is lower for composite **FAl21** shows better frictional characteristic at lower as well as high applied brake pressure

Preference of composites on the basis of μ_{Fade} at applied pressures

FAl23>FAl21>FAl24 (0.7 MPa) FAl24>FAl21 (0.5

Fade (%): **Table 5.8(b)** shows the fade (%) of composite **FAl21** decreases from 11 to 9% and increases from 10 to 15% for composite **FAl24** corresponding to increase in applied brake pressure from 0.5 to 0.7 MPa. It may be concluded that the nature of fade of composite **FAl21** is low at high applied pressure (0.7 MPa). It is lower than resin based friction materials **[29].**
Preference of composites on the basis of fade (%) is ,

FAl21>FAl23>FAl24 (0.7 MPa) FAl24>FAl21 (0.5 MPa)

Recovery (%): The recovery (%) is increased about 3 and 20% corresponding composites **FAl23** and **FAl24** and is decreased abut 12 % for composite **FAl21** corresponding to increase in applied brake pressure from 0.5 to 0.7 MPa **(Table 5.8(b)).** It may be concluded that Al based composites FAl23 and FAl24 recovers its frictional characteristics at high applied pressure. Recovery (%) for Al based composite friction materials is higher than resin based friction materials **[29,147].**
Preference of composites on the basis of recovery (%) is

FAl24>FAl21>FAl23 (0.7 MPa) FAl21>FAl24>FAl23 (0.5

It may be concluded that the performance of the developed Al based composites (friction materials) which are based on the different combinations is distinct from each other. It is also observed that the rule of mixture does not hold well for all the cases.
Temperature rise: **Table 5.8(b)** shows that the temperature rise increases from 170 to 200^{0}C corresponding to increase in pressure from 0.5 to 0.7 MPa. It is obvious that temperature increases corresponding to increase in pressure.

5.4.2 Full scale test/Product test

In this type of tribo-test, brake pads of actual size were used as test specimens to characterize the reliability and tribological properties and asses the suitability under standard input parameters. Two type of tribo- tests were carried out namely **i) light duty vehicle tests ii) heavy duty vehicle tests.**
Test preferences of developed Al based composites for light and heavy duty applications are compared to the corresponding type of test performances of commercially used resin based friction materials in different applications. The test performances of developed Al based composites are evaluated on the basis of recommended friction materials by friction materials manufacturers federal motor vehicle safety standard-105 (FMVSS-105) [73]. The test performances of developed Al based composites for other applications are also evaluated on the basis of test performances of using brake materials in different application.

Table 5.9(a) Friction test performances for light duty vehicles

Samples	Test codes	Temp. rise		Coefficient of friction				Wear					
								Pad thickness (mm)		Wt.(gm)		Avg. wear	
		T_{min}, (^{0}C)	T_{max}, (^{0}C)	μ_{min}	μ_{max}	$\Delta\mu = \mu_{max} - \mu_{min}$	$\mu_{av.}$	Pad1	Pad2	Pad1	Pad2	Thick. (mm)	Wt. (gm)
FAI21	LCVHY/ ADB-0130	40	200	0.36	0.63	0.27	0.49	0.19	0.11	2.8	2.3	0.2	2.6
FAI23	LCVHY/ ADB-0130	40	200	0.28	0.41	0.13	0.37	0.21	0.18	1.9	1.7	0.2	1.8
FAI24	LCVHY/ ADB-0130	40	200	0.26	0.39	0.13	0.34	0.17	0.15	1.5	1.3	0.2	1.4
FAI25	LCVHY/ ADB-0130	40	200	0.27	0.40	0.13	0.35	0.23	0.19	1.8	1.8	0.2	1.8
FAI26	LCVHY/ ADB-0130	40	200	0.31	0.46	0.15	0.41	0.19	0.25	2.0	2.3	0.2	2.2

Table 5.9(b) Fade and recovery test performance for light duty vehicles

Out put parameters	Test code: LCVHY/ADB-0130						
	FR3	FR4	FAI21	FAI23	FAI24	FAI25	FAI26
$\mu_{performance}$	-	-	0.516	0.342	0.316	0.328	0.380
$\mu_{recovery}$	-	-	0.633	0.378	0.349	0.363	0.419
μ_{fade}	-	-	0.511	-	-	-	-
Fade (%)	-	-	99	-	-	-	-
Recovery (%)	-	-	123	111	111	111	110
Wear, cm^3			0.89	0.63	0.50	0.62	0.77
Temp rise., ^{0}C	40-250	40-250	40-200	40-200	40-200	40-200	40-200

Table 5.10 Performance of resin based brake pads for light/heavy duty vehicles

Samples	Test codes for Heavy:FR1, FR2 and Light:FR3, FR4 Vehicle Test	Tem. rise		Coefficient of friction			Wear					
							Pad thickness (mm)		Wt.(gm)		Avg. wear	
		$T_{max.}$ (^{0}C)	$T_{min.}$(^{0}C)	μ_{min}	μ_{max}	$\mu_{av.}$	Pad1	Pad2	Pad1	Pad2	Thick. (mm)	Wt. (gm)
FR1*	AN700/ADB-0130	40	600	0.31	0.48	0.42	0.29	0.32	3.1	3.2	0.31	3.15
FR2*	NAO-507/ADB-256	40	400	0.28	0.49	0.40	0.02	0.04	2.1	3.0	0.03	2.55
FR3*	JBNH/ADB-0130	40	250	0.30	0.44	0.36	0.06	0.08	0.2	0.1	0.07	0.15
FR4*	LCVHY/ADB-0130	40	250	0.25	0.42	0.35	0.05	0.07	0.1	0.1	0.06	0.10

* Resin based commercial samples with unknown ingredients

5.4.2.1 Light duty vehicle tests

The tribo-tests were conducted on a Krauss rig type RWDC 100C (450 V/50 Hz) machine conforming to ECR R-90 standard regulation test for developed Al based and commercially available resin based brake pad materials (pad area; 18.5 cm^2). The output performances are characterized to asses the reliability and suitability of developed Al based friction composites in comparison to resin based friction composites for light duty application. The performances in terms of wear, coefficient of friction (μ), fluctuation in coefficient of friction, $\mu_{performance,}$, $\mu_{recovery,}$ $\mu_{performance,}$ $\mu_{fade,}$ fade (%), recovery (%) and temperature rise of selected developed composites under applied brake pressure about 1.0 MPa at constant speed 660 rpm are measured and recorded. The tribo-test performances are given in **Table 5.9(a), Table 5.9(b) and Table 5.10 (pp.141).**

Wear (gm): Table 5.9(a) shows the wear varies with in a range from 1.4 to 2.6 gm. The wear decreases for the composites FAl21 to FAl24 and increases for the composites FAl25 to FAl26. It is lower for composite FAl24 (1.4 gm). Wear for resin based composites FR3 and FR4 is 0.15 and 0.10 gm respectively **(Table 10).** It may be concluded that wear of Al based composites is higher than wear of resin based composites.

Preference of composites on the basis of wear performance is

FAl24>FAl23≈FAl25>FAl26>FAl21

Coefficient of friction (μ_{Aavg}): Table 5.9(a) shows the coefficient of friction for composite **FAl21** is about 0.49 which is maximum and beyond the range of **automotive industry standard range of 0.3 to 0.45 [155]** but it is equivalent to the coefficient of friction of brake materials which is commercially used in racing cars, touring cars and also applicable where exceptional life required **[194,195],** so that it is suitable for these applications. For other composites **FAl23** to **FAl26**, it varies with in a range from 0.34 to 0.41. It may conclude that the composites **FAl23, FAl24, FAl25** and **FAl26** is suitable for brake pads in automotive industries because the range of coefficient of friction for these composites lies with in a range of automotive industry standard range. It is also observed from **Table 10** that average coefficient of friction (μ_{avg}) for resin based composites **FR3** and **FR4** varies with in range of 0.35-0.36 which is equivalent to Al based composites except of **FAl21.** It may be also concluded that developed Al based composites can be used for road vehicles and also used in racing cars, touring cars and also applicable where exceptional life required.

Preference of composites on the basis of average frictional performance is

FAl23>FAl25>FAl26>FAl24>FAl21

Temperature rise: The temperature rise for developed Al based composites varies with in a range from 40 to 200^{0}C **Table 5.9(a)** corresponding to no. of brake cycles 50 whereas the temperature rise for resin based composites varies with in a range from 40 to 250^{0}C **(Table 10).** It may be concluded that temperature rise of developed Al based brake pads is lower than commercially used resin based friction materials **[29, 150, 190].**

Fluctuation in coefficient of friction: Amplitude of frictional fluctuation for composite FAl21 is about 0.27 which is 2 times higher than the amplitude of frictional fluctuation of other composites. It is noticed that amplitude of frictional fluctuation of composites **FAl23, FAl24** and **FAl25 (Table 5.9(a)** is constant and in comparison to resin based composites, **FR3 and FR4** is lower **(Table 10).** It may be concluded that feeling of jerk for resin based friction material is higher than that of Al based composites.

Preference of composites on the basis of frictional fluctuation performance is

FAl23≈FAl25≈ FAl24>FAl26>FAl21

Performance friction coefficient ($\mu_{Performance}$): Table 5.9(b) shows the friction performance ($\mu_{Performance}$) of Al based composites **FAl21** to FAl26 varies with in a range from 0.32 to 0.52. It is inferred that friction performance of composite **FAl21** is 1.6 times more than that of other composites.

Preference of composites on the basis of $\mu_{Performance}$ corresponding to chemistries alteration is

FAl21>FAl26>FAl23>FAl25>FAl24

Performance recovery coefficient ($\mu_{Recovery}$): Table 5.9(b) shows that the performance recovery coefficient ($\mu_{Recovery}$) of Al based composites **FAl21** to **FAl26** varies with in a range from 0.35 to 0.63. It is noticed that friction performance of composite **FAl21** is 1.5 times more than that of others.

Preference of composites on the basis of $\mu_{Recovery}$ corresponding to chemistries alteration is

FAl21>FAl26>FAl23>FAl25>FAl24

Recovery (%): Table 5.9(b) shows the recovery (%) (≈111) is equal for composites **FAl23, FAl24 FAl25** and **FAl26** whereas for composite **FAl26**, it is higher **(≈ 123).** It may be concluded that recovery for Al based composites is higher than recovery (%) of resin based composites **[29].**

Preference of composites on the basis of recovery (%) at applied pressures

FAl21>FAl23≈FAl24≈FAl25>FAl26

5.4.2.2 Heavy duty vehicle tests

Table 5.11 (a) and **Table 5.11 (b) (pp.145)** shows the performances obtained from the ECR R-90 standard regulation test carried out on Krauss rig test machine under applied brake pressure 1.3 MPa for heavy duty application. The output parameters of Al based brake pad materials are compared to corresponding output parameters of commercially used resin based brake pad materials which are tested under identical conditions and performances, are recorded in **Table 5.10 (pp.141) and Table 5.11(b) (pp.145).**

Wear (gm): Table 5.11 (a) shows the wear varies with in a range from 2.7 to 3.6 gm for the composites **FAl23 to FAl26.** It is noticed that for composite **FAl21** (≈7.6 gm), it is significantly increased. The wear for resin based composites **FR1** and **FR2 (Table 5.10)** is about 3.15 and 2.55 gm respectively, which is equivalent to the wear of Al based composites except of wear in composite **FAl21.**

Preference of composites on the basis of wear performance is

FAl23>FAl26>FAl24>FAl25>FAl21

Coefficient of friction (μ_{Aavg}): Table 5.11 (a) shows the coefficient of friction for composites **FAl21** to **FAl26** varies with in a range from 0.36 to 0.43 lie in the range of automotive industry standard range ≈ 0.3 to 0.45 **[155].** It is also observed from **Table 10** that average coefficient of friction (μ_{avg}) for resin based composites **FR1** and **FR2** varies with in range of 0.40-0.42 which is equivalent to coefficient of friction of Al based composites. It may concluded that the all Al based composites is suitable for production of brake pads and their use in automobiles because the range of coefficient of friction for these composites lies with in a range of automotive industry standard range. It is also concluded that the coefficient of friction for composite **FAl23** and **FAl24** lie in mid of automotive industry standard range, which confirms optimal tribological performance during test.

Preference of composites on the basis of average frictional performance is:

FAl23>FAl25>FAl26>FAl24>FAl21

Temperature rise: Table 5.11 (a) shows the temperature rise varies with in a range from 40 to 200^{0}C in a friction test is stable and equal for developed Al based composites. The temperature rise for resin based composites **FR1** and **FR2** varies with in a range from 40 to 600^{0}C and 40 to 400^{0}C respectively **(Table 5.10),** which is higher in comparison to developed Al based composites. It is noticed that temperature rise for Al based brake pads is 1.5 to 3 times lower than commercially used friction materials **[29,150,190].**

Fluctuation in coefficient of friction: Table 5.11 (a) shows that the amplitude of frictional fluctuation for composites **FAI21** and **FAI25** is 1.1 to 1.3 times more than that of amplitude of frictional fluctuation of other composites. It is maximum for composite **FAI21** and minimum for composite **FAI23**. The amplitude of frictional fluctuation for resin based composites **FR1** and **FR2** is about 0.17 and 0.21(**Table 5.10**) which is equivalent to amplitude of frictional fluctuation of developed Al based composites. It may be concluded that formation of vibration and judder resulting feeling of jerk during braking for Al based friction materials application is equivalent to resin based friction materials.

Preference of composites on the basis of frictional fluctuation performance is:

FAI23>FAI24> FAI26>FAI25>FAI21

Table 5.11 (a) Friction test performance for heavy duty vehicles

Samples	Test code	Tem. rise		Coefficient of friction				Wear					
								Pad thickness (mm)		Wt. (gm)		Avg. wear	
		T_{min}, (^{0}C)	T_{max}, (^{0}C)	μ_{min}	μ_{max}	$\Delta\mu = \mu_{max} - \mu_{min}$	$\mu_{av.}$	Pad1	Pad2	Pad1	Pad2	Thick. (mm)	Wt. (gm)
FAI21	AN-700/ADB-0130	40	200	0.26	0.52	0.26	0.41	0.4	0.43	6.3	8.9	0.42	7.6
FAI23	AN-700/ADB-0130	40	200	0.26	0.46	0.20	0.36	0.4	0.35	2.9	2.5	0.37	2.7
FAI24	AN-700/ADB-0130	40	200	0.27	0.49	0.22	0.38	0.3	0.35	3.0	3.2	0.33	3.1
FAI25	AN-700/ADB-0130	40	200	0.31	0.55	0.24	0.43	0.3	0.41	3.3	3.8	0.36	3.6
FAI26	AN-700/ADB-0130	40	200	0.30	0.53	0.23	0.42	0.4	0.30	3.0	2.8	0.33	2.9

Table 5.11(b) Fade and recovery performance for heavy duty vehicles

Parameter	TQ: AN-700/ADB-0130 (1.3 MPa)						
	FR1	FR2	FAI21	FAI23	FAI24	FAI25	FAI26
$\mu_{performance}$	0.429	0.394	0.388	0.344	0.365	0.413	0.396
$\mu_{recovery}$	0.454	0.426	0.465	0.413	0.438	0.495	0.475
μ_{fade}	0.386	0.328	0.360	0.320	0.339	0.383	0.386
Fade(%)	10	17	7	7	7	7	3
Recovery(%)	106	108	120	120	120	120	120
Wear (cm^3)	-	-	2.62	0.94	1.11	1.23	1.02
Disc temp. (^{0}C)	0-600	00-400	0-200	0-200	0-200	0-200	0-200

Performance friction coefficient ($\mu_{Performance}$): Table 5.11(b) shows the performance friction coefficient ($\mu_{Performance}$) of developed Al based composites **FAI21** to **FAI26,** varies with in a

range from 0.34 to 0.41. For resin based composites **FR1** and **FR2, Table 5.11(b)**, it is about 0.43 and 0.39 respectively, which is equivalent to friction performance of developed Al based composites.

Preference of composites on the basis of $\mu_{Performance}$ is:

FAl25>FAl26>FAl21>FAl24>FAl23

Performance recovery coefficient ($\mu_{Recovery}$): Table 5.11(b) shows that the performance recovery ($\mu_{Recovery}$) of developed Al based composites **FAl21** to **FAl26** varies with in a range from 0.41 to 0.50. It is noticed that $\mu_{Recovery}$ of composite **FAl25** is 1.5 times more than that of others. The performance recovery corresponding to Al based composites are higher than that of resin based friction materials **[29,147].**

Preference of composites on the basis of $\mu_{Recovery}$ is:

FAl25>FAl26>FAl21>FAl24>FAl23

Fade (%): From **Table 5.11(b)**, it is inferred that the fade (%) for composite **FAl26** is about 3, whereas for other composites **FAl21, FAl23, FAl24** and **FAl25**, the fade (%) is stabilized and equal about 7. For resin based friction materials **FR1** and **FR2, Table 5.11(b)**, it is about 10 and 17 respectively, which is higher than fade of Al based composites. It may be concluded that fade for developed Al based composites is lower and stable.

Preference of composites on the basis of fade (%) at applied pressures:

FAl26>FAl21≈FAl23≈FAl24≈FAl25

Recovery (%): From **Table 5.11(b)**, it is inferred that recovery (%) is stable and equal about 120 for all the developed Al based composites. For resin based composites **FR1** and **FR2 (Table 5.11(b))**, it is about 106 and 108 respectively, which is lower than recovery of Al based composites. It may be concluded that recovery for developed Al based composites is higher and stable than recovery (%) of resin based composites.

Preference of composites on the basis of recovery (%) at applied pressures:

FAl21≈FAl23≈FAl24≈FAl25≈FAl26

5.5 Effect of brake pressures on friction test performance

The effects of brake pressures on friction and wear properties of developed Al based composites are characterized. The purpose of characterization is to optimize the compositions

of friction materials. **Table 5.12** shows the effect of brake pressure on friction and wear properties.

Table 5.12 Effect of brake pressure on friction and wear

Pad area: 18.86 cm^2

Samples/Test codes	Brake pressure (MPa)	Tem. rise		Coefficient of friction				Wear	
								Pad thickness mm	Wt.(gm)
		$T_{min,}$ ^0C	$T_{max,}$ ^0C	μ_{min}	μ_{max}	$\Delta\mu = \mu_{max} - \mu_{min}$	$\mu_{av.}$	Thick.(mm)	Wt.(gm)
FAl21/RS5	0.5	40	200	0.27	0.40	0.13	0.35	0.2	1.8
FAl21/RS7	0.7	40	200	0.34	0.43	0.09	0.40	.16	1.5
FAl21/RS9	0.9	40	200	0.28	0.42	0.14	0.37	0.17	1.3
FAl21/LCVHY/ ADB-130	1.0	40	200	0.36	0.63	0.27	0.48	0.2	2.6
FAl23/ RS5	0.5	40	170	0.31	0.41	0.10	0.41	2.3	0.20
FAl23/ RS7	0.7	40	200	0.35	0.41	0.06	0.42	1.3	0.10
FAl23/LCVHY/ ADB-0130	1.0	40	200	0.28	0.41	0.13	0.37	0.2	1.8
FAl24/RS5	0.5	40	170	0.35	0.54	0.19	0.43	0.9	0.15
FAl24/RS7	0.7	40	170	0.34	0.50	0.16	0.41	0.6	0.10
FAl24/LCVHY/ ADB-0130	1.0	40	200	0.26	0.39	0.13	0.36	0.2	1.4

Note: Tribo-test data at brake pressure 0.9 MPa for composites FAl23 and FAl24 are not recorded due to technical error in system and this test is not carried out for composites FAl25 and FAl26.

Wear (gm): Fig. 5.6 (i) shows that the wear of composites is low at applied pressure about 0.7 MPa. The wear of composites is low and stable corresponding to increase in pressure from 0.5 to 0.7 MPa and it increases linearly corresponding to increase in pressure from 0.7 to 1.0 MPa.

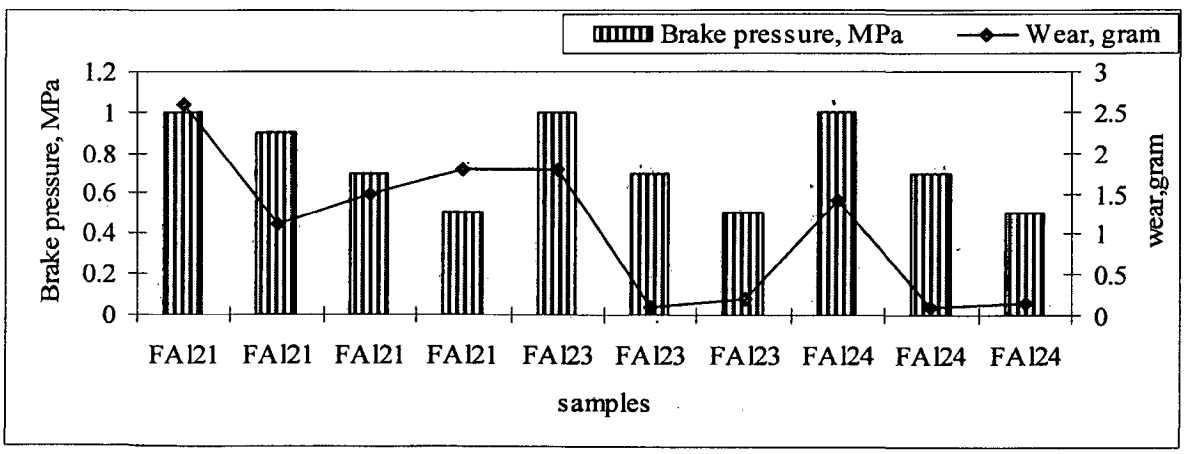

Fig. 5.6(i) Effect of brake pressure on wear

Coefficient of friction (μ_{avg}): Fig. 5.6(ii) shows that the coefficient of friction of composites is almost stable corresponding to change the applied brake pressure. It is noticed that for composite FAl21, the coefficient of friction is slightly higher ($\approx$ 0.48) corresponding to pressure 1.0 MPa, whereas for other composites the coefficient of friction lies in industrial range 0.3 to 0.45 **[188]**. It may be concluded that there is no significant effect of applied brake pressure on coefficient of friction of developed Al based friction composites.

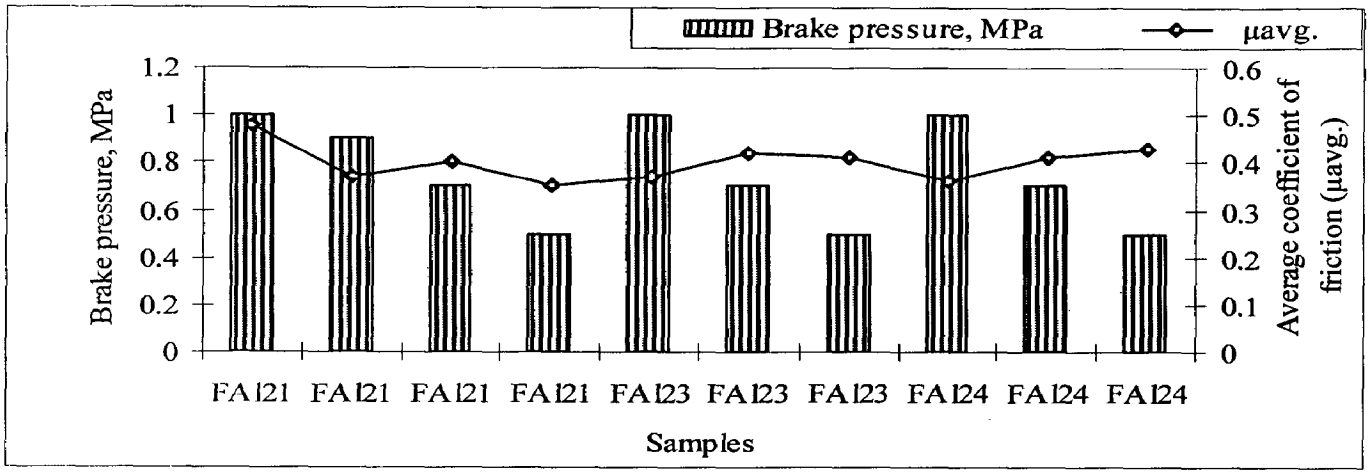

Fig. 5.6(ii) Effect of brake pressure on average coefficient of friction

Performance friction coefficient ($\mu_{performance}$): Fig. 5.6(iii) shows that the performance friction coefficient of Al based composites decreases corresponding to increase in pressure from 0.5 to 1.0 MPa. It may be concluded that friction performance for developed composites is stable with slight variation.

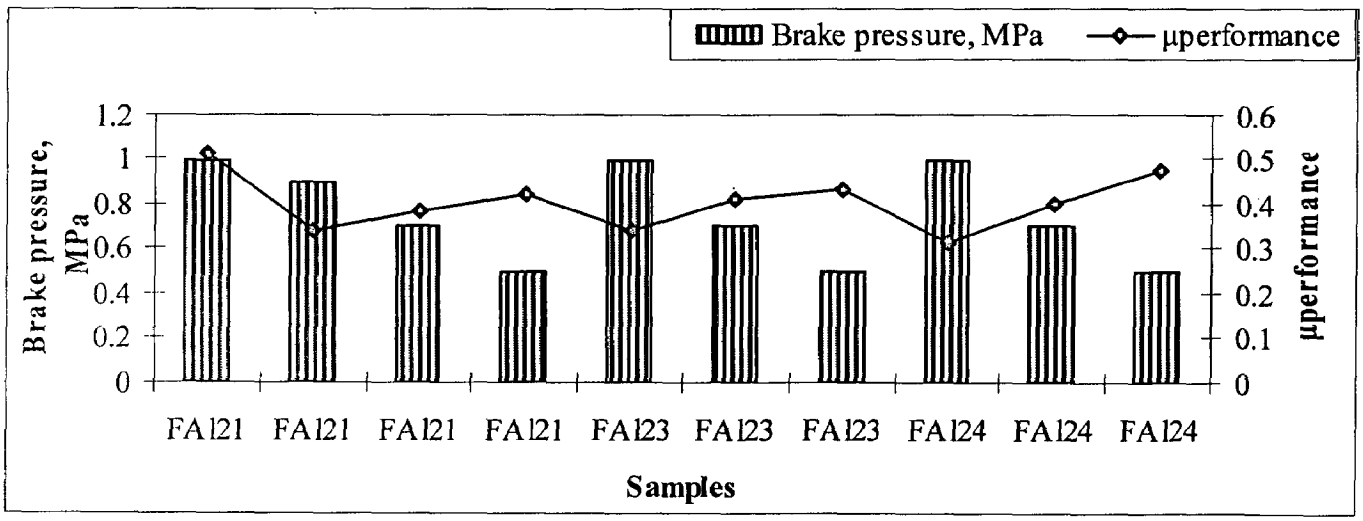

Fig. 5.6(iii) Effect of brake pressure on friction performance ($\mu_{performance}$)

Performance recovery ($\mu_{recovery}$): Fig.5.6 (iv) shows that the variation in recovery performance of developed Al based composites corresponding to applied brake pressure is similar to variation of performance friction coefficient ($\mu_{performance}$).

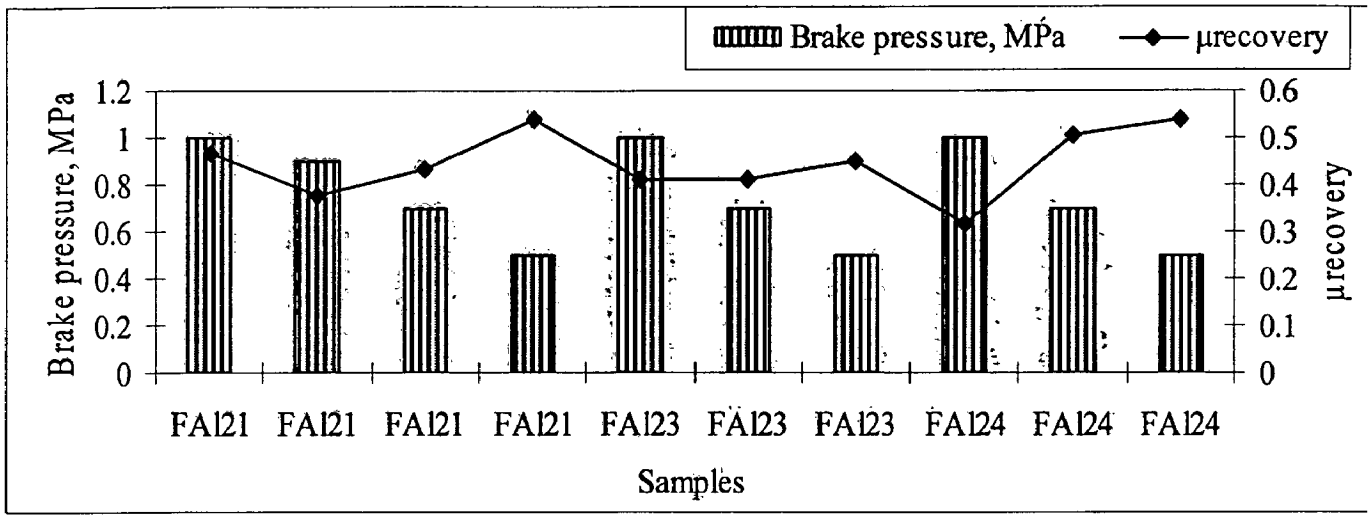

Fig. 5.6(iv) Effect of brake pressure on recovery ($\mu_{recovery}$)

Fluctuation in coefficient of friction (Δμ): It is inferred from fig. 5.6 (v) that fluctuation in coefficient of friction for composites decreases corresponding to increase the applied brake pressure from 0.5 to .7 MPa and increases linearly with increasing the brake pressure from 0.7 to 1.0 MPa. It may conclude that fluctuation in coefficient of friction for developed Al based composite depends upon applied brake pressure and their chemistry.

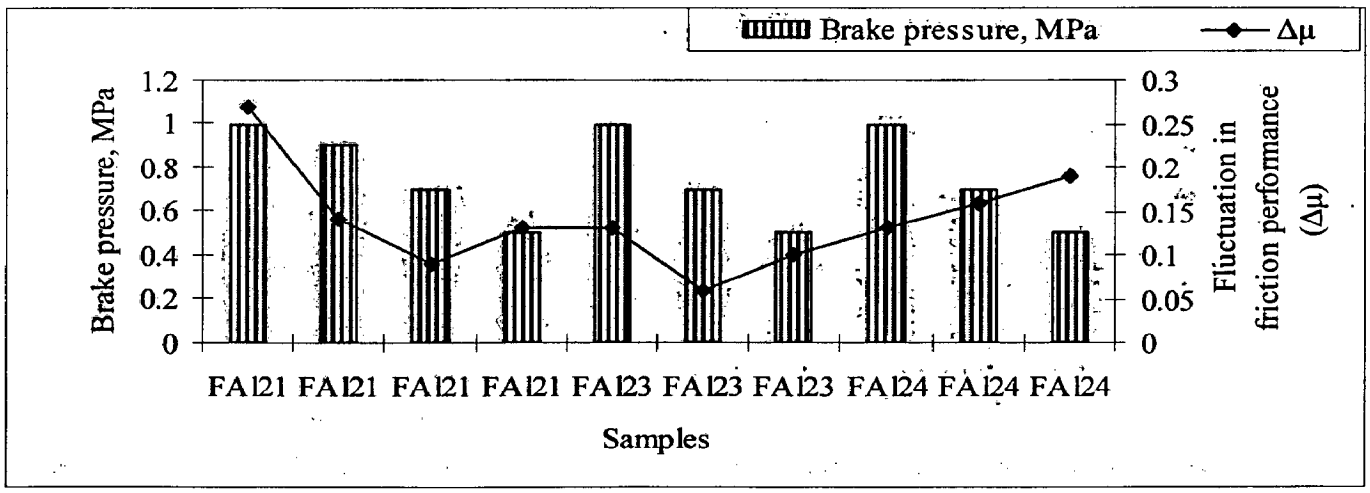

Fig. 5.6 (v) Effect of brake pressure on fluctuation in friction performance (Δμ)

Recovery (%): It is inferred from fig. 5.6(vi) that recovery performance (%) of Al based composites is high and stable. There is no significant effect of applied brake pressures with in a range from 0.5 to 1.0 MPa on recovery (%) of composites.

The overall effect of brake pressure on wear and fluctuation in coefficient of friction has been noticed.

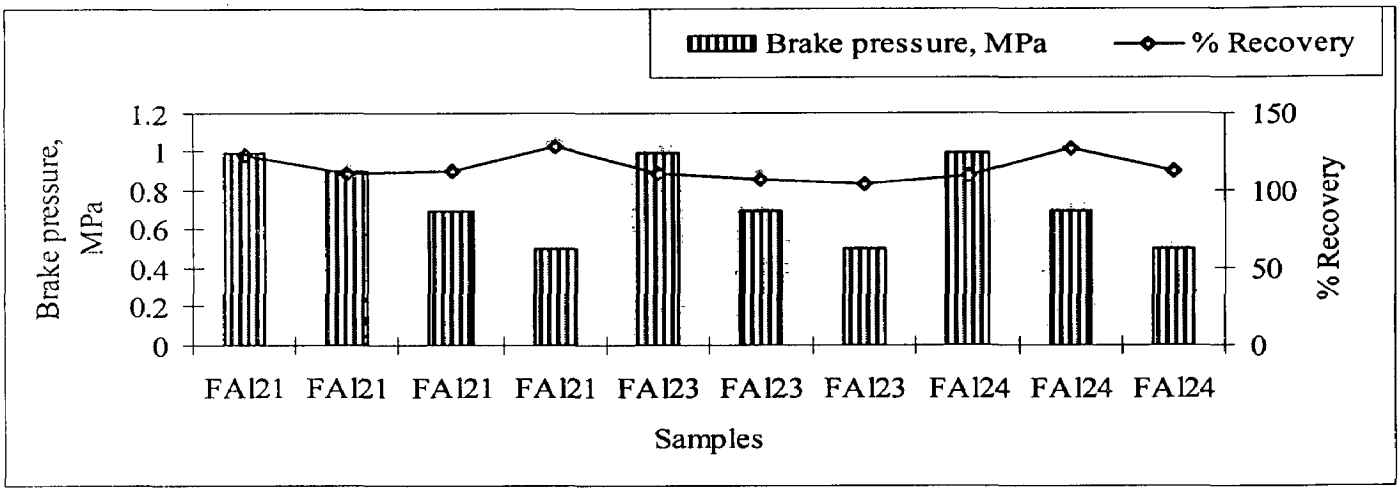

Fig. 5.6(vi) Effect of brake pressure on recovery (%)

It may be concluded that wear of composites increases with increasing the applied pressure whereas other tribological properties are largely unchanged. Xiang Xiong et al. have reported that wear increases with increasing the applied pressure whereas coefficient of friction decreases with increasing the applied pressure [185].

5.6 Effect of contact area on tribological properties

Pin-on-disc tests were conducted at constant applied pressure to asses the effect of contact area on tribological characteristics of Al based composites.

Pin-on-disc output test parameters are summarized in **Tables 5.13(a) and (b).** The wear and coefficient of friction in **Tables 5.13(a)** and temperature rise in **Tables 5.13(b)** are summarized.

Table 5.13(a) Wear and coefficient of friction

Pressure: 1.02 MPa, speed =1040 rpm, sliding time = 90 min

Contact area of test specimen (mm^2)	Wear, gram (01 hr)					Coefficient of friction (μ_{avg})				
	FAl21	FAl23	FAl24	FAl25	FAl26	FAl21	FAl23	FAl24	FAl25	FAl26
49	1.33	1.30	1.36	1.39	1.29	0.41	0.32	0.46	0.39	0.40
58	1.35	1.27	1.31	1.35	1.29	0.39	0.34	0.49	0.37	0.33
69	1.39	1.24	1.27	1.33	1.23	0.39	0.37	0.43	0.37	0.39
78	1.41	1.22	1.22	1.42	1.20	0.43	0.4	0.44	0.40	0.42

Table 5.13(b) Temperature rise

Pressure: 1.02 MPa, speed =1040 rpm sliding time = 90 minut

Contact area of test pin (mm^2)	Normal load (kgf)	Temperature rise ^0C				
		FAl21	FAl23	FAl24	FAl25	FAl26
49	5	143	140	149	138	145
58	6	139	136	140	135	139
69	7	137	131	137	130	129
78	8	132	127	127	130	125

Wear (gm): From Fig. 5.7 (i), it is inferred that wear is not the linear function of contact area because it is also depend upon compositions of composites. The relation between wear and contact area is different for different composites. It may be concluded that area of contact of developed Al based composites can be reduced/increased with slight variation in wear.

Coefficient of friction (μ_{avg}): From Fig. 5.7 (ii), it is inferred that coefficient of friction is not the linear function of contact area because it is also depend upon compositions of composites. It is noticed that the coefficient of friction of Al based composites varies corresponding to change the contact area but the range of variation of coefficient of friction lies in automotive industry standard range. For composite FAl23, area is proportional to coefficient of friction whereas for other composites there is no unique relationship between them.

Temperature rise: It is inferred from Fig. 5.7 (iii) that the temperature rise decreases corresponding to increase in contact area. It varies with in a short range from 125 to 149^{0}C. It may be concluded that temperature is inverse function of contact area.

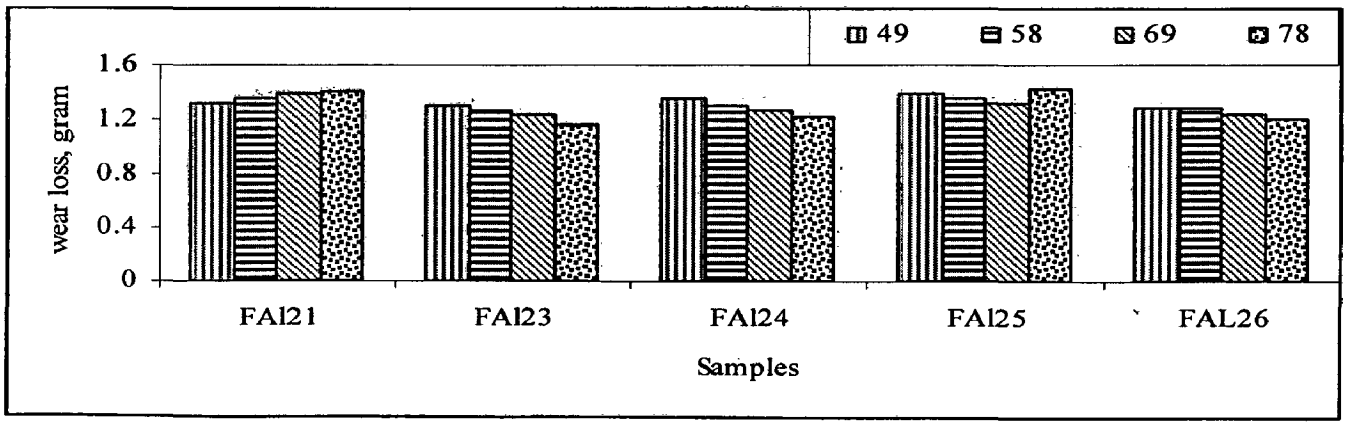

Fig. 5.7(i) Effect of contact area on wear

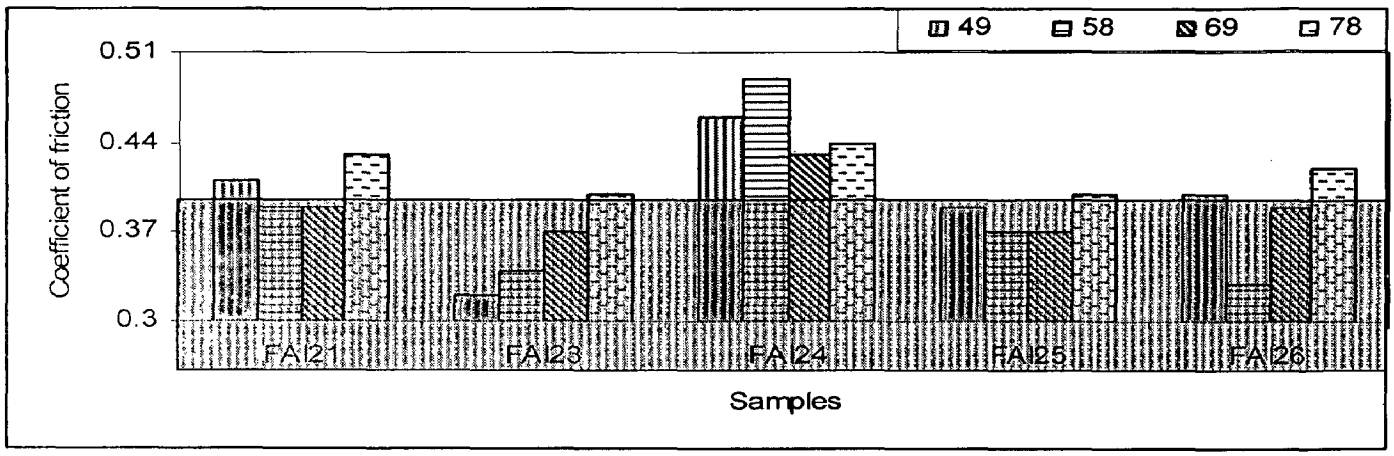

Fig. 5.7(ii) Effect of contact area on avg. coefficient of friction

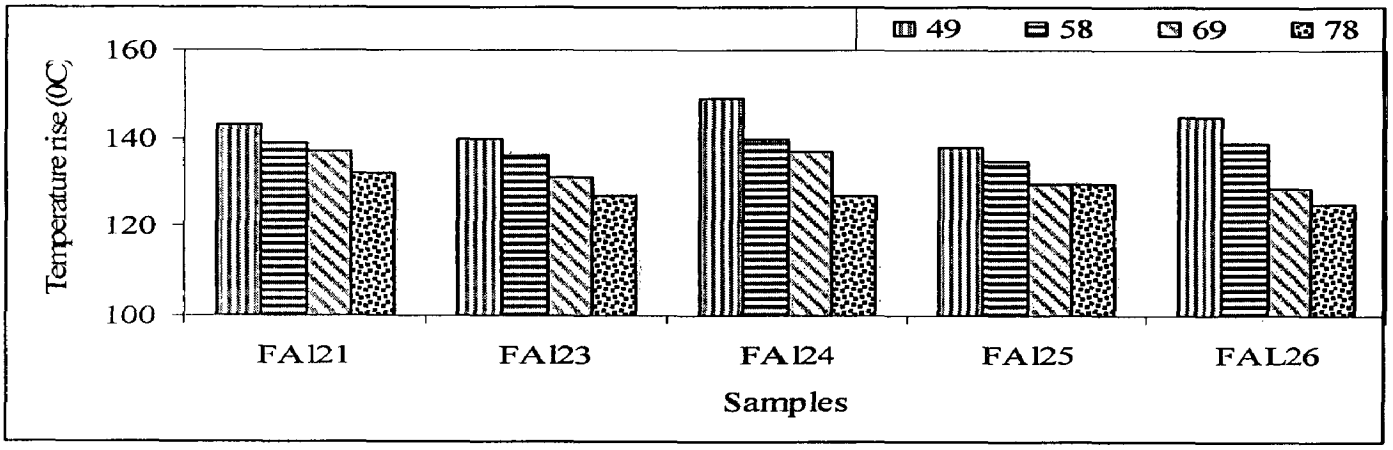

Fig. 5.7(iii) Effect of contact area temp. rise

It may be concluded that wear of composites slightly varies with increasing the contact area from 49 to 78 mm^2 whereas coefficient of friction of composite FAl23 is significantly increased with increase in contact area and for other composites like FAl21and FAl25, it varies similarly. Temperature rise decreases with increase the area. Yang et al. [187] have found lower wear coefficient values obtained by an average of about 12%, from the pins with a smaller nominal contact due to the availability of smaller asperity wear volumes.

5.7 Comparisons of developed Al based with existing resin based brake pad materials

5.7.1 Light duty: The friction test performance parameters of Al based friction materials for light duty application are compared to corresponding parameters of existing resin based friction materials.

Note: The performance parameters for developed Al based friction materials and existing resin based friction materials are shown in **Tables 5.9(a) (pp.141), 5.9(b) (pp.141), 5.10 (pp. 141), 5.11(a), 5.11(b) (pp.145) and 5.14 (pp.153).**

The following observations are recorded:

(i) Wear of developed Al based brake pad materials is higher than that of wear of resin based friction materials.

(ii) Coefficient of friction of developed Al based brake pad materials is equivalent to coefficient of friction of resin based friction materials.

(iii) Temperature rise of developed Al based brake pad materials ($\approx$ 40 to 200^{0}C) is lower than that of temperature rise of resin based friction materials ($\approx$ 40 to 250^{0}C).

(iv) Fluctuation in coefficient of friction of developed Al based brake pad materials is equivalent to fluctuation in coefficient of friction of resin based friction materials.

5.7.2 Heavy duty: The friction test performance parameters of Al based friction materials for heavy duty application are compared to corresponding parameters of existing resin based friction materials (**Table 5.14**).

Wear (cc): It is inferred from fig. 5.8(i) that the wear in developed Al based composite friction materials is lower than wear in resin based friction materials **[29]**. The wear in developed Al based composites varies within a range from 0.94 to 2.62 cc whereas for resin based friction materials, it varies within a range from 3.20 to 8.8 cc.

Wear (mm): It is inferred from fig. 5.8(ii) that the wear in developed Al based brake pad thickness is lower than wear in resin based brake pad thickness **[60]**. The wear in pad thickness of Al based composites varies within a range from 0.33 to 0.42 mm whereas for resin based friction materials, it varies within a range from 1.76 to 3.9 mm. It is noticed that wear in Al based composite is 6 to 9 times lower than wear in resin based composites RA, RB and RC. It may be concluded that fluctuation in resin based brake pads is much higher than Al based brake pads.

Table 5.14 Fade and recovery test performance of resin based friction materials [29]

Parameter	NAO Friction composites (Resin based)					
	AC	MC	OC	PC	Ph	C*
μ_{max}	0.387	0.374	0.399	0.365	0.409	-
μ_{min}	0.359	0.354	0.369	0.332	0.300	-
$\mu_{avg.}$	0.37	0.36	0.38	0.35	0.35	
$\mu_{performance}$	0.389	0.398	0.43	0.443	0.386	0.430
$\mu_{recovery}$	0.408	0.421	0.451	0.475	0.411	0.471
μ_{fade}	0.357	0.356	0.386	0.382	0.329	0.379
% Fade	8	11	10	14	15	12
% Recovery	105	106	105	107	106	109
Wear (cm^3)	5.32	3.20	3.52	3.65	6.89	8.8
Disc. Temp.(^{0}C)	387	469	446	495	456	439

*Commercial samples with unknown ingredients but based on phenolic resin

Avg. coefficient of friction: It is inferred from fig. 5.8(iii) that the coefficient of friction in developed Al based composite friction materials is equivalent to coefficient of friction of resin based friction materials **[29].** The coefficient of friction in developed Al based composites varies with in a range from 0.36 to 0.43 whereas for resin based friction materials; it varies with in a range from 0.35 to 0.38.

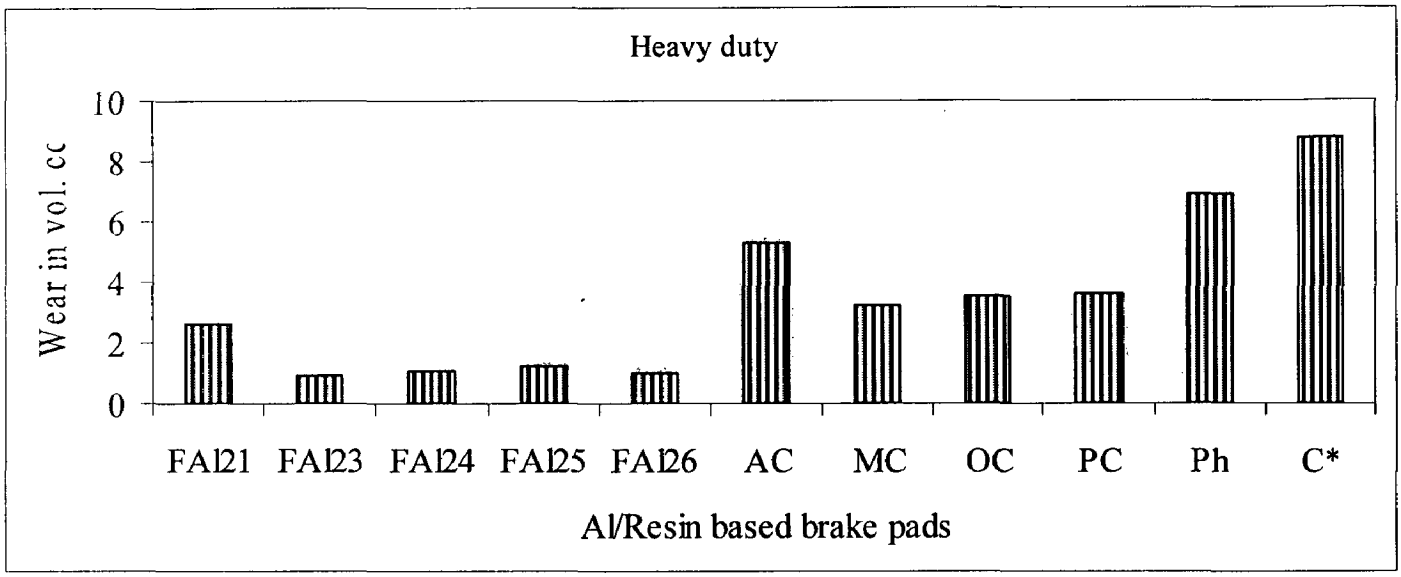

Fig. 5.8(i)

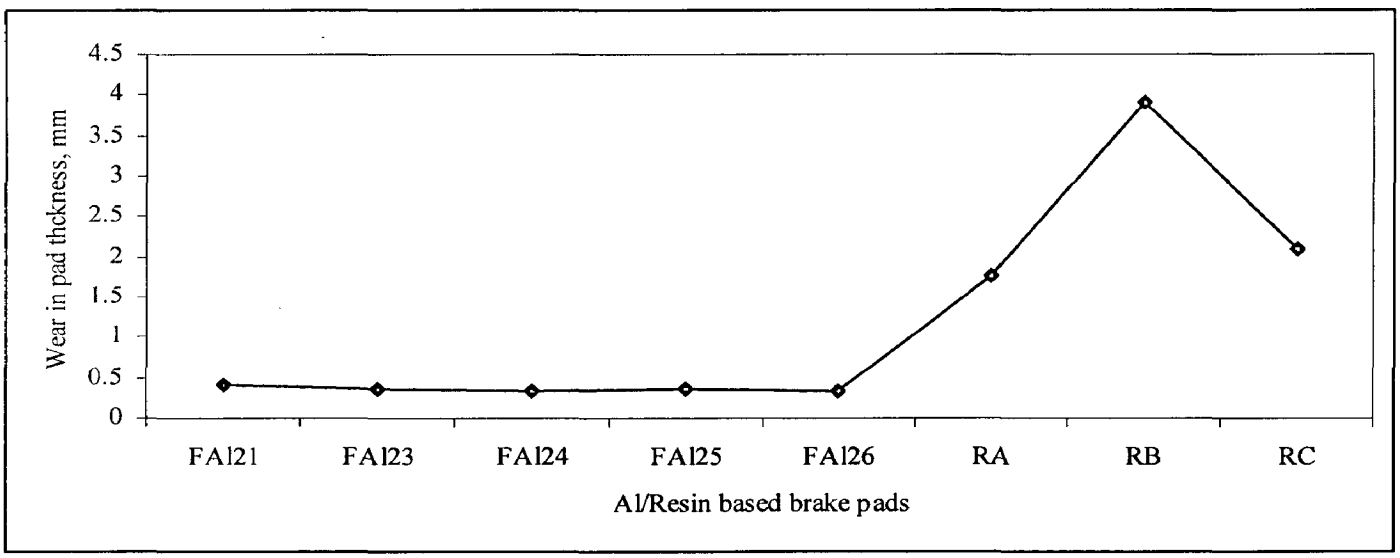

Fig. 5.8(ii)

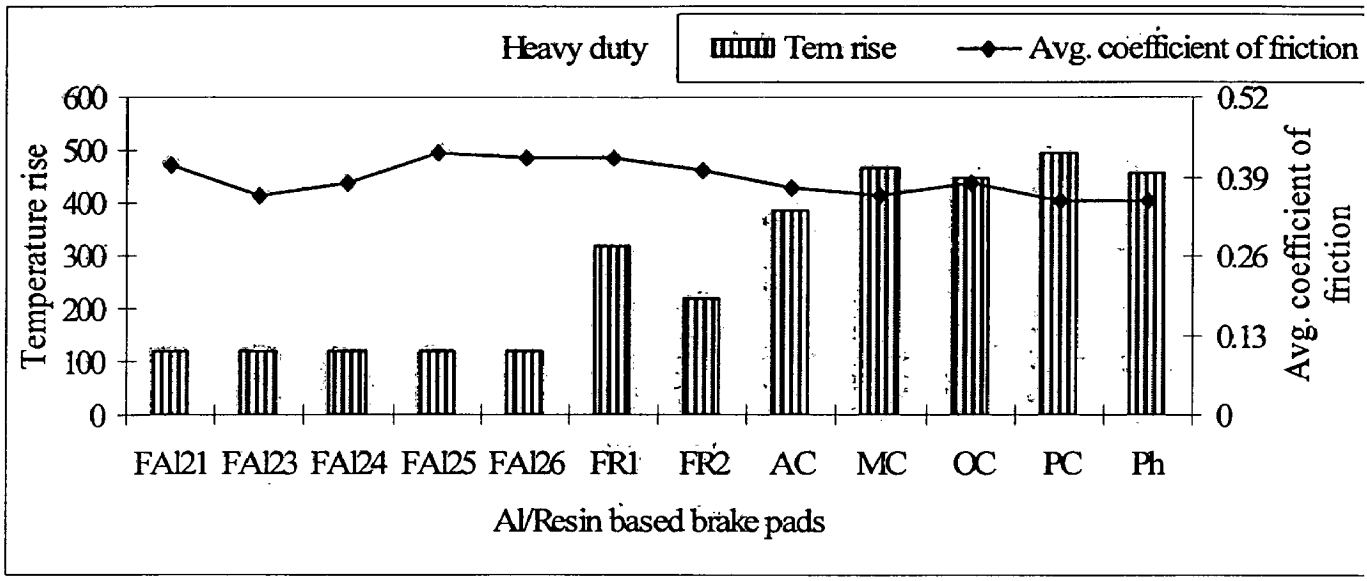

Fig. 5.8 (iii)

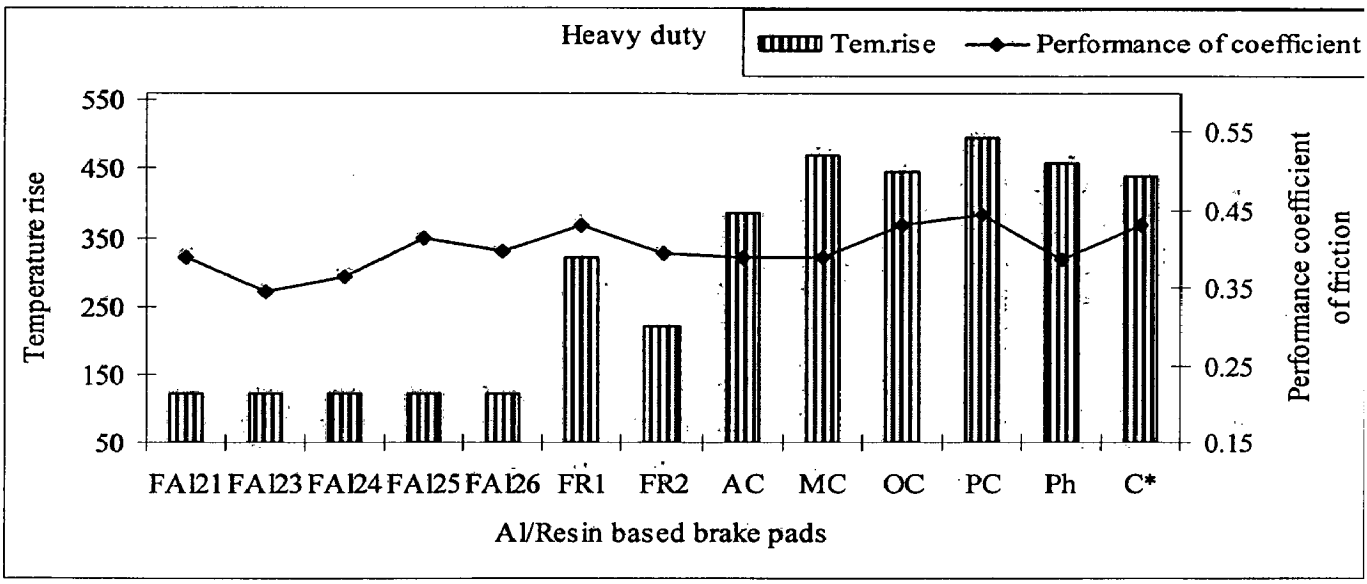

Fig. 5.8 (iv)

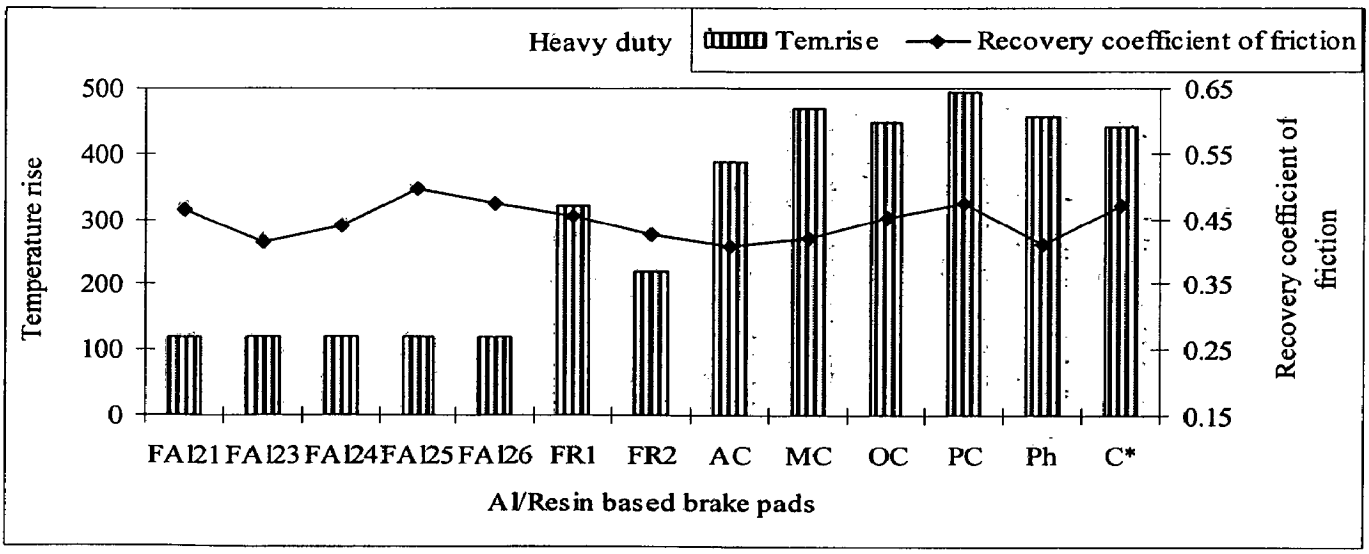

Fig. 5.8 (v)

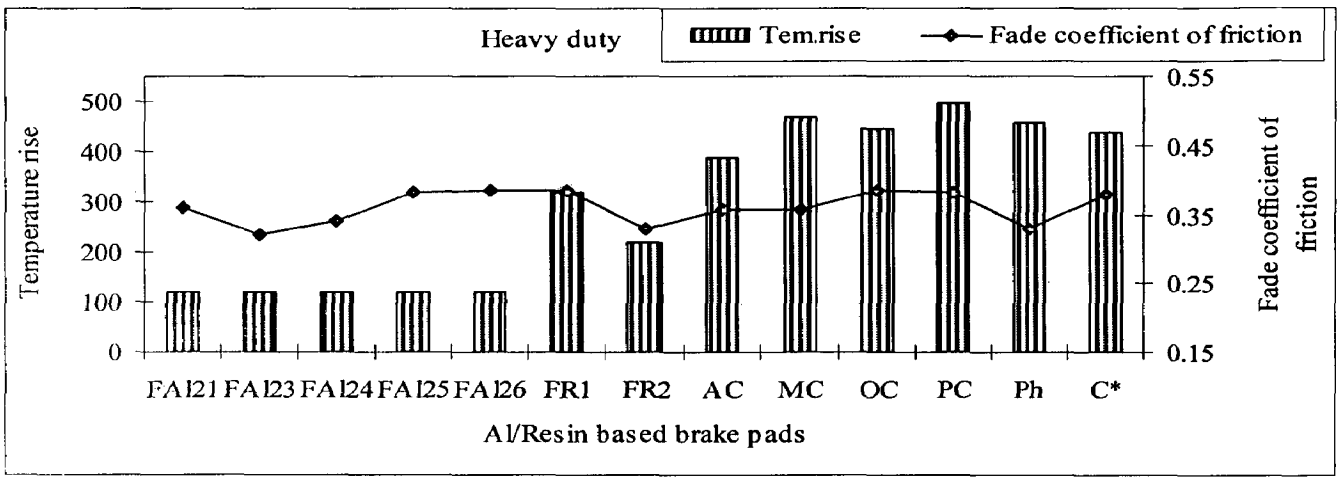

Fig. 5.8 (vi)

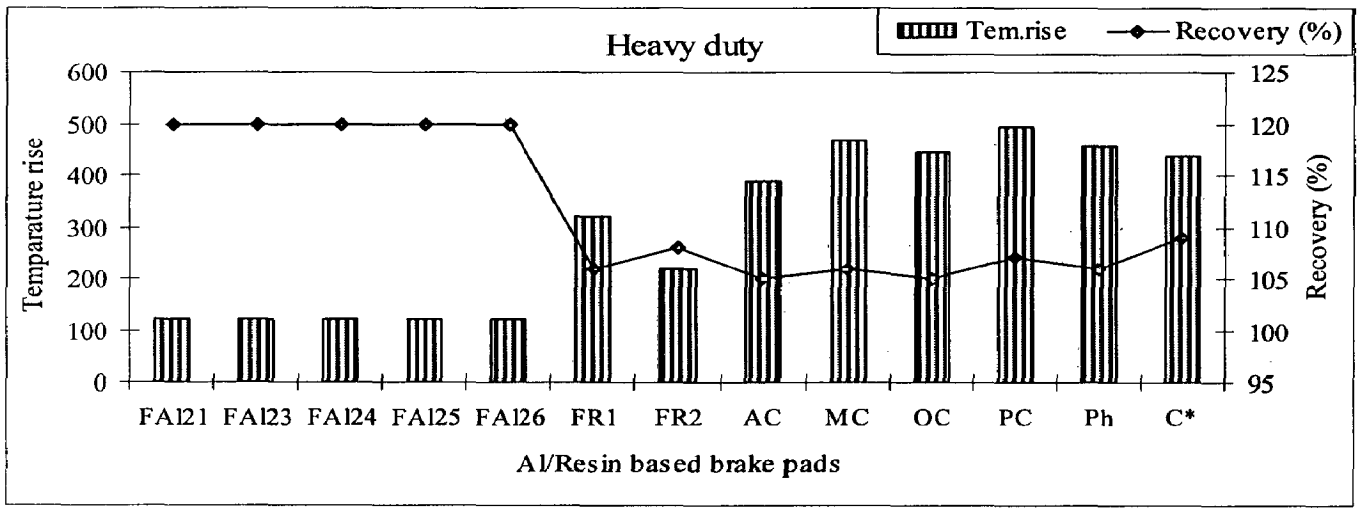

Fig. 5.8 (vii)

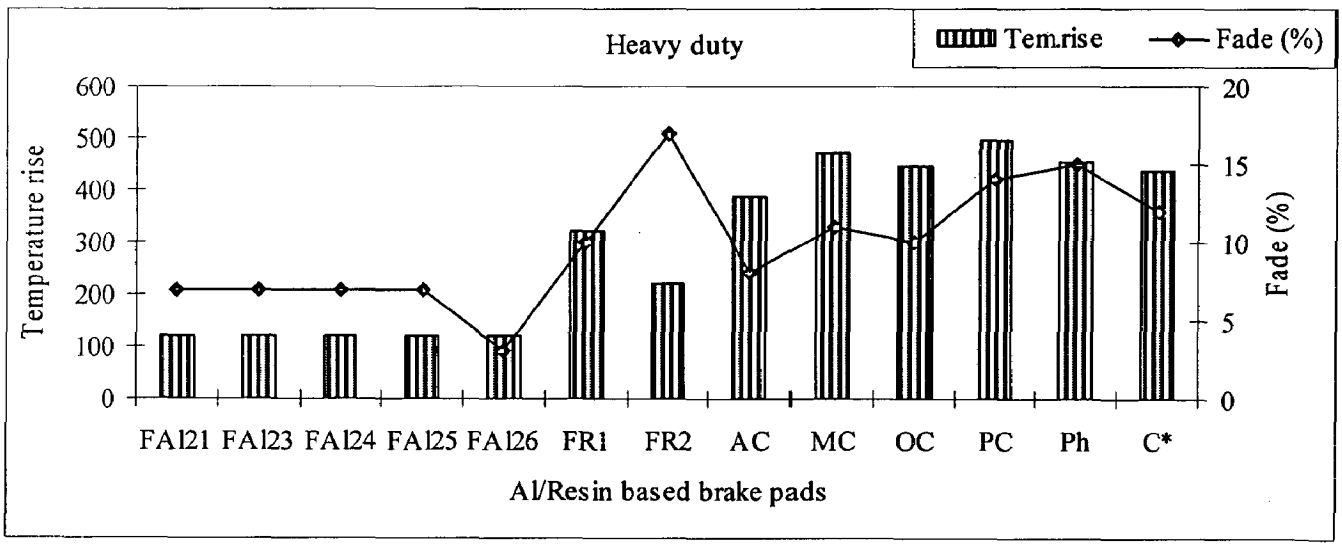

Fig. 5.8 (viii)

Fig. 5.8 Comparison of output parameters namely i) wear, cc ii) wear in pad thickness, mm iii) coefficient of friction iv) performance coefficient of friction v) recovery coefficient of friction vi) fade coefficient of friction vii) recovery (%) viii) fade (%) of Al based friction material with resin based friction material

Performance coefficient of friction: It is inferred from fig 5.8 (iv) that the performance coefficient of friction of Al based composite friction materials is stable and equivalent to performance coefficient of friction of resin based friction materials.

Recovery coefficient of friction: It is inferred from fig 5.8 (v) that the recovery coefficient of friction in Al based composite friction materials is stable and equivalent to recovery coefficient of friction of resin based friction materials **[29].**

Fade coefficient of friction: It is inferred from fig 5.8(vi) that the fade coefficient of friction for Al based composite friction materials is equivalent to the fade coefficient of friction of resin based friction materials **[29].**

Recovery (%): It is inferred from fig 5.8 (vii) that the recovery (%) for Al based composite friction materials is higher than the recovery of resin based friction materials **[29].** The recovery (%) for Al based composites is constant about 120 corresponding to temperature varies in a range from 40 to 200 ^{0}C whereas for resin based friction materials; it varies with in a range from 105 to 109 corresponding to temperature varies in a range from 387 to 495 ^{0}C **[29].** It may be concluded that recovery (%) is 14% higher for developed Al based composites than resin based composites.

Fade (%): It is inferred from fig 5.8 (viii) that the fade (%) in developed Al based composite friction materials is lower than the fade (%) of resin based friction materials **[29].** The fade (%) for Al based composites varies with in a range from 3 to 7 whereas for resin based friction materials; it varies with in a range from 8 to 15.

Temperature rise (^{o}C): It is obvious and inferred from Tables that the temperature rise in Al based composite friction materials is lower than temperature rise in resin based friction materials. The temperature rise in Al based composites varies with in a range fro 40 to 200 ^{0}C whereas for resin based friction materials; it varies with in a range from 387 to 495 ^{o}C **[29].**

5.8 Comparison of worn surfaces

In this stion the characteristics of the worn surface of developed Al based friction materials are compared to characteristics of the worn surface of resin based friction materials.

Characteristics of the friction surface [60]

Figures.5.9(i) and (iii) show the typically observed worn surfaces of the brake linings after completed tribo-tests. Several characteristic features can be observed on the friction surface of linings. The leading edge (LE) of the friction layer (brightness) always develops a better contact with the rotor. This is due to distribution of the friction force over the lining surface. Less intimate contact on the trailing edge facilitates the access of air and uneven wear related to a higher oxidation (burn-off) of phenolic resin. In case of Al based composites, oxidation

effect is not significant due to low temperature rise whereas another cause may be tribolayer formation at contact surface reduces the uneven wear. The researchers identified the transition temperature required for the tribolayer formation is about 24-215 ^{O}C **[45].**

Figure.5.9 shows the wear surfaces like i) Al based, ii) Resin based-A and iii) Resin-B after the tribo-test (sliding direction is marked by arrow). From fig.5.9 (i), it can be observed that materials wear off from surface of Al based brake pads is uniform and there is no excessive wear at the leading or trailing edge is noticed. Figures.5.9 (ii) and (iii) show the excessive oxidation at the trailing edge of resin based brake pads, which influenced the wear rate. When the pads heated up during braking, the resin tended to expand and crack, and at very high temperatures the resin turns into glassy carbon. Carbonized resins weaken the matrix and accelerate pad wear. The glassy phase lost support and was torn off from the surface by shear force. In spite of excessive oxidation on trailing edges, the leading edges wore out faster due to more intimate contact and higher pressure. Due to thermal expansion and heterogeneity of brake lining materials, the contact is highly uneven. The real and apparent contact areas are dramatically different. A good example of lining heterogeneity and its impact on contact between the disc and lining is shown in fig. 9(ii) and iii) whereas for Al based brake pad, homogeneous contact between the disc and lining is shown in fig.9 (i). The dark area marked by the arrow represents a valley with no contact, while the surrounding bright surface touches the rotating disc.

Due to thermal and shearing stresses, cracking of brake linings can be observed (fig. 9(ii)). Apparently, the friction layers formed from the wear particulates generated during friction. The chemistry and structure of a friction layer depends on bulk materials (lining and disc), testing conditions, and environment. The role of the friction layer may vary depending on its character.

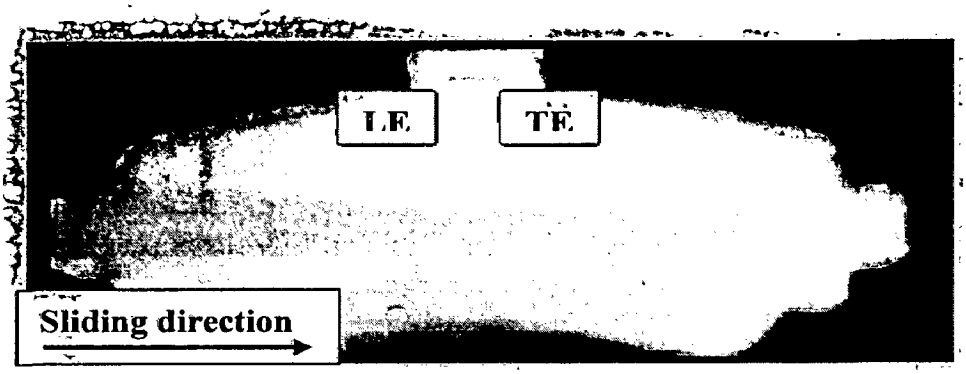

Fig.5.9 (i)

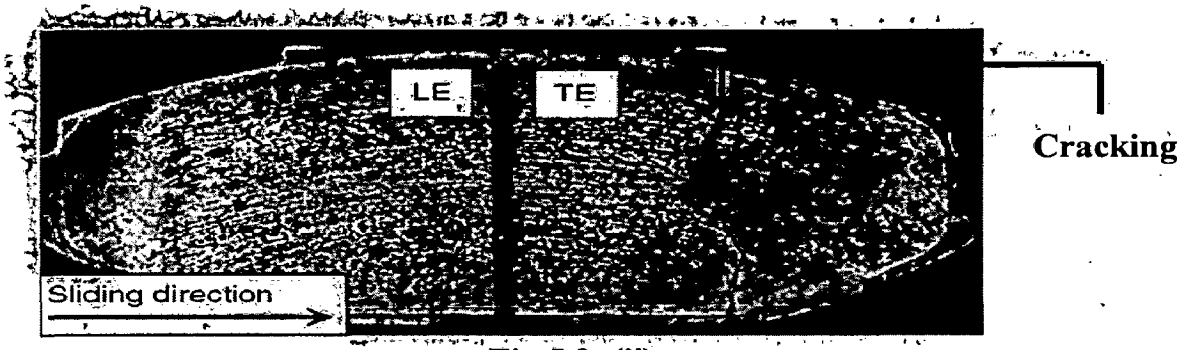

Fig.5.9 (ii)

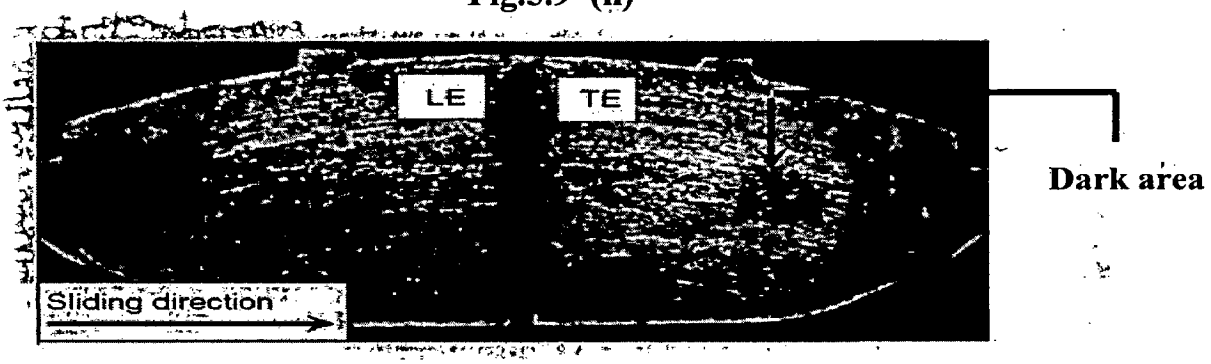

Fig.5.9 (iii)

Fig.5.9 Surface of brake lining samples i) Developed Al based brake pad (FAl26), ii) Resin-A and iii) Resin based-B after the tribo-test (sliding direction is marked by arrow) **[60]**. The leading edge (LE) and trailing edge (TE) are marked on the pad.

5.9 Suitability of developed Al based brake pad materials

Tribo-test output parameter ranges of developed Al based brake pad materials are compared to corresponding standard ranges of tribo-parameters, which are implemented/defined by automotive industries on the basis of performance of different brake pad materials in working field, to judge the suitability of Al based brake materials for different application. The standard performance evaluations have been carried out in two steps.

5.9.1 Standard performance evaluation-I

The tribo-performance of developed Al based brake pad materials are evaluated on the basis of comparison to tribo-performance of friction materials in different applications namely i) Resin based brake pads in heavy duty ii) Sintered/resin based brake pads in automobiles

iii) sintered/resin based friction materials used in railway applications iv) high speed composite friction materials v) traditional brake materials used for brakes and clutches.

5.9.1.1 Resin based brake pads in heavy duty application

Table **5.15 (a) shows** the performance evaluation of developed Al powder based brake pad materials to resin based brake pad materials **[60].** It is noticed that the wear, cc of resin based brake pads is 4 to 12 times higher than that of wear in Al based composites brake pads. Similarly wear in pad thickness of resin based brake pads is 5 to 9 times higher that wear in pad thickness of Al based composites. It is inferred that coefficient of friction of Al based composites is equivalent to coefficient of friction of resin based composites.

It may be concluded that:

i) Wear of developed Al based composites is lower.

ii) Coefficient of friction lies in standard industries range; 0.30-0.45 **[155]** and is equivalent to coefficient of friction of resin based friction materials.

Table 5.15 (a) Performance evaluation of developed Al based brake pad materials against resin based brake pad materials [60]

FM code	Ref.	Heavy duty application					
		Wear		μ_{max}	μ_{min}	$\mu_{avg.}$	$\Delta\mu$
		Weight loss (gm)	Pad thickness, mm				
FAI21	Developed	7.6	0.42	0.52	0.26	0.41	0.26
FAI23	Developed	2.7	0.37	0.46	0.26	0.36	0.20
FAI24	Developed	3.1	0.33	0.49	0.27	0.38	0.22
FAI25	Developed	3.6	0.36	0.55	0.31	0.43	0.24
FAI26	Developed	2.9	0.33	0.53	0.30	0.42	0.23
FA*	[60]	44	1.8	0.71	0.19	0.54	0.52
FB*	[60]	57	4.3	0.43	0.24	0.34	0.19
FC*	[60]	25	1.7	0.35	0.19	0.30	0.16

* Resin based brake pad materials

5.9.1.2 Brake pad performance in automobiles

Table 5.15 (b) shows the performance evaluation of developed Al powder based brake pad materials to brake pad performance in automobiles.

It is noticed that the temperature rise of resin based brake pads is 1.5 to 3 times higher than that of temperature rise in Al based composites brake pads. The coefficient of friction is not stable for resin based friction materials because it increases corresponding to increase in temperature. It reaches upto a maximum value within a range of 0.47 to 0.54, which is beyond the automotive industry standard range. In case of developed Al based composites, coefficient of friction is stable and there is no significant effect of temperature rise on it.

It may be concluded that:

(i) Temperature rise is high, which is 1.5 to 3 times higher than Al based brake pac materials.

(ii) For resin based friction materials, coefficient of friction increases corresponding tc increase in temperature rise, resulting COF is not stable during brake application. Foi developed Al based brake pad materials, there is no significant effect of temperature rise is observed on COF. It is approximately stable during braking.

(iii) COF of developed Al based friction composites is equivalent to maximum COF oi sintered friction material brake pads; AFA (0.42) and AFB (0.45) at temperature 450^{0}C and OEM level brake pads: RS4-2-1 BLACK(0.42-0.45) and RS4-7 BLACK(0.35-0.37) at temperature 300 to 650^{0}C whereas COF of developed Al based friction materials is slightly lower than max. COF of RS4-4 ORANGE, RS4-14BLACK and RS-19 YELLOW [195].

Table 5.15 (b) Brake pad performance in automobiles

FM code	Heavy duty applications			
	Ref.	Temp.rise.(^{0}C)	μ	Application
FAI21	-	40-200	0.41	Developed
FAI23	-	40-200	0.36	Developed
FAI24	-	40-200	0.38	Developed
FAI25	-	40-200	0.43	Developed
FAI26	-	40-200	0.42	Developed
AFA	[150]	450	0.42	Automobile vehicles (sintered friction material) for tractor, trucks, military vehicles, motorcycles brake disc and parking brakes
AFB	[194]	450	0.45	Kateel Brake liners for automobile vehicles (sintered friction material)
OEM-level	[194]	327-427	0.30-0.40	Street use only
RS4-2-1 BLACK	[194]	Cold	0.36	High performance road vehicles
		100	0.38	
		300-500	0.42-0.45	
RS4-4 ORANGE	[194]	Cold	0.39	For rear axle use on Touring Car, Porsche racing
		100	0.40	
		350-650	0.48-0.53	
RS4-7 BLACK	[194]	Cold	0.32	For rear axle of front wheel use on Racing Cars
		100	0.33	Touring car, WRC, GT and other forms of medium weight single seated race cars that have good levels of grip
		350-650	0.35-0.37	
RS4-14 BLACK	[194]	Cold	0.44	Touring car, WRC, GT and other forms of medium weight single seater race cars that have good levels of grip
		100	0.47	
		350-650	0.49-0.54	
RS-19 YELLOW	[194]	Cold	0.4	Suitable for endurance racing or application where exceptional life required
		100	0.43	
		400-700	0.47-0.49	

5.9.1.3 Sintered/resin based friction materials used in railway applications

Table 5.15 (c) shows the performance evaluation of developed Al powder based brake pad materials compare to sintered/resin based friction materials which are used in railway applications. Temperature rise is 1.5 to 2 times higher than that temperature rise of developed Al based friction materials. The coefficient of friction of developed Al based friction materials is higher than coefficient of friction of sintered friction materials for railway brake blocks.

Table 5.15 (c) Comparison of developed Al based brake pad materials with sintered/resin based friction materials used in railway

FM code	Ref.	Tem. rise	Coefficient of friction			Applications
		T_{max} ^0C	μ_{min}	μ_{max}	$\mu_{avg.}$	
FAl21	-	120	0.26	0.52	0.41	Developed
FAl23	-	120	0.26	0.46	0.36	Developed
FAl24	-	120	0.27	0.49	0.38	Developed
FAl25	-	120	0.31	0.55	0.43	Developed
FAl26	-	120	0.30	0.53	0.42	Developed
RFA	[150]	120	0.36	0.41	0.39	Railway disc (resin bonded)
RFB	[150]	440	0.12	0.35	0.24	Railway brake block (resin bonded)
RFC	[150]	-	0.34	0.44	0.39	Railway disc (sintered friction material)
RFD	[150]	<600	0.14	0.36	0.25	Railway brake block (sintered friction material)
RFE	[150]	350	-	-	0.4	Railway brake block (sintered friction material)
RFF	[191]	350	0.15	0.6	0.38	Brakes and clutches (Resin/sintered friction materials) for automobile vehicles
RFG	[150]	<600	.08	0.15	0.12	Railway brake block (GCI)

It may be concluded that:

(i) Temperature rise varies with in a range from 350 to 600 ^0C, which is 1.5 to 3 times higher than Al based brake pad materials. .

(ii) COF of developed Al based friction materials is equivalent to COF of sintered/resin based friction material brake disc (**Table 5.15 (c)**). It is inferred that Al based composites are not suitable for railway brake blocks, where low coefficient of friction with in a range from 0.12 to 0.24 is required (**Table 5.15 (c)**) **[150].**

5.9.1.4 High speed friction materials

Table 5.15(d)(pp.163) shows the tribo-performance evaluation of developed Al powder based brake pad materials compare to tribo-performance of high speed composite friction materials [157].

The following observations are recorded:

(i) Temperature rise varies with in a range from 331 to 422 °C, which is 1.5 to 2 times higher than Al based brake pad materials.

(ii) Performance coefficient of friction ($\mu_{performance}$) of developed Al based friction materials varies with in a range from 0.34 to 0.41 where as for high speed friction material it varies with in a range from 0.28 to 0.39. For high speed friction materials, $\mu_{performance}$ is lower.

(iii) Fluctuation in coefficient of friction of developed Al based friction materials is higher than fluctuation in coefficient of friction of high speed friction materials. Jerk is more effective in developed Al based friction materials than that of high speed friction materials.

(iv) Fade coefficient of friction is low for high speed friction materials. Fading in frictional properties for high speed friction materials, (high temperature) is higher than the fading in developed Al based friction materials.

(v) Fade (%) for high speed friction materials is 2 times higher than developed Al based friction materials.

(vi) Recovery coefficient of friction for developed Al based friction materials is 1.5 times higher high speed friction materials.

It is noticed that wear of developed Al based friction materials is equivalent to high speed friction materials except of composite FAl21.

Table 5.15(d) Performance standard evaluation of Al powder based friction materials against high speed friction materials [147]

FM code	Ref.	Heavy duty applications							
		$\mu_{performace}$	$\mu_{ma} - \mu_{min}$	μ_{fade}	Fade (%)	$\mu_{recovery}$	Recovery (%)	Tem. °C	Wear (gm)
FAl21	-	0.39	0.26	0.36	7.0	0.47	120	120	7.60
FAl23	-	0.34	0.20	0.32	7.0	0.41	120	120	2.70
FAl24	-	0.37	0.22	0.34	7.0	0.44	120	120	3.10
FAl25	-	0.41	0.24	0.38	7.0	0.50	120	120	3.55
FAl26	-	0.40	0.23	0.39	3.0	0.48	120	120	2.90
FM1	[147]	0.39	0.20	0.34	14	0.40	104	422	2.40
FM2		0.37	0.21	0.31	16	0.40	110	389	2.35
FM3		0.33	0.11	0.29	13	0.35	107	373	1.35
FM4		0.30	0.09	0.26	13	0.32	110	331	1.95
FM5		0.29	0.15	0.20	31	0.33	111	413	2.93
FM6		0.28	0.14	0.22	24	0.32	115	372	3.27
FM7		0.28	0.21	0.19	44	0.32	114	362	3.12

corresponding to increase in pressure from 1.0 to 2.0 MPa and decreases corresponding to increase in pressure from 0.5 to 0.7 MPa.

(ii) Coefficient of friction varies within a range from 0.34 to 0.43. This range is optimum because it lies in a automotive standard range from 0.3 to 0.45 **[155].** H. Jang et. al. **[61]** has reported the optimum average coefficient of friction (μ) value of 0.42.

(iii) Temperature rise varies within a lower range from 40 to 200^{0}C (Table 5.5.18). H. Jang et. al. **[61]** has also reported low temperature rise for the friction material containing Al metal as fibers $\approx$ 40 to 300^{0}C. It is lower than resin based friction materials **[150].**

(iv) The fluctuation in coefficient of friction of developed composites is equivalent to resin based friction materials.

(v) Thickness reduction in outer brake pads of developed Al based composites varies within a range of 1.3 to 3.8 mm where as for resin based brake pads; it varies within a range from 1.76 to 3.6 mm. On other hand, thickness reduction in inner pads of developed brake pads varies a range of 0.11 to 4.1 mm where as for resin based brake pads; it varies with in a range from 1.76 to 4.3 mm **[60].** For composite FAl21, it is higher for both inner as well as out side brake pads.

(vi) Recovery coefficient of friction of developed Al based brake pads is equivalent to resin based brake pads.

(vii) Performance recovery coefficient ($\mu_{recovery}$), of developed Al based brake pads is equivalent to recovery coefficient of friction of resin based brake pads.

(viii) Performance friction fade coefficient (μ_{fade}) of Al based friction materials is higher than that of resin based friction materials. The range of variation of μ_{fade} for Al based is about 0.328 to 0.386 whereas the range of variation of μ_{fade} for resin based $\approx$0.185 to 0.336 **[147].**

(ix) Fade (%) for Al based composites is 1.4 to 2.5 times lower than resin based friction composites).

(x) Recovery (%) is about 120 which is higher than the recovery of resin based composites ($\approx$ 106).

(xi) Weight per pad of developed Al based brake pad material is about 40% less than that of weight per pad of resin based brake pad material.

(xii) Developed Al based brake pad material is most economical because it can be used for fabrication of brake rotor after recycling.

On the basis of overall performances and their evaluation in comparison to commercially used sintered iron based friction materials in light/medium/heavy application, it may be concluded that developed Al based composites namely FAl21, FAl23 FAl24 FAl25 and FAl26 qualify the standard parameters and have been found to suitable for light/medium/heavy brake application.

Priority Order of Tested Friction Materials Based on Tribological Characteristics: Standard Light Duty Test (LCVHY/ADB-0130)

Wear (gm):	FAl24>FAl23≈FAl25>FAl26>FAl21
Coefficient of friction (μ):	FAl23>FAl25>FAl26>FAl24>FAl21
Amplitude of frictional fluctuation:	FAl23≈FAl25≈ FAl24>FAl26>FAl21
Friction performance (μPerformance):	FAl21>FAl26>FAl23>FAl25>FAl24
Performance recovery (μRecovery):	FAl21>FAl26>FAl23>FAl25>FAl24
Recovery (%):	FAl21>FAl23≈FAl24≈FAl25>FAl26

Priority Order of Tested Friction Materials Based on Tribological Characteristics: Standard Heavy Duty Test (AN-700/ADB-0130)

Wear (gm):	FAl23>FAl26>FAl24>FAl25>FAl21
Coefficient of friction (μ):	FAl23>FAl25>FAl26>FAl24>FAl21
Amplitude of frictional fluctuation:	FAl23>FAl24> FAl26>FAl25>FAl21
Friction performance (μPerformance):	FAl25>FAl26>FAl21>FAl24>FAl23
Performance recovery (μRecovery):	FAl21>FAl26>FAl23>FAl25>FAl24
Recovery (%):	FAl21≈FAl23≈FAl24≈FAl25≈FAl26

Table 5.17 Summary of friction test performance

Friction test for Al-based brake pads														
Samples	Brake pressure, MPa	Tribo-tests	Temp. rise		Coefficient of friction				Wear					
									Pad thickness (mm)		Wt.(gm)		Avg. wear	
			$T_{max,}$ ^0C	$T_{min,}$ ^0C	μ_{min}	μ_{max}	$\mu_{av.}$	$\Delta\mu = \mu_{max} - \mu_{min}$	Pad1	Pad2	Pad1	Pad2	Pad thickness (mm)	Wt., (gm)
FAI21	0.5	Reduce scale test	40	170	0.27	0.40	0.35	0.13	0.23	0.19	1.8	1.8	0.20	1.8
FAI23	0.5		40	170	0.31	0.41	0.41	0.15	0.19	0.25	2.0	2.3	0.20	2.2
FAI24	0.5		40	170	0.35	0.54	0.43	0.19	0.07	0.23	0.6	0.9	0.15	0.8
FAI21	0.7		40	200	0.34	0.43	0.4	0.09	0.02	0.03	1.2	1.7	0.14	1.5
FAI23	0.7		40	200	0.35	0.41	0.42	0.10	0.01	0.09	1.1	1.3	0.10	1.2
FAI24	0.7		40	170	0.34	0.50	0.41	0.17	0.04	0.18	0.3	0.6	0.10	0.5
FAI21	1.0	Light duty test	40	200	0.36	0.63	0.27	0.49	0.19	0.11	2.8	2.3	0.2	2.6
FAI23	1.0		40	200	0.28	0.41	0.13	0.37	0.21	0.18	1.9	1.7	0.2	1.8
FAI24	1.0		40	200	0.26	0.39	0.13	0.34	0.17	0.15	1.5	1.3	0.2	1.4
FAI25	1.0		40	200	0.27	0.40	0.13	0.35	0.23	0.19	1.8	1.8	0.2	1.8
FAI26	1.0		40	200	.31	0.46	0.15	0.41	0.19	0.25	2.0	2.3	0.2	2.2
FAI21	2.0	Heavy duty test	40	200	0.26	0.52	0.26	0.41	0.4	0.43	6.3	8.9	0.42	7.6
FAI23	2.0		40	200	0.26	0.46	0.20	0.36	0.4	0.35	2.9	2.5	0.37	2.7
FAI24	2.0		40	200	0.27	0.49	0.22	0.38	0.3	0.35	3.0	3.2	0.33	3.1
FAI25	2.0		40	200	0.31	0.55	0.24	0.43	0.3	0.41	3.3	3.8	0.36	3.6
FAI26	2.0		40	200	0.30	0.53	0.23	0.42	0.4	0.30	3.0	2.8	0.33	2.9

Table 5.18 Summary of fade and recovery test performance

Parameters	*Test code:RS7, RS5*				*Reduced scale*	
	FAI21		FAI23		FAI24	
	RS7	RS5	RS7	RS5	RS7	RS5
$\mu_{performance}$	0.383	0.424	0.412	0.433	0.400	0.478
$\mu_{recovery}$	0.433	0.538	0.442	0.452	0.506	0.539
μ_{fade}	0.349	0.376	0.364	-	0.341	0.431
Fade (%)	9	11	12	-	15	10
Recovery (%)	113	128	107	104	127	113
Wear (cm^3)	0.51	0.41	0.42	0.77	0.18	0.27
Temp.rise, °C	40 -170	40-200	40- 170	40-200	40 - 170	40-200

Parameter	*TC: LCVHY/ADB-0130*				*Light duty test*		
	FR3	FR4	FAI21	FAI23	FAI24	FAI25	FAI26
$\mu_{performance}$	-	-	0.516	0.342	0.316	0.328	0.380
$\mu_{recovery}$	-	-	0.633	0.378	0.349	0.363	0.419
μ_{fade}	-	-	0.511	-	-	-	-
Fade (%)	-	-	99	-	-	-	-
Recovery(%)	-	-	123	111	11	111	110
Wear (cm^3)			0.89	0.63	0.50	0.62	0.77
Disc temp., °C	40-250	40-250	40-200	40-200	40-200	40-200	40-200

Parameter	*TC : AN-700/ADB-0130*				*Heavy duty test*		
	FR1	FR2	FAI21	FAI23	FAI24	FAI25	FAI26
$\mu_{performance}$	0.429	0.394	0.388	0.344	0.365	0.413	0.396
$\mu_{recovery}$	0.454	0.426	0.465	0.413	0.438	0.495	0.475
μ_{fade}	0.386	0.328	0.360	0.320	0.339	0.383	0.386
Fade (%)	10	17	7	7	7	7	3
Recovery (%)	106	108	120	120	120	120	120
Wear (cm^3)	-	-	2.62	0.94	1.11	1.23	1.02
Disc temp., °C	40-600	40-400	0-200	0-200	0-200	0-200	0-200

5.11 Sub-scale inertia dynamometer tests for AN-32 aircraft brake rotor

Subscale inertia dynamometer tests against cast iron inertia wheel were carried out at HAL Bangalore, INDIA for assessing the suitability of Al-based friction material composites namely **FAl20** to **FAl30**, for AN-32 aircraft brake rotor application. The detailed test reports namely HAL20 to HAL30 corresponding to the tested samples are available in **Annexure-B1-B24**. The tribo-test input parameters are shown in **Table 5.19** designated as test codes: TQ1, TQ2 and TQ3.

Table 5.19 Sub-scale dynamometer friction test input parameters [157]

Brake pad contact area: 25.8 cm^2

Kinetic Energy levels	Test Codes	Input test parameters			
		Kinetic Energy (kgfm)	Brake speed (rpm)	Brake pressure (kgf/cm^2)	Brake Force (kgf)
High	TQ1	17300	1000	18.0	160
Medium	TQ2	12000	835	12.83	100
Low	TQ3	8000	687	7.50	70

Note: The lower and medium input kinetic energy level tribo-tests were carried out to assess the performance of tribological characteristics to provide a basis for selection of composites for higher energy test. High kinetic energy level test-TQ1 is a standard test in aeronautics for AN-32 aircraft brake rotor **[157].**

Table 5.20 shows the range of standard output test parameters for AN-32 rotor brake pads namely run down time (RD time), coefficient of friction (COF) and maximum wear for iron based sintered friction material. Developed Al-based brake pads were tested and compared with above output parameters as applicable to iron based brake pads, to judge their suitability for AN-32 aircraft applications. The tribo-tests of commercially used brake pad materials are performed on subscale dynamometer friction tester under rejected-take-off **(RTO)** condition (regarded as the most extreme condition, wherein the brake assembly has to absorb a quantum of energy within the available airstrip length) **[USP.3844800].**

Table 5.20 Standard sub-scale dynamometer friction test performance

AN32	Test code: TQ1					
	RD Time (s)		COF		Maximum wear (50 cycles)	
	Min	Max	Min	Max	Wear (gm)	Wear in pad thickness (mm)
Standard output	6	12	0.18	0.40	14	1.25

Note: Corresponding to the maximum and minimum limits of sub-scale dynamometer friction test output parameters for AN-32 brake rotor application **(Table 5.20)**, shaded regions are presented in following figures. The tribo-test output parameters of developed composites that appear in the shaded region are found suitable for AN-32 aircraft application.

The different test parameters as obtained from subscale inertia dynamometer tribo-tests are as follows **[157]**.

1. **Run down time**: This parameter relates to the time required for a pair of brake pads in absorbing the energy fed from the dynamometer. This time should preferably be on the lower side for efficient brake application.
2. **Run down revolution**: This is also a parallel parameter corresponding to run down time. However, it is the number of revolutions of the inertia wheel until complete stoppage. Like RD time, RD revolutions should also be on the lower side for efficient braking.
3. **Coefficient of friction (COF):** This is the ratio of absorbed energy by the pair of brake pads to the input kinetic energy under dynamic conditions. This should be preferably on the higher side for efficient braking. However, at the same time, not too high, because it tends to increases the fluctuation in coefficient of friction, resulting in vibration and judder.
4. **Brake torque:** It is the force developed by the brakes under dynamic conditions and it is parallel to the COF. This parameter like COF should be moderate.
5. **Wear loss:** The wear loss has been investigated in two forms, one corresponding to weight loss and the other corresponding to thickness of brake pad for 50 braking cycles. This parameter should also be low.
6. **Temperature rise:** During braking operation, temperature of brake pad always rises. This rise might adversely affect the test parameters described above. It should be therefore low/moderate only. Furthermore, the number of test cycles and temperature rise are parallel parameters, larger the number of cycles higher the temperature rise.

5.12 Tribo-test performance of developed Al-based composites

The output test parameters of developed Al based composites lie in the standard output parameter range for AN32 (**Table 5.20 pp.172**), therby qualifying the composites for further high input energy evaluations.

There is a general trend in these figures, such that the performance variations are more severe up to 22 nos. of braking cycles. Thereafter, the performance tends to stabilize. This is possibly because of the initial mechanical adjustment of stationary brake pads against moving inertia wheel.

5.12.1 Low energy level tribo-test: TQ3 (KE = 8000 kgfm)

The low energy level tribo-test is conducted to evaluate the tribo-performance of randomly selected composite **FAl26**. The purpose of this test is to observe the variation in tribological characteristics of **FAl26** at low input energy **(Table 5.24 pp.189)** and provide a basis for selection of composites for medium energy level test.

Variation of coefficient of friction and RD time

Figure 10(i) shows that coefficient of friction (μ) and run down (RD) time vary within a range of 0.36 to 0.40 and 11.2 to 12.3 s respectively in 50 nos. of braking cycles.

Coefficient of friction: From fig. 5.10 (i), it is observed that coefficient of friction varies within a range from 0.36 to 0.40 up to 22 nos. of braking cycles and thereafter it stabilizes at about 0.38. It lies in standard range ≈ 0.18 to 0.40 (**Table 5.20**) as shown in fig. 5.10(i). The coefficient of friction is also stable corresponding to gradual temperature rise in 22-50 nos. of braking cycles fig. 5.10 (ii). It may be concluded that initially coefficient of friction varies up to 22 nos. of brake cycles and stabilizes thereafter.

RD time: Run down time varies within a range of 11.2 to 12.3 s upto 22 nos. braking cycles and in remaining nos. of braking cycles, it stabilizes with little fluctuation shown in fig. 5.10(i), lying within the standard range (**Table 5.20**)

It may be concluded that COF, RD time and temperature rise of developed composite **FAl26** at lower input energy, stabilize after 22 nos. of braking cycles.

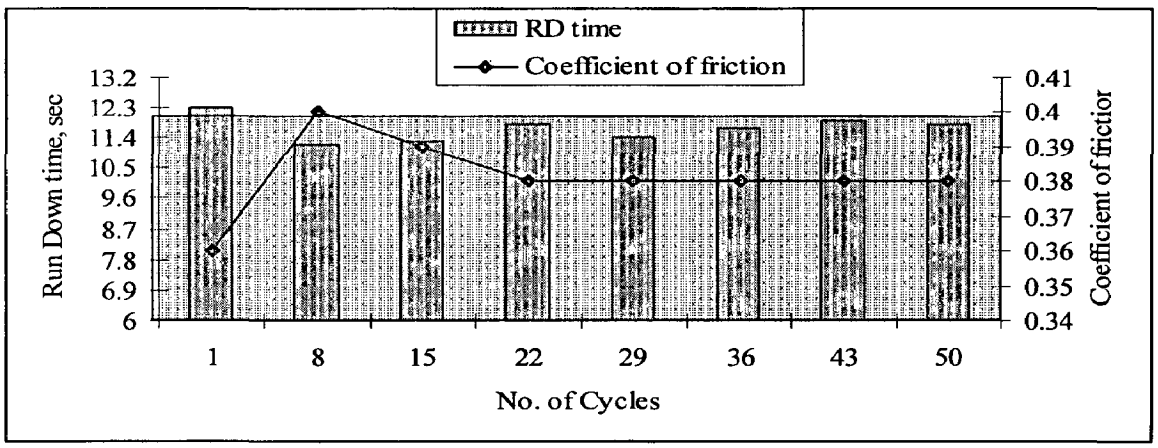

Fig. 5.10(i)

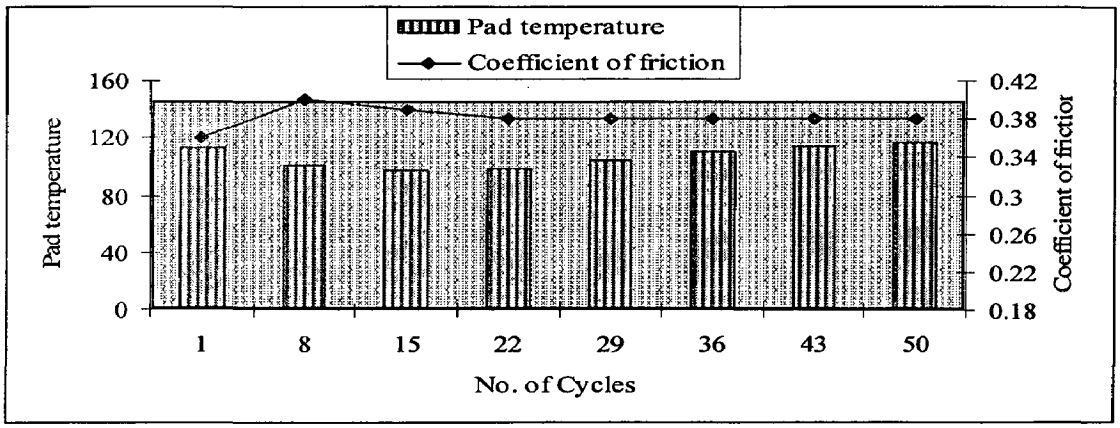

Fig. 5.10(ii)

Fig. 5.10 i) Run down time and coefficient of friction ii) Pad temperature; °C and coefficient of friction in 50 brake cycles

5.12.2 Medium energy level tribo-test: TQ2 (KE = 12000 kgfm)

Figure 5.11(a) shows the variation in coefficient of friction, RD time, temperature rise and mean brake torque corresponding to 50 nos. of braking cycles under medium energy range (TQ2). Fig. 5.11(b) shows the average coefficient of friction, average RD time; average temperature rise and average mean brake torque corresponding to 50 nos. of braking cycles The purpose of this test is to evaluate the tribo-performance and establish a basis for selection of composites for standard high-energy test (TQ1).

5.12.2.1 Variation of coefficient of friction and RD time

Fig. 5.11(a) show the variation of coefficient of friction (COF) (μ) within a range of 0.23 to 0.42, run down (RD) time within a range of 7 to 16.5 s, temperature rise upto 120 ^{0}C and brake toque from 16 to 24 kgfm corresponding to 50 nos. of braking cycles. It is inferred that the range of variation of coefficient of friction and RD time is higher in comparison to low energy level test.

Coefficient of friction (COF): Fig. 5.11(a) (i) shows that the coefficient of friction of composites namely **FAI21** to **FAI26** varies within a range of 0.23 to 0.42 in 50 nos. of braking cycles. It lies in standard range (0.18 to 0.40) **(Table 5.20)** (which has been shown in fig. 5.11(a)(i) by shaded region).

Based on performance wise comparison, preferences are in the following order:

FAI24>FAI25>FAI26>FAI21>FAI23>FAI22

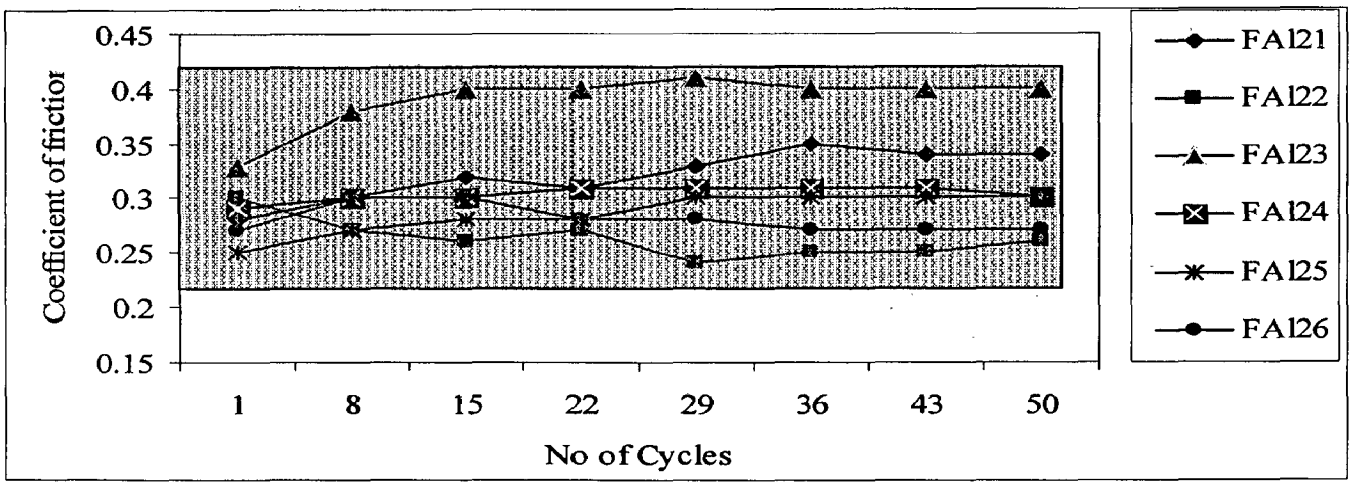

Fig. 5.11(a) (i)

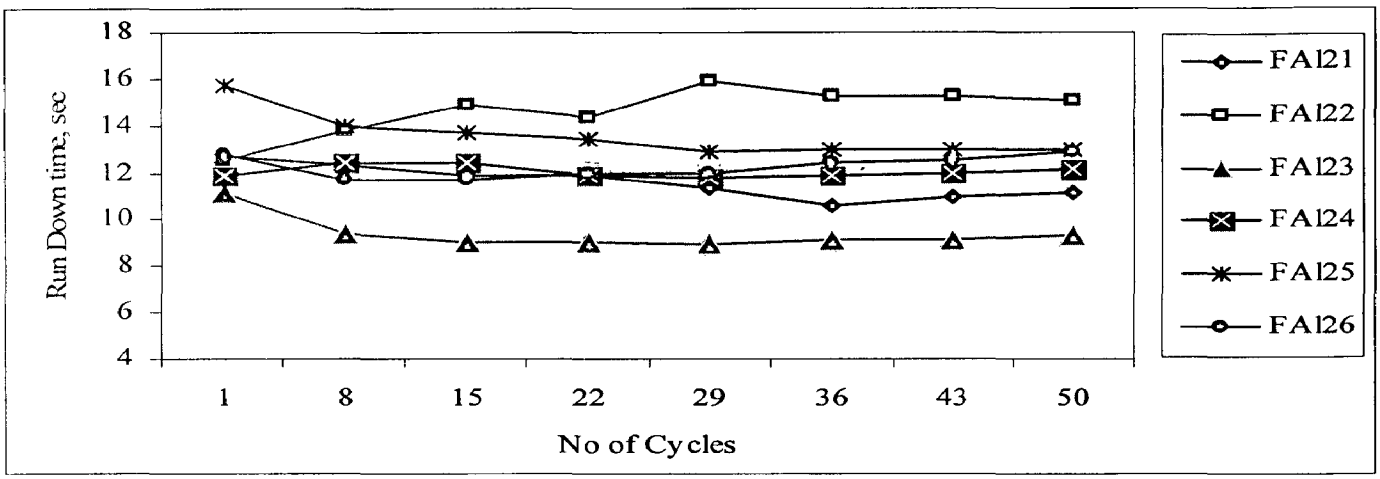

Fig. 5.11(a) (ii)

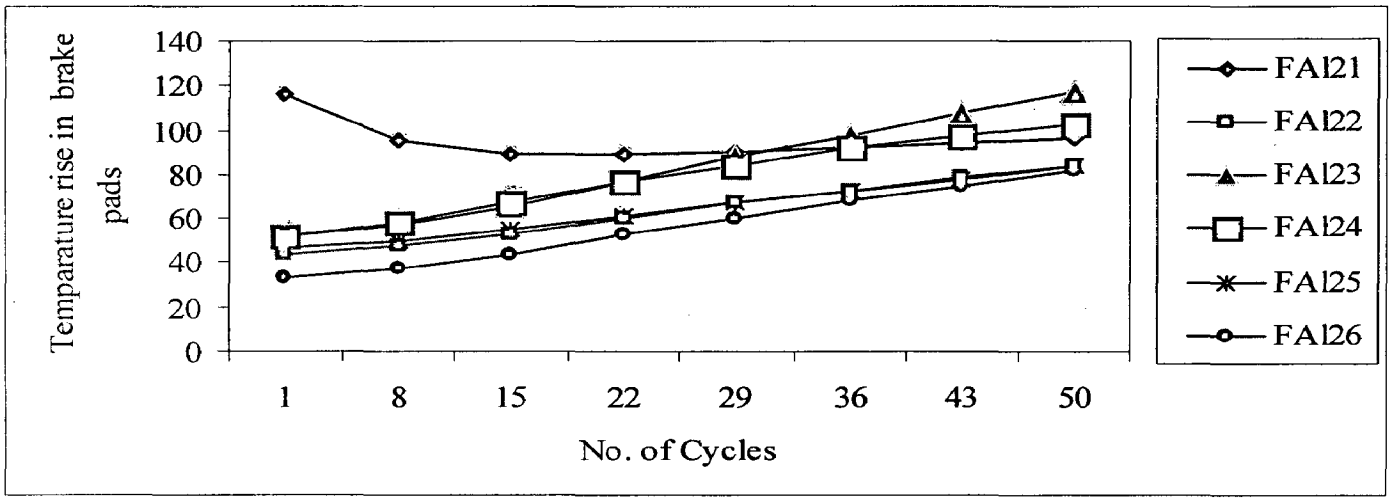

Fig. 5.11(a) (iii)

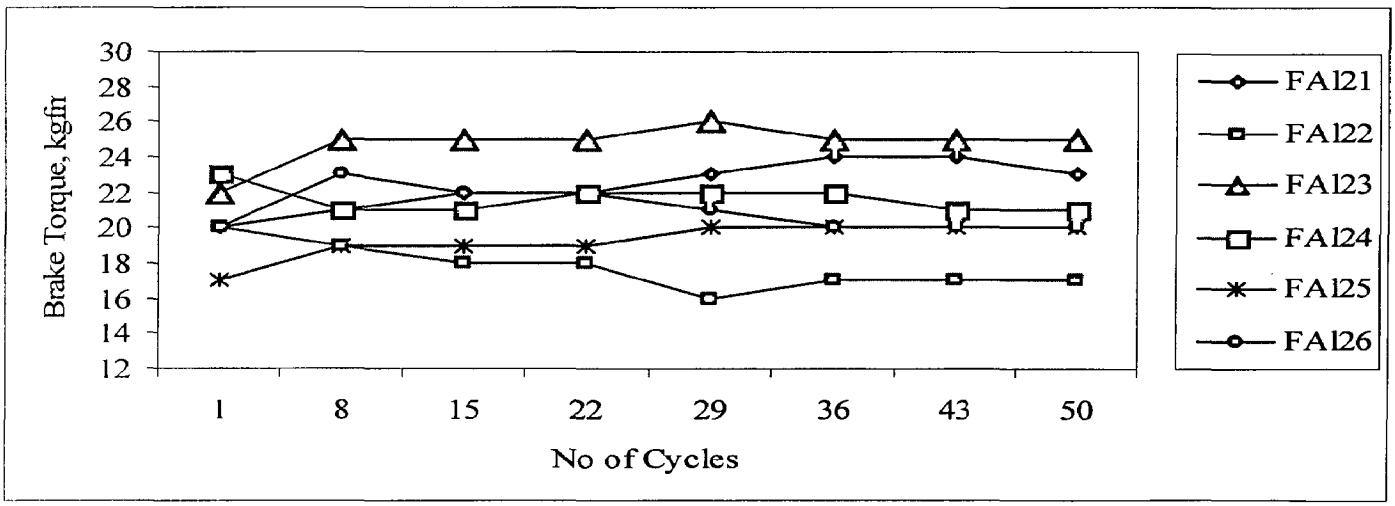

Fig. 5.11(a) (iv)

Fig. 5.11(a) Variation in output parameters i) Coefficient of friction ii) Run down time iii) Temperature rise iv) Brake torque in 50 braking cycles

RD time: From Fig. 5.11(a) (ii), it is observed that the run down time (RD time) of composites corresponding to 50 nos. of braking cycles varies from 9.2 to 14.7 s. The RD time for composites **FAI22** and **FAI25** is high and does not lie in standard range. It may be concluded that composites **FAI22** and **FAI25** are not found to suitable for standard high-energy test TQ1. Based on performance wise comparison, preferences are in the following order:

FAI23>FAI21>FAI24>FAI26

Temperature rise: Fig. 5.11(a) (iii) shows that temperature rise varies within a range from 33 to 120 ^{0}C corresponding to 50 nos. of braking cycles. It is noticed that the maximum temperature rise is about 120^{0}C for composite **FAI23** in 50th braking cycle, which is much lower than temperature rise in sintered brake pad material; 350^{0}C **[62].**

Based on performance-wise comparison, preferences are in the following order:

FAI26>FAI22>FAI25>FAI21>FAI24>FAI23

Mean Brake torque: Fig. 5.11(a) (iv) shows that the mean brake torque corresponding to 50 nos. of braking cycles varies from 15 to 26 kgfm. It increases initially upto the 8th braking cycle, thereafter it stabilizes.

5.12.2.2 Average output parameters of composites: The average output parameters; wear loss, run down time, coefficient of friction, temperature rise and fluctuation in frictional characteristic of composites namely **FAI21** to **FAI26** in 50 nos. of braking cycles are shown in fig. 5.11(b). Standard ranges **(Table 5.20)** have been shown in figs. figs. 5.11(b) (i) to fig. 5.11(b) (v) by shaded region.

Average wear loss: Fig. 5.11(b) (i) shows that the average wear loss of brake pads of different composites in 50 nos. of braking cycles varies from 2.5 to 25.5 gm. It may be concluded the composite **FAI20** is not suitable for high energy test because of the high wear; 25.5 gm **(Table 24 pp.190)**, which is 1.8 times higher than standard wear ≈ 14 gm **(Table 5.20)**

Based on performance wise comparison, preferences are in the following order:

FAI21>FAI25>FAI22>FAI24>FAI23>FAI26

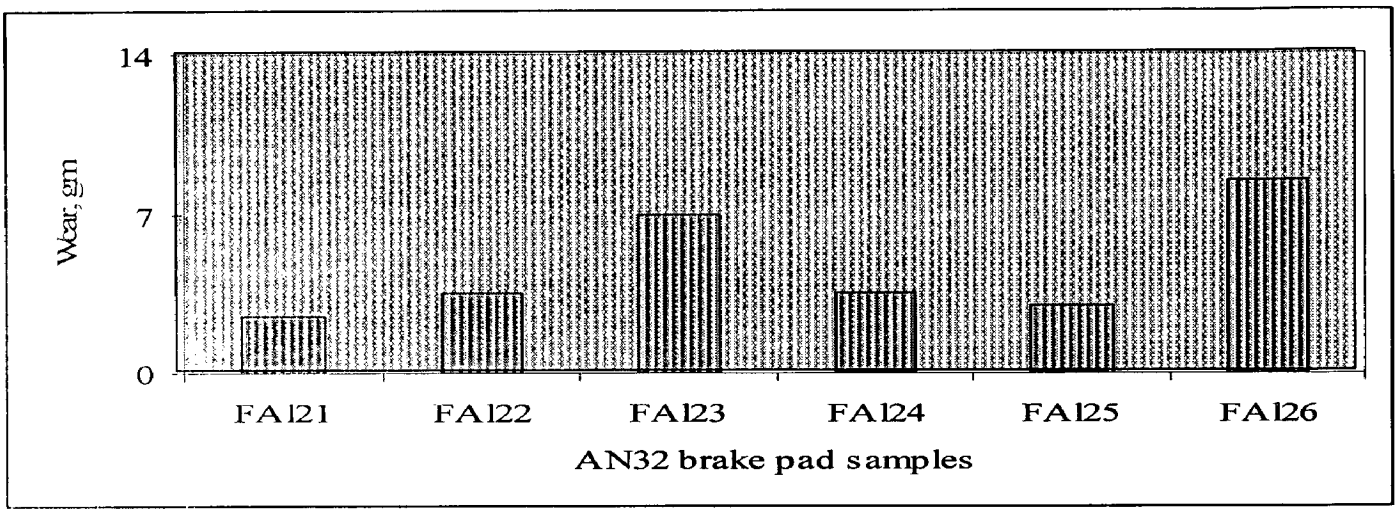

Fig. 5.11(b)(i)

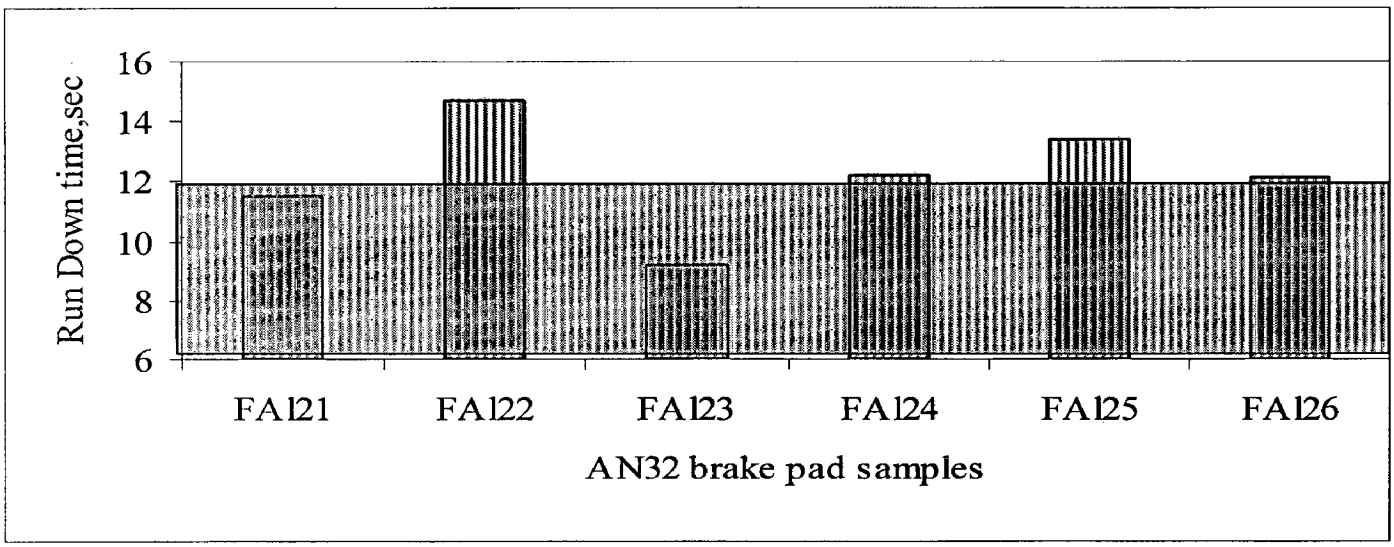

Fig. 5.11(b)(ii)

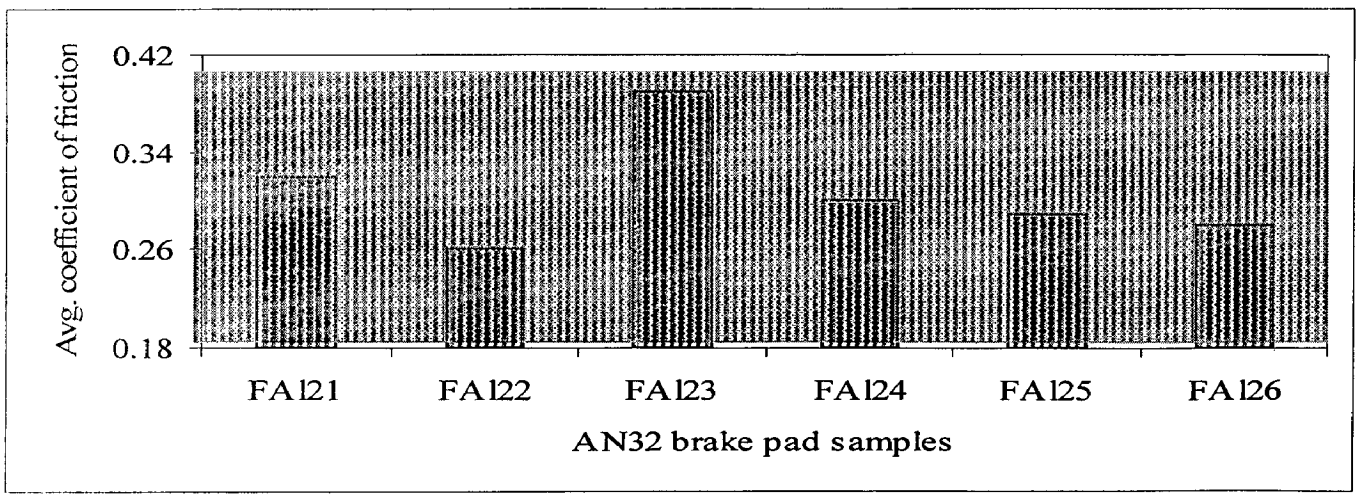

Fig. 5.11(b)(iii)

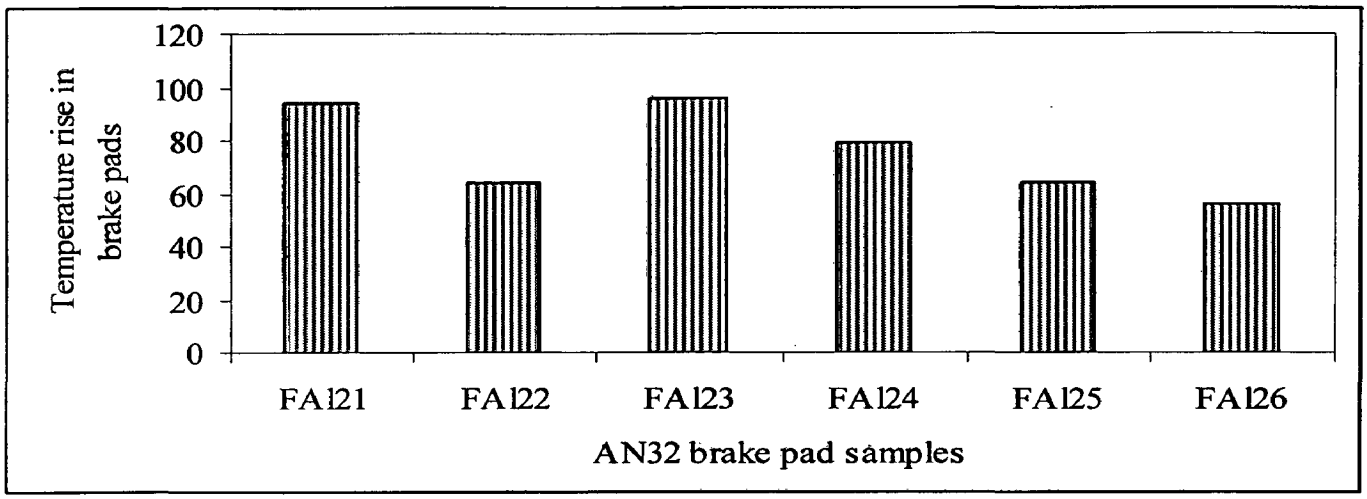

Fig. 5.11(b)(iv)

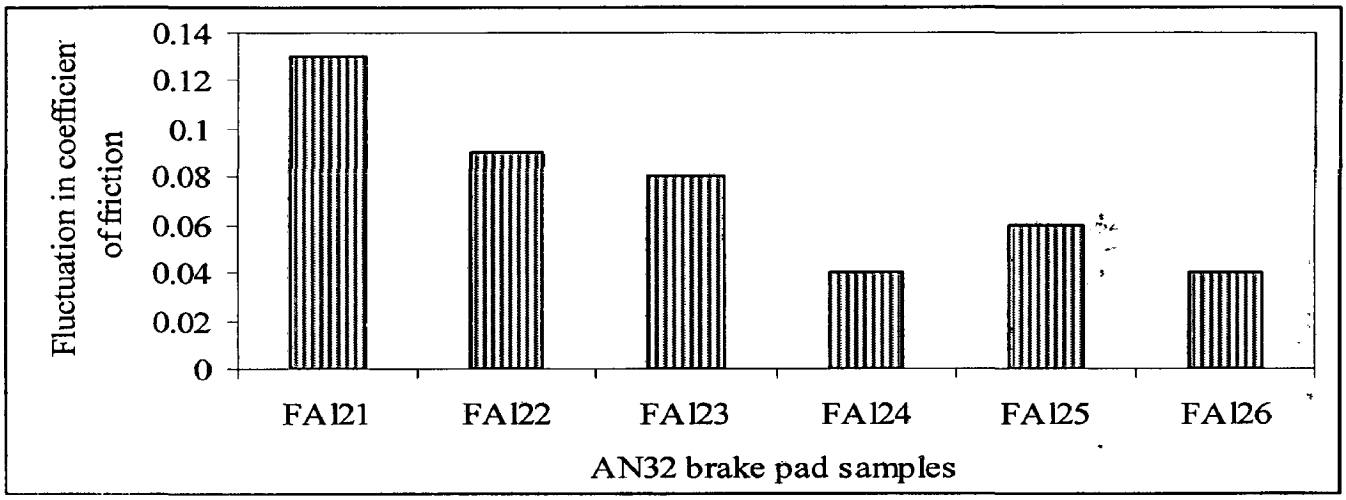

Fig. 5.11(b)(v)

Fig. 5.11 (b) Average output parameters i) Wear (gm)ii) Rum Down time, s iii) Coefficient of friction iv) Temperature in brake pad (higher side) v) Fluctuation in coefficient of friction

Run down time: Fig. 5.11(b) (ii) shows that the RD time varies from 9.5 to 14.7 s in 50 nos. of braking cycles. The RD time for composites **FAI22** and **FAI25** is high and does not lie in standard range.

Based on performance wise comparison, preferences are in the following order:

FAI23>FAI21>FAI26>FAI24>FAI25> FAI22

Coefficient of friction: Coefficient of friction of composites varies from 0.26 to 0.39 in 50 nos. of braking cycles. All the composites qualify for higher energy test as the COF lies in the shaded region (Fig. 5.11(b) (iii).

Based on performance wise comparison, preferences are in the following order:

FAl26>FAl25>FAl24>FAl21>FAl23>FAl22

Temperature rise: Temperature rise varies from 59 to 96 ^{0}C (Fig. 5.11(b) (iv).

Fluctuation in frictional characteristics: Fluctuation in coefficient of friction of composites varies from 0.04 to 0.13 (fig. 5.11(b) (v).

Based on performance wise comparison, preferences are in the following order:

FAl24>FAl26>FAl25>FAl23>FAl22>FAl21

It may be inferred that fluctuation for Al based brake pads is low resulting in low vibration and judder. On the basis of tribo-performance evaluation, composite **FAl22** has not been found suitable for high energy level test-TQ1 **(Table 20).**

5.12.3 High energy level tribo-test: TQ1 (KE = 17300 kgfm)

High energy level/standard test (TQ1) has been conducted in two phases. In first test phase, selected composites FAl21, FAl23, FAl24, FAl25 and FAl26 (on the basis of low and medium energy level test); and in the sond test phase, composites FAl27, FAl28, FAl29 and FAl30 (selected for high energy level test without undergoing low/medium energy level tests): are tested to judge their suitability for AN32 aircraft brake rotor application.

The tribo-test output parameters of developed composites are compared to corresponding output parameters of existing Fe based sintered brake pads for AN32 aircraft.

Table 5.21 High energy/standard friction test performance

Samples	Test Code	50 Cycles.	R.D. Revolution	R.D. time, s	COF (μ)	Higher side pad temp. rise	Δμ	Wear report					
								Thick., mm			Wt. gm		
								Pad1	Pad2	Avg.	Pad1	Pad2	Avg.
FAl26	TQ1	Max	71	8.5	0.42	142	0.08	1.47	2.44	1.95	12	27	19.5
		Min	58	7.0	0.34	84							
		Avg.	63	7.6	0.39	114							
FAl28	TQ1	Max	64	7.7	0.36	122	0.06	0.55	0.68	0.62	7	6	6.5
		Min	49	5.9	0.30	38							
		Avg.	54	6.5	0.34	80							
FAl29	TQ1	Max	60	7.2	o.35	135	0.04	1.1	-	11	9	21	15
		Min	51	6.2	0.31	35							
		Avg.	56	6.7	0.33	86							
FAl30	TQ1	Max	59	7.1	0.38	132	0.05	0.42	0.52	0.47	9	8	8.5
		Min	50	6.1	0.33	41							
		Avg.	53	6.4	0.36	83							

The variation in tribological properties of optimized composites FAl26, FAl28, FAl29 and FAl30 corresponding to 50 nos. of braking cycles are shown in graphic and numeric terms synchronously- **Annexure- B1-B24.** The values of output test parameters from data sheets are summarized in **Table 5.21 pp.179.**

Average wear (gm): It is observed that the wear of Al based composites; **FAl28** (6.5 gm) and **FAl30** (8.5 gm) **(Table 5.21)** is two times lower in comparison to aeronautics industries standard wear (≈14 gm) **(Table 20).** The wear of composite **FAl29** is equivalent to standard wear whereas wear of composite FAl26 is 1.4 times higher in comparison to standard wear The wear for Al based brake pads is 35 to 53% lower than wear of iron based aircraft brake pads **[157]** and 49% lower than copper based aircraft brake pads **[62].**

Run down time (RD time): The RD time of Al based composites FAl26, FAl28, FAl29 and FAl30 in 50 nos. of braking cycles varies from 6.4 to 7.6 s **(Table 5.21).** It lies within aeronautics industries standard RD time range ≈ 6-12 s **(Table 20).**

Coefficient of friction: The coefficient of friction of developed Al based composites FAl26, FAl28, FAl29 and FAl30 varies from 0.33-0.39 **(Table 5.21).** It lies within aeronautics industries standard coefficient of friction range of 0.18-0.40 **(Table 5.20) [157].** It is also noticed that the range of coefficient of friction of Al based composite brake pads; 0.33-0.39 is equivalent to recommended operating coefficient of friction for non-asbestos friction material (μ=0.2 to 0.45) **[39].**

Temperature rise: The temperature rise of developed Al based composites FAl26, FAl28, FAl29 and FAl30 varies with in a range of 35-142 ^{0}C **(Table 5.21),** which is lower than the acceptable temperature rise range of aircraft brake material **[62].**

Fluctuation in coefficient of friction: ($\Delta\mu \approx \mu_{max}$-$\mu_{min}$): The fluctuation in coefficient of friction of composites varies with in a range of 0.04- 0.08, which is 3 to 5 times lower than standard acceptable fluctuation in coefficient of friction (0.22) **(Table 5.20).** The lower value of fluctuation in coefficient of friction reduces the noise, judder and vibration during braking.

It may be concluded that the developed Al based composites namely **FAl28, FAl29** and **FAl30** are qualified for AN32 aircraft application on the basis of wear.

It may be finally concluded that developed Al based composites FAl28, FAl29, FAl30 and FAl26 qualify the aeronautics industries standard parameters and are suitable for AN32 aircraft brake application.

On the basis of overall friction test performances, preferences of composites is

FAl28>FAl30>FAl29>FAl26

5.13 Comparison of wear characteristics of Al and Fe based brake pad composites for AN32

Sub-scale dynamometer friction test output parameters under high energy test (TQ1) of developed Al based brake pads and Fe based brake pads prepared by P/M route for AN32 aircraft rotor applications is shown in **Tables 5.21 pp.178 and 5.22 pp.180** respectively.

Wear (gm): It is observed from fig. 5.12(i) that the wear of Al based brake pad composites like **FAI28, FAI29** and **FAI30** lies in standard region and is lower (≈two times) in comparison to wear of Fe based sintered brake pads. On the basis wear it may concluded that the Al based composites are more suitable than Fe based composites.

Table 5.22 Wear characteristics of earlier developed Fe based brake pads [157]

Samples	Test Codes	Range	RD time, s	COF (μ)	Δμ	Wear					
						Thick., mm			Wt., gm		
						Pad1	Pad2	Avg.	Pad1	Pad2	Avg.
FM11N*	TQ1	Max	13.8	0.34	0.12	2.40	2.35	2.4	38	37	37.5
		Min	8.80	0.22							
		Avg	12.1	0.25							
FM12N*	TQ1	Max	12.3	0.35	0.10	1.88	2.29	2.1	29	32	30.5
		Min	8.40	0.25							
		Avg	9.30	0.32							
FM15ABN*	TQ1	Max	13.9	0.25	0.02	2.12	2.49	2.3	31	31	31.0
		Min	12.50	0.23							
			12.9	0.25							

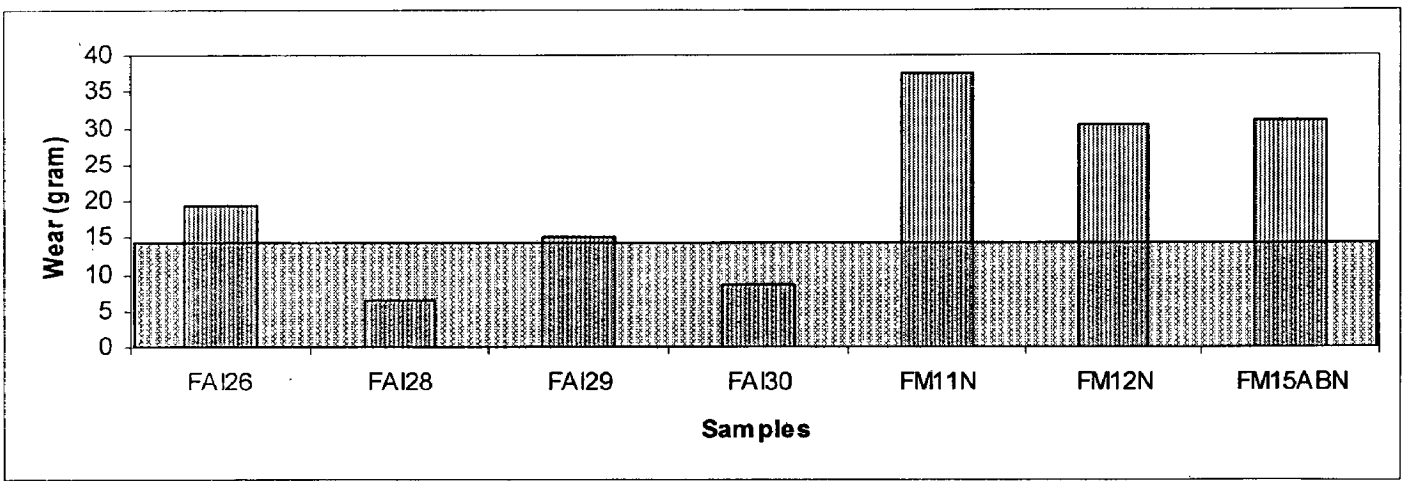

Fig. 5.12(i)

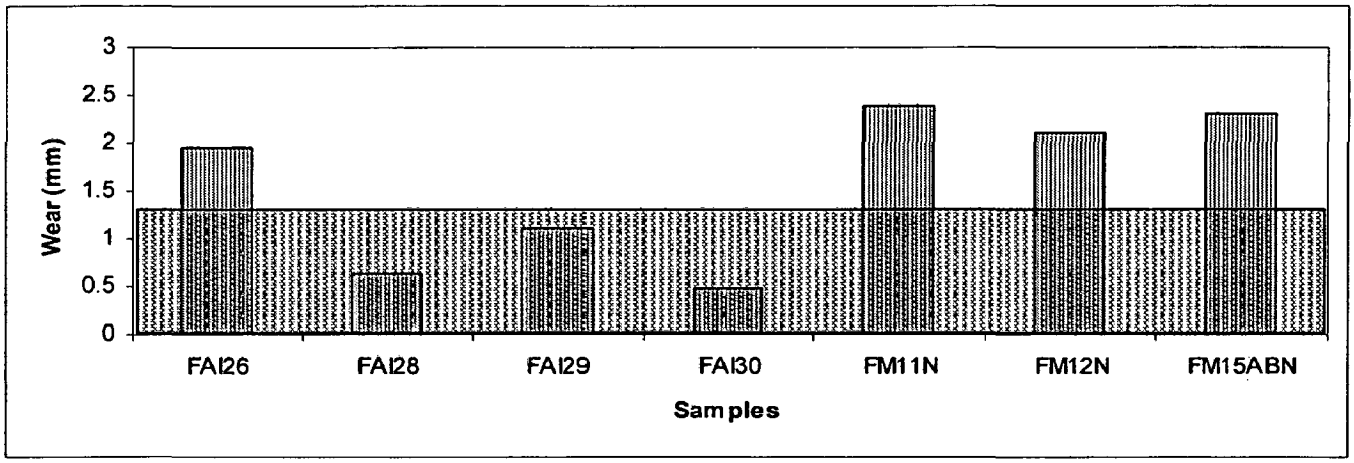

Fig. 5.12(ii)

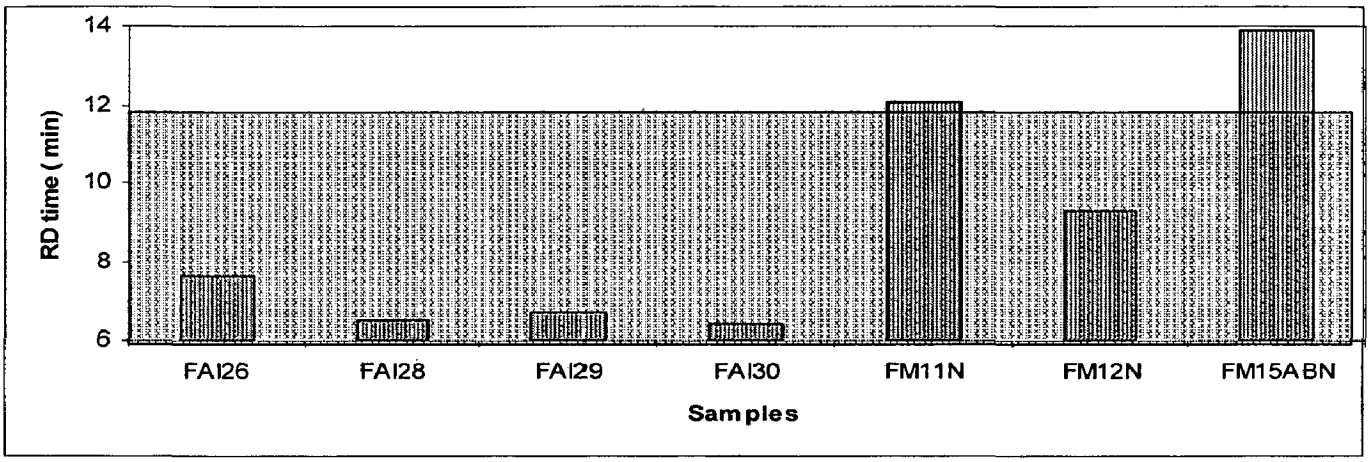

Fig. 5.12 (iii)

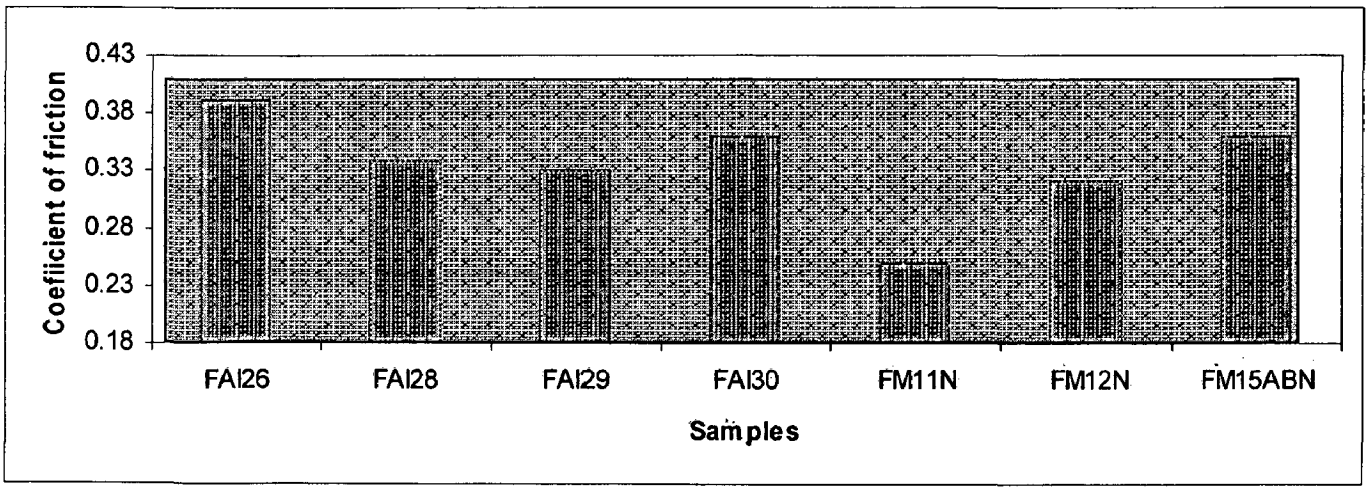

Fig. 5.12(iv)

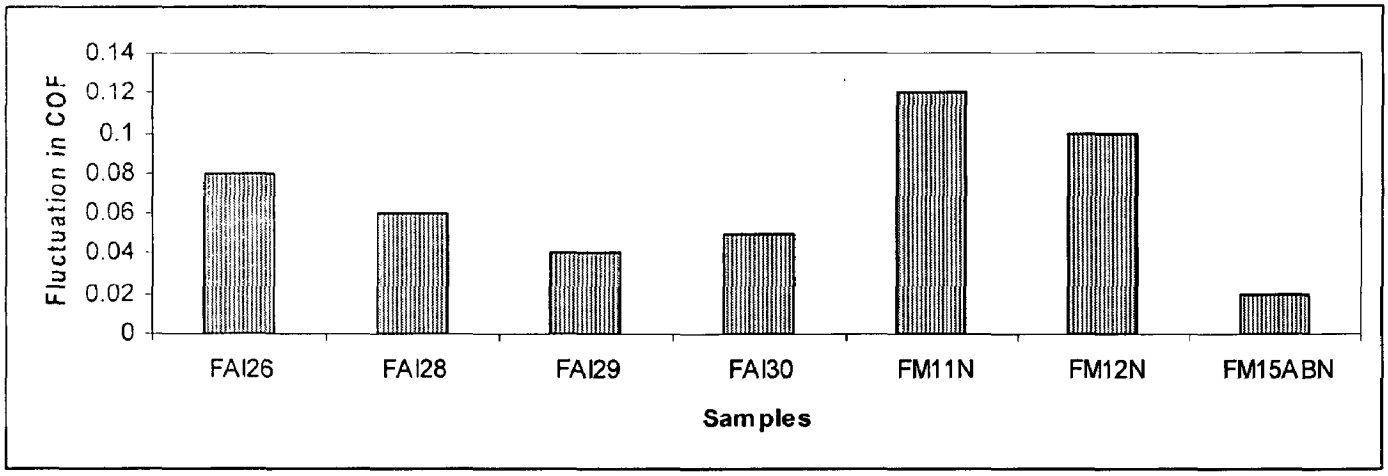

Fig. 5.12(v)

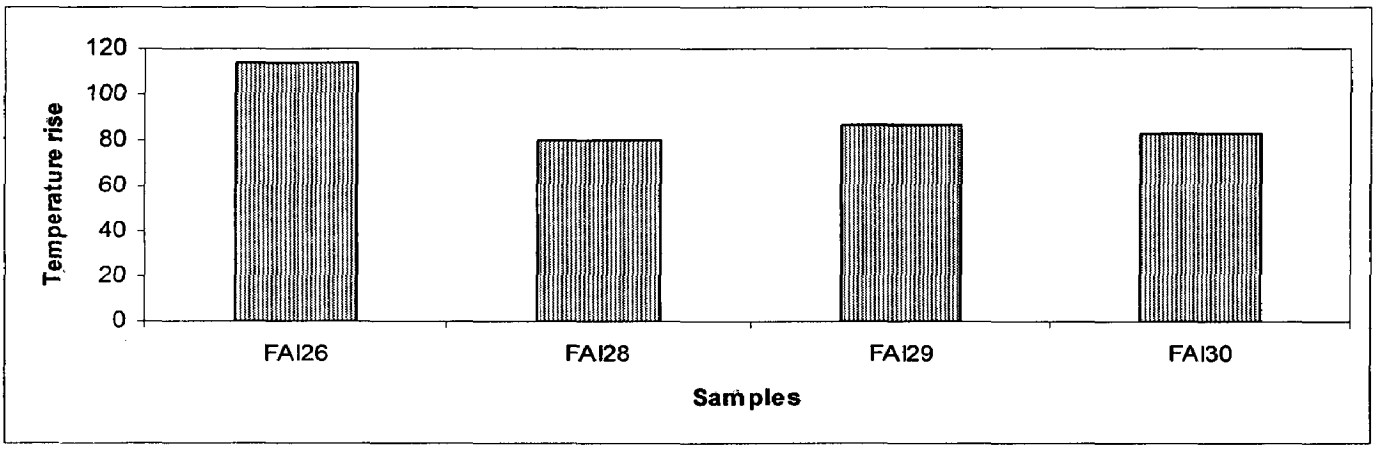

Fig. 5.12(vi)

Fig. 5.12 Comparison of tribo-performance of Al/Fe brake pads i) wear in gram ii) wear of pad in thickness, mm iii) Run Down time, s iv) coefficient of friction v) Fluctuation in coefficient of friction vi) Temperature rise

Wear loss (mm): The wear of Al based brake pads is lower than Fe based brake pads (fig. 5.12 (ii)). It is observed that wear in terms of pad thickness of Al based brake pad is about 1.1 to 1.2 times lower than Fe based brake pads namely FM11N, FM12M and FM15ABN **(Table 5.22 pp.180)**. It is inferred that wear of Al based composite (FAI26) and Fe based composites is higher than the upper limit of standard range (1.25 mm- **Table 5.20 pp.170**), whereas for other Al based composites, wear lies in standard region. It may be concluded that developed Al based composites **FAI28, FAI29** and **FAI30** are found more suitable than Fe based composites for AN32 aircraft brake application.

RD time: RD time for Al based brake pads is about 1.1 to 1.6 times lower than RD time of Fe based brake pads namely FM11N, FM12N and FM15ABN (fig. 5.12 (iii)). It is inferred that the RD time of Al based and Fe based composites lies in the standard region except for composite

FM15ABN. It may be concluded that the developed Al based composites are found more suitable than Fe based composites for AN32 aircraft brake application

Avg. coefficient of friction: Figure 5.12 (iv) shows that the coefficient of friction for Al based composites is equivalent to Fe based composites and lies in standard region. For Al based composites, it varies within a range of 0.33 to 0.39 whereas for iron based composites, it varies within a range of 0.23 to 0.32. On the basis of coefficient of friction, it may be concluded that the developed Al based composites are suitable for AN32 aircraft brake application.

Fluctuation in coefficient of friction: Fluctuation in coefficient of friction for Al based brake pad is lower than Fe based brake pads except of FM15ABN (fig. 5.12 (v)). It may be concluded that judder, vibration and noise of Al based composites are lower than that of Fe based composites.

Temperature rise: Fig. 5.12 (vi) shows that the temperature rise of Al based composites is similar except for FAl26. For composite FAl26, it is higher than others.

Based on performance wise comparison, preferences are in the following order:

FAl28>FAl30>FAl29>FAl26

5.14 Effects of input kinetic energy on tribological characteristics

Table 5.23 shows friction test output parameters of developed composite **FAl26** under different input kinetic energy level test. This test has been conducted to assess the effect of input kinetic energy on wear properties of developed Al-based friction material.

Table 5.23 Friction test performance

Sample	Test Codes	50 Cycles	R.D. Revolution	R.D. time (s)	COF	Max. Temp. rise	Wear report					
							Thickness (mm)			Weight (gm)		
							Pad1	Pad2	Avg.	Pad1	Pad2	Avg.
FAl26	TQ1	Max	71	8.5	0.42	142	1.47	2.44	1.95	12	27	19.5
		Min	58	7.0	0.34	84						
		Avg	63	7.6	0.39	114						
FAl26	TQ2	Max	90	13.0	0.30	82	1.10	1.01	1.10	7	10	8.5
		Min	79	11.4	0.26	33						
		Avg	84	12.1	0.28	56						
FAl26	TQ3	Max	70	12.3	0.40	129	0.35	0.19	0.27	3	3	3.0
		Min	64	11.2	0.36	81						
		Avg	67	11.7	0.38	105						

Wear loss (gm): Figure 5.13 (i) shows that wear increases corresponding to increase in input kinetic energy. The wear ratio (the ratio of wear at different energy levels) in higher energy range **(wear ratio = wear at high energy level to wear at low energy level)** is 1.2 times lower than that the wear ratio in lower energy range. This is a significant characteristic of Al based composites for higher energy range application.

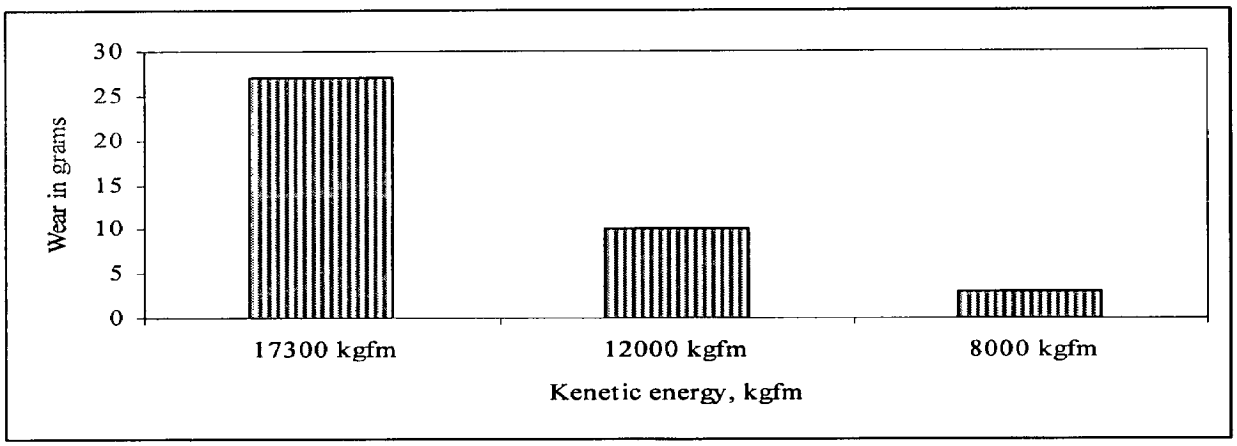

Fig. 5.13(i)

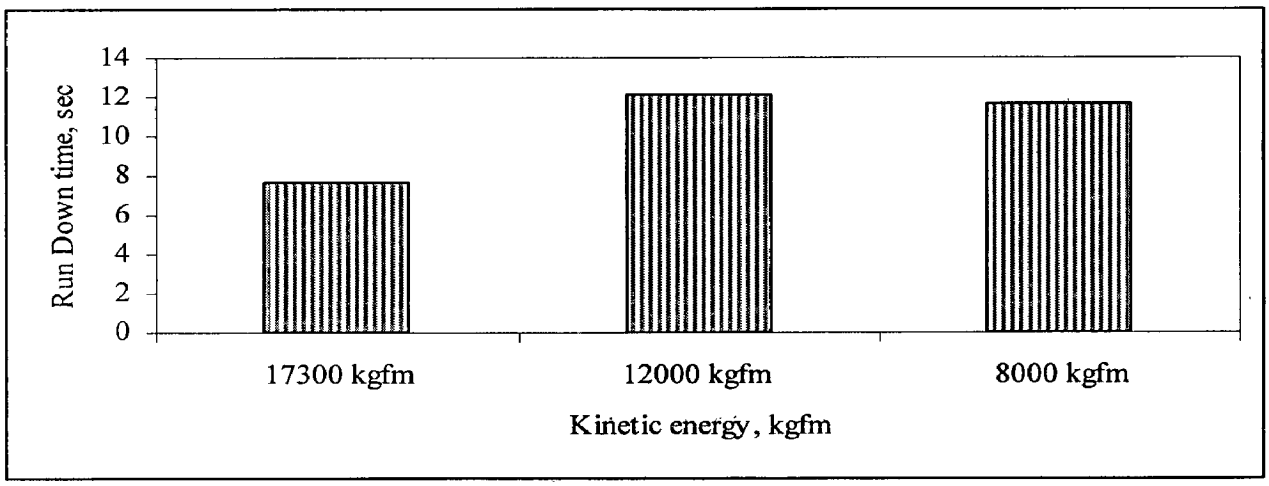

Fig. 5.13(ii)

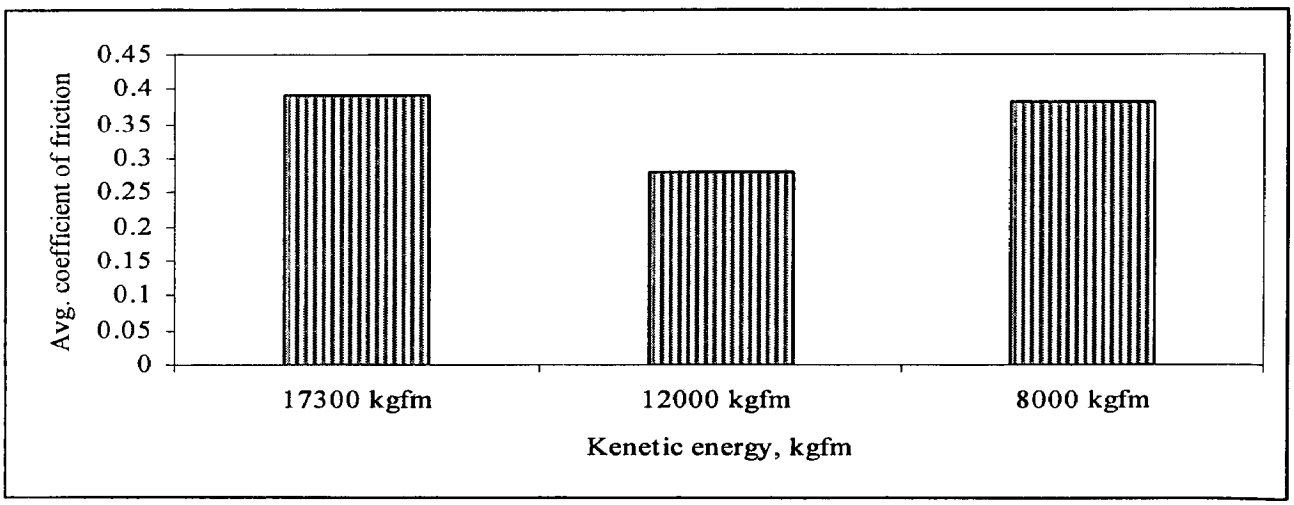

Fig. 5.13(iii)

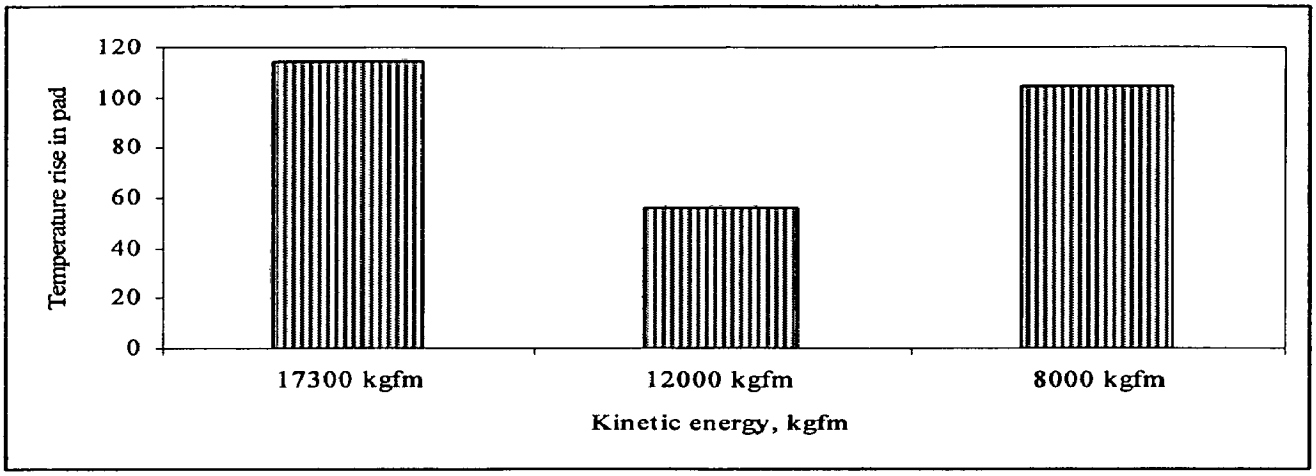

Fig. 5.13(iv)

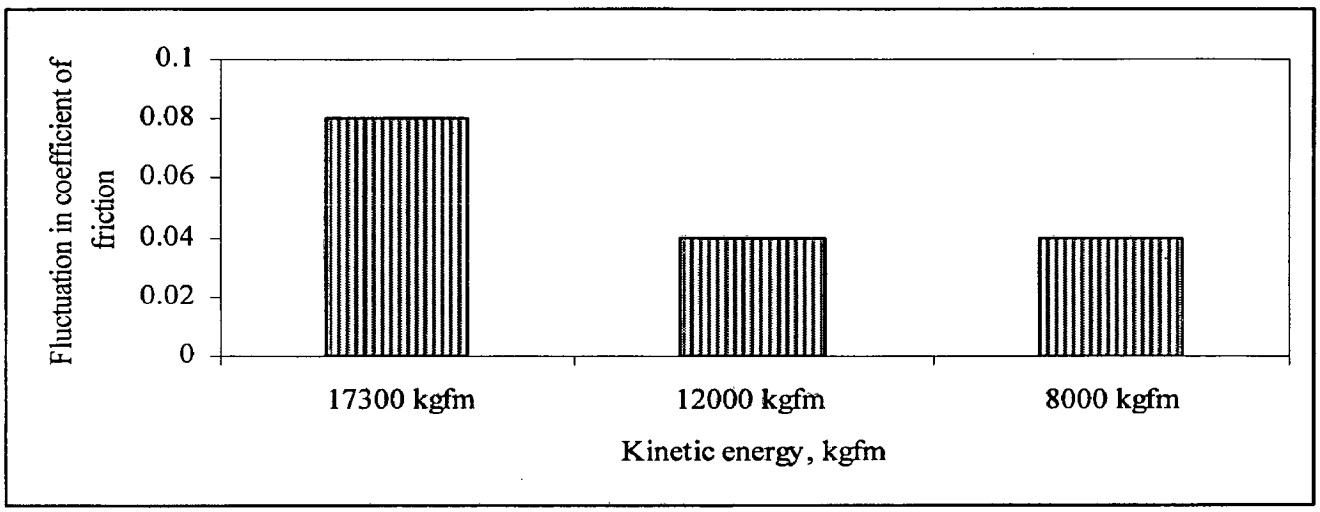

Fig. 5.13(v)

Fig. 5.13 Effects of input kinetic energy on performance of Al/Fe brake pads i) Wear, gm ii) Run Down time, s iii) Avg. coefficient of friction iv) Temperature rise v) Fluctuation in coefficient of friction

Run down time: It is inferred from fig.5.13 (ii) that run down time decreases corresponding to increase in input kinetic energy from 12000 to 17300 kgfm. There is no significant effect of increase in input K. E from 8000 to 12000 kgfm on RD time.

Coefficient of friction: The average coefficient of friction of composite FAl26 is low at medium input energy, whereas at low and high input energy, it is high and constant (fig.5.13 (iii)).

Temperature rise: The temperature rise varies similarly as coefficient of friction corresponding to input kinetic energy (fig.5.13 (iv)). It decreases corresponding to increase in kinetic energy from 8000 to 12000 kgfm, thereafter it tends to increase with input energy from 12000 to 17300 kgfm.

Fluctuation in coefficient of friction: Figure 5.13(v) shows that fluctuation in coefficient of friction increases corresponding to increase in input kinetic energy. The fluctuation in coefficient of friction is steady at low input kinetic energy range (from 8000 to 12000 kgfm), whereas it increases in a multiple of 2.0 in high input kinetic energy range (from 12000 to 17300 kgfm). It is noted that the fluctuation in coefficient of friction ($\Delta\mu$) is 3.4 times lower than that of the standard fluctuation in coefficient of friction. It may be concluded that the probability of vibration or judder is low.

On the basis of overall performances, it may be concluded that the variation in wear and fluctuation in coefficient of friction corresponding to input kinetic energy is of similar nature whereas the variation in average coefficient of friction and temperature rise corresponding to input energy is also of similar nature.

Discussion: The change in tribological characteristics of composites upto 22 nos. of braking cycles is observed. It may be a cause of mechanical mismatching between the static surface of brake pad and the dynamic surface of disc rotor, burnish stops etc.

The wear of composite FAl26 jumps from 8.5 to 19.5 gm when input energy is increased from 1200 to 17300 kgfm (increase of braking force from 100 to 160 kgf with speed from 835 to 1000 rpm). Kwok *et. al. (I)* **[84]** have reported that generally, wear loss increases with increasing the load/brake pressure, but it varies in a complex manner with energy/pressure/speed depending on which regime the sliding condition falls into. Three regimes of tribological behavior are observed for the Al based composites (Al/SiC; fabricated by P/M). In Regime I, mild wear is observed while in Regime II, catastrophic failures occur when a certain critical load is exceeded, resulting in the rapid adhesion of a large amount of specimen material to the counter-face: it is no longer possible to continue the test when this happens. In Regime III, extensive melting of the pads takes place, and under such a sliding condition, the size of reinforcement particles appears to have an important influence on the rate of wear of these composites. A significant effect of input kinetic energy on wear resistance, coefficient of friction, temperature rise and fluctuation in coefficient of friction has been reported in higher energy range than in lower energy range. In lower energy range, wear increases by about 3 times whereas in higher energy range it increases by about 2 times. The magnitude of wear is a complex function of load and speed since it can increase or decrease when certain combinations of load and speed are raised; such a behavior appears to be dependent upon the dominant wear-mechanism. Kwok **[85]** has reported about five dominant mechanisms namely (i) abrasive and delamination wear; (ii) a combination of abrasion, delamination, adhesion and melting; (iii) melt wear; (iv) severe adhesion and (v) severe melting of Al/SiC composites. The regions of dominance of the various mechanisms are also

presented in terms of the applied load and sliding speed. He has also found that the size of the particulate SiC reinforcement controls the high-speed wear resistance of the composites; massive wear occurs if the particles are smaller than a threshold value. Al/SiCp composites with small SiC particles (lower wt. %) are therefore more suitable for low-speed applications. Ho *et. al.* **[132]** have also reported that initially the relation between wear and load is linear up to sliding time of about 20s and thereafter it becomes non linear with higher wear loss. The wear loss corresponding to sliding time increases due to increase in the temperature at contact surface; thereby composites become soft by loosing their hardness. Rhee's wear equation ($\Delta W = K L^a V^b t^c$ where ΔW = wear loss, K= the wear factor, L= load, V= speed, t= time and a, b and c are one set of parameters for a specific friction material) also supports the above discussion.

The fluctuation in coefficient of friction of brake pads as a function of applied brake pressure and ingredients is a very important issue because drivers/pilots expect the same level of friction force at various braking conditions. The fluctuation in the COF gives rise to noise, anti-fade, and vibration [9]. The COF of friction material often varies with sliding speed and this COF variation is highly dependent on ingredients of the friction material. When the COF increases as the sliding speed decreases, the friction force increases at the end of the stop, and can then cause an unpleasant forward jerking. The increase of the COF at the end of a stop is called anti-fade and is often concomitant with noise and judder **[123,124].**

5.15 Summary of sub-scale dynamometer test results

The results pertaining to sub-scale dynamometer under low, medium and standard/high energy level for non qualified/qualified composites mentioned above are summarized in **Table 5.24 pp.189** for simplicity. As a conclusion, following observations are recorded:

(i) The wear for Al based composites varies from 6.5 to 19.5 gm. For composites FAl28 and FAl30, the wear is two times lower than standard wear, whereas for FAl29, is equivalent to standard wear. For composite FAl26, it is 1.5 times higher than standard wear but in comparison to Fe based composites for AN32 aircraft **[157],** it is two times lower.

(ii) The wear in terms of pad thickness (mm) of developed Al based composites is lower than standard wear in pad thickness (mm) except for composite FAl26 (**Table 5.24**).

(iii) RD time range for developed Al based composites lies in the standard RD time range for AN32 aircraft.

(iv) Max temperature rise for developed Al based composites at high energy level is 142 °C, which is much lower than commercially used Cu based sintered metallic brake pads **[62].**

(v) Fluctuation in coefficient of friction for developed Al based composites is lower in comparison to standard fluctuation in coefficient of friction for AN32 **(Table 20),** resulting in low vibration and judder.

(vi) Coefficient of friction, temperature rise and mean brake torque for developed Al based composites are steady throughout 50 nos. of braking cycles.

(vii) Fade is low and recovery is high for developed Al based composites.

(viii) Mass reduction per pad is about 40 %.

The most significant aspect of the developed Al based composites relates to stability in coefficient of friction (μ≈0.33-0.39), low temperature rise (T ≈ 114 °C), low RD time (≈ 6.4-7.6 min) and low fluctuation in coefficient of friction in 50 nos. of braking cycles. It is also noteworthy to report that the aforementioned properties in the developed Al based brake pads have been achieved with low SiC content in the chemistry (6-9 wt.%). This novel aspect has emerged from the present work. On the basis of overall performance and comparison to commercially used sintered iron based friction materials in AN32 aircraft brake application, it may be concluded that developed Al based composites namely FAl28, FAl29 and FAl30 qualify the standard parameters and have been found to suitable for AN32 aircraft brake rotor application.

Table 5.24 Summary of sub-scale dynamometer friction test performance

Friction test output parameters													
Sample	Test code	50 Cycles	R.D. Revolution	Run Down time (s)	COF	Max. temp. rise(°C)	Δμ	Wear					
								Pad thickness (mm)			Wt. (gm)		
								Pad1	Pad2	Avg.	Pad1	Pad2	Avg.
FAI20	TQ2	Max	112	16.2	0.30	116	0.05	1.76	1.3	1.53	19	32	25.5
		Min	92	13.3	0.25	87							
		Avg	102	14.7	0.27	99							
FAI21	TQ2	Max	91	13.1	0.35	116	0.07	0.13	0.25	0.19	2.0	3.0	2.5
		Min	73	10.5	0.28	89							
		Avg	80	11.5	0.32	94							
FAI22	TQ2	Max	129	16.5	0.32	84	0.09	0.23	-	0.23	3.5	-	3.5
		Min	87	10.3	0.23	44							
		Avg	105	14.7	0.26	64							
FAI23	TQ2	Max	77	11.1	0.41	133	0.08	0.79	0.63	0.70	7.0	7.0	7.0
		Min	60	8.6	0.33	47							
		Avg	64	9.2	0.39	96							
FAI24	TQ2	Max	93	13.4	0.31	103	0.08	0.35	0.38	0.37	3.0	4.0	3.5
		Min	82	11.8	0.27	52							
		Avg	85	12.2	0.30	79							
FAI25	TQ2	Max	109	15.7	0.31	84	0.06	0.12	0.25	0.19	3.0	3.0	3.0
		Min	86	12.4	0.25	47							
		Avg	94	13.4	0.29	64							
FAI26	TQ2	Max	90	13	0.30	82	0.04	1.1	1.01	1.1	7.0	10	8.5
		Min	79	11.4	0.26	33							
		Avg	84	12.1	0.28	56							
FAI26	TQ3	Max	70	12.3	0.40	129	0.04	0.35	0.19	0.27	3.0	3.0	3.0
		Min	64	11.2	0.36	81							
		Avg	67	11.7	0.38	105							
FAI26	TQ1	Max	71	8.5	0.42	142	0.08	1.47	2.44	1.95	12	27	19.5
		Min	58	7.0	0.34	84							
		Avg.	63	7.6	0.39	114							
FAI28	TQ1	Max	64	7.7	0.36	122	0.06	0.55	0.68	0.62	7	6	6.5
		Min	49	5.9	0.30	38							
		Avg.	54	6.5	0.34	80							
FAI29	TQ1	Max	60	7.2	o.35	135	0.04	1.1	-	11	9	21	15
		Min	51	6.2	0.31	35							
		Avg.	56	6.7	0.33	86							
FAI30	TQ1	Max	59	7.1	0.38	132	0.05	0.42	0.52	0.47	9	8	8.5
		Min	50	6.1	0.33	41							
		Avg.	53	6.4	0.36	83							

5.16 Estimation and comparison of thermo-mechanical properties

Estimation of properties of selected developed Al based friction materials/composites are categorized into two parts namely i) thermal and ii) mechanical. These properties are compared with the properties of commercially used friction materials in different applications.

5.16.1 Estimation of thermal properties of developed Al based friction materials

The thermo-tests of developed Al based composites were carried out at Delhi Metro Railway corporation-Delhi, India for characterization of the thermo-physical properties of Al-based friction material composites namely FAl21 to FAl26, to judge their suitability for light to heavy duty and AN-32 aircraft rotor brake application. In this stion, thermo-tests of composites under different temperature ranges are covered.

The thermo-tests input parameters are shown in **Table 5.25** as test codes (TH1 to TH8).

Table 5.25 Thermal test input parameters

Test Code	Temperature Range	Specimen Geometry and Dimension			Thermal Tester
		Shape	Dimension (mm)		
TH1	20 (RT)- 350 °C	Disc	d x t	10 x 3.5	Lesser Flash
TH2	350- 575 °C				
TH3	20 (RT)- 350 °C	Cube	a x a x a	5 x 5 x 5	TAP 607- 1
TH4	350- 575 °C				
TH5	20 (RT)- 350 °C	Cylindrical	d x l	10 x 22	TCT426
TH6	350- 575 °C				
TH7	100-500 °C				
TH8	20 (RT)- 350 °C	Rectangular	l x b x t	10 x 5 x 2	Dilatometer

This part of thesis shows an overview about thermal properties of developed Al based friction materials at different temperature ranges and at particular temperatures, which were measured using of different thermometers.

The average values of thermal properties of al based friction composites namely thermal diffusivity D, specific heat c_p, thermal expansion coefficient ϵ and thermal conductivity λ, are measured directly using different thermometers (Chapter 4). Thermal conductivity λ can also be calculated from equation; $\lambda = \rho c_p d$.

The different test parameters as obtained from thermo- tests are as follows:

Thermal diffusitivity

A measure of the hear transfer rate at which a temperature disturbance at one point in a body travels to another point.

It is expressed by the relationship $\lambda/\rho C_p$, where λ is the coefficient of thermal conductivity, ρ is the density, and C_p is the specific heat at constant pressure.

The diffusitivity is a measure of how quickly a body can change its temperature. It increases with the ability of a body to conduct heat and decreases with the amount of heat needed to change the temperature of body (C_p).

Specific heat

The specific heat of material is defined as the amount of energy required to raise a unit mass of material by one unit of temperature at constant pressure. The relationship between heat and temperature change is usually expressed in the form shown below where where: C_p = specific heat, m = mass, ΔT = change in temperature, and Q is the energy. The relationship does not apply if a phase change is encountered, because the heat added or removed during a phase change does not change the temperature.

$C_p = Q/(m\ \Delta T)$ Where: C_p = specific heat, m = mass, ΔT = change in temperature, Q = energy

Thermal conductivity- λ

It is the quantity of heat transmitted, due to unit temperature gradient, in unit time under steady conditions in a direction normal to a surface of unit area. Thermal Conductivity is used in the Fourier's equation.

Thermal expansion coefficient

Materials expand because an increase in temperature leads to greater thermal vibration of the atoms in a material, and hence to an increase in the average separation distance of adjacent atoms.

The linear coefficient of thermal expansion a describes by how much a material will expand for each degree of temperature increase, as given by the formula: $\alpha=dl/(l \times dT)$, where, dl = change in length of material, l = overall length of material in the direction being measured, dT = change in temperature.

Although ratio is dimensionless, expansion has the unit k^{-1}, and is normally quoted in parts per million per °C rise in temperature. There is a related volume coefficient of thermal expansion, but the acronym CTE typically refers just to the linear expansion.

5.16.2 Thermo-test performance of developed Al-based friction materials

Tables 5.26 (a) and **5.26 (b)** show the thermo-test output parameters in different temperature ranges; i.e. RT- 350 °C and 350- 575 °C. The absolute thermal conductivities of composites at

different temperatures are also measured and summarized in **Table 5.26(c)**. **Table 5.26 (d)** shows the thermal properties of friction materials/composites, which are being used in different applications. The thermo-test output parameters of developed Al based composites are compared to the thermal properties of friction materials/composites (**Table 5.26 (d)**) to judge their suitability of composites for different applications. The ranges of thermal properties of friction materials/composites are shown in figures by shaded region.

Table 5.26 (a) Thermo-test performance: 20 (RT)- 350 °C

Test codes Samples	TH1	TH3	TH5	TH8
	Thermal diffusitivity, D (10^{-5} m^2 s^{-1})	Specific Heat- C_p (J kg^{-1} K^{-1})	Thermal conductivity- ($Wm^{-1}K^{-1}$)	Thermal expansion coefficient- (10^{-6}/ K)
FAl21	6.70	851.0	171.2	7.80
FAl23	5.21	860.1	167.1	7.10
FAl24	5.20	873.5	168.3	9.10
FAl25	4.10	829.8	168.3	10.3
FAl26	5.10	850.9	171.0	9.60

Table 5.26 (b) Thermal test performance: 350- 575 °C

Test codes Samples	TH2	TH4	TH6	TH9
	Thermal-diffusitivity, D(10^{-5} m^2 s^{-1})	Specific Heat- C_p (J kg^{-1} K^{-1})	Thermal conductivity- ($Wm^{-1}K^{-1}$)	Thermal expansion- coefficient- (10^{-6}/ K)
FAl21	7.233	854.3	172.2	9.78
FAl23	6.921	863.7	171.5	8.89
FAl24	7.200	876.1	172.9	10.9
FAl25	7.021	834.8	173.4	11.7
FAl26	7.130	855.3	174.2	11.66

Table 5.26(c) Absolute thermal conductivity at different temperatures

Test code	TH7				
Samples	100 °C	200 °C	300 °C	400 °C	500 °C
FAl21	168	173	196	178	171
FAl23	169	174	171	172	174
FAl24	172	177	181	173	168
FAl25	168	175	178	172	174

Table 5.26 (d) Thermal properties of composites for different applications

Composites for different applications	Properties	Density, gm/cc	Thermal-Diffusivity, ($\times 10^{-5}$ m^2/s)	Specific-heat, J/kgK	Thermal-Conductivity, W/m/K
	Range	2.7-2.94	4.2 -8.5	821-898	110-175
	Ref.	-	-	-	-
*AMC600	[189]	2.75	7.1	897.6	174.6
*AMC610	[189]	2.8	7.2	870.9	174.8
*AMC620	[189]	2.82	7.1	844.6	169.8
*AMC630	[189]	2.90	6.5	820.4	154.4
*AMC640	[189]	2.94	5.7	795.9	134.0
Railway brake disc	[59]	2.7	6.32	850.0	145.0
Composites brake application	[190]	-	4.2 -8.5	-	110.0
Automotive disc brake	[61]	2.85	-	1027	148.0

*AMC-Aerospace Metal Composites for brake discs of trains and cars.

5.16.2.1 Estimation of thermal diffusitivity: Fig. 5.14(a) shows that thermal diffusitivity of composites increases corresponding to increase in temperature range from 20-350 to 350-575 °C. It varies slightly at low temperature range whereas stabilizes at high temperature range. It is inferred that thermal diffusitivity varies within a range of 4.10 to 6.70 (10^{-5} m^2 s^{-1}) at low temperature range whereas at high temperature range, it varies with in a range from 6.92 to 7.23 (10^{-5} m^2 s^{-1}). It is maximum for composite **FAl21** and minimum for composite **FAl25** at low temperature range where as at high temperature range, it is maximum for composite **FAl21** and minimum for composite **FAl23**. It may be concluded that the diffusitivity of Al based composites is function of temperature rise because diffusitivity increases with increase in temperature rise. It may also be concluded that the range of diffusitivity variation at low and high temperature ranges lies in shaded region can be preferred for brake applications. .

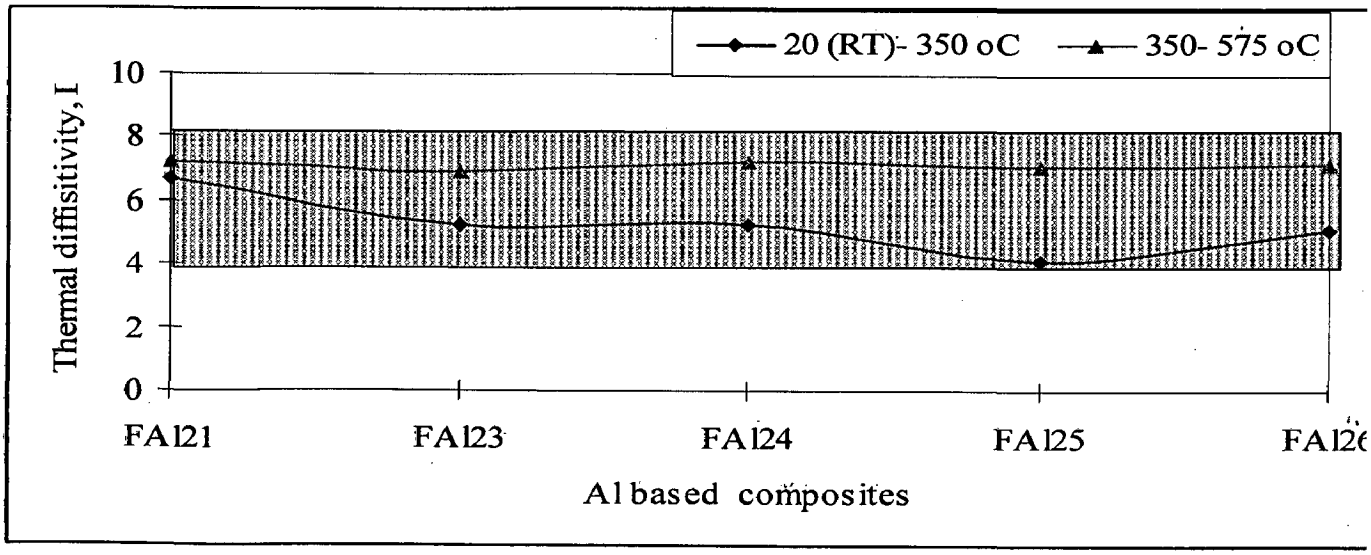

Fig. 5.14(a) Thermal diffusitivity

5.16.2.2 Estimation of specific heat: Fig. 5.14(b) shows that specific heat of composites increases corresponding to increase in temperature range from 20-350 to 350-575 °C. The thermal diffusitivity varies with in a range from 830 to 874 (J $kg^{-1} K^{-1}$) at low temperature range whereas at high temperature range, it varies with in a range from 835 to 876 (J $kg^{-1} K^{-1}$). It is maximum for composite **FAl24** and minimum for composite **FAl25** at low temperature range where as at high temperature range, it is maximum for composite **FAl24** and minimum for composite **FAl25**. It is noticed that the fluctuation in specific heat of Al based composites is higher at low temperature range than fluctuation in specific heat at high temperature range. It shows that the specific heat capacity of composites increases with stability corresponding to increase in temperature range. It may be concluded that range of specific heat variation at low and high temperature ranges lies in shaded region can be preferred for above given applications **(Table 5.26(d)).**

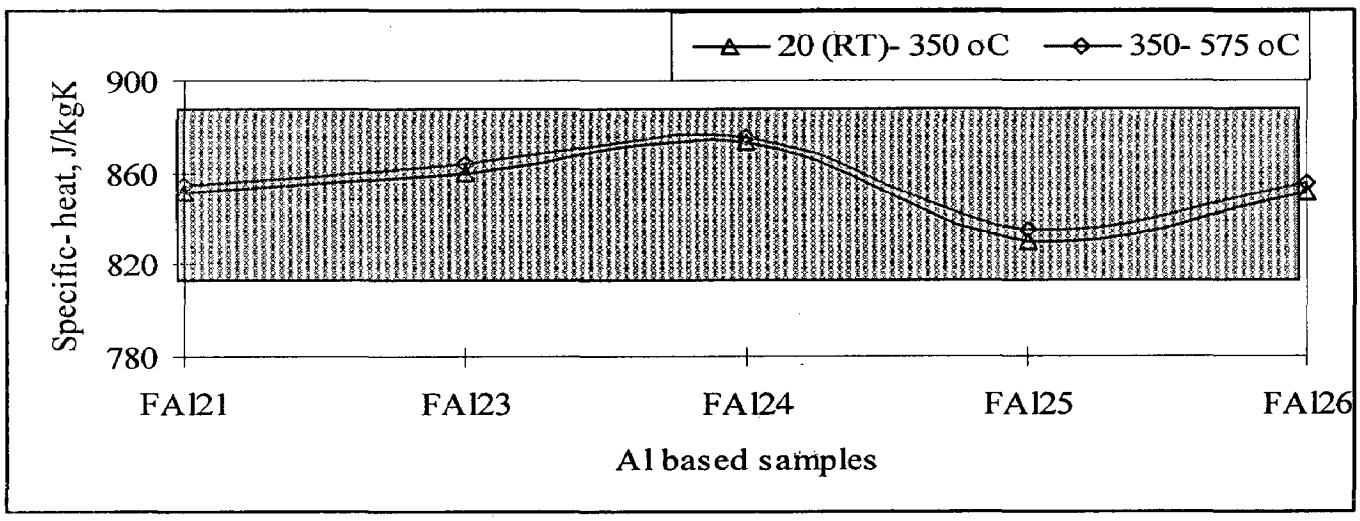

Fig. 5.14(b) Specific heat

5.16.2.3 Estimation of thermal conductivity: Figure 5.14(c) shows that thermal conductivity of composites increases corresponding to increase in temperature. The thermal conductivity varies with in a range from 167 to 171 (W $m^{-1}K^{-1}$) at low temperature range whereas at high temperature range, it varies with in a range from 172 to 174 ($Wm^{-1}K^{-1}$). It is noticed that the fluctuation in thermal conductivity of Al based composites is 2.0 times higher at low temperature range than fluctuation ($\lambda_{max} - \lambda_{min}$) in thermal conductivity at high temperature range. It shows that the thermal conductivity of composites increases with stability corresponding to increase in temperature range. It may be concluded that thermal conductivity range of developed composites lies in shaded region can be preferred for applications **(Table 5.26).**

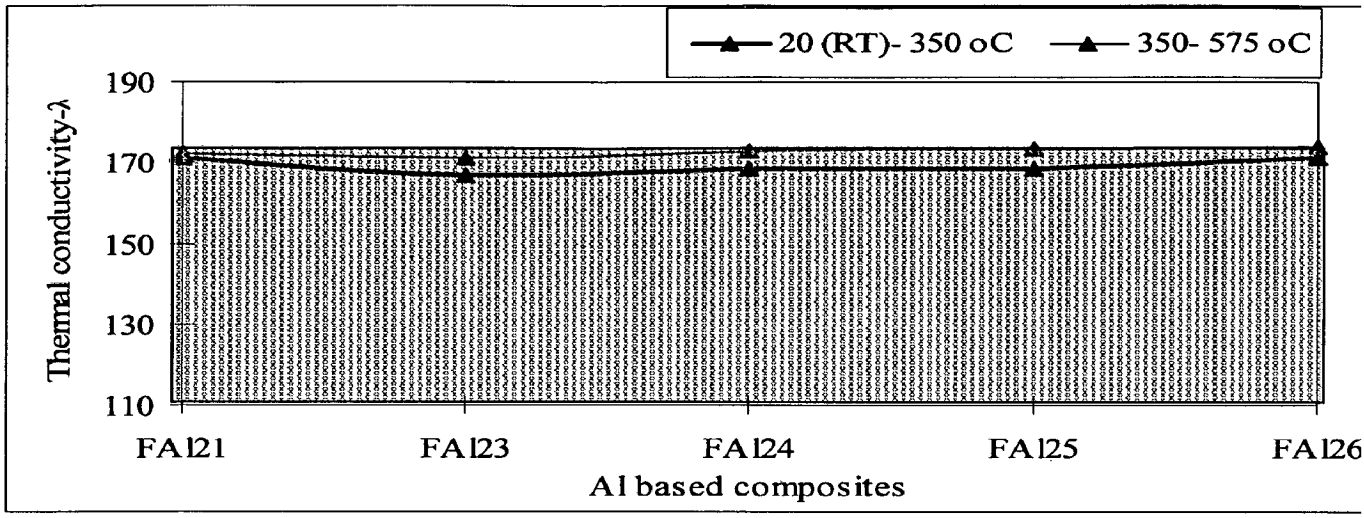

Fig. 5.14(c) Thermal conductivity

5.16.2.4 Estimation of thermal expansion coefficient: Fig. 5.14(d) shows that thermal expansion coefficient of Al based composites increases corresponding to increase in temperature range from 20-350 to 350-575 °C. The thermal expansion coefficient varies with in a range from 7.10 to 10.3 (10^{-6}/ K) at low temperature range whereas at high temperature range, it varies with in a range from 9 to 12 (10^{-6}/ K). It is maximum for composite **FAl25** and minimum for composite **FAl23** at low temperature range where as at high temperature range, it is maximum for composites **FAl25** and FAl26 and minimum for composite **FAl23**. It is noticed that the fluctuation (CTE_{min}- CTE_{max}) in thermal expansion coefficient of Al based composites at low temperature range is equal to fluctuation in thermal expansion coefficient at high temperature range. It shows that the thermal expansion coefficient is stable and constant at low temperature range as well as high temperature range. Form figure, it is inferred that thermal expansion coefficient at low and high temperature range varies simultaneously corresponding to composites.

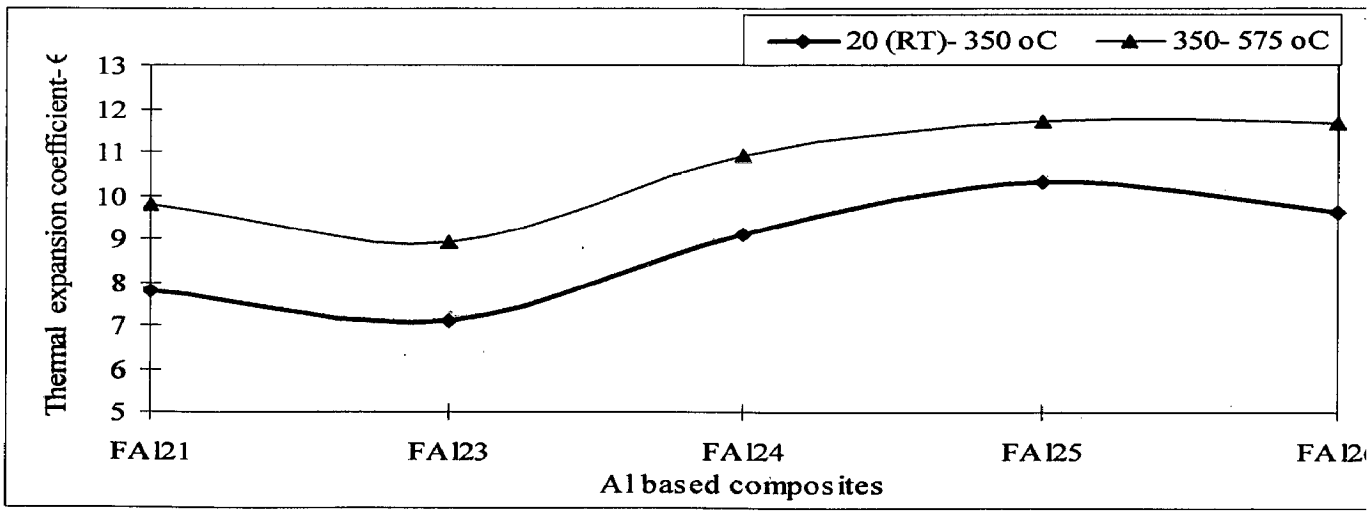

Fig. 5.14(d) Thermal expansion coefficient

5.16.2.5 Estimation of absolute thermal conductivity of composites: Table 5.26(c) pp.192 shows the variation in absolute thermal conductivities of composites corresponding to temperatures; 100, 200, 300, 400 and 500 °C.

Variation in absolute thermal conductivity: Fig. 5.14 (e) shows that the variation in absolute thermal conductivity of Al based composites corresponding to temperatures. The thermal conductivity of composites increases corresponding to increase in temperature up to 300 °C thereafter it tends to decrease. It stabilizes with in a temperature ranges from 400 to 500 °C. For composite FAl21, it reaches up to peak value at temperature 300^0C. It is noticed that for all composites, thermal conductivity increases up to 300 °C thereafter it tends to decrease. It is inferred that thermal conductivity stabilizes for the composites with in a temperature range from 200 to 400 °C. It may be concluded that thermal conductivity of Al based composites is stable and high up to 500 °C.

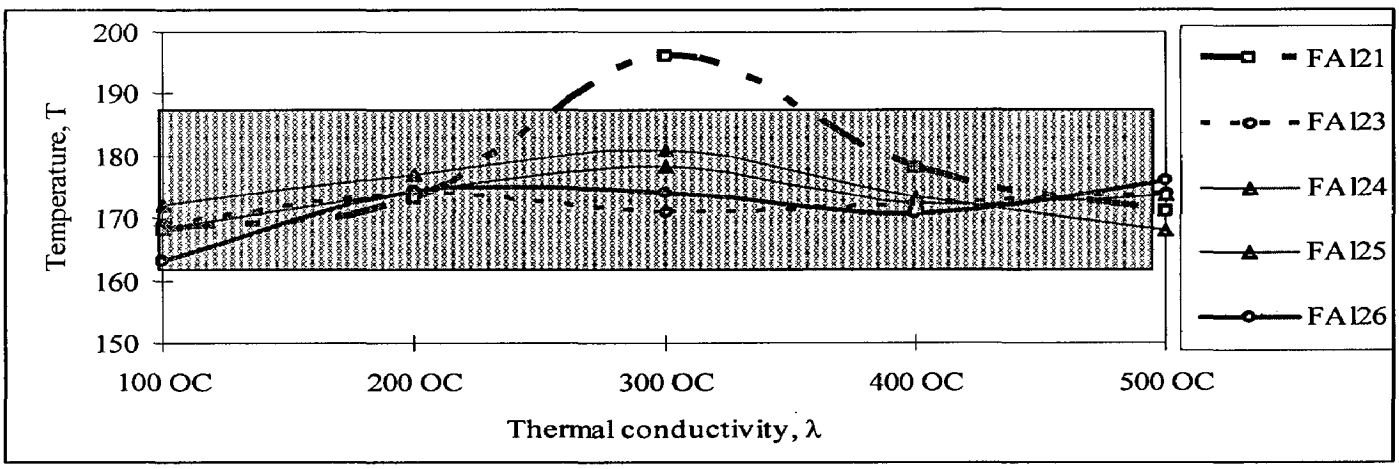

Fig. 5.14(e) Absolute thermal conductivity

It may be concluded that range of thermal conductivity variation at low well as high temperatures lies in shaded region can be preferred for different applications, especially in brakelining.

5.17 Summary

1. Thermal diffusitivity of developed Al based composites lies in shaded region except of composite FAl25 whereas at higher temperature range, thermal diffusitivity of composites stabilizes.
2. Specific heat of developed composites lies with in shaded region. It is noticed that there is no significant effect of variation in temperature range on specific heat of composites.

3. Thermal conductivity of Al based composites is stable at low and high temperature range There is no significant effect of variation in temperature range on thermal conductivity o composites.
4. Thermal expansion coefficient of Al based composites increases with increase ir temperature range.
5. Absolute thermal conductivity of composites initially increases and then stabilizes for al composites except of FAl21. Absolute thermal conductivity of composite FAl21 reache their peak value at temperature 300 ^{0}C.

5.18 Estimation of mechanical properties of developed Al based friction materials

The mechanical property tests of developed Al based composites were carried out at Delh Metro Railway corporation-Delhi, India for characterization of the mechanical properties o Al-based friction material composites namely FAl20 to FAl26, to judge their suitability fo light/heavy duty and AN-32 aircraft rotor brake application.

The mechanical test input parameter: test code (ME) are shown in **Table 5.27.**

Table 5.27 Mechanical test input parameters

Test code	Specimen Geometry and Dimension			Mechanical Tester
	Shape	Dimension (mm)		Laser flash method - ULVAC TC-7000
ME	rectangular	l x b x t	10 x 5 x 2	

Note: The mechanical properties of developed composites namely young's modulus, tensile strength, compressive strength, shear modulus and shear strength are measured at room temperature and compared to mechanical properties of friction materials used in different applications.

The different test parameters as obtained from mechanical tests are as follows.

Young's modulus, E

In solid mechanics, Young's modulus is a measure of the stiffness of an isotropic elastic material. It is defined as the ratio of the uniaxial stress over the uniaxial strain in the range of stress in which Hooke's Law holds. This can be experimentally determined from the slope of a stress-strain curve created during tensile tests conducted on a sample of the material during tensile tests conducted on a sample of the material.

Tensile strength, Y

The greatest longitudinal stress, a substance can bear without tearing apart.

Compressive strength, £e

By definition, the compressive strength of a material is that value of uniaxial compressive stress reached when the material fails completely. The compressive strength is usually obtained experimentally by means of a compressive test. The apparatus used for this experiment is the same as that used in a tensile test. However, rather than applying a uniaxial tensile load, a uniaxial compressive load is applied. As can be imagined, the specimen.

Shear modulus, G

It is defined as the ratio of the shear stress over the shear strain .

Shear strength, S

Shear strength in engineering is a term used to describe the strength of a material or component against the type of yield or structural failure where the material or component fails in shear.

5.19 Mechanical tests performances of developed Al-based friction materials

Table 5.28 (a) and ***5.28*** **(b)** show the mechanical test results and mechanical properties of friction materials which have been drawn from different applications.

Table 5.28 (a) Mechanical test performance of developed Al based friction materials

Samples	Mechanical test output parameters of Al based friction materials Test code: ME						
	Longitudinal young's Modulus, GPa, E_{11}	Transverse Young's Modulus, GPa, E_{22}	Yield Tensile strength, MPa, Y_e	Ultimate Tensile strength, MPa, Y_u	Yield Compressive strength, MPa, £e	Shear Modulus (x.-y), Gpa G_{12}	Sear Strength, Mpa (at strain 2%).S_{12}
FAl21	227.8	99.7	321.5	366.0	265.2	25.0	76.7
FAl22	229.0	100.0	308.2	345.1	253.2	22.0	75.7
FAl23	242.9	97.0	309.7	349.0	253.3	23.6	79.1
FAl24	246.9	105.1	323.3	346.9	261.9	24.6	88.0
FAl25	235.6	104.3	321.8	358.7	266.2	24.3	79.0
FAl26	232.6	99.9	318.1	366.2	268.3	32.3	76.0

The mechanical output test parameters of developed Al based composites are compared with corresponding parameters of mechanical properties of commercial friction materials for different applications (**Table 5.28 (b)**). The upper and lower limits of ranges of mechanical

properties of friction materials are presented in figures by shaded region. The ranges of mechanical properties of developed Al based composites lie in this region are known as qualified composites and preferred for applications.

Table 5.28 (b) Mechanical properties of friction materials for different applications at room temperature (RT)

Friction materials	Reference	Longitudinal young' Modulus, GPa, E_{11}	Transverse Young's Modulus, GPa, E_{22}	Yield Tensile strength, MPa, Y_e	Ultimate Tensile strength, MPa, Y_u	Compressive strength, MPa, $\pounds_e$	Sear Strength, Mpa (at strain 2%). S_{12}
CFAMC [a]	**[193]**	240	130	-	-	-	70
FMS [b]	**[194]**	-	-	26	-	-	53
Fe based friction materials [c]	**[150]**	-	-	-	-	50	70-90
Disc brake materials [d]	**[150].**	-	-	-	-	130-470	-
Al composites [e]	**[123]**	-	54-98	208-405	236-460	-	-
Al based alloy	**[171]**	58-116		167-630			

[a] 3M is developing two compositions of Continuous Fiber Reinforced Aluminum Matrix Composites (CFAMC)

[b] Designed by KATEEL engineering industry for a dry friction use

[c] Railway applications

[d] For railway applications

[e] Fabricated by Duralcan company **[123].**

5.19.1 Longitudinal Young's modulus: Table 5.28 (a) shows that longitudinal young's modulus of developed Al based composites varies with in a short range from 228 to 247 GPa. It is noticed that longitudinal young's modulus of developed Al based composites is equivalent to longitudinal young's modulus of developed Al based matrix composite (AMC) **[193].**

5.19.2 Transverse Young's modulus: Table 5.28 (a) shows that transverse young's modulus of developed Al based composites varies with in a range from 97 to 105 GPa. It is noticed that transverse young's modulus of developed Al based composites is lower than the transverse young's modulus of Al based matrix composite (AMC) **[193],** on other hand it higher than Al composites fabricated by Duralcan composite manufacturing company **[123].**

5.19.3 Yield tensile strength: Table 5.28 (a) shows that yield tensile strength of developed Al based composites vary with in a range from 308 to 323 MPa. It is noticed that yield tensile strength of developed Al based composites is 12 times higher than yield tensile strength of sintered iron based friction materials **[194].** Fig 5.15(a) shows that yield tensile strength of developed Al based composites lies with in standard range from 208 to 405 MPa of Al composites, fabricated by Duralcan composite manufacturing company **(Table 5.28 (b))**

[123]. It may be concluded that yield tensile strength of developed Al based composites lie in shaded region shows better mechanical property.

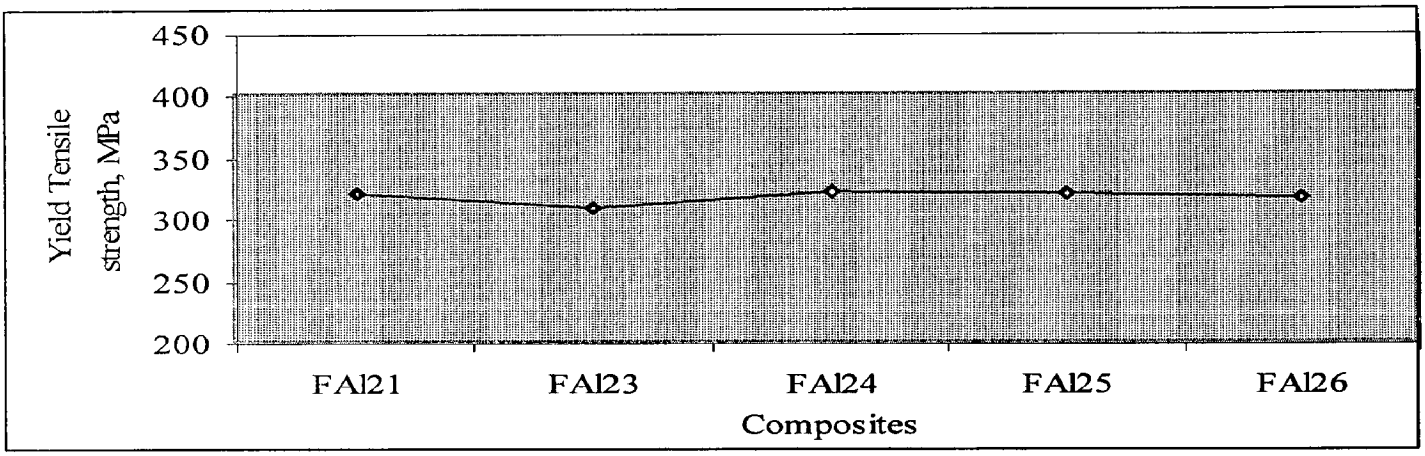

Fig 5.15(a) Yield Tensile strength

5.19.4 Ultimate tensile strength: Table 5.28 (a)shows that ultimate tensile strength of developed Al based composites varies with in a range from 345 to 366 MPa. Figure 5.15(b) shows that yield tensile strength of developed Al based composites lies with in range from 236 to 460 MPa of Al composites fabricated by DURALCAN composite manufacturing company **(Table 5.28 (b)) [123].** It may be concluded that ultimate tensile strength of developed Al based composites lie in shaded region shows better mechanical property.

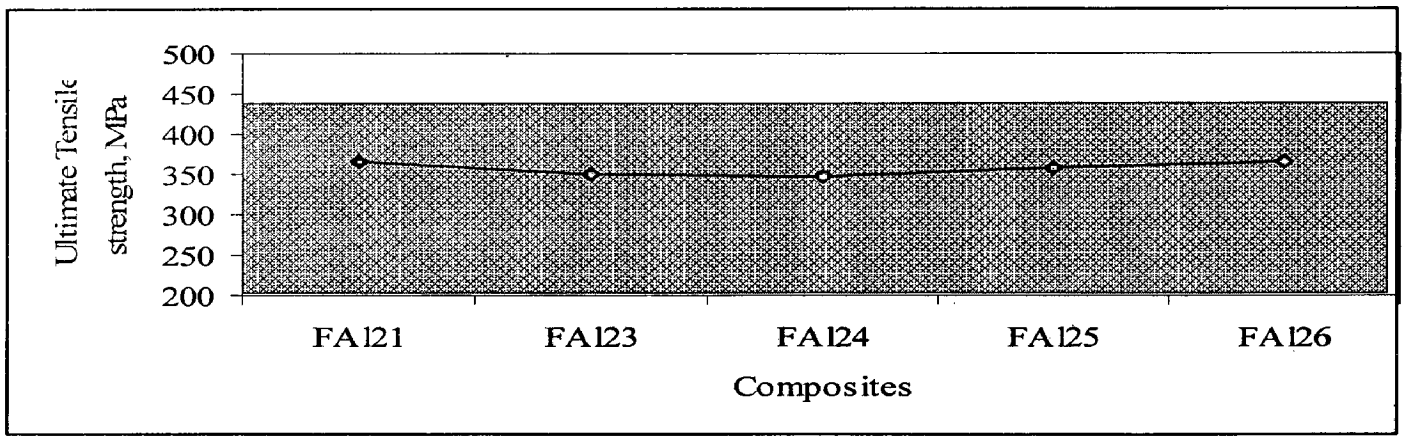

Fig 5.15(b) Ultimate tensile strength

5.19.5 Compressive strength: Table 5.28 (a) shows that yield compressive strength of developed Al based composites varies with in a range from 253 to 268 MPa **(Table 5.28 (b)).** It is maximum for composite **FAl26.** It is noticed that yield compressive strength of developed Al based composites is 5 times higher than yield compressive strength of PM friction materials **[150].** Fig 5.15(c) shows that yield compressive strength of developed Al based composites lies with in a range from 130 to 470 MPa of disc brake materials. It may be concluded that

yield compressive strength of developed Al based composites lie in shaded region shows better mechanical property.

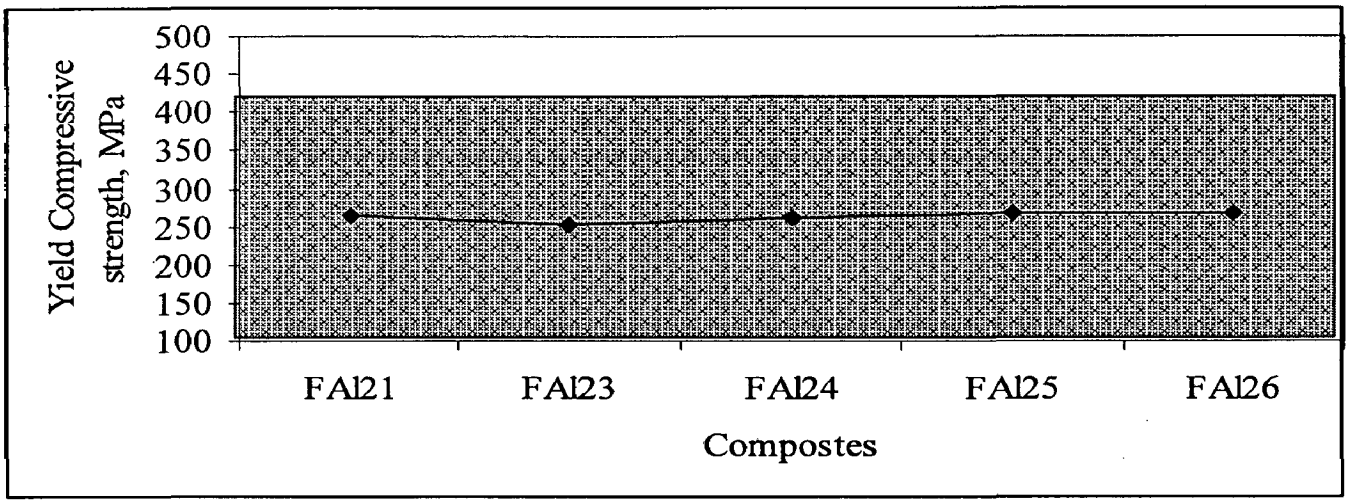

Fig 5.15(c) Compressive strength

5.19.6 Shear strength: Fig. 5.15(d) shows that shear strength of developed Al based composites varies with in a range from 76 to 88 MPa. It is maximum for composite FAl24. Fig. 5.15(d)shows that shear strength of developed Al based composites lies with in a shaded range from 70 to 90 MPa of disc brake materials **(Table 5.28 (b))[150].**

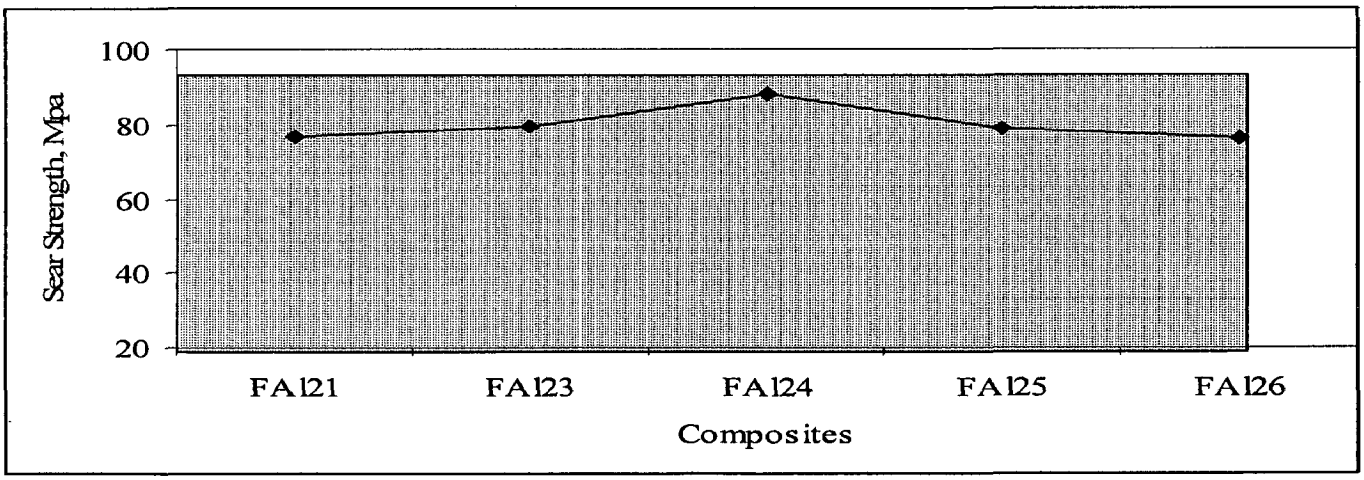

Fig. 5.15(d) Shear strength

5.20 Summary

(i) Mechanical properties for all Al based composites lie with in shaded region which shows the standard range of properties of composites/friction materials are used in different applications.

(ii) Fluctuation in shear modulus of composites is high corresponding to compositions of developed Al based composites.

(iii)Mechanical properties of Al based composites varies with in a short range and these are stable correspond to alternating of compositions.

5.21 Metallographic examination

Metallographic examinations of selected developed Al based friction materials/composites are categorized in namely i) SEM with EDAX analysis (fig. 5.16) ii) X-Ray mapping (fig. 5.17) and iii) optical microscope examination(Fig. 5.18).

5.21.1 Metallographic examination of friction, interface and back plate layer of selected developed Al based brake pads

Selected samples of Al brake pads were microscopically examined. Microstructures of selected developed samples FAl21, FAl23, FAl24, FAl25 and FAl26 were recorded at the magnification of 200X. These samples were polished to study the distribution of graphite, Al and SiC using optical microscope (shown by fig. 5.18 (i-v)). No etching was performed to ascertain void distribution at the polished surface. Three locations were identified for each samples namely friction layer, interface and backing plate. In all the cases, backing plate contains Al with 30 wt. % of fine (50μm) SiC and therefore the structure is very uniform with Al as white matrix and SiC as shaded particles. The interface in all the cases is distinctly visible as the boundary of friction layer with coarse distribution of graphite and Al on one side and backing plate with finely distributed SiC particles and Al on the other side, however the interface is somewhat diffused having combination of both fine and coarse features. This is indicative of a sound interface free of any cracks, discontinuities etc. It is therefore expected that bonding between friction layer and backing plate will be sound and chances of failure by separation will be slim. Friction layer consists of largely continuous coarse Al matrix separated by coarse graphite flakes. Occasionally few yellow colored particles also appear in the friction material which is probably a Cu phase. Their revelation has been highlighted by adjusting the contrast and intensity of the image and recorded pictures separately. SiC particles in friction material are embedded in the regions of graphite flake and are visible but could not be recorded in microstructures. Different phases as mentioned above are also marked in microstructures.

In order to get the detailed information about different constituents EDAX analysis was also performed including their micro-analysis (shown by fig. 5.16 (i-v)). For this fractured samples containing backing plate at one side and friction layer at other were extracted from finished brake pads. Here also three fields were chosen one consisting of friction layer, the other one consisting of interface between backing plate and friction layer and the third consisting of backing plate alone. Figure 5.17(i-v) provide micro-analysis report of friction material, interface and backing plate respectively corresponding to each of FAl21, FAl23, FAl24, FAl25 and FAl26, simultaneously from FAl21 to FAl26 shows X-rays mapping (fig. 5.17) of different element and their combination from above samples. The common observation about

these samples is that Cu is present as an impurity; SiC is very uniformly and finely distributed in region of backing plate however, it is occasionally present in friction layer as relatively coarse constituents. Graphite is also coarse in the form of flakes. Barium sulphate ($BaSO_4$) and antimony tri sulphide (Sb_2S_3) as well as zinc spots are present in friction layer only because they were not mixed with backing plate material. This way EDAX analysis confirms (fig.5.16 (i-v)) our expectation with reference to friction layer and backing plate. The distribution of their phases is as per our expectation. Except Cu, there are no unusual features observed. Presence of Cu is possibly due to impurity in Al powder as raw material.

Microanalysis report of the samples should be treated as relative only and not absolute because the analysis is field specific limited to a narrow area.

The micro examination as given above has been done for expected samples and has been also done for selected samples and it is expected that all these samples are similar in their constituents since they consist of gradual chemistry variation and all of them have been processed commonly.

All the samples appear to be fully dense with no trace of porosity. Obliviously because they have been hot forged. Differences in apparent density are on account of chemistry variations of samples.

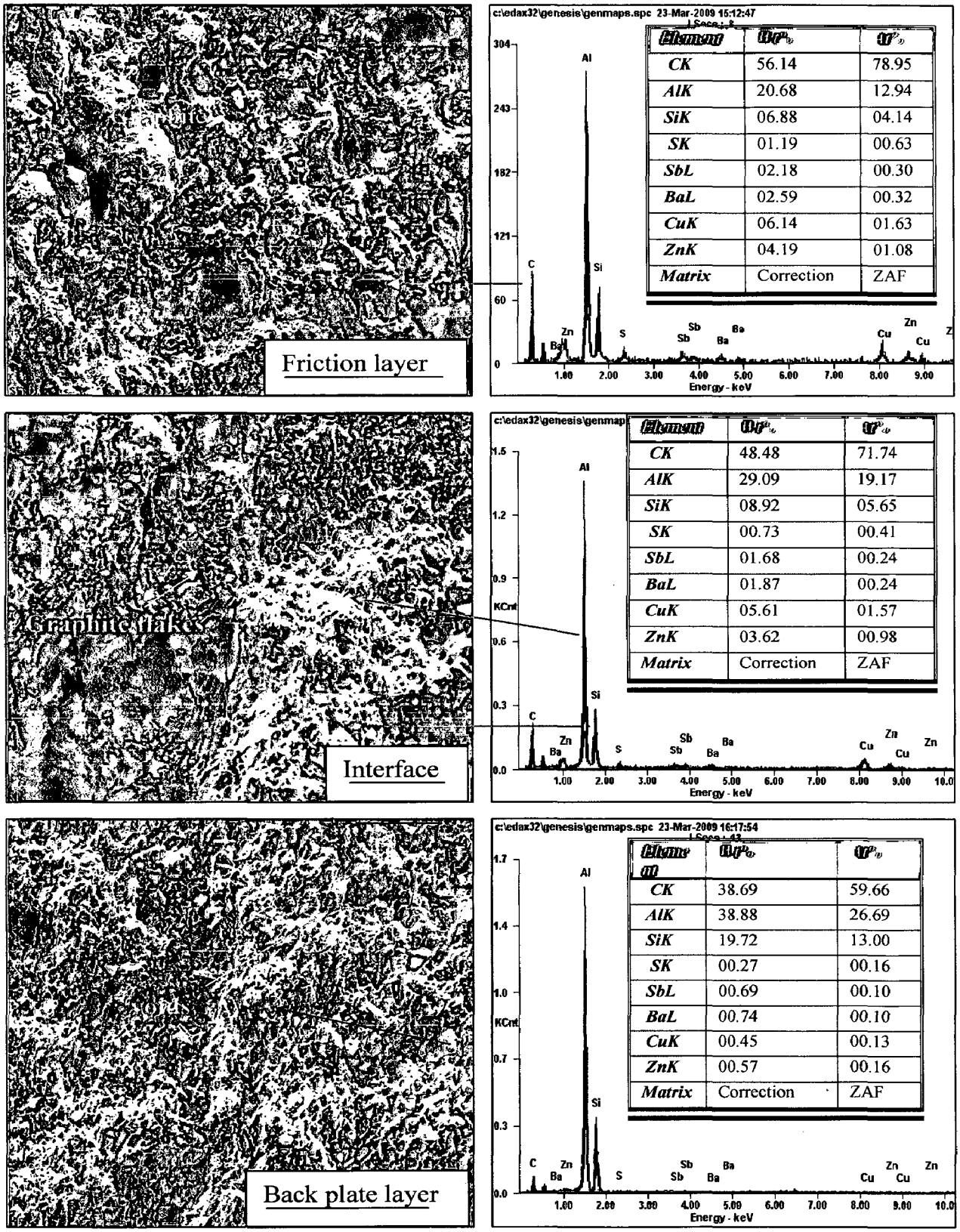
Friction layer
Graphite flakes
Interface
Back plate layer
Energy - keV

Fig. 5.16(i)

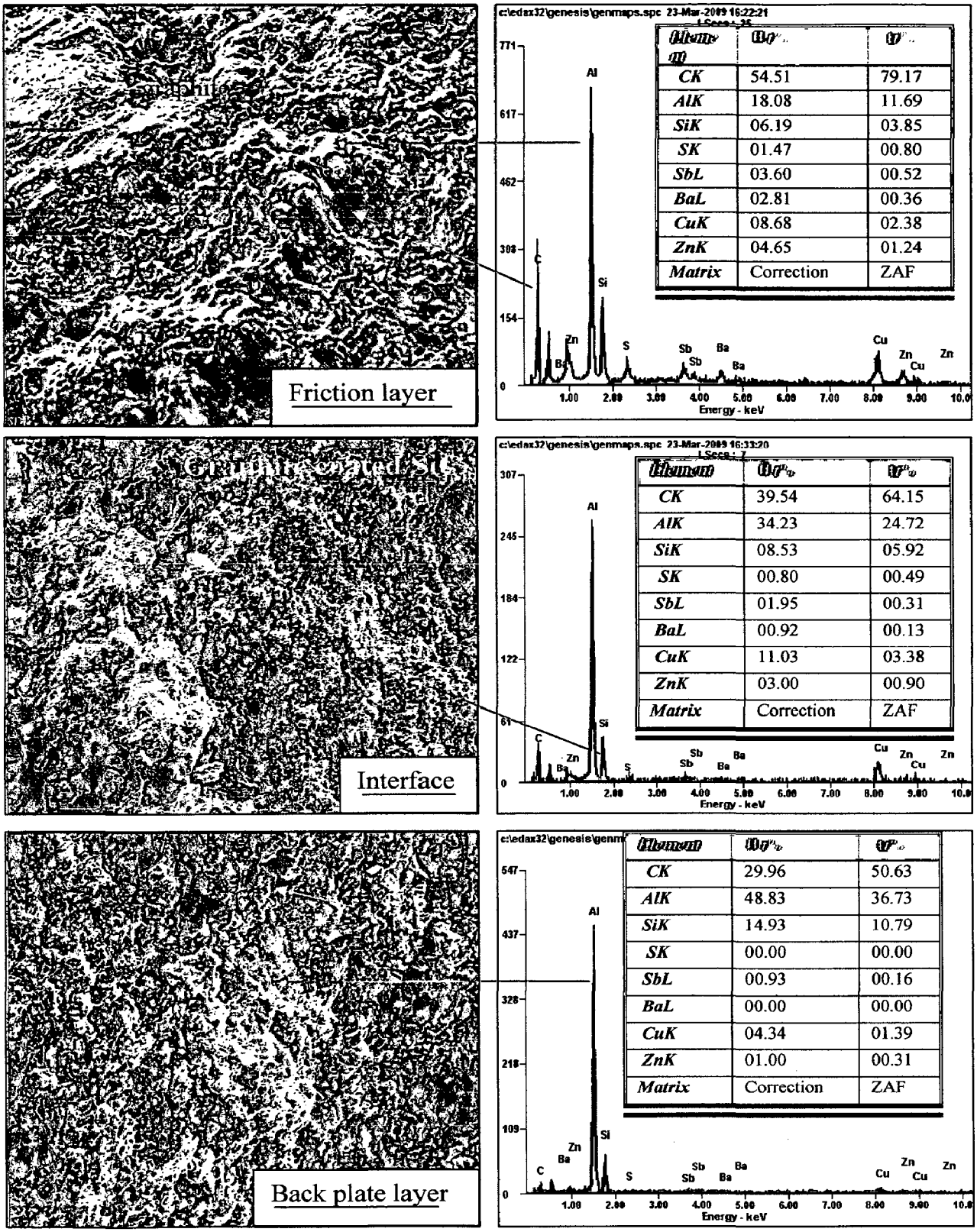

Fig. 5.16(ii)

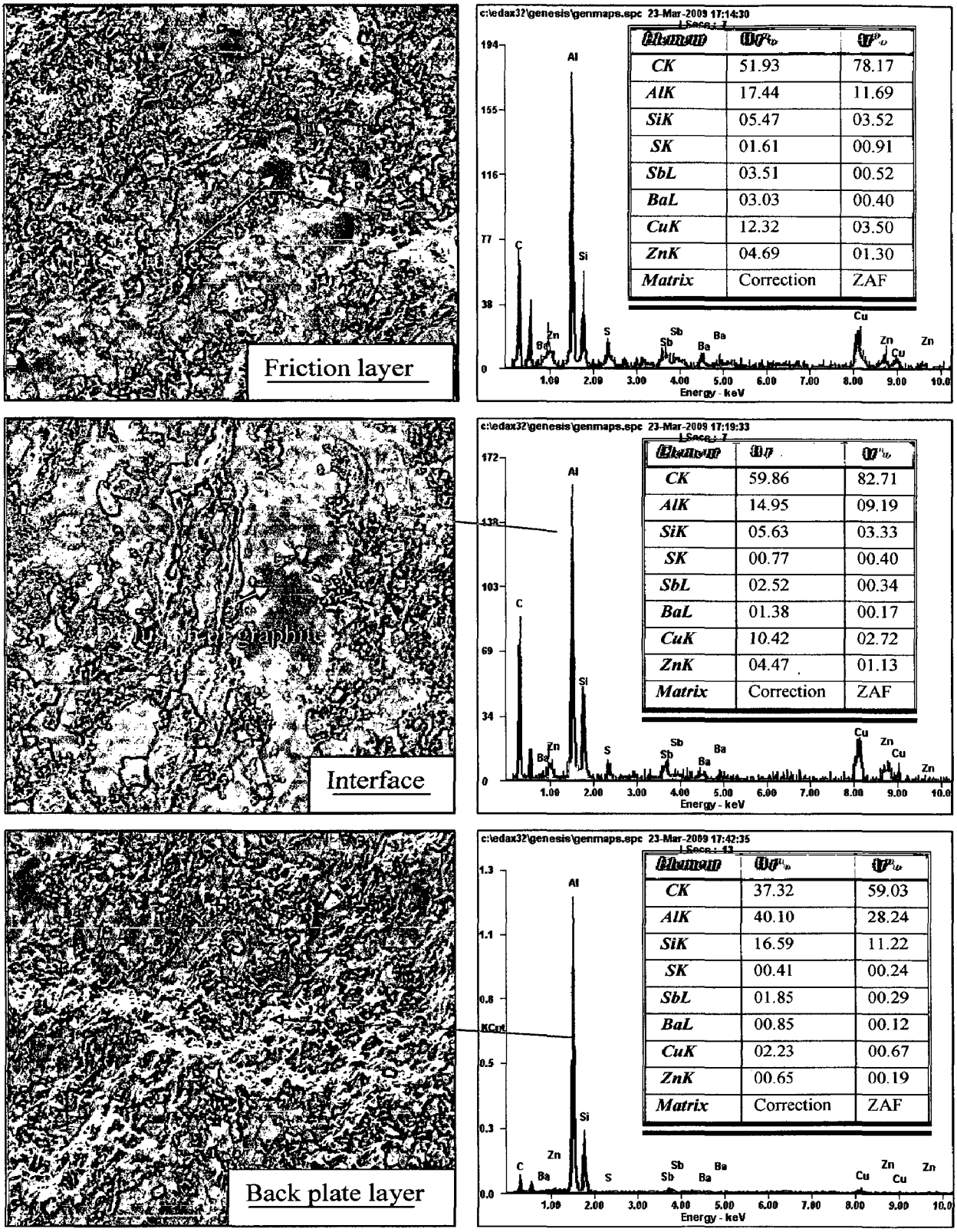
Friction layer
c:\edax32\genesis\genmaps.spc 23-Mar-2009 17:14:30
Element | Wt% | At%
CK | 51.93 | 78.17
AlK | 17.44 | 11.69
SiK | 05.47 | 03.52
SK | 01.61 | 00.91
SbL | 03.51 | 00.52
BaL | 03.03 | 00.40
CuK | 12.32 | 03.50
ZnK | 04.69 | 01.30
Matrix | Correction | ZAF
Energy - keV
Interface
c:\edax32\genesis\genmaps.spc 23-Mar-2009 17:19:33
Element | Wt% | At%
CK | 59.86 | 82.71
AlK | 14.95 | 09.19
SiK | 05.63 | 03.33
SK | 00.77 | 00.40
SbL | 02.52 | 00.34
BaL | 01.38 | 00.17
CuK | 10.42 | 02.72
ZnK | 04.47 | 01.13
Matrix | Correction | ZAF
Energy - keV
Back plate layer
c:\edax32\genesis\genmaps.spc 23-Mar-2009 17:42:35
Element | Wt% | At%
CK | 37.32 | 59.03
AlK | 40.10 | 28.24
SiK | 16.59 | 11.22
SK | 00.41 | 00.24
SbL | 01.85 | 00.29
BaL | 00.85 | 00.12
CuK | 02.23 | 00.67
ZnK | 00.65 | 00.19
Matrix | Correction | ZAF
Energy - keV

Fig. 5.16(iii)

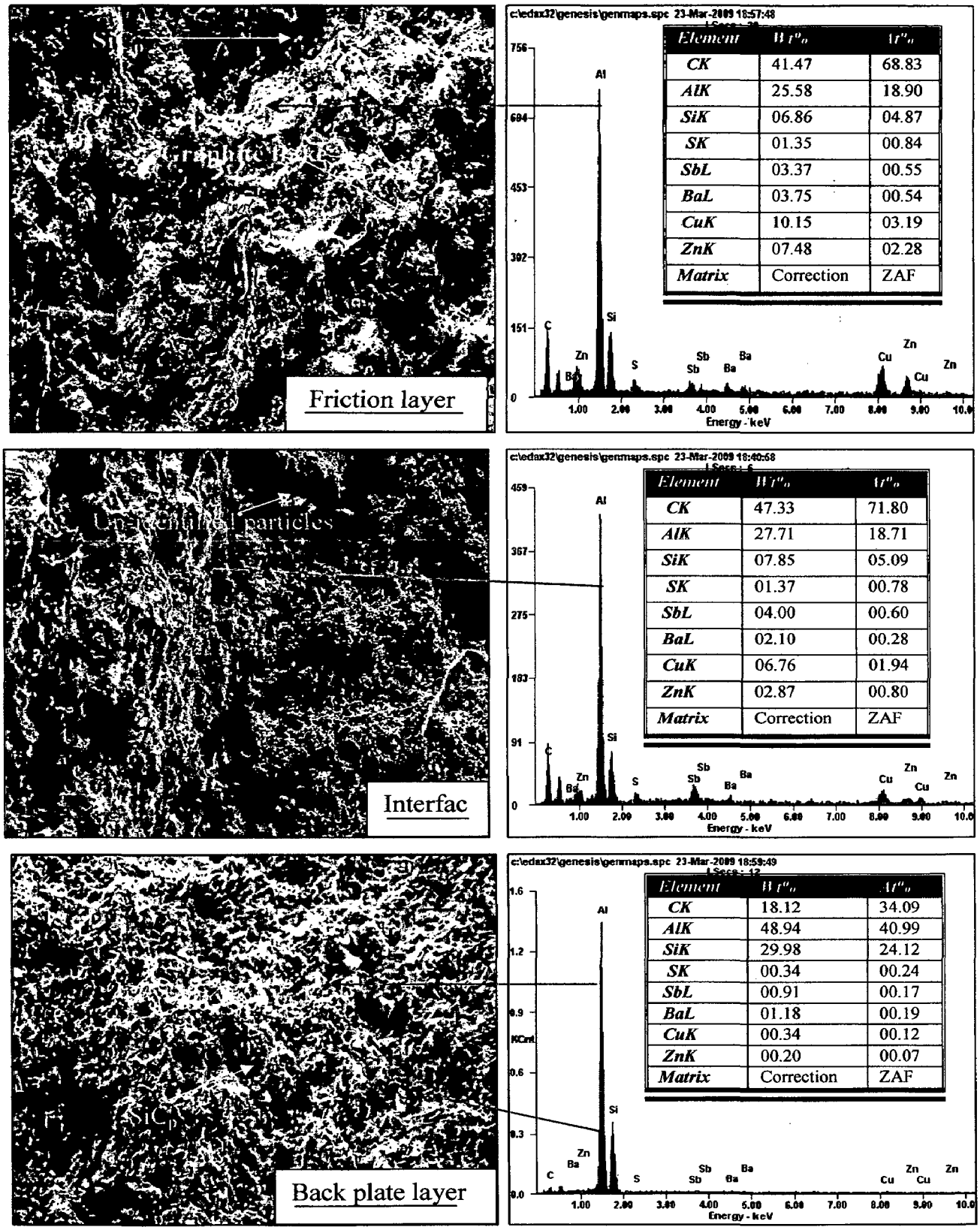

Element	Wt%	At%
CK	41.47	68.83
AlK	25.58	18.90
SiK	06.86	04.87
SK	01.35	00.84
SbL	03.37	00.55
BaL	03.75	00.54
CuK	10.15	03.19
ZnK	07.48	02.28
Matrix	Correction	ZAF

Element	Wt%	At%
CK	47.33	71.80
AlK	27.71	18.71
SiK	07.85	05.09
SK	01.37	00.78
SbL	04.00	00.60
BaL	02.10	00.28
CuK	06.76	01.94
ZnK	02.87	00.80
Matrix	Correction	ZAF

Element	Wt%	At%
CK	18.12	34.09
AlK	48.94	40.99
SiK	29.98	24.12
SK	00.34	00.24
SbL	00.91	00.17
BaL	01.18	00.19
CuK	00.34	00.12
ZnK	00.20	00.07
Matrix	Correction	ZAF

Fig. 5.16(iv)

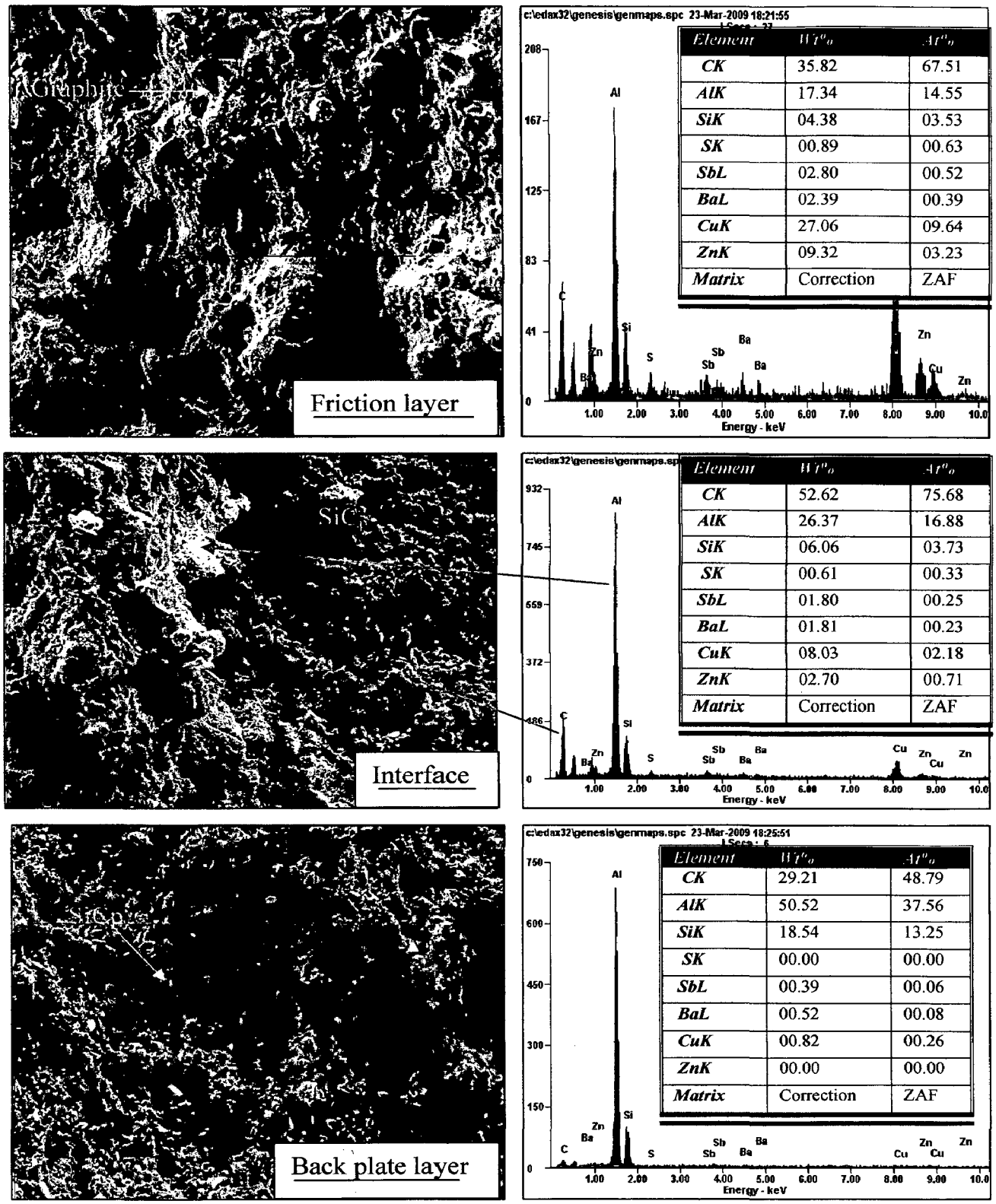

Fig. 5.16 EDX analysis of fractured selected developed Al based friction composites i) FAl21 ii) FAl23. iii) FAl24 iv) FAl25 and v) FAl26 at 200X

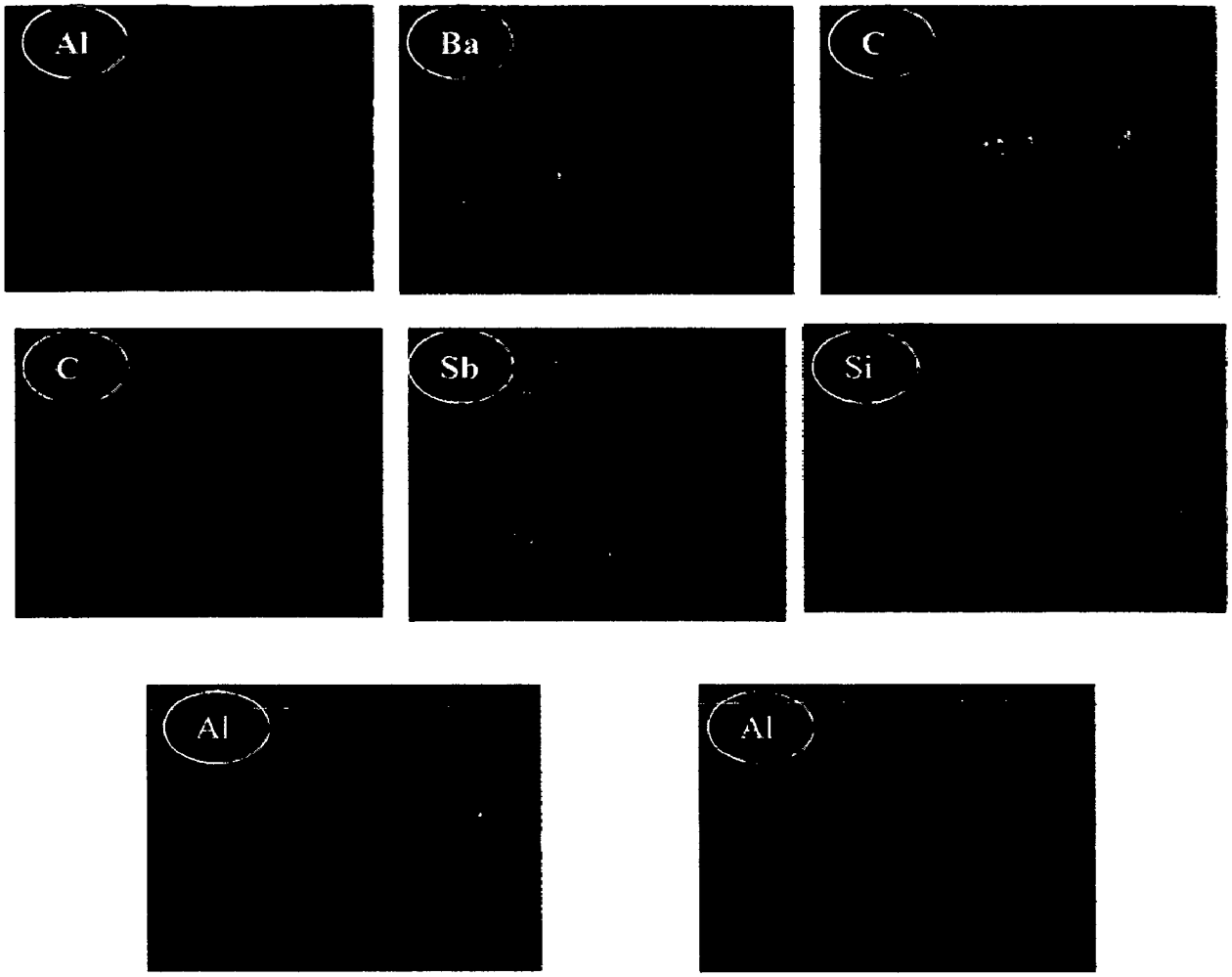

Fig. 5.17(a)(i) Mapping of different constituents

Fig. 5.17(b)(i) Overlapping of maps of different constituents

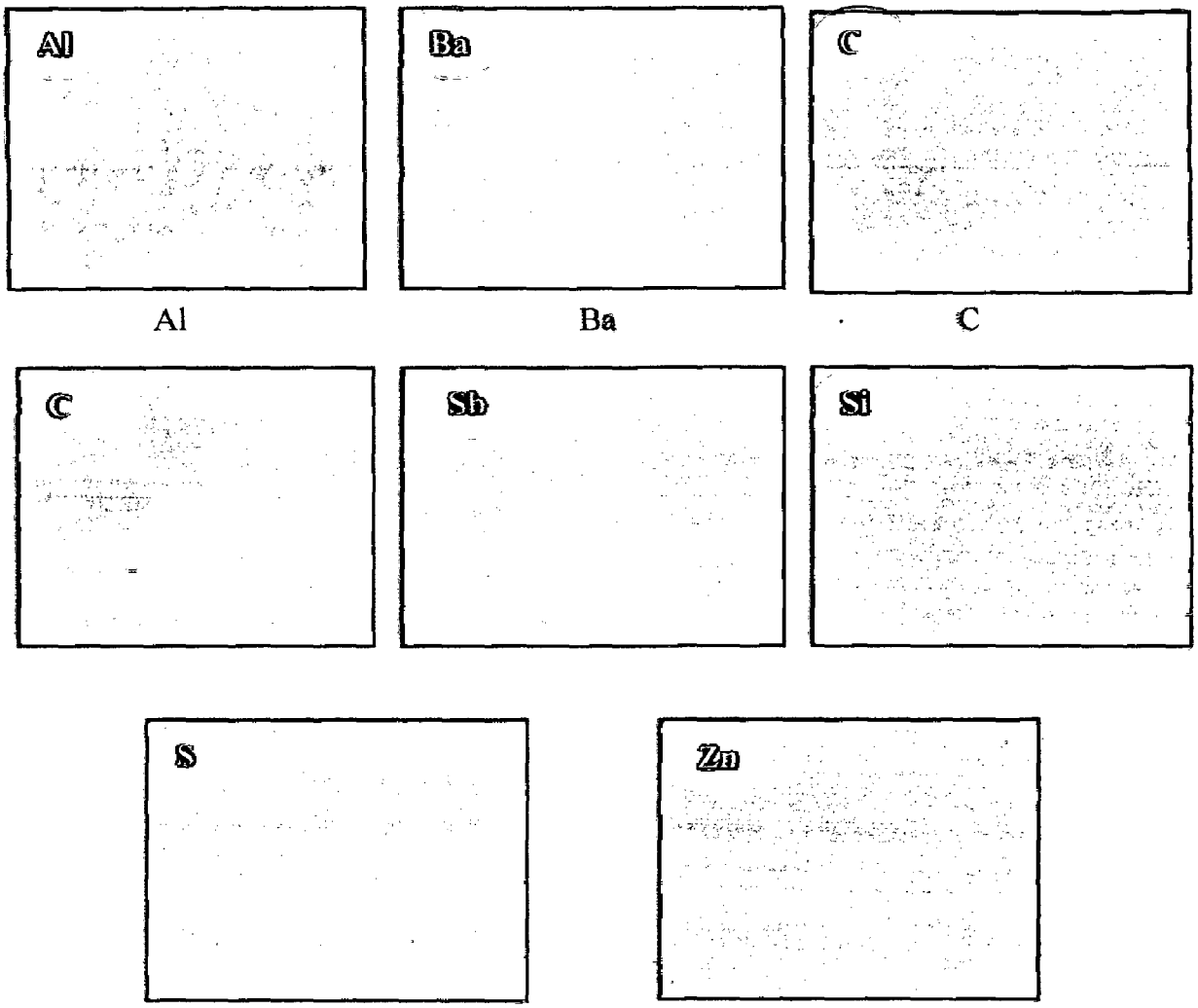

Fig. 5.17(a)(ii) Mapping of different constituents

Fig. 5.17(b)(ii) Overlapping of maps of different constituents

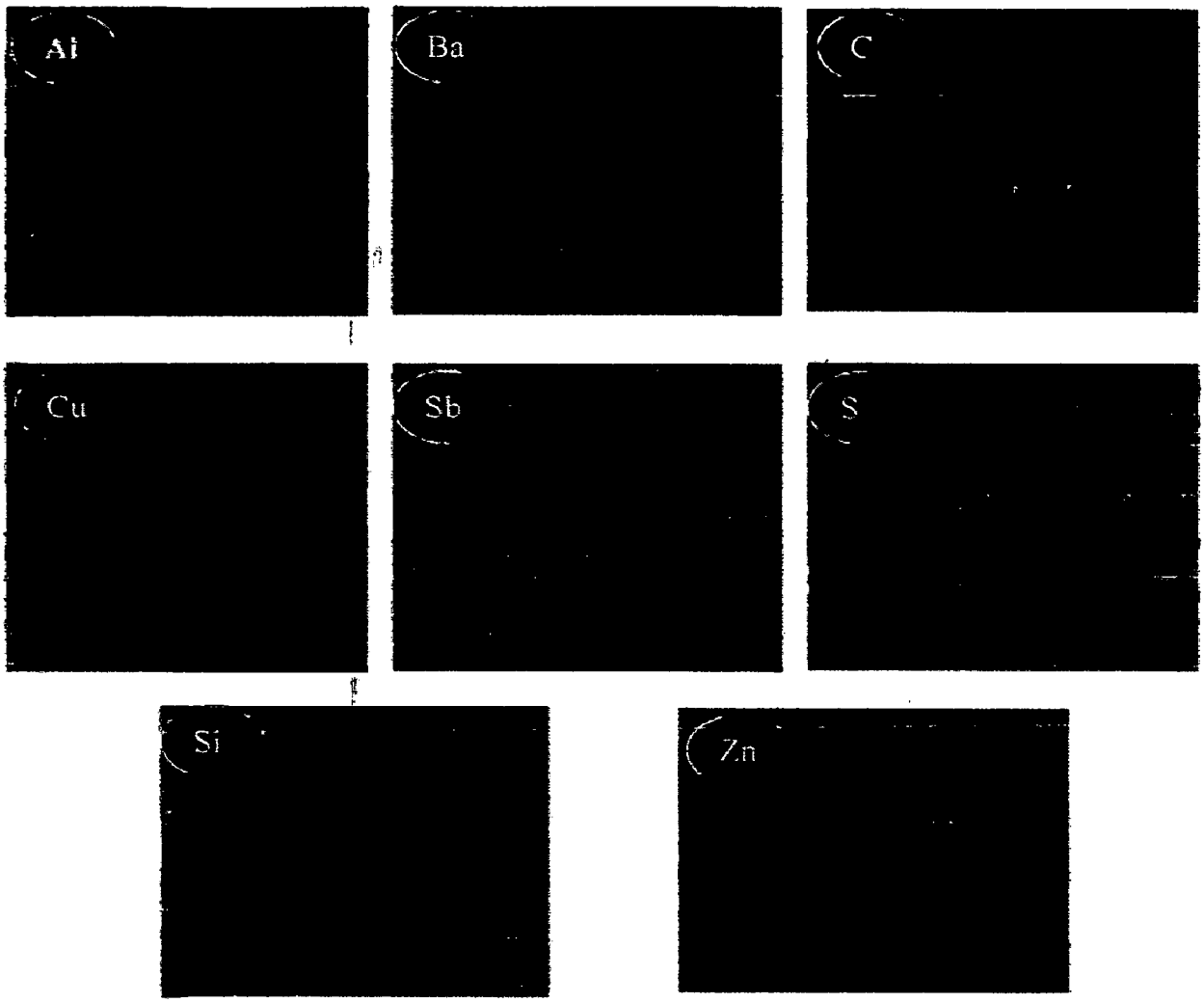

Fig. 5.17 (a)(iii) Mapping of different constituents

Fig. 5.17 (b)(iii) Overlapping of maps of different constituents

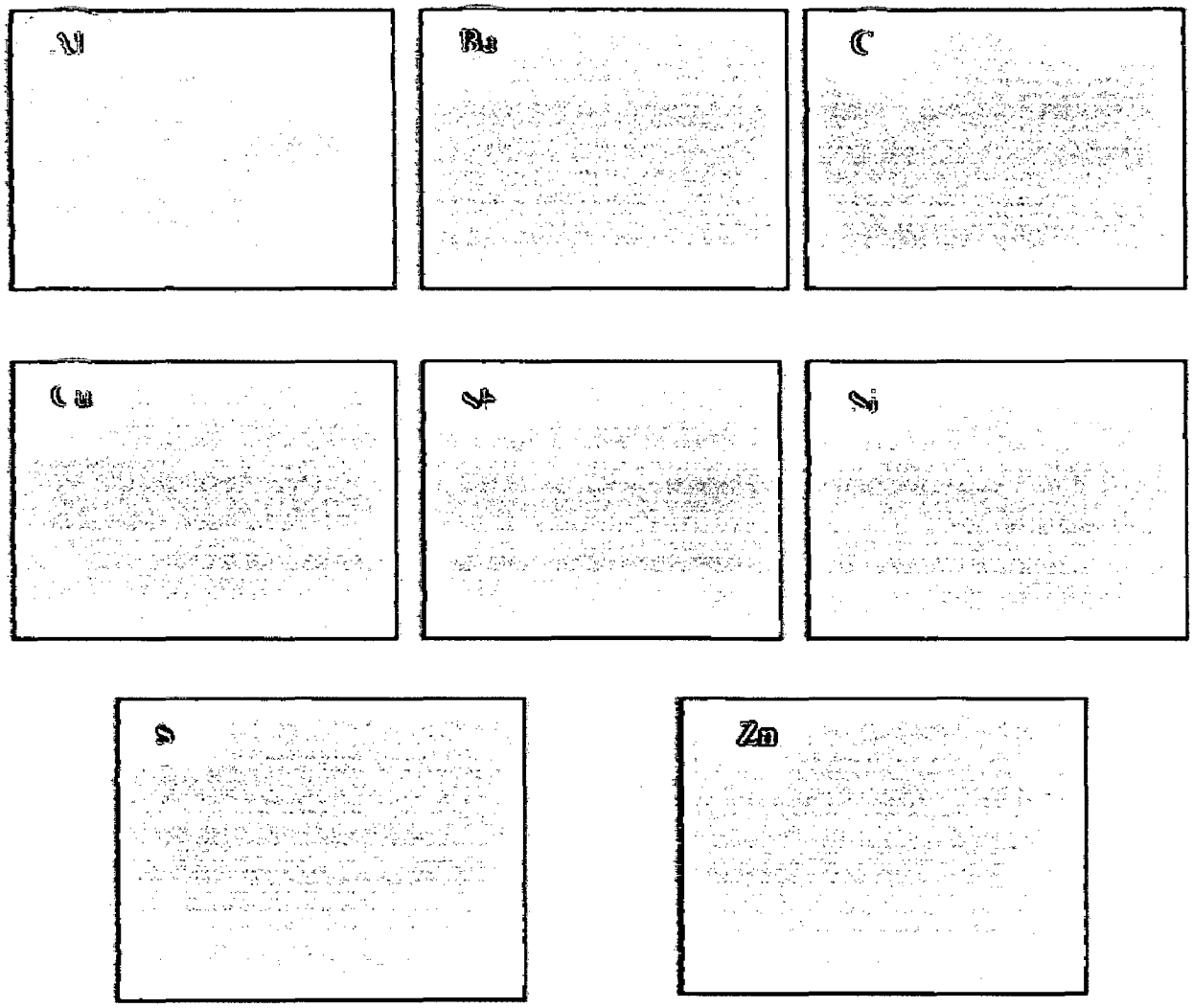

Fig. 5.17 (a)(iv) Mapping of different constituents

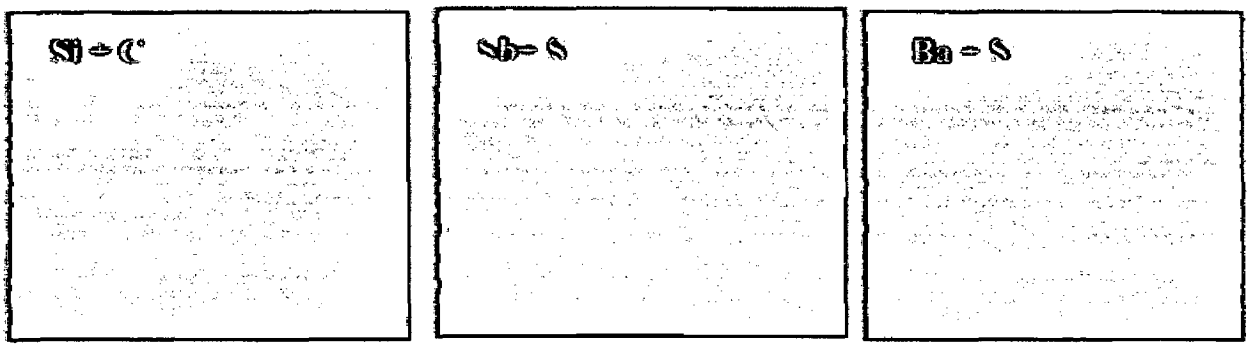

Fig. 5.17 (b)(iv) Overlapping of maps of different constituents

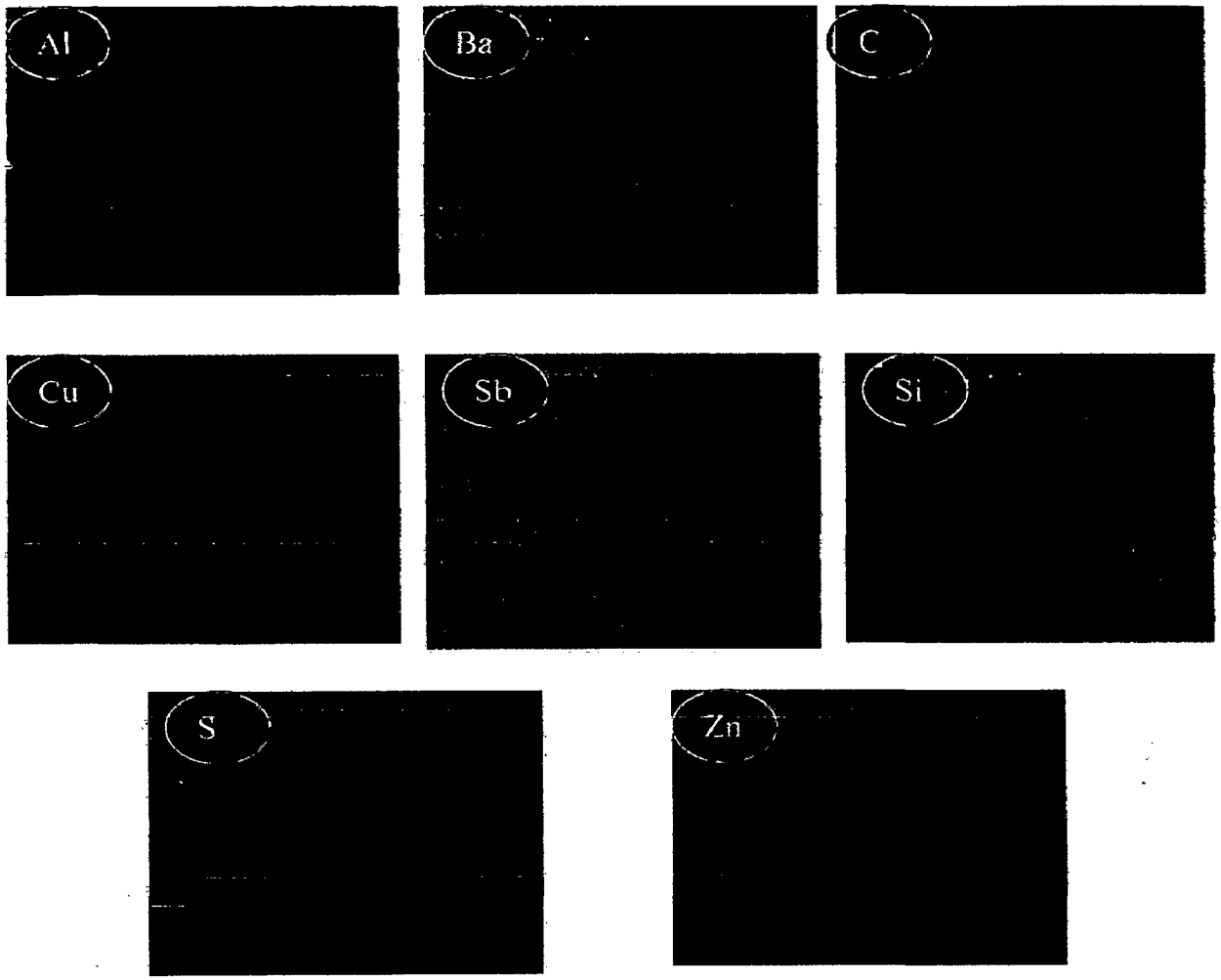

Fig. 5.17 (a)(v) Mapping of different constituents

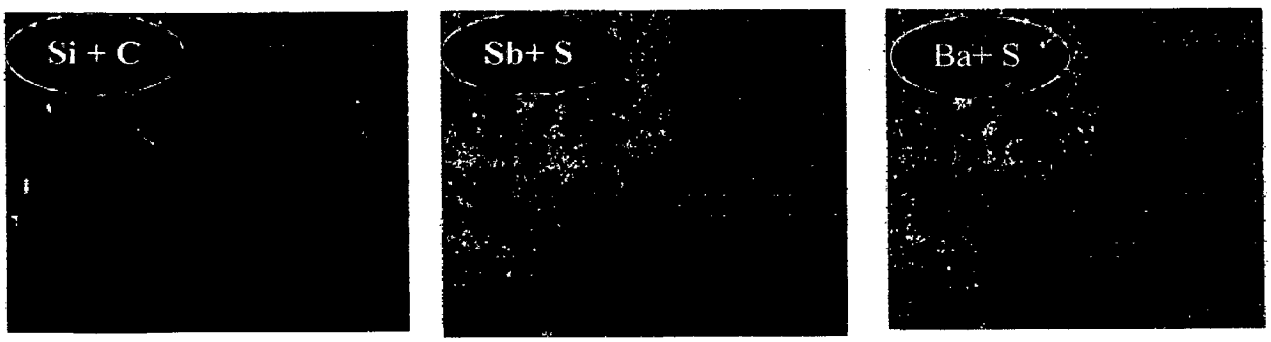

Fig. 5.17 (b)(v) Overlapping of maps of different constituents

Fig. 5.17 X-Ray Mapping of fractured selected developed Al based friction composites i) FAl21 ii) FAl23. iii) FAl24 iv) FAl25 and v) FAl26 at 200X

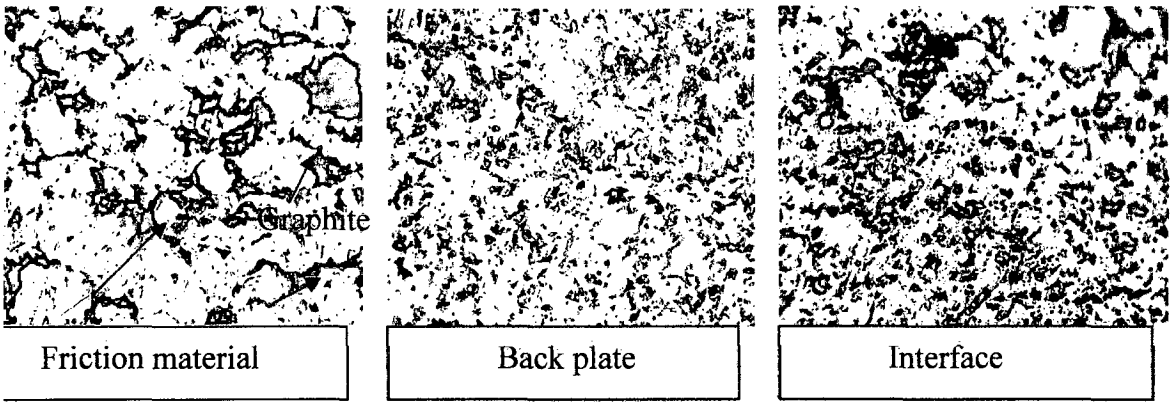

Fig. 5.18(i)

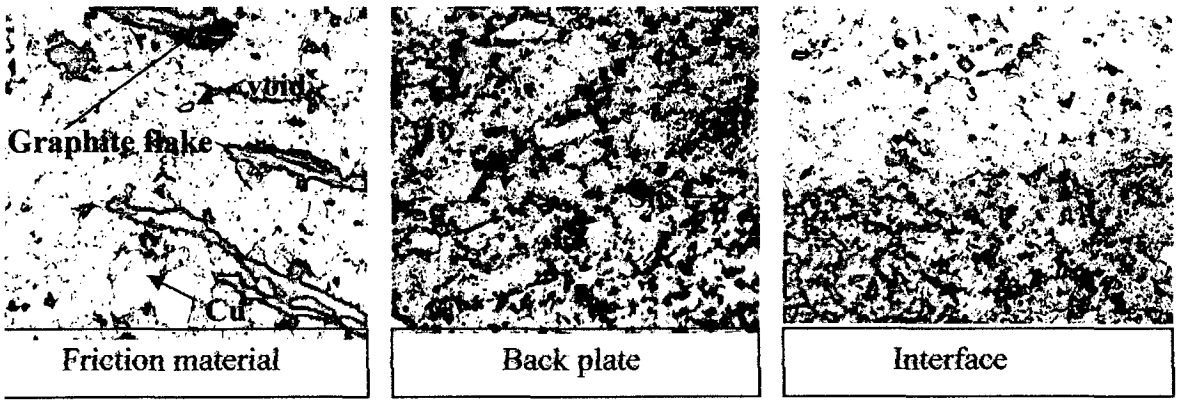

Fig. 5.18(ii)

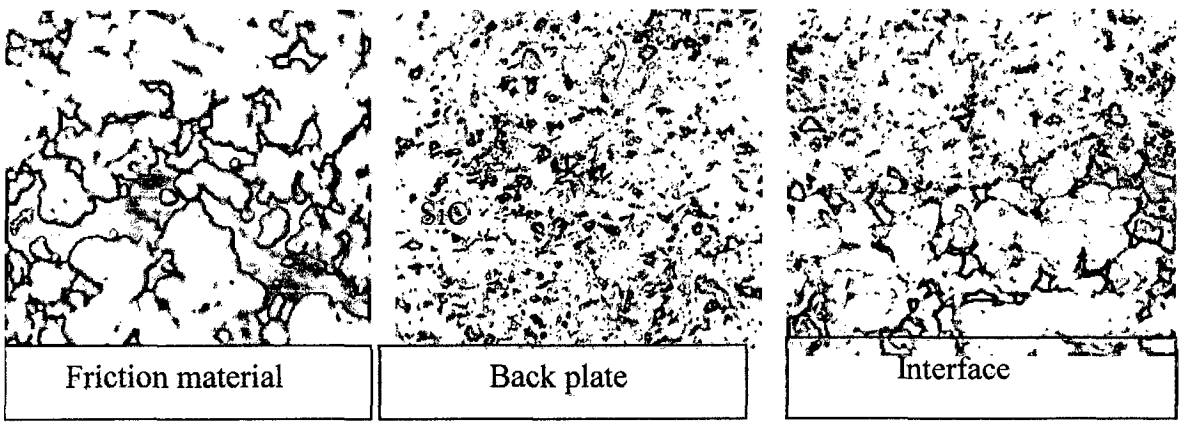

Fig. 5.18(iii)

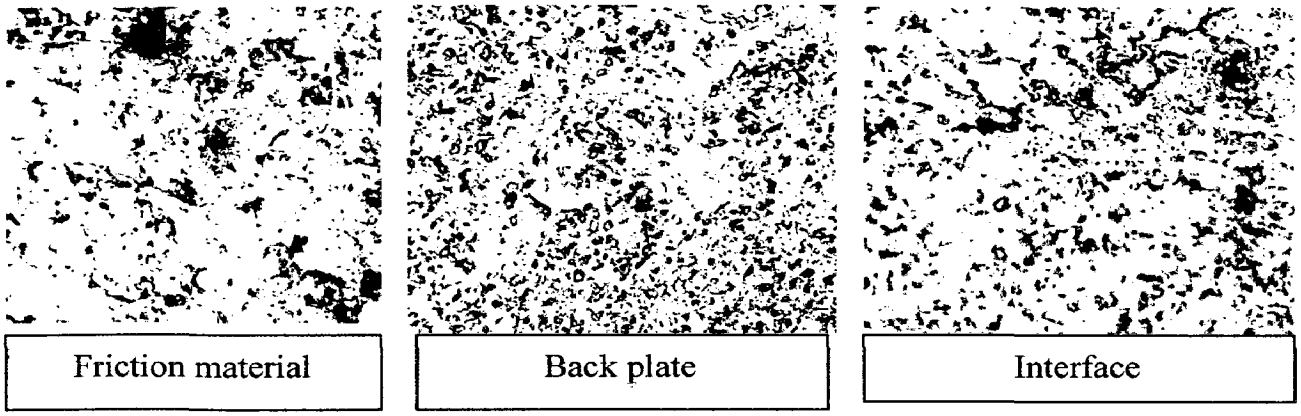

Fig. 5.18(iv)

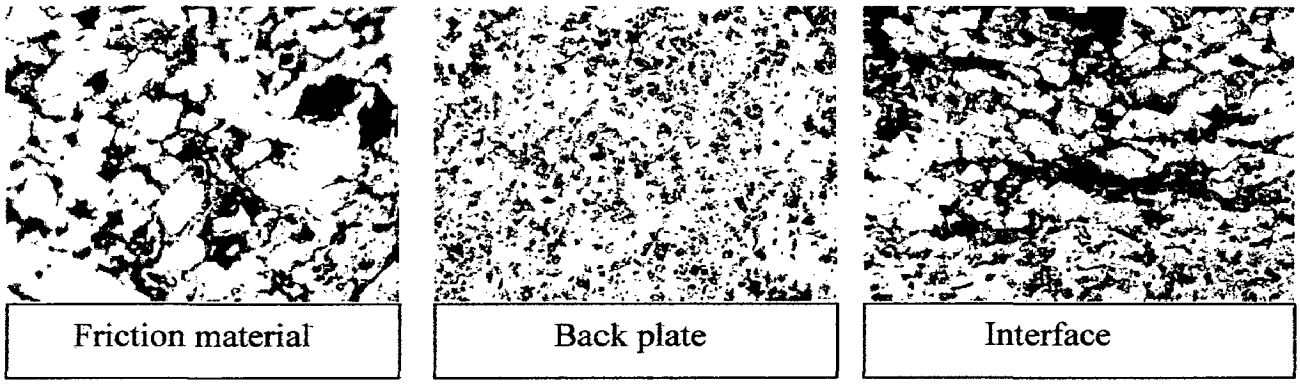

Fig. 5.18(v)

Fig. 5.18 Optical micrographs of polished surface of friction material, back plate material and interface of friction and backing plate material of developed Al based composites i) FAl21 ii) FAl23. iii) FAl24 iv) FAl25 and v) FAl26 at 200X

5.22 The choice of processing technology

In the present investigation, Al friction pads were made for first time by employing **"Preform Hot Powder Forging"** technology as described in chapter 4. However no justification for its choice has been provided till now for the simple reason that sufficient literature was not available on this processing method during the course of literature review. Now it is apt, having described the results as above to justify our expectations, to elaborate on the choice of this processing technology.

First and foremost Al pads can only be made employing powder route because large quantity of non-metallic constituents including ceramics are involved in their manufacture. Therefore, powder route is only option for their manufacture.

Sondly joining of backing with friction element is the biggest challenge involving Al as matrix. So it was decided to employ strong Al powder based backing plate as a composite layer over

which Al based friction layer of differing chemistry would be placed. Both need to be compacted simultaneously with proper adjustment of thickness of each layer. This way, problem of joining with adequate adhesion is sorted out.

Thirdly sintering of Al based material always leads to poor densification, resulting in increased porosity whereas friction materials should have as low porosity as possible. Therefore choice of sintering route is ruled out for manufacturing of brake pads.

Accordingly **"Preform Hot Powder Forging"** technology is the only option left to process these products to simultaneously achieve:

1. Zero level porosity in friction material
2. Adequate joining of backing plate to friction element
3. Fabrication of tough and strong Al based backing plate

The need for a controlled atmosphere (inert/reducing) is eliminated. Two-step forging, namely cold consolidation of powder for getting a green preform and subsequent hot forging of heated powder preform to net shape of sufficient density.

The results reported above amply justify that the processing technology chosen in present investigation is most suitable for manufacturing Al based brake pads covering a wide range of applications from automobiles to aircrafts.

Chapter 6

CONCLUSIONS AND SUGGESTIONS

6.1 Conclusions

The present investigation has been primarily focused to develop an alternative technology for the manufacture of brake pads for light to heavy-duty automobiles and AN-32 aircraft and to characterize the quality of the developed pads against conventionally used phenolic- resin/sintered products. This primary objective has been successfully achieved and it can be reasonably concluded that this investigation has seeded the development of Al based brake pads for the first time using an alternative processing route.

The detailed significant achievements have been listed as follows, chronologically, in accordance with objectives:

(i) 'Preform Hot Powder Forging' technology for the manufacturing of friction materials overcoming the limitations of sintering process has been successfully developed for the first time.

(ii) Inert/vacuum/reducing environments associated with conventional sintering and secondary processes have been completely eliminated.

(iii) The technology overcomes the problems of joining between backing plate and friction element because of simultaneous application of pressure and temperature.

(iv) Temperature rise range is lowest ($\approx$ 40-200^{0}C) in comparison to iron based and resin based brake pads.

(v) Coefficient of friction can be adjusted to cover a wide range of applications.

(vi) Weight per pad of developed Al based brake pad material is about 40% less than resin based materials whereas for AN-32 aircraft, it is 60 % less than Fe based brake pads currently being used.

(vii) Developed Al based brake pad material is most economical because it can also be used for fabrication of brake rotor after recycling.

(viii) Detailed characterization of brake pads developed in the present investigation and their comparison with sintered counterpart has led to possible substitution in actual application.

(ix) Overall performance of the product made by 'Perform Powder Forging' technology has led to significant improvement in quality in comparison to existing sintering technology.

(x) Significant reduction in mass/pad is shown in **Table 6.1.**

Table 6.1 Mass reduction per brake pad

Materials	Brake pad weight , gm		Mass reduction, %	
	Marutee-800	AN-32	Marutee-800	AN-32
Al	150	95	-	-
Fe	250	150	67	67
Resin base	190	-	27	-

6.2 Suitability of developed Al based brake pads for different applications

Based on detailed investigations, following compositions are suitable for given applications follows **(Table 6.2)**:

Table 6.2 Suitability of developed Al based brake pads

Applications	*Preference and suitability of chemistry on the basis of over all tribo-performance for braking elements*
Aircrafts-AN-32	*FAl28>FAl30>FAl29>FAl26*
Tractors	*FAl23>FAl24>FAl25=FAl21*
Racing cars	*FAl21>FAl24>FAl25*
Tractors, trucks	*FAl23>FAl24>FAl25=FAl21*
Tractors, trucks, military vehicles	*FAl23>FAl24>FAl25=FAl21*
High speed composite friction materials	*FAl21>FAl24>FAl23*
Railway disc and brake block	*FAl21>FAl25*
Brakes and clutches	*FAl23>FAl24>FAl25=FAl21*
High performance road vehicles	*FAl23>FAl24>FAl25=FAl21*

6.3 Suggestions for future work

Some of the points that emerged during the present investigation need to be further investigated in detail, these are as follows:

(i) To improve the wear resistance of friction layer and strength of back plate with addition of fine/ ultra fine SiC powder in compositions.

(ii) To investigate in detail the role of tribo-layers at brake pad surface and development of a wear map.

(iii) To investigate in detail the performance of graphite and antimony tri sulphide lubricants with respect to coefficient of friction and wear resistance.

(iv) To extend the application of Al based brake pads for high-speed military aircrafts.

PAPERS PUBLISHED/PRESENTED

1. Chaturvedi A. K., Chandra K., Misra P.S. "Characterization of Al/Ingredients MMFC" **Tribology-ASME, 131**, 2009, pp.1-7.

2. Chaturvedi A.K. Chaturvedi, K. Chandra, P.S. Misra "Development and for light/heavy duty applications" presented in **International conference PM'09**, at Goa-INDIA held on Feb. 16-18, 2009.

3. Ghazi A.A.S, Chandra K, Misra P.S., Chaturvedi A.K., Asif M. "Development and characterization of iron based metal matrix composite for brake pads applications" presented in **International conference PM'09**, at Goa-INDIA held on Feb. 16-18, 2009.

4. Chaturvedi A. K., Chandra K., Misra P.S "Wear behavior of al-based friction composites under dry sliding conditions" accepted for presentation in **International conference PM'10**, at Goa-INDIA held on Jan. 28-30 2010.

PATENT FILED

The Patent titled "**Aluminium powder based stator brake pads/discs for light, medium and heavy duty automobiles and the materials thereof**" has been cleared for filing by Intellectual Property Rights Cell, IIT Roorkee, Roorkee.

References

Journals/Books

1. Abouelmagd G., "Hot deformation and wear resistance of P/M aluminium metal matrix composites", Journal of Materials Processing Technology, **155-156,** 2004, pp. 1395-1401.
2. Ahlatci H, Kocer T, Candan E, Cimenoglu H "Wear behavior of Al/(Al_2O_{3p} + SiC_p) hybrid composites", Tribology International, **39**, 2006, pp. 213-2
3. Aigbodian V. S., Hassan S.B., "Effects of silicon carbide reinforcement on microstructure and properties of cast Al-Si-Fe/SiC particulate composites", Material Science and Engineering, **A 447**, 2007, pp. 355-369.
4. Abachi P., Masoudi A., Purazrang K., "Dry sliding wear behavior of SiC_p/QE22 magnesium alloy matrix compodites", Material Science and Engineering, **A435-436**, 2006, pp. 653-657.
5. Aleksandrova A.B., Kryachek V.M., Levit G.B., Rozenshtein D.G., Fedorchenko I.M., Prikhod'ko P. Lzvekov G.V., "Effect of technological factors on the properties of friction materials ii) effect of sintering conditions on the structure and frictional and wear properties of powder metallurgy friction disks", Powder Metallurgy and Metal Ceramics, **11**, No. 10, 1972, pp. 831-833.
6. Alpas A.T. Zhang J., "Wear rate transition in cast aluminum silicon alloys reinforced with SiC particles", Scripta Metallurgica, **26**, 1992, pp. 505-509.
7. Alpas A.T., Embury J.D., "Sliding and abrasive wear behavior of an aluminum (2014)-Sic particle reinforced composite", Scripta Metallurgica, **24**, 1990, pp. 931-935.
8. Alpas A.T., Embury J.D., "Wear mechanisms in particle reinforced and laminated metal matrix composites", Wear of Materials, ASME, New York, **1**, 1991, pp. 159-166.
9. Alpas A.T., H. Hu, Zhang J., "Plastic deformation and damage accumulation below the worn surfaces", Wear, **162-164**, 1993, pp. 188-195.
10. Alpas A.T., Zhang J., "Effect of microstructure (particulate size and volume fraction) and counterface material on the sliding wear resistance of particulate-reinforced aluminum matrix composites", Metall. Trans., **25A**, 1994, pp. 969-983.
11. Alpas A.T., Zhang, J., "Effect of SiC particle reinforcement on the dry sliding wear of aluminum-silicon alloys (A356)", Wear, **155**, 1992, pp. 83-104.
12. Altuzarra Oscar, Amezua Enrique et al., "Judder vibration in disc brakes excited by thermo elastic instability ", Engineering computations, **19**, No. 4, 2002, pp. 411-430.

13. Anand K., Kishore, "On the wear of aluminum-corundum composites", Wear, **85**, 1983, pp. 163-169.

14. Anderson A.E., "ASM hand book", Friction, Lubrication, and wear technology, ASM International, Metal Park,OH, **18**, 1992, pp. 569-577.

15. Andrew W. Batchelor, Gwidon W. Stachowiak, "Tribology in materials processing", Journal of Materials Processing Technology **48**, 1995, pp. 503-515.

16. Archard J.F., "Contact and rubbing of flat surfaces", Journal of Applied. Physics, **24**, 1953, pp. 981-988.

17. Argon A.S., Im J., Safoglu R., "Cavity formation from inclusions in ductile fracture", Metallurgical and Materials Transactions A, **6**, No. 3, 1975, pp. 825-837.

18. Arunachalam V.S, "Powder Metallurgy – Recent advances", Oxford and IBM Publishing Co. Pvt. Ltd., 1989, pp. 156-167.

19. Akhlaghi F., Bidaki-A. Zare "Influence of graphite content on the dry sliding and oil impregnated sliding wear behavior of Al 2024-graphite composites produced by in situ powder metallurgy method", Wear, **266**, 2009, pp. 37-45.

20. Axen N., Alahelisten A., Jacobson S., "Abrasive wear of alumina fiber-reinforced aluminium", Wear, **173**, 1994, pp. 95–104.

21. Babu G., Golla Dheeraj, "Sintered metallic disc brake pads for automobiles", Transactions of PMAI, **34**, 2008, pp. 43-44.

22. Berns H., "Comparison of wear resistant MMC and white cast iron", Wear, **254**, 2003, pp. 47–54

23. Basavarajappa S., Chandramohan G., Subramanian R., Chandrasekar A., ''Dry sliding behavior of hybrid metal matrix composites'', Material. Science, Medziagotyra, **11**, No.3, 2005, pp. 253-257.

24. Bijway J., Nidhi, Majumdar N., Sathapathy B.K., "Influence of modified phenolic resins on the fade and recovery behavior of friction materials", Wear, **259**, 2005, pp. 1068-1078.

25. Bhabani K., Satapathy, Bijwe J., "Wear data analysis of friction materials to investigate the simultaneous influence of operating parameters and compositions", Wear, **256**, Issues 7-8, 2004, pp. 797-804.

26. Bhabani K., Satapathy, Jayashree Bijwe, "Composite friction materials based on organic fibres: Sensitivity of friction and wear to operating variables", Composites: Part A, **37**, Issue 10, 2006, pp. 1557-1567.

27. Bhansali K.J., Mehrabian R., "Abrasive wear of aluminum-matrix composites", Journal of Metals, **34**, issue 9, (Sept. 1982), 30-34

28. Bhanuprasad V.V., Bhat R.B.V., Kuruvilla A.K., Mahajan Y.R., Ramamrishnan P., "Effect of extrusion parameters on structure and properties of 2124 aluminium alloy matrix composites", Materials and Manufacturing processes., **16**,2001, pp. 841-853.

29. Bijwe Jayashree, "Novel green resins for NAO friction composites", Paper presented at second international workshop on advances in asbestos free friction composites (IWAAFC-2) held at IIT-Delhi, on 7-8, Feb 2008. pp. 79-90.

30. Blau Peter J., "Friction science and technology", CRC Press, Taylor and Francis group, Boca Raton Landon, New York, 2009, pp. 345-403.

31. Brechet Y., Embury J.D. Tao, S., Luo L., "Damage initiation in metal matrix composite", Acta Metall., **39**, No.8, 1991, pp. 1781-1786.

32. Bryant D. Michael, Tiwari Atul, Lin Jau-Wen "Wear rate reductions in carbon brushes, conducting current, and sliding against wavy copper surfaces" IEEE Tractions on components, packing, and manufacturing technology-part A, **18**, 1995, pp. 375-381.

33. Cao L., Wang Y., Yao C.K., "The wear properties of a SiC-whisker-reinforced aluminum composite", Wear, **140**, 1990, pp. 273-277.

34. Chan D., Stachowiak G.W., "Review of automotive brake friction materials", Proc. Instn. Mech. Engrs, **218**, Part D: J. Automobile Engineering, 2004, pp. 953-966.

35. Chen M.Y., Breslin M.C., "Friction behavior of co-continuous Alumina/aluminium composites with and without SiC reinforcement", Wear, **249**, 2002, pp.868-876.

36. Cho M.H., Cho K.H., Kim S.J., Kim D.H. , Jang Ho., "The role of transfer layers on friction characteristics in the sliding interface between friction materials against gray iron brake disks", Tribology Letters, **20**, No. 2, 2005, pp 101-108.

37. Cho M.R. Kim, S.J., Basch R.H., Fash J.W., Jang H., "Effects of ingredients on characteristics of brake linings: an experimental case study", Wear, **258**, 2005, pp. 1682-1687.

38. Cho Min Hyung, Jeong Ju, Kim Seong Jin, Jang Ho "Tribological properties of solid lubricants (graphite, Sb_3S_3, MoS_2) for automotive brake friction materials", Wear, **260**, 2006, pp. 855-860.

39. Chichinadze A.V. et al., "Assesment of friction and wear characteristics of domestic friction composite materials in loaded aircraft brakes", Journal of Friction and Wear, **30**, No.4, 2009, pp. 261-270.

40. Czichos H., Molgaard J., "Towards a general theory of tribological systems", Wear, **14**, 1977, pp. 247-264.

41. Dashwood R.J., Schaffer G.B., "Powder forging of a sintered Al-3.8Cu-1mg-0.8Si-0.1 Sn alloy", Material Science and Engineering, **A1323**, 2002, pp. 206-212.

42. Das S, "Cast aluminium based MMC- development of products: an experience" On metal matrix composites, Institute industry interaction, Depatment of metallurgical and materials engg., UOR, Roorkee and regional research laboratory (CSIR), Thiruvanathapuram, October 9, 1999 pp. 41-50.

43. Dautzenberg J.H., Zaat J.H, "Quantitative determination of deformation by sliding wear", Wear, **23**, 1973, pp.9-19.

44. Derkacheva G.M., Panaioti I.I.,"Trends in the compositions and manufacture of friction powder materials(survey)", Powder Metallurgy and Metal Ceramics, **34** No. 3-4, 1995, pp. 207-212

45. Deuis R.L. Subramanian, Yellup J.M.," Dry sliding wear of aluminium composites-A review", Composite Science and Technology, **57**, 1997, pp. 415-435.

46. Ekşi A. and Sarıtaş S. "Effects of Powder Hardness and Particle Size on the Densification of Cold isostatically Pressed Powders", Turkish Journal of Engineering & Environmental Sciences, **26** (5), 2002, pp. 377-384.

47. Eksi A.K., Yuzbasioglu A.H., "Effect of sintering and pressing parameters of cold isostatically pressed Al and Fe powders", Materials and Design, **28**, 2007, pp.1364-1368.

48. Fedorchenko I.M. "Sintered materials for friction units, Powder Metallurgy and Metal Ceramics", **6**, No. 10, 1967, pp. 806-813.

49. Fedorchenko I.M. panaioti I.I., Derkacheva G.M., "Studies of friction materials", Part-1, Powder Metallurgy and Metal Ceramics, **4**, No. 5, 1965, pp. 391-393.

50. Fedorchenko I.M., "Tendencies in creating composite materials for equipping friction assemblies", Powder Metallurgy and Metal Ceramics, **5**, 1992, pp. 44-53.

51. Federal Motor Vekicle Safety Stand.-105, "National Highway Traffic Safety Administration, Department of Transportation", U.S. Government Printing Office, Washington-DC, Chap. V, **1975**.

52. Geiger A.L., Haselman D.P.H., Donaldson K.Y., "Effect of reinforcement particle size on the thermal conductivity of a particulate silicon carbide-reinforced aluminium – matrix composites", J. Material Science Letters, **12**, 1993, pp. 420-423.

53. Geiger A.L., Walker J.A., "Processing and properties of discontinuous reinforced aluminum composites", JOM, **43**, 1991, pp. 8-1.5.

54. Girot F.A., Quenisset J.M., Naslin R., "Discontinuously reinforced aluminum matrix composites", Composite Science and Technology., **30**, 1989, pp. 155-184.

55. Gome G.,, Garcia, "Particles distribution on wear behavior of an Al-Grp composites", Industrial lubrication and tribology , **59**, No.2, 2007, pp. 77-80.

56. Godet M., "The third-body approach: A mechanical view of wear", Wear, **100**, 1984, pp. 437-452.

57. Gopinath, K, The influence of speed on the wear of sintered iron based materials, Wear, **71**, 1981, pp 161-178,.

58. Gurunath P.V., Bijwe J. "Friction and wear studies on brake pad materials based on newily developed resin", Wear, **263**, 2007, pp. 1212-1219.

59. Guerin J.D., Bricout J.P., Laden K., Watremez., "High thermal diffusitivity materials for railway brake discs", Tribology Letters, **3**, 1997, pp. 257-267.

60. Hee K.W. Filip P., "Performance of ceramic enhanced phenolic matrix brake lining materials for automotive brake linings", Wear, **259**, 2005, pp. 1088-1096.

61. H. Jang, Seong Jin Kim, Kim S.J., Basch R.H., Fash J.W. "The effect of metal fibers on the friction performance of automotive brake friction materials" Wear, **256**, 2004, pp. 406-414.

62. Ho T.L., Peteson M.B., "Wear formulation for aircraft brake material sliding against steel", Wear, **43**, 1977, pp. 199-210.

63. Hosking F.M., Folgar Portillo F., Wunderlin R., Merhabian R., "Composites of aluminum alloys: Fabrication and wear behavior", J. Material Science, **17**, 1982, pp. 477-498.

64. Howell G., J., Ball A., "Dry sliding wear of particulate –reinforced aluminium alloys against automobile friction materials", Wear, **181-183**, 1995, pp. 379-390.

65. Hozumi Goto, Claudiu V., Suciu, Takahiro Inokuchi , "Friction and Wear Properties of Aluminum-Silicon Alloy Impregnated Graphite Composite (ALGR-MMC) under Lubricated Sliding Conditions", Tribology Transactions, **52**, Issue 3, May 2009,

66. Hu M.S., "Some effects of particle size on the flow behavior of Al- SiC composites", Scripta Matallurgica, **25**, 1991, pp. 695-700.

67. Huang Scott Xaiaodi, Paxton Kip, "A macrocomposite Al brake rotor for reduced weight and improved performance", JOM, **part IV**, 1998, pp. 26-28.

68. Huber T, Degischer H.P., Lefranc G., Schmitt T., ''Thermal expansion study on aluminium-matrix composites with different reinforcements architecture on Sic particles'', Composite Science and technology, **66**, 2006, pp. 2206-2217.

69. Hunt W.H., Brockenbrough J.R., Magnusen P.E, "An Al-SiC-Mg composite model system: Microstructural effects on deformation and damage evolution", Scripta Matallurgica, **25**, 1991, pp.15-20.

70. Hutchings I.M., "Tribological properties of metal matrix composites", Materials Science and Technology, **10**, 1994, pp. 513-517

71. Hutchings I.M., "Mechanisms of wear in powder technology: A review", Powder Technol., **76**, 1993, pp. 3-13.

72. Hutchings I.M., "Tribology-Friction and Wear of Engineering Materials", CRC Press, Boca Raton London, FL, 1992, pp. 503-515-240.

73. Jacko M.G., Tsang H.S., Rhee U.S., "Automotive friction materials evolution during the past decade", Wear, **100**, 1984, pp. 503-515.

74. Jiang J., Ma A., Liu H., Tan R., "The wear properties of an alumina-aluminosilicate fiber hybrid reinforced Al-Si alloy in a lubricated condition", Wear, **171**, 1994, pp. 163-168.

75. Jokinen A., Anderson P., "Tribological properties of PM aluminum alloy matrix composites", Annual Powder Metallurgy Conf. Proc., Metal Powder Industries Federation, American Powder Metallurgy Institute, Princeton, NJ, 1990, pp. 517-530.

76. Joaquin Aguilar-Santillan., "Wetting of Al_2O_3 by Molten Aluminium:The influence of $BaSO_4$ additions", Journal of Nanomaterials., **2008**, , 2008, pp. 1-12.

77. Kato K., "Classification of wear mechanisms/models", Proc Instn Mech Engrs **216**, 2002, pp. 349-355.

78. Kennedy F.E., "Thermal and thermomechanical effects in dry sliding", Wear, **100**, 1984, pp. 453-476.

79. Kim Seong Jin., "Complementary effects of solid lubricants" Tribology International, **40**, 2007, pp. 15-20.

80. Kozama Mihaly, "Friction and wear of aluminium matrix composite", National Tribology conference, ROTRIB'03, GALATI, **24-26**, September, 2003, pp. 99-106.

81. Kragel'skii V., Silin Ao A., 'The design of low-wear friction materials, Powder Metallurgy and Metal Ceramics, **5**, No. 2, 1969, pp 245-248.

82. Krishnadas C.G., Dutta D., Mohan G., "Development of Metalloceramic Friction Materials for aircrafts brake", published in proceedings (ISBN 0-87339-251-5) of International Conference on Advanced Composites: Advanced Composites 93, held on Feb. 15-19 at Woolongong (Australia), 1993, pp. 61-67.

83. Kumar S., Balasubramanian V., "Developing a mathematical model to evaluate wear rate of AA7075/SiCp powder metallurgy composites", Wear, **264**, 2008, pp. 1026-1034.

84. Kwok J.K.M., Lim S.C., "High-speed tribological properties of some Al/SiCp composites; I-Frictional and wear-rate characteristics", Composite Science. and Technology, **59**, 1999, pp. 55–63.

85. Kwok J.K.M., Lim S.C., "High speed tribological properties of some Al/SiCp composites: II wear mechanisms", Composites Science and Technology, **59**, 1999, pp. 65-75.

86. Landheer D., Zaat J.H., "The mechanism of transfer in sliding friction", Wear, 27, 1974, pp. 129-145.

87. Lazarev G.E., "Evaluation of wear resistance of friction materials", Powder Metallurgy and Metal Ceramics, 7, No. 10, 1971, pp. 903-905.

88. Lee C.S., Kim Y.H., Han K.S.., "Wear behaviour of aluminum matrix composite materials", J. Material Science, **27**, 1992, pp. 793- 800.

89. Lee H.L., Lu W.H., Chan S., "Abrasive wear of powder metallurgy: Al alloy 6061-SiC particle composites", Wear, **159**, 1992, pp. 223–231.

90. Lemieux S., Elomari S., "Thermal expansion of isotropic duralcan metal matrix composites", Journal of Materials Science, **33**, 1998, pp. 4381-4387.

91. Lewandowski J.J, Liu C., Hunt W.H., "Effect of matrix microstructure and particle distribution on fracture of aluminum metal matrix composite", J. Material Science, Engineering., **A107**, 1989, pp. 241-255.

92. Lim S.C., Ashby M.F., Brunton J.H., "Wear rate transitions and their relationship to wear mechanisms", Acta Metal., ***35***, No. 6, 1987, pp. 1343- 1348.

93. Li K., Li W., Zhao X., Tu M., ''A study on tribological behavior of Al_2O_3/Al composites at elevated temperature'', Chengdu University of Science and Technology, China, personal communication, 1992.

94. Lloyd D.J., "Aspects of fracture in particulate reinforced metal matrix composites", Acta Metallurgical Material., **39**, No. 1, 1991, pp. 59-71.

95. Lo H.J., Dionne S., Sahoo M., Hawthorne H.M., " s", J. Material Science., **27**, 1992, pp. 5681-5691.

96. Long T.T., Nishimura T., Aisaka T., Ose M., Morita M., "Mechanical properties and wear resistance of 6061 alloy reinforced with a hybrid of Al_2O_3 fibers and SiC whiskers", Trans. Jpn. Inst. Met., **29**, 1988, pp. 920-927.

97. Luciano Afferrante, Paolo Decuzzi, "The effect of engagement laws on the thermomechanical damage of multidisk clutches and brakes", Wear, **257**, 2004, pp 66-72.

98. Ludema K.C., "Introduction to wear", Friction, Lubrication and Wear Technology, ASM International, New York, **18**, 1992, page 1.

99. Luise Gudmand-Heyer, Allan Bach, Georg T. Nielsen, Per Morgen, 'Tribological properties of automotive disc brakes with solid lubricants, Wear, **232**, 1999, pp 168-175.

100. Manoharan M.., Lewandowski J.J, "Crack initiation and growth toughness of an aluminum metal-matrix composite", Acta Metallurgical Material, **38**, No. 3, 1990, pp. 489-496.

101. Martinez M.A., Martin A., Lorca J.L., "Wear of Al-Si alloys and Al-Si/SiC composites at ambient and elevated temperatures", Scripta Metallurgy, **28**, 1993, pp. 207-212.

102. Mazlee M.N., "Fabrication of aluminium composite from recycled automotive component" Research of Aluminium Alloys and Composites, (February 11,2007) pp. 1-6

103. Matejka V., Lu Yafei, Kratosova G., Leskova J., "Efects of silicon carbide in semi-metallic brake materials on friction performance and friction layer formation", Wear, **265**, 2008, pp 1121-1128.

104. Moore M.A., Douthwaite R.M., "Plastic deformation below worn surfaces", Metallurgical and Materials Transactions A, **7A**, 1976, pp. 1833-1839.

105. Miyoshi K. et al., "Adhesion and transition metal in contact with non metallic hard materials", Wear, **77**, **1982**, pp. 253-264.

106. Nair S.V., Tien J.K., Bates R.C., "SiC reinforced aluminium metal matrix composites", International Material Review, **30**, No.6, 1985, pp. 275–290.

107. Natarajan N., Vijayarangan S., Rajendran I., "Wear behaviour of A356/25SiCp aluminium matrix composites sliding against automobile friction material", Wear, **261**, 2006, pp. 812-822.

108. Noguchi M., Fukizawa K., "Alternate materials reduce weight in automobiles", Advanced Material Process, **243**, No.6, 1993, pp. 20-26.

109. Osterle W. Klob H., Urban I., Dmitriev A.I., "Towards a better understanding of brake friction materials" , Wear, **263**, 2007, pp.1189-1201.

110. Ostermeyer G.P., "On the dynamics of the friction coefficient", Wear, **254**, 2003, pp. 852-858.

111. Pan Y.M., Fine M.E., Gheng H.S., "Aging effects on the wear behavior of P/M aluminum alloy SiC particle composite", Scripta Metallurgy., **24**, 1990, pp. 1341-1345.

112. Pan Y.M., Fine M.E., Gheng H.S., "Sliding wear of an alloy SiC whisker composite", Tribologt. Transactions, **35**, 1992, pp. 482-490.

113. Prasad Naresh., "Development and characterization of metal matrix composite using red mud an industrial waste for wear resistant applications", Ph.D. Thesis, Mechanical Engineering department, National institute of technology (Deemed university) Rourkela, India, **2006**.

114. Peterson. M. B, "Advanced in tribo-materials I Achievements in Tribology", Amer, Soc, Mech. Eng., **1**, New York, 1990, pp. 91-109.

115. Panier S, P. Dufrenoy, D. Weichert, "An experimental investigation of hot spots in railway disc brakes", Wear, **256**, 2004, pp. 764-773.

116. Pavlygo T.M., Skhnenko A. V., Serdyuk G.G., "Development of powder material hot forging in the Ukraine", Powder Metallurgy and Metal Ceramic, **39**, 2000, pp.183-194.

117. Peter J. Blau, "The significance and use of the friction coefficient", Tribology International, **34**, 2001, pp. 585-591.

118. Peter J. Blau, Brian C. Jolly, "Wear of truck brake lining materials using three different test methods", Wear, **259**, 2005, pp 1022-1030.

119. Peter J. Blau, Harry M. Meyer, "Case study characteristics of wear particles produced during friction tests of conventional and unconventional disc brake material", Wear, **225**, 2003, pp 1261-1269.

120. Peter J. Blau, Kenneth G. Budinski, "Compositions, functions and testing of friction brake materials and their additives" and use of ASTM standards for wear testing" Wear, **225-229**, 1999, pp. 1159-1170.

121. Peter J. Blau, "Friction science and technology", CRC Press, Taylor and Francis group, Boca Raton Landon, New York, 2009, pp. 345-403.

122. Pramila Bai B.N., Ramasesh B.S., Surappa M. K., "Dry sliding wear of A356Al-SiC, composites", Wear, **157**, 1992, pp. 295-304.

123. Prasad B.K, Das S., " The significance of the matrix microstructure on the solid lubrication characteristics of graphite in auminium alloys", Materials Science and Engineering, **A144**, 1991, pp. 229-235.

124. Prasad S.V., Asthana R., "Aluminium metal-matrix composites for automotive applications: tribological considerations", Tribology Letters, **17**, 2004, pp. 445-453.

125. Prasad S.V., Mecklenburg K.R., "Friction behavior of ceramic fiber-reinforced aluminum metal-matrix composites against a 440C steel counterface", Wear, **162-164**, 1993, pp. 47-56.

126. Prasad S.V., Rohatgi P.K., "Tribological properties of Al alloy particle composites" , J. Met., **39**, 1987, pp. 22-26

127. Rack H.J., "Fabrication of high performance powder-metallurgy aluminum matrix composites", Advance Material Manufacturing Processes, **3**, 1988, pp. 327-358.

128. Rack H.J., "Light-weight, high-performance metal matrix composites", Processing *and* Properties for Powder Metallurgy Composites, The Metallurgical Society, Warrendale, PA, 1988, pp. 155-167.

129. Ramakrishnan N., "An analytical study of strengthening of particulate reinforced metal matrix composites", Acta Metallurgical Material., **44**, No.1, 1996, pp. 69-77.

130. Rawal Suraj, "Metal-matrix composites for space applications", JOM, **53,** No. 4, 2001, pp. 14-17.

131. Ravi K.R., Pai B.C., Pillai R.M., Chakraborty M.," Separation and recovery of Aluminium from aluminium metal matrix composites by salt flux addition" International Symposium of research students on materials science and engineering, December, 20-22, 2004, Department of Metallurgical and Materials Engineering, Indian Institute of Technology Madras, Chennai, pp.1-6.

132. Rhee S.K., M.G. Jacko, P.H.S. Tsang, "The role of friction film in friction, wear and noise of automotive brakes", Wear 146 (1991) 89–97.

133. Rhee S.K., Tsang P.H.S., Wang Y.S. "Friction-induced noise and vibration of disc brakes", Wear, **133**, 1989, pp. 39-45.

134. Riahi A.R., Alpas A.T., " The role of tribo-layers on the sliding wear behavior of graphitic aluminium matrix composites", Wear, **251**, 2001, pp. 1396-1407.

135. Rohatgi P. K., "Metal-matrix composites", Defence Science Journal, **43,** 1993, pp. 323-349.

136. Rohatgi P.K., Liu Y., Ray S., "Friction and wear of metal-matrix composites", Friction, Lubrication and Wear Technology, ASM International, New York, **8**, 1992, pp. 801-811.

137. Roy M., Venkataraman B., Bhanuprasad.V.V., Mahajan Y.R., Sudararajan G., "The effect of particulate reinforcement on the sliding wear behavior of aluminum matrix composites", Metallurgical Transactions, **23A,** 1992, pp. 2833-2847.

138. Ruff A.W., "Considerations on data requirements for tribological modeling", Tribological Modeling for Mechanical Designers, ASTM, Philadelphia, PA, **1991,** pp. 127-142.

139. Rules and regulations standard for exposure to asbestos dust, "Occupational and Safety Health Administration", **37 FR 11318**, June 1972, pp. 1972-1976.

140. Sadanandam J., Bikshamaiah G, Gopalakrishna B., Mahajan Y.R. "Effect of different reinforcements on the thermal expansion of 2124 aluminium metal-matrix composites" Journal of . Material Science Letter., **11,** 1992, pp.1518-1520.

141. Sadanandam J., Bikshamaiah G, Gopalakrishna B., Mahajan Y.R. "Effect of different reinforcements on the thermal expansion of 2124 aluminium metal-matrix composites" Journal of . Material Science Letter, **11**, 1992, pp. 1518-1520.

142. Sahin Y., Ozdin K., "A model for the abrasive wear behaviour of aluminium based composites" J. Material and Design, **29**, 2008, 7 pp. 28-733.

143. Sanders, P.G., Dalka T. Basch M.R.H., "A reduced–scale brake dynamometer for friction characterization", Tribology International, **34**, 2001, pp. 609-615.

144. Sands C.R. Shakespeare R.I., "Powder Metallurgy–Practice and Applications", George Newnes Limited, London, 1966, pp 198-199.

145. Sannino A.P., "Sliding wear of a SiC particulate reinforced Al-Cu-Mg alloy composite/ 17-4 PH stainless steel system", Master's Thesis ,Clemson University, Clemson, SC, December 1993.

146. Sannino A.P., Rack H.J., "Dry sliding wear of discontinuously reinforced aluminium composites: review and discussion", Wear, **189**, 1995, pp. 1-19.

147. Satapathy B.K., Bijway J., Kolluri D.K." Assessment of fiber contribution to friction material performance using grey relation analysis (GRA)", Journal of composite matarials, **40**, 2006, pp. 483-501.

148. Sato A., Mehrabian R., "Aluminum matrix composites: Fabrication and properties", Metallurgical Transaction, **7B**, 1976, pp. 443-450.

149. Sawla S, Das S "Combined effect of reinforcement and heat treatment on the two body abrasive wear of aluminum alloy and aluminum particle composites", Wear, **257**, 2004, pp. 555-561.

150. Schneider L., "8- Friction materials", Springer Berlin Heidelberg, **2A1**, 2006, pp. 1-8.

151. Seong Jin Kim, Min Hyung Cho, Keun Hyung Cho, Ho Jang, "Complementary effects of solid lubricants in automotive brake lining", J. Tribology International, **40**, 2007, pp. 15-20.

152. Severin D., Dorsch S., "Friction mechanism in industrial brakes", Wear, **249**, 2001, pp. 771-779.

153. Shetty Raviraj, Pai R., Pai S., Rao S., "Tribological Studies on Discontinuously Reinforced Aluminum Composites Based on the orthogonal Arrays", ARPN Journal of Engineering and Applied Sciences,. **3**, no. 1, February, 2008, pp. 84-92.

154. Shevehuk, Yu. F., Zozulya , V.D., Khrieko, A.F., "Friction of materials with additions of substances acting as solid Lubricants", Poroshkovaya metallurgiya, **12**, Dec. 1968, pp. 69-73.

155. Shorowordi K.M., Haseeb A.S.M.A., Celis J.P., "Velocity effects on the wear, friction and tribochemistry of aluminum MMC sliding against phenolic brake pad", Wear, **256**, Issue, 11-12, 2004, pp. 1176-1181.

156. Shorowordi K.M., Haseeb A.S.M.A., Celis J.P. "Tribo-surface characteristics of Al-B_4C and Al-SiC composites worn under different contact pressures", Wear, **261**, 2006, pp. 634-641.

157. Singaravelu Lenin D, "Development of friction materials through powder metallurgy", Ph.D. Thesis, 2007, MMED, IIT Roorkee, India.

158. Sinha S.K., Biswas S.K., "Frictional characteristics of Al-SiC composite brake disc, Journal of Materials Science", **30**, No. 9, 1995, pp. 237-247.

159. Skolianos S., Kattamis T.Z., "Tribological properties of SiC,-reinforced A1-4.5%Cu-15%Mg alloy composites", Material Science Engineering., **Al63**, 1993, pp. 107-113.

160. Srivatsan T. S. et al., "Processing techniques for particulate-reinforced metal aluminium matrix composites", Journal of materials science, **26,** 1991, pp. 5965-5978.

161. Straffelini G., Pellizzari M. Molinari A., "Influence of load and temperature on the dry slinding behavior of Al-based metal-matrix-composites against friction material" Wear, **256**, Issues 7-8, 2004, pp. 754-763.

162. Suckehoon Kang, "A study of friction and wear characteristics of copper-and iron-based sintered materials", Wear, **162-164**, 1993, pp. 1123-1128.

163. Suryanarayana C., IvanovE., Boldyrev V.V., "The science and technology of mechanical alloying", Materials science and technology, **A304-306**, 2001, pp. 151-158.

164. Surappa M.K., Rohatgi P.K., "Preperation and properties of cast aluminium–ceramic particle composites", Journal of Material Science, **16,** 1981 pp. 983-993.

165. Talib R.J., Muchtar, Azhari C.H., "Microstructural characteristics on the surface and subsurface of semimetallic automotive friction materials during braking process", Journal of Materials Processing Technology, **140**, 2003, pp 694-699.

166. Talib R.J., Muchtar, Azhari C.H., "The performance of semi-metallic friction materials for passenger cars", Journal of Technology, **46(A),** 2007, pp. 53-72

167. Tiwari A.N., "Composite materials for automotive brakes", published in 'Powder Metallurgy: Processing for Automotive electrical, Electronics and Engaging Industry' - edited by P. Ramakrishnan, New Age International Pub., New Delhi, 2007, pp 86-102.

168. Torralba, J. M., da Costa, C. E., & Velasco, F. "P/M aluminum matrix composites: an overview". Journal of Materials Processing Technology, **133** No.1-2, 2003, pp. 203-206.

169. Uyyuru R.K, Surappa M.K., Brusethaug S., "Effect of reinforcement volume fraction and size distribution on the tribological behavior of Al-composite/brake pad tribo-couple, wear", Wear, **260,** Issues 11-12, June, 2006, pp. 1248-1255.

170. Uyyuru R.K., Surappa M.K., Brusethaug S., "Tribological behavior of Ai-Si-SiCp composites/automobile brake and system under dry sliding conditions", Tribology International, **40**, Issue 2, 2007, pp. 365-373.

171. Vencl A., Rac A., Bobic I., "Tribological behavior of Al-based MMCs and their application in automotive industry", Tribology in industry, **26** No.3-4, 2004, pp.31-38.

172. Vingsbo O., "Fundamentals of friction and wear", Engineering materials for Adv. Friction and Wear Applications, ASM International, Gaithersburg, MD, 1988, pp. l-9.

173. Wallbridge N.C., Dowson D., "Distribution of wear rate data and a statistical approach to sliding wear theory", Wear, **119**, 1987, pp. 295-312.

174. Wang A., Rack H.J., "A statistical model for sliding wear of metals in metal/composite systems", Acta Metall. Mater., **40**, 1992, pp. 2301-2305.

175. Wang A., Rack H.J., "Abrasive wear of silicon carbide particulate and whisker-reinforced 7091 aluminum matrix composites", Wear, **146**, 1991, pp. 337-348.

176. Wang A., Rack H.J., "Dry sliding wear in 2124 Al-SIC/174 PH stainless steel systems", Wear, **148**, 1991, pp. 355-374.

177. Wang A., Rack H.J., "The effect of aging on the abrasion behavior of SiC,/2124 metal matrix composites", Metal and Ceramic Minerals, Metals and Materials Society, Warrendale, PA,1990, pp. 487-498.

178. Wang A., Rack H.J., "Transition wear behavior of SiC-particulate and SiC-whisker-reinforced 7091 Al metal matrix composites", Material Science Engineering., **Al47**, 1991, pp. 21 l-224.

179. Wan Y, Xue Q.J., "Effect of phospforus- containing additives on the wear of aluminium in the lubricated aluminium-on-on steel contact", Tribology Letteres, **2**,1996, pp. 37-45.

180. Wan Y, Liu W., Xue Q.J., "Effects of diol compounds on the friction and wear of aluminium alloy in a lubricated aluminium-on-steel contact", Wear, **193**, 1996, pp. 99-104.

181. Weng B.J., Chang S.T., Shiau J.S., "Micro fracture mechanisms of SiC-6061 aluminum composite after hipping", Scripta Metalllurgica, **27** , 1992, pp. 1127-1132.

182. Werner Osterle, Ingrid Urban, "Third Body formation on brake pads and rotors, Tribology International" **39**, 2006, pp. 401-408.

183. Wojtaszek Marek "Properties of aluminium-ceramic phase composites produced from P/M compacts in hot forging and extrusion process", Metallurgy and foundry engineering, **33**, 2007, pp. 63-71.

184. Wilson S., Alpas A.T., "Effect of temperature on the sliding wear performance of Al alloys and Al matrix composites", Wear, **196**, 1996, pp. 270-278.

185. Xiang Xiong , Jiang-hong Li, Bai-yun Huang, "Impact of brake pressure on the friction and wear of carbon/carbon composites" Science Direct, Carbon **45,** 2007 pp. 2692–2716.

186. Yang L.J., "A test methodology for the determination of wear coefficient", Wear, **259,** 2005, pp. 1453-1461.

187. Yang L.J., "The effect of nominal specimen contact area on the wear coefficient of A6061 aluminium matrix composite reinforced with alumina particles", Wear, **263,** 2007, pp. 939-948.

188 Yafei Lu, Choong-Fong Tang, Maurice A.Wrieght, " Optimization of a commercial brake pad formulation", Journal of applied polymer science, **84,**2002, pp. 2498-2504.

189 Yibin Xu, Yoshihisa Tanaka, "Thermal conductivity of SiC fine particles reinforced Al alloy matrix composite with dispersed particle size", Journal of applied physics, **95,** No. **2,** 2004, pp. 722-725.

190 Zmago Stadler, Kristoffer Krnel, Tomaz Kosmac, "Friction behavior of sintered metallic brake pads on a C/C–SiC composite brake disc", Journal of the European Ceramic Society, **27,** 2007, pp.1411–1417

References from internet:

191. Clutch/Brake material properties.
www.roymech.co.uk/Useful_Tables/Drive/Brake_Clutch_mat.html

192. Hecht R.L., "Thermal transport properties of aluminium metal matrix composites for brake application", pp. 1-5.
http://www.html.ornl.gov/tpuc/brakes.html

193. Aluminium Matrix Composites, Typical Properties Data Sheet, pp.1-9.
http//solutions.3m.com

194. Kateel Industry ltd. 'Brake liners, brake block, asbestos brake liners, railway brake blocks, India'p.1-3.
http://www.indiamart.com/kateelengineering/brake-liners.html

195. VW vortex Forums: Brake pad performance: Friction coefficient & operating temperature, pp.1-10.
http://forums.vwvortex.com

196. The brake bible, url:http://www.carbibles.com/brake_bible.html

Research and Business Survey Reports

Research Report RR.1

Research report on " Composition, Functions, and Testing of friction brake materials and their additives" prepared by Peter J. Blau, Oak Ridge National Laboratory, Oak Ridge, Tennessee, managed by UT-B ATTELLE, LLC, sponsored by U.S. Department of Energy, under contract DE-AC05-00OR22725, submitted in august 2001.
http://www.ornl.gov/~webworks/cppr/y2001/rpt/110463.pdf

Business Survey Report

AVM028C: The friction products and material market Feb. 2007 by BCC Research.

AVM028C: The friction products and material market Aug. 2009 by BCC Research

00046784G: Report on 2009 World Market Forecasts for imported Friction Material and Articles Thereof, Oct. 2008 Bharat Book Bureau.

USA/ European patents

US Patent No.	Date of publication	Title of patent	Investigator(s)
US.P-7087318	08/08/06	Copper based sintered contact material and double-layered sintered contact member	Takayama, Takemori et. al.
US.P-6918970	19/07/05	High strength Al. alloy for high temperature applications	Lee et. al.
US.P-0175544	09/09/04	Non Asbestos-based friction materials	Iwao et. al.
US.P-6439353	27/08/02	Aircraft wheel brake with exchangeable brake segments	Gerd Roloff
US.P-6382368	07/05/02	Drum-in disc brake	Iwata, Yukio
US.P-6093482	25/07/00	Carbon-carbon composite for friction products and method of making same	Hyun Cheol Park
US.P-6068094	30/05/00	Sintered friction materials	Takahashi et al.
US.P-5902943	05/11/99	Al. alloy powder blends and sintered aluminium alloys	Schaffer et. al.
US.P-5976456	02/11/99	Method for producing aluminium alloy powder compacts	Ziani et. al.
US.P-5925837	20/07/99	Manufactering method and products of metallic friction material	Chien-ping et. al.
US.P-5856278	01/05/99	Friction material for use with Al. alloy rotor	Brewer, et al.
US.P-5841042	24/11/98	Brake lining material for heavy load braking device	Yoshinari Kato
US.P-5830309	03/11/98	Resin bonded friction material	McCord, H.Lee
US.P-5824923	20/10/98	Sintered friction materials, composite copper alloy powder used therefore and manufacturing method thereof.	Kondoh et al.
US.P-5712029	27/01/98	Friction material	Kazuo et. al.
US.P-5620791	15/04/97	Brake rotors and methods for making the same	Dwivedi et al
US.P-5620042	15/04/97	Method of casting a brake rotor	Marh Ket al.

US Patent No.	Date of publication	Title of patent	Investigator(s)
US.P-5595266	21/01/97	Bonding a friction material brake lining element to a metallic backing plate element	Cecere, James A.
US.P-5538104	07/23/96	Brake pad	Katz et al.
US.P-5407035	18/04/95	Composite disc brake rotor and method of making	Cole, Gerald et al.
US.P-5384087	24/01/95	Aluminium –silicon carbide composite and process for making the same	Scorey, Clive
US.P-5339931	23/08/94	Porous copper powder modified friction material	Jacko et al.
US.P-5372222	13/12/94	Light weight and high thermal conductivity brake rotor	Seong K. Rhee
US.P-5325941	05/07/94	Composite brake rotors and clutches	Farinacci et al.
US.P-5028494	02/07/91	Brake disc material for road vehicles	Tsujimura et. al.
US.P-4946647	07/08/90	Process for the manufacture of aluminium–graphite composite for automobile and engg. applications.	Rohatgi et. al.
US.P-4865806	12/09/89	Process for preparation of composite materials containing nonmetallic particles in a metallic matrix	Michael D. et al.
US.P-4661154	28/04/87	Process for the production by powder metallurgy of components subjected to friction	Lechert Jr., Stephen J.
US.P-4409298	10/11/83	Castable metal composite friction materials	Albertson, et. al.
US.P-4415363	15/11/83	Sintered iron base friction material	Sanftleben et al.
US.P-4311524	19/01/02	Sintered iron-based friction material	Genkin, Valery A.
US.P-4350530	21/09/82	Sintered alloy for friction materials	Kamioka et al.
US.P-4391641	07/05/83	Sintered powder metal friction material	Lloyd et al.
US.P-4203936	05/20/80	Water slurry process for manufacturing phenolic resin bonded friction materials	Kiwak et al.
US.P-4173681	11/06/79	Brake pad with integral organic back plate	Durrieu et. al.
USP-4069042	17/01/78	Method of pressing and forging metal powder	Milton R. Rearick
US.P-3844800	29/12/74	Friction material	Bendix Corp.

European Patent No.	Date of publication	Title of patent	Investigator(s)
EuP-0567284	20/04/93	Aluminium-based metal matrix composite	Rohatgi et. al.
EuP-0539011	07/05/97	Nickel coated carbon preforms	Bell et. al.

Annexure- I

Krauss test (ECR R90 standard regulation test) for brake pads of light to heavy duty road vehicles

(Page A1to A21)

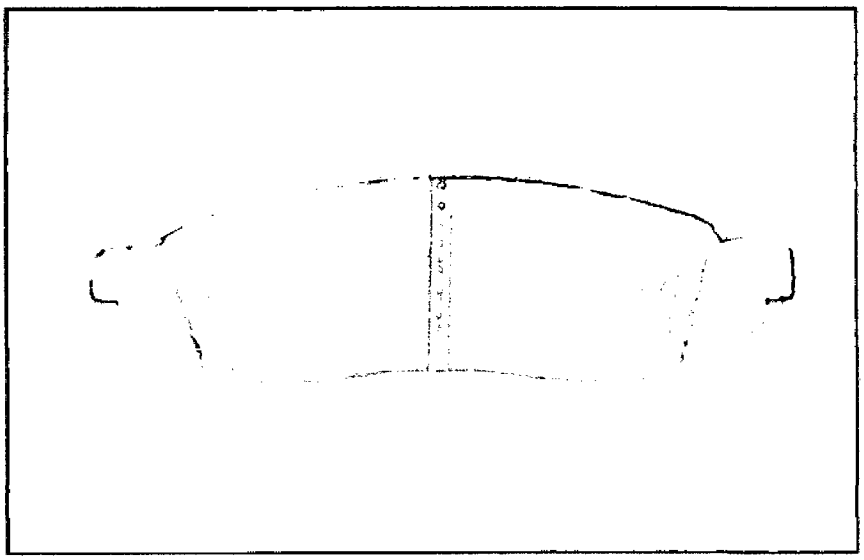

DEVELOPED BRAKE PAD FOR MARUTI-800 CAR

ALLIED NIPPON LTD.

(A joint venture with Japan Brake Ind. Co.)

TEST PROTOCOL
FRICTION TEST

A1.

Test program	STANDARD TEST
Program no.	0051
Protocol no.	11T (21)
Operator	HARENDER
Tester	RW118
Test Date	18.09.2008
WVA no.	20731 00
Index	ADB130 FM 18.5
Batch	SAMPLE
Customer	
Customer no.	ADB-0130

Comment:
STANDERD TEST

Technical Data:

Caliper	SLIDING
Disc dia	215mm
Disc thickness	10.5mm
Disc no.	0
Test no.	11T (9BAR)
Frict. Radius	95.5mm
Pad Area	18.5 cm²
Test Pressure	9.0 Bar

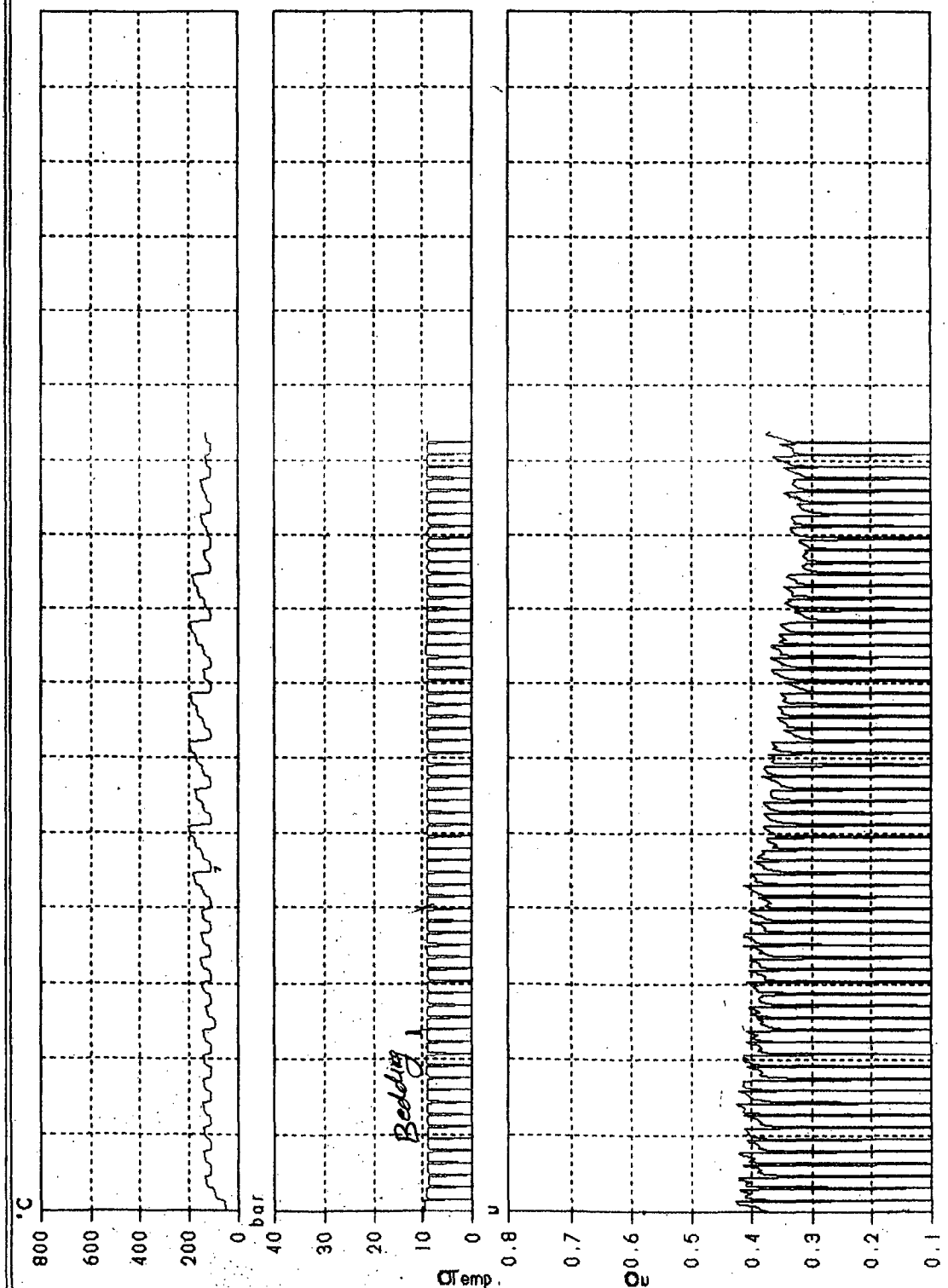

processed	verified	
passed	failed	

Wear: '01/02 1.0 1.2

Pad 1	0.00 mm	0.00 g
Pad 2	0.00 mm	0.00 g
Disc	0.00 mm	0.00 g

Friction Values:

umin.	=0.282
umax	=0.417
Perf.u	=0.342
Fade mue	=0.307
Recovery u	=0.378
Test Av. Mue	=0.365

SML_AN01P

ALLIED NIPPON LTD.

(A joint venture with Japan Brake Ind. Co.)

TEST PROTOCOL FRICTION TEST

PART 2

AR

Test program	STANDARD TEST
Program no.	0051
Protocol no.	IIT (21)
Operator	HARENDER
Tester	RW118
Test Date	18.09.2008
WVA no.	20731 00
Index	ADB130 FM 18.5
Batch	SAMPLE
Customer	
Customer no.	ADB-0130
Comment:	

STANDERD TEST

Technical Data:

Calliper	SLIDING
Disc dia	215mm
Disc thickness	10.5mm
Disc no.	0
Test no.	IIT (7BAR)
Frict. Radius	95.5mm
Pad Area	18.5 cm²
Test Pressure	7.0 Bar

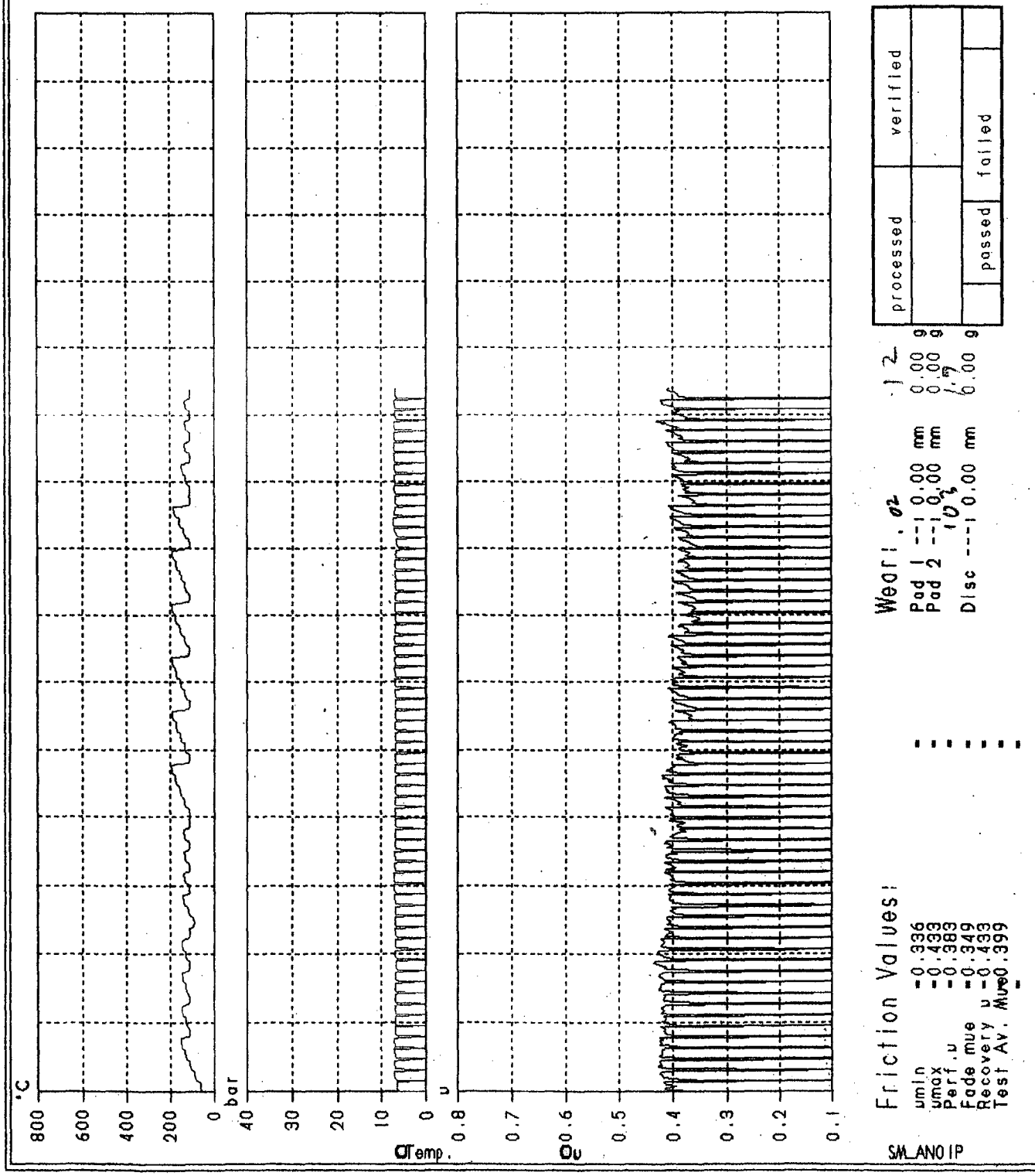

ALLIED NIPPON LTD.

(A joint venture with Japan Brake Ind. Co.)

TEST PROTOCOL FRICTION TEST

A3

Test program ---: STANDARD TEST
Program no. ----: 0051
Protocol no. ---: IIT (23)
Operator -------: HARENDER
Tester ---------: RW118
Test Date ------: 18.09.2008
WVA no. --------: 20731 00
Index ----------: ADB130 FM 18.5
Batch ----------: SAMPLE
Customer -------:
Customer no. ---: ADB-0130
Comment:
STANDERD TEST

Technical Data:

Caliper -------: SLIDING
Disc dia ------: 215mm
Disc thickness : 10.5mm
Disc no. ------: 0
Test no. ------: IIT (7BAR)
Frict. Radius -: 95.5mm
Pad Area ------: 18.5 cm²
Test Pressure--: 7.0 Bar

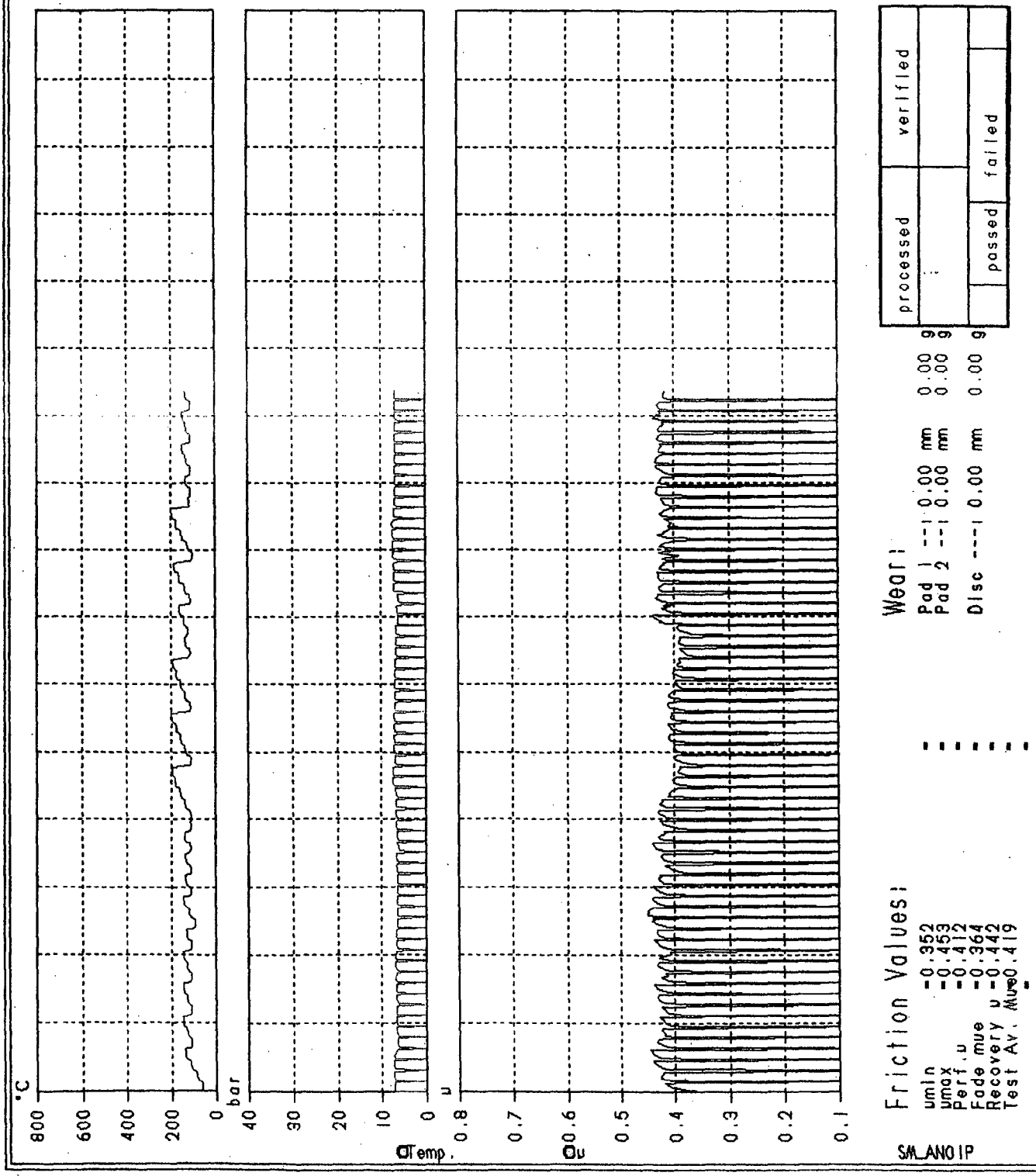

ALLIED NIPPON LTD.

(A joint venture with Japan Brake Ind. Co.)

TEST PROTOCOL
FRICTION TEST

A4

Test program ---: STANDARD TEST
Program no. ----: 0051
Protocol no. ---: IIT SAMPLE(660)18
Operator -------: VIJAY
Tester ---------: RW118
Test Date ------: 03.09.2008
WVA no. --------: 20731 00
Index ----------: ADB130 FM 18.5
Batch ----------: SAMPLE
Customer -------:
Customer no. ---: ADB-0130
Comment:
STANDERD TEST

Technical Data:

Caliper --------: SLIDING
Disc dia -------: 215mm
Disc thickness : 10.5mm
Disc no. -------: 0
Test no. -------: 8801
Frict. Radius -: 95.5mm
Pad Area -------: 18.5 cm²
Test Pressure--: 7.0 Bar

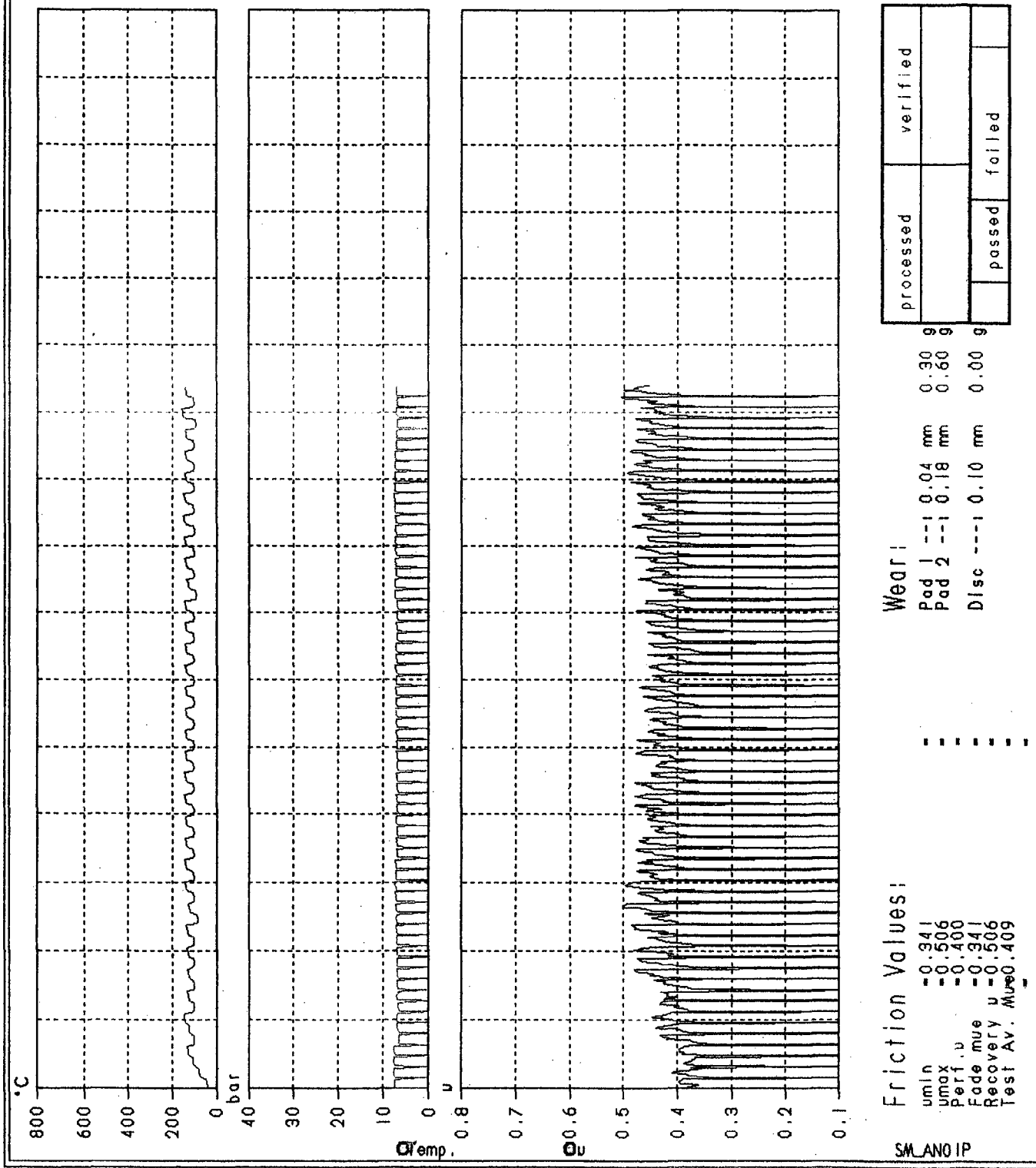

ALLIED NIPPON LTD.

(A joint venture with Japan Brake Ind. Co.)

TEST PROTOCOL
FRICTION TEST

A5

Test program ---: STANDARD TEST
Program no. ----: 0051
Protocol no. ---: IIT SAMPLE(660) 18
Operator -------: VIJAY
Tester ---------: RW118
Test Date ------: 03.09.2008
WVA no. --------: 20731 00
Index ----------: ADB130 FM 18.5
Batch ----------: SAMPLE
Customer -------:
Customer no. ---: ADB-0130
Comment:
STANDERD TEST

Technical Data:

Caliper -------: SLIDING
Disc dia ------: 215mm
Disc thickness : 10.5mm
Disc no. ------: 0
Test no. ------: 8800
Frict. Radius -: 95.5mm
Pad Area ------: 18.5 cm²
Test Pressure--: 5.0 Bar

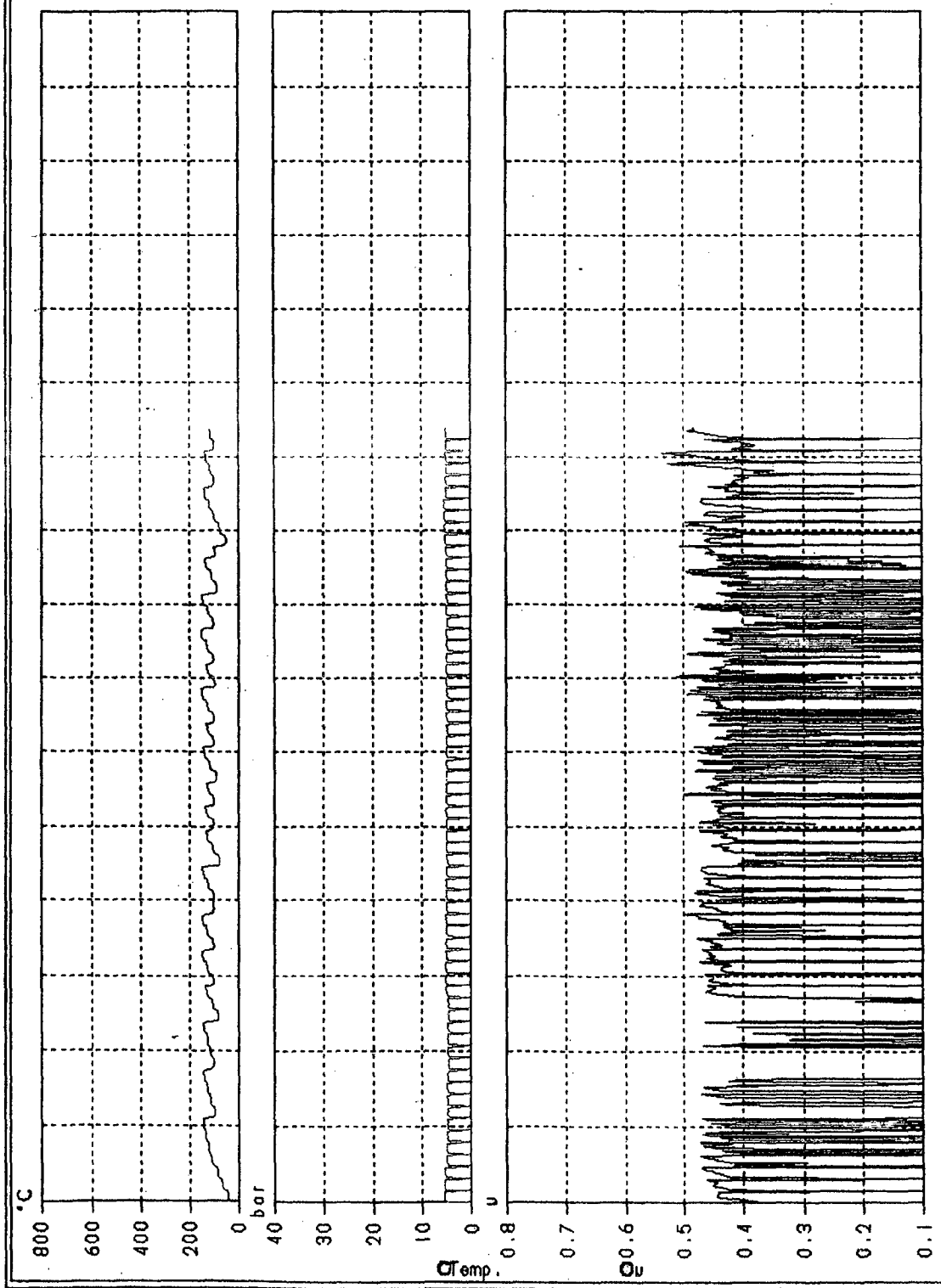

Wear:

Pad 1 --: 0.07 mm 0.60 g
Pad 2 --: 0.23 mm 0.90 g
Disc ---: 0.12 mm 0.00 g

Friction Values:

μmin -0.347
μmax -0.538
Perf.u -0.424
Fade mue -0.376
Recovery u -0.538
Test Av. Mue 0.433

SM_AN01P

ALLIED NIPPON LTD.

(A joint venture with Japan Brake Ind. Co.)

TEST PROTOCOL FRICTION TEST

A6

Test program ---: STANDARD TEST
Program no. ----: 0051
Protocol no. ---: IIT (23)
Operator -------: HARENDER
Tester ---------: RW118
Test Date ------: 18.09.2008
WVA no. --------: 20731 00
Index ----------: ADB130 FM 18.5
Batch ----------: SAMPLE
Customer -------:
Customer no. ---: ADB-0130
Comment:
STANDERD TEST

Technical Data:

Caliper -------: SLIDING
Disc dia ------: 215mm
Disc thickness : 10.5mm
Disc no. ------: 0
Test no. ------: IIT (5BAR)
Frict. Radius -: 95.5mm
Pad Area ------: 18.5 cm²
Test Pressure--: 5.0 Bar

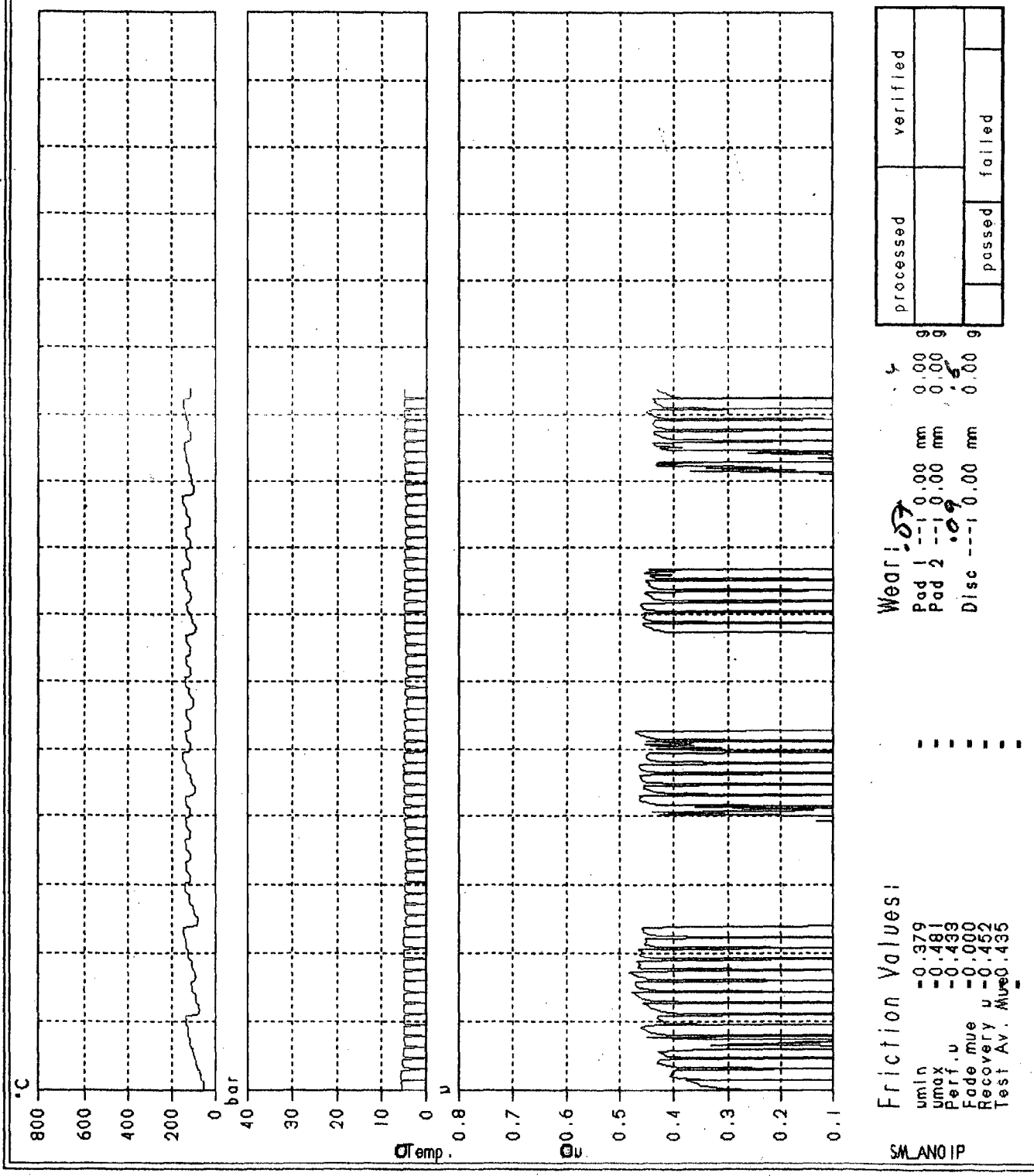

ALLIED NIPPON LTD.

(A joint venture with Japan Brake Ind. Co.)

TEST PROTOCOL FRICTION TEST

A7

Test program ---: STANDARD TEST
Program no. ----: 0051
Protocol no. ---: IIT (21)
Operator -------: HARENDER
Tester ---------: RW118
Test Date ------: 18.09.2008
WVA no. --------: 20731 00
Index ----------: ADB130 FM 18.5
Batch ----------:
Customer -------: SAMPLE
Customer no. ---: ADB-0130
Comment:
STANDERD TEST

Technical Data:

Caliper -------: SLIDING
Disc dia ------: 215mm
Disc thickness : 10.5mm
Disc no. ------: 0
Test no. ------: IIT (5BAR)
Frict. Radius -: 95.5mm
Pad Area ------: 18.5 cm²
Test Pressure--: 5.0 Bar

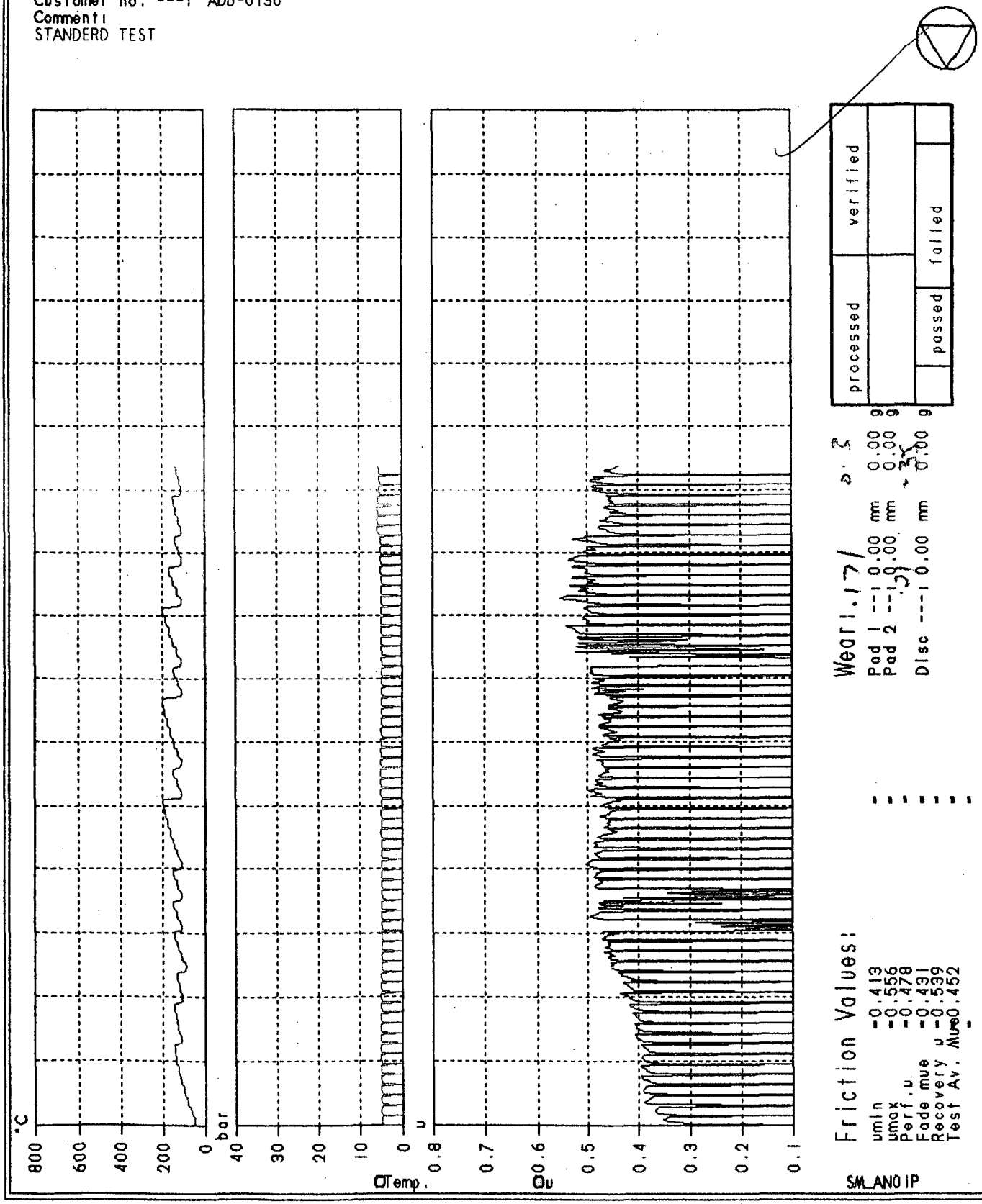

ALLIED NIPPON LTD.

(A joint venture with Japan Brake Ind. Co.)

TEST PROTOCOL
FRICTION TEST

A8

Test program ---: CV LINING TEST
Program no. ----: 0018 PKI
Protocol no. ---: JBNH
Operator -------: HARENDRA
Tester ---------: RW118
Test Date ------: 19.06.2008
WVA no. --------: 20731 00
Index ----------: ADB130 FM 18.5
Batch ----------: SAMPLE
Customer -------:
Customer no. ---: ADB-0130
Comment:
STANDERD TEST

Technical Data:

Caliper -------: SLIDING
Disc dia ------: 215mm
Disc thickness : 10.5mm
Disc no. ------: 0
Test no. ------: 8727
Frict. Radius -: 95.5mm
Pad Area ------: 18.5 cm²
Pressure-------: 10.0 Bar

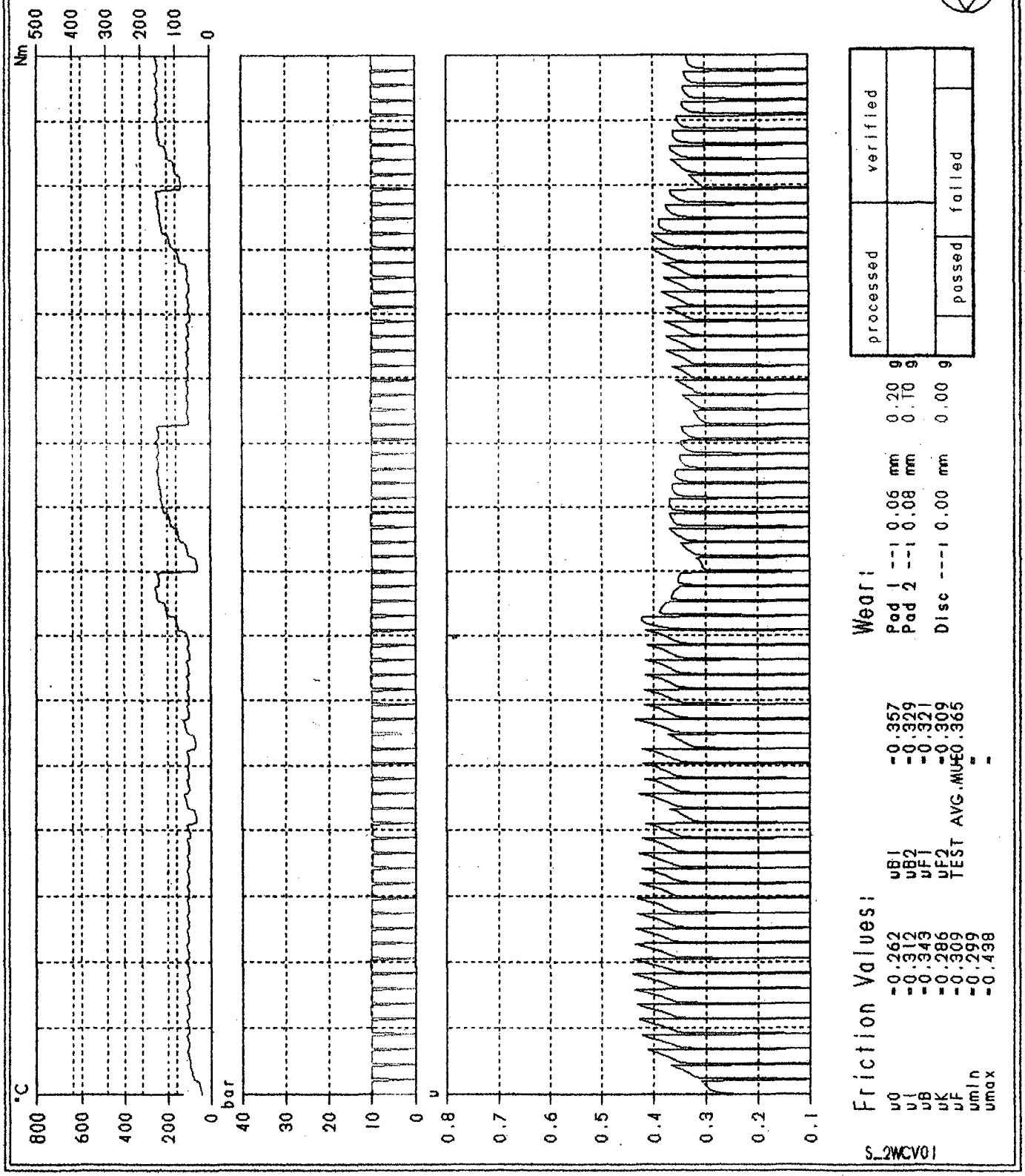

ALLIED NIPPON LTD.

(A joint venture with Japan Brake Ind. Co.)

TEST PROTOCOL FRICTION TEST

A9

Test program ---: CV LINING TEST
Program no. ----: 0018 PKI
Protocol no. ---: DEV
Operator -------: RAJU
Tester ---------: RWI18
Test Date ------: 30.04.2008
WVA no. --------: 20731 00
Index ----------: ADB130 FM 18.5
Batch ----------: SAMPLE
Customer -------:
Customer no. ---: ADB-0130
Comment:
STANDERD TEST

Technical Data:

Caliper -------: SLIDING
Disc dia ------: 215mm
Disc thickness : 10.5mm
Disc no. ------: 0
Test no. ------: 8656
Frict. Radius -: 95.5mm
Pad Area ------: 18.5 cm²
Pressure-------: 10.0 Bar

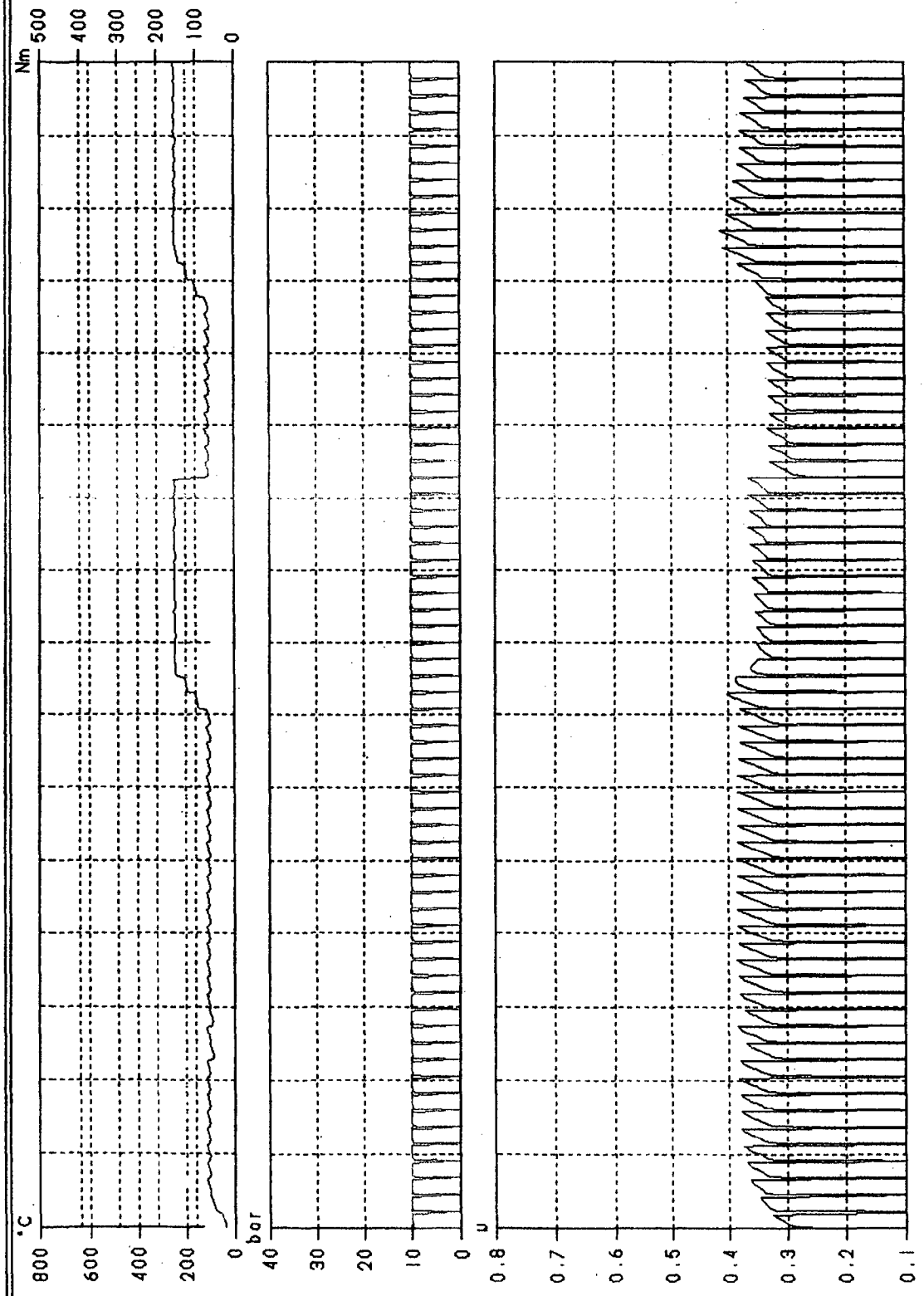

processed	verified
passed	failed

Wear:

Pad 1 --:	0.05 mm	0.10 g
Pad 2 --:	0.07 mm	0.10 g
Disc ---:	0.00 mm	0.00 g

Friction Values:

u0	=0.274	uB1	=0.330
u1	=0.329	uB2	=0.301
uB	=0.316	uF1	=0.320
uK	=0.297	uF2	=0.328
uF	=0.320	TEST AVG.MU	=0.349
umin	=0.274		
umax	=0.416		

S_2WCV01

ALLIED NIPPON LTD.

(A joint venture with Japan Brake Ind. Co.)

TEST PROTOCOL
FRICTION TEST

A10

Test program	STANDARD TEST
Program no.	0051
Protocol no.	ADB-0130
Operator	HARENDRA
Tester	RW118
Test Date	01.12.2008
WVA no.	20731 00
Index	ADB130 FM 29.1
Batch	SAMPLE
Customer	
Customer no.	ADB-0130

Comment:
STANDARD TEST

Technical Data:

Caliper	SLIDING
Disc dia	215mm
Disc thickness	10.5mm
Disc no.	0
Test no.	8873
Frict. Radius	95.5 mm
Pad Area	29.1 cm²
Test Pressure	10.0 Bar

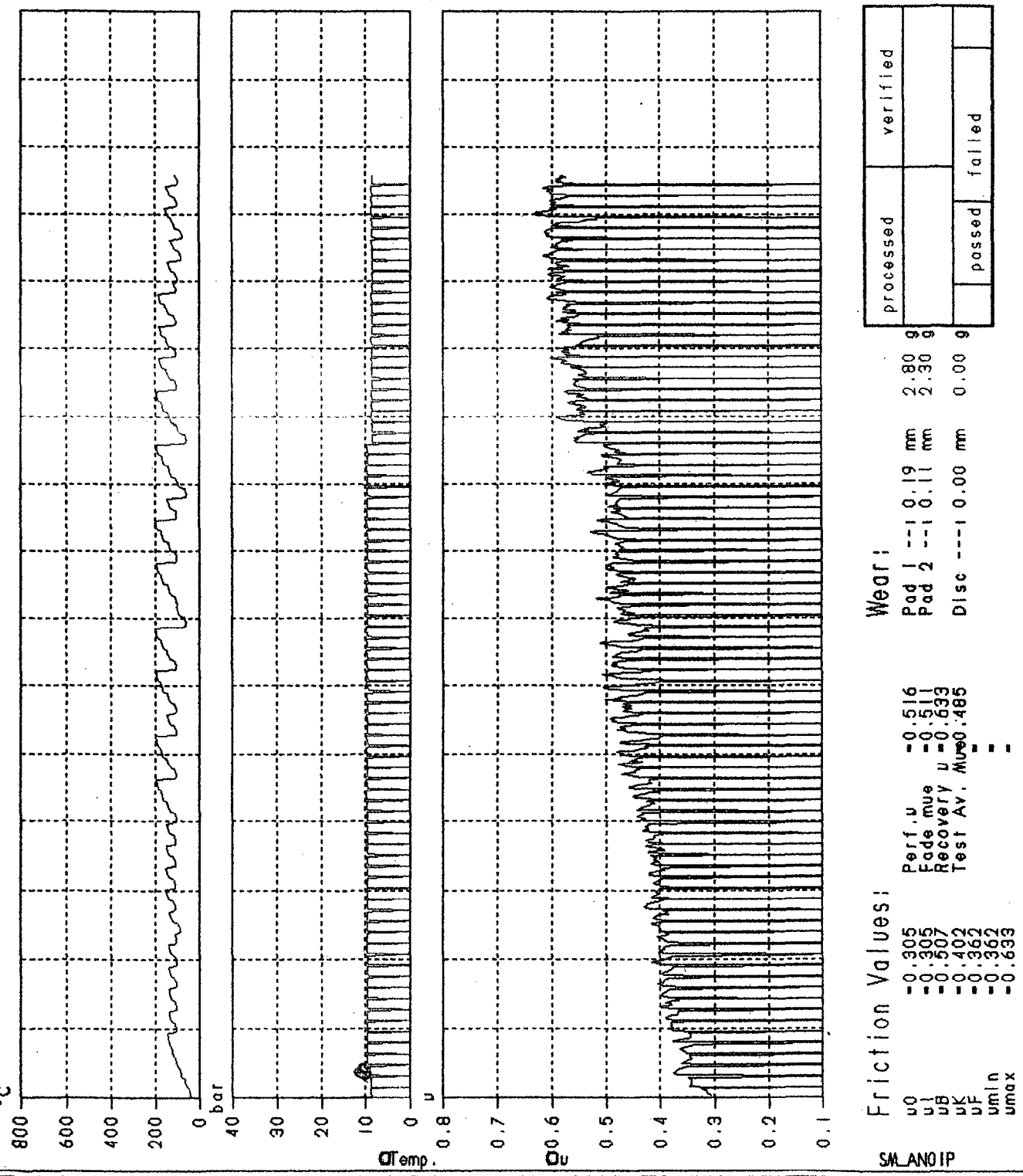

ALLIED NIPPON LTD.

(A joint venture with Japan Brake Ind. Co.)

TEST PROTOCOL
FRICTION TEST

A11

Test program	STANDARD TEST
Program no.	0051
Protocol no.	IIT (23)
Operator	HARENDER
Tester	RW118
Test Date	17.01.2009
WVA no.	20731 00
Index	ADB130 FM 18.5
Batch	SAMPLE
Customer	
Customer no.	ADB-0130
Comment:	STANDERD TEST

Technical Data:

Caliper	SLIDING
Disc dia	215mm
Disc thickness	10.5mm
Disc no.	0
Test no.	IIT (9BAR)
Frict. Radius	95.5mm
Pad Area	18.5 cm²
Test Pressure	10.0 Bar

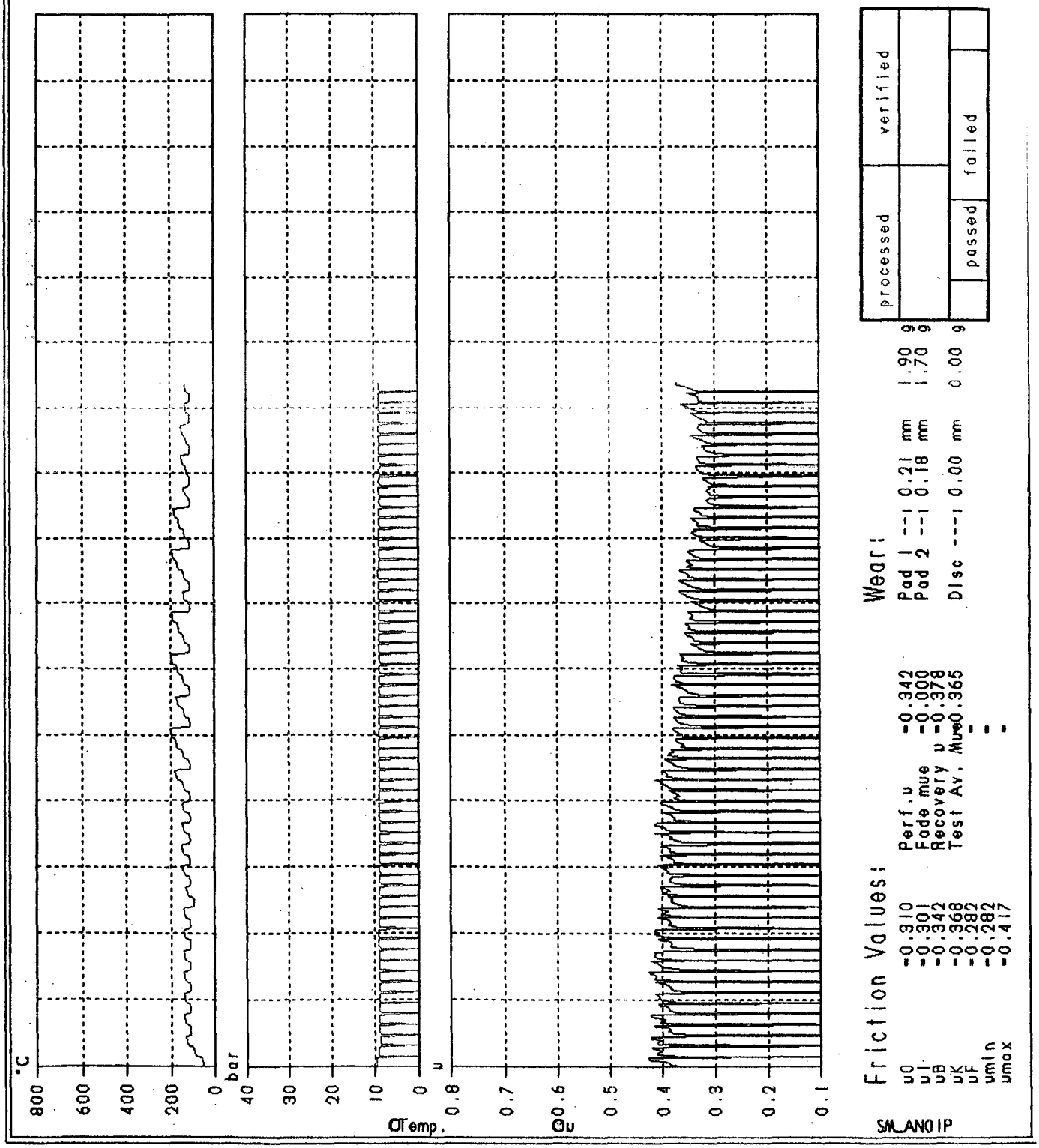

ALLIED NIPPON LTD.

(A joint venture with Japan Brake Ind. Co.)

TEST PROTOCOL
FRICTION TEST

AIR

Test program ---: STANDARD TEST
Program no. ----: 0051
Protocol no. ---: IIT (24)
Operator -------: HARENDER
Tester ---------: RW118
Test Date ------: 19.01.2009
WVA no. --------: 20731 00
Index ----------: ADB130 FM 18.5
Batch ----------: SAMPLE
Customer -------:
Customer no. ---: ADB-0130
Comment:
STANDERD TEST

Technical Data:

Caliper -------: SLIDING
Disc dia ------: 315mm
Disc thickness : 10.5mm
Disc no. ------: 0
Test no. ------: IIT (98AR)
Frict. Radius -: 95.5mm
Pad Area ------: 18.5 cm²
Test Pressure--: 10.0 Bar

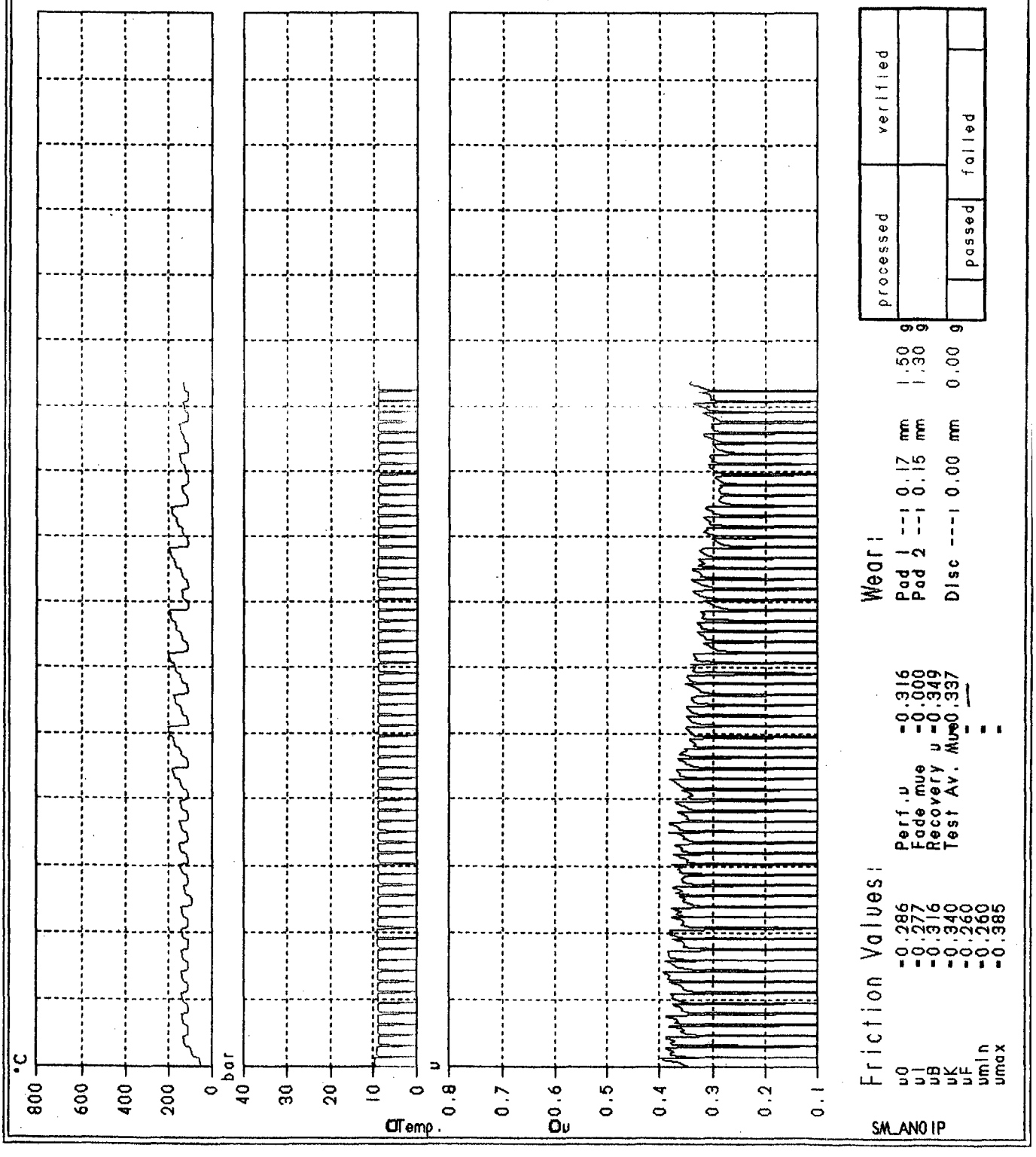

ALLIED NIPPON LTD.

(A joint venture with Japan Brake Ind. Co.)

TEST PROTOCOL FRICTION TEST

A13

Test program ---: STANDARD TEST
Program no. ----: 0051
Protocol no. ---: IIT (25)
Operator -------: HARENDER
Tester ---------: RWI18
Test Date ------: 19.01.2009
WVA no. --------: 20731 00
Index ----------: ADB130 FM 18.5
Batch ----------: SAMPLE
Customer -------:
Customer no. ---: ADB-0130
Comment:
STANDERD TEST

Technical Data:

Caliper -------: SLIDING
Disc dia. ------: 315mm
Disc thickness : 10.5mm
Disc no. ------: 0
Test no. ------: IIT (9BAR)
Frict. Radius -: 95.5mm
Pad Area ------: 18.5 cm²
Test Pressure--: 9.0 Bar

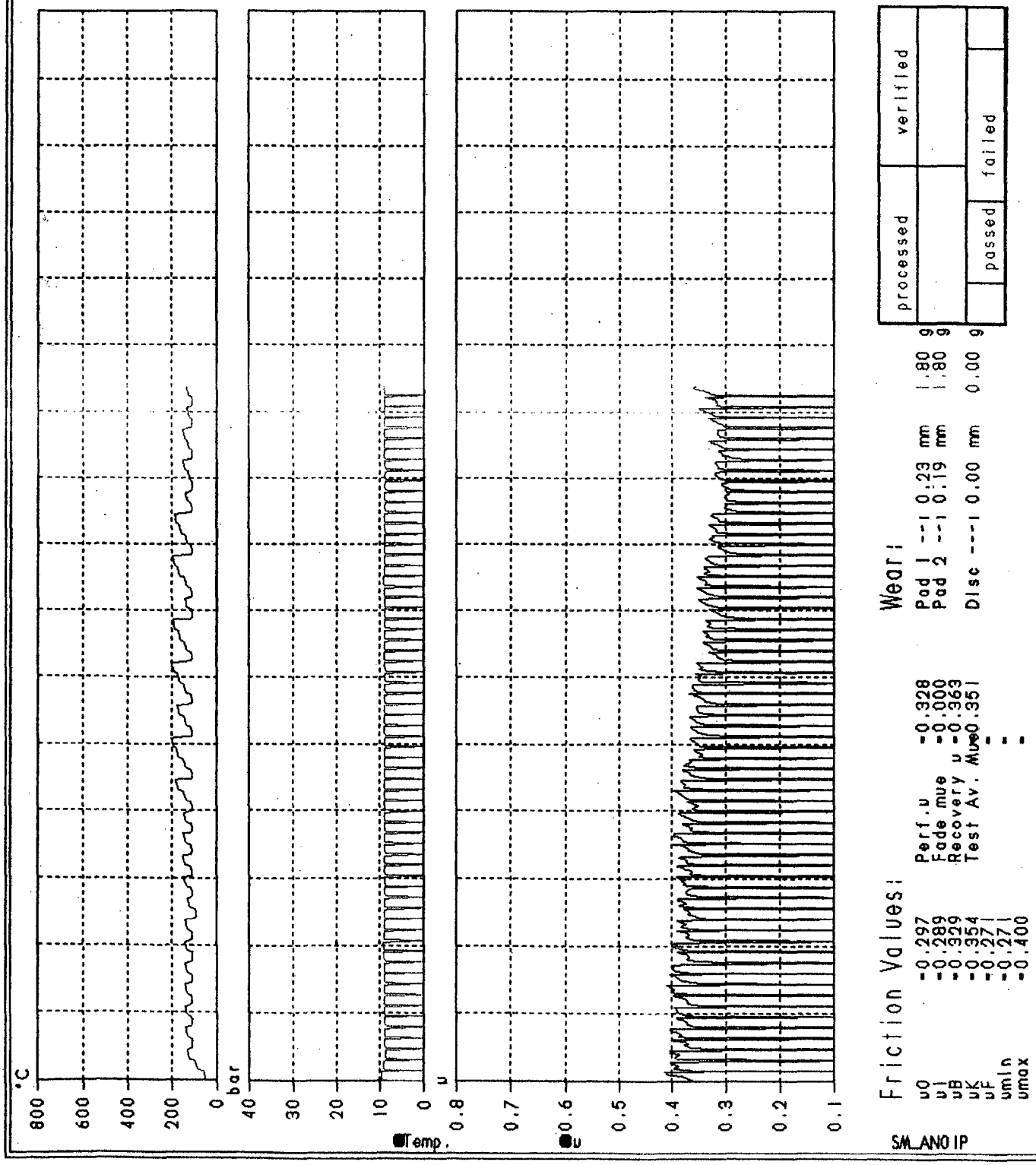

ALLIED NIPPON LTD.

(A joint venture with Japan Brake Ind. Co.)

TEST PROTOCOL
FRICTION TEST

A14

Test program	STANDARD TEST
Program no.	0051
Protocol no.	IIT (26)
Operator	HARENDER
Tester	RW118
Test Date	19.01.2009
WVA no.	20731 00
Index	ADB130 FM 18.5
Batch	SAMPLE
Customer	
Customer no.	ADB-0130

Comment:
STANDERD TEST

Technical Data:

Caliper	SLIDING
Disc dia	215mm
Disc thickness	10.5mm
Disc no.	0
Test no.	IIT (9BAR)
Frict. Radius	95.5mm
Pad Area	18.5 cm²
Test Pressure	10.0 Bar

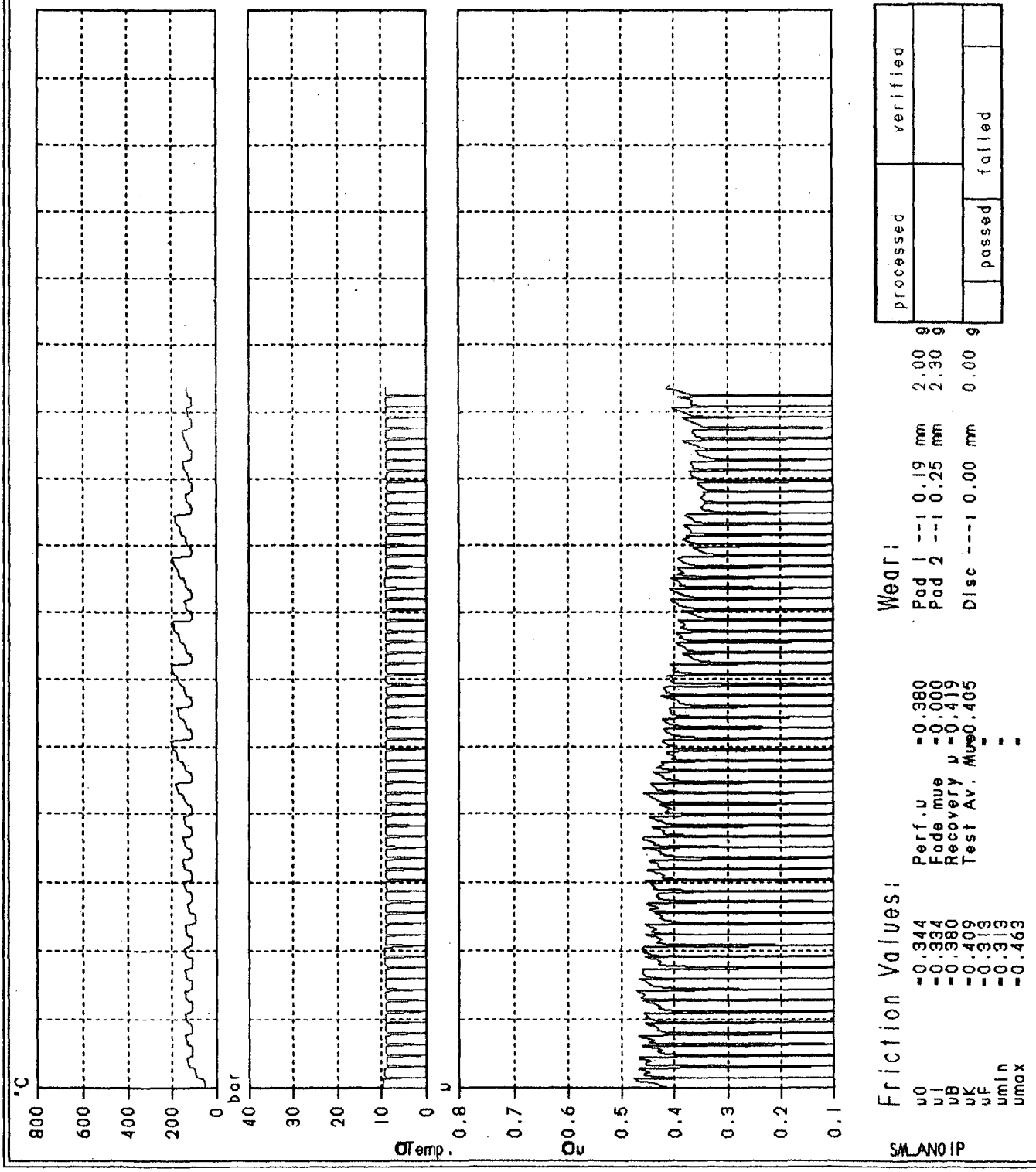

ALLIED NIPPON LTD.

(A Joint venture with Japan Brake Ind. Co.)

TEST PROTOCOL
FRICTION TEST

A15

Test program ---: STANDARD TEST
Program no. ----: 005
Protocol no. ---: ADB-0130
Operator -------: VIJAY
Tester ---------: RW118
Test Date ------: 10.10.2008
WVA no. --------: 20731 00
Index ----------: ADB130 FM.29.1
Batch ----------: NAM-114 (Reg)
Customer -------: REG.
Customer no. ---: ADB-0130
Comment:
STANDARD TEST

Technical Data:

Caliper -------: SLIDING
Disc dia ------: 215mm
Disc thickness : 10.5mm
Disc no. ------: 0
Test no. ------: 8363
Frict. Radius -: 95.5mm
Pad Area ------: 29.1 cm²
Test Pressure--: 20.0 Bar

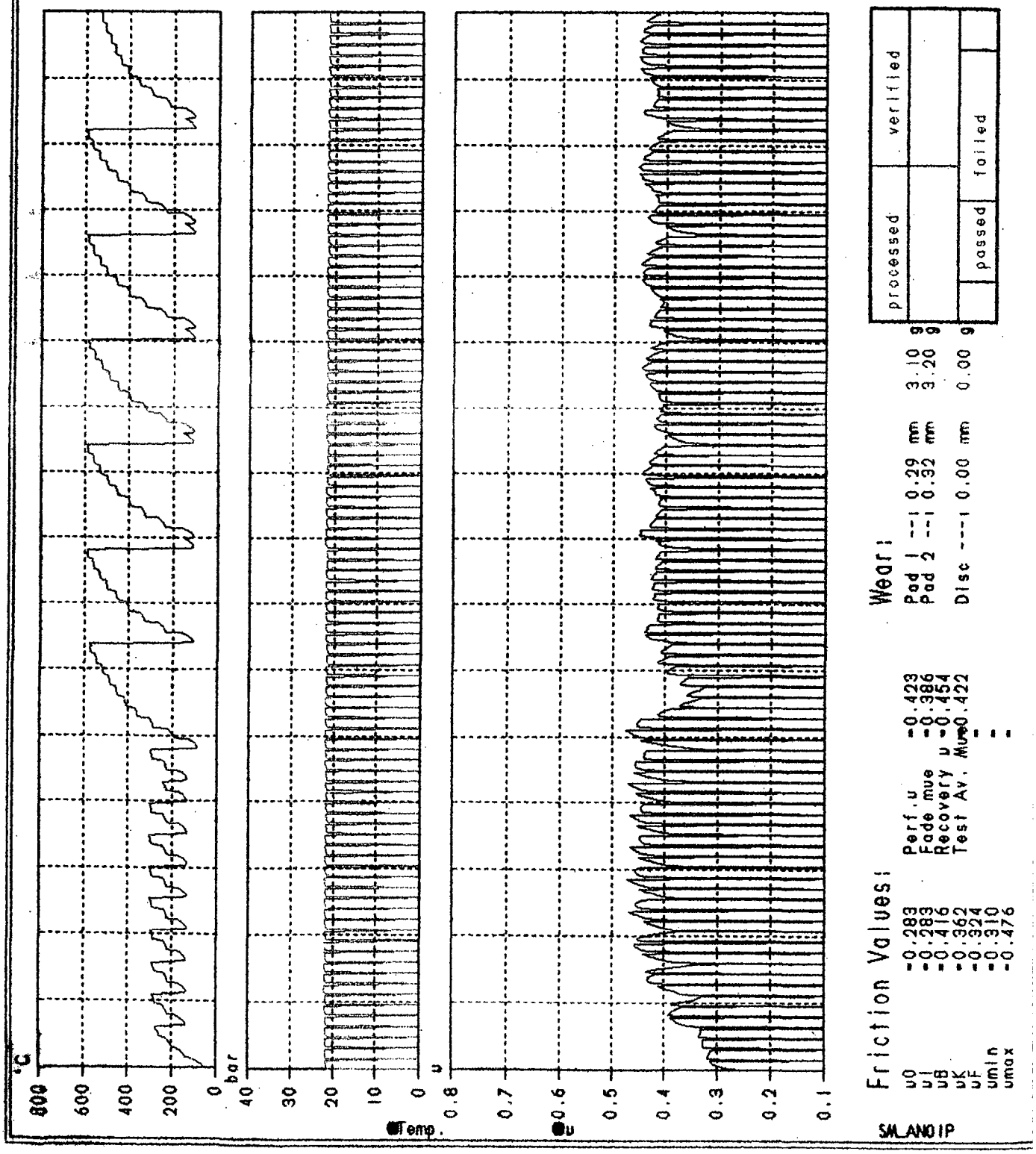

ALLIED NIPPON LTD.

(A joint venture with Japan Brake Ind. Co.)

TEST PROTOCOL
FRICTION TEST

A16

Test program ---: STANDARD TEST
Program no. ----: 005
Protocol no. ---:
Operator -------: VIJAY
Tester ---------: RW118
Test Date ------: 11.09.2008
WVA no. --------: (P0256)
Index ----------: 0256/ADB
Batch ----------: SAMPLE
Customer -------:
Customer no. ---: ADB-0256
Comment:
R-90 REGULATION TEST

Technical Data:

Caliper -------: SLIDING
Disc dia ------: 263mm
Disc thickness : 21.0mm
Disc no. ------: 0
Test no. ------: 8816
Frict. Radius -: 106.3mm
Pad Area ------: 48.5 cm²
Test Pressure--: 20.0 Bar

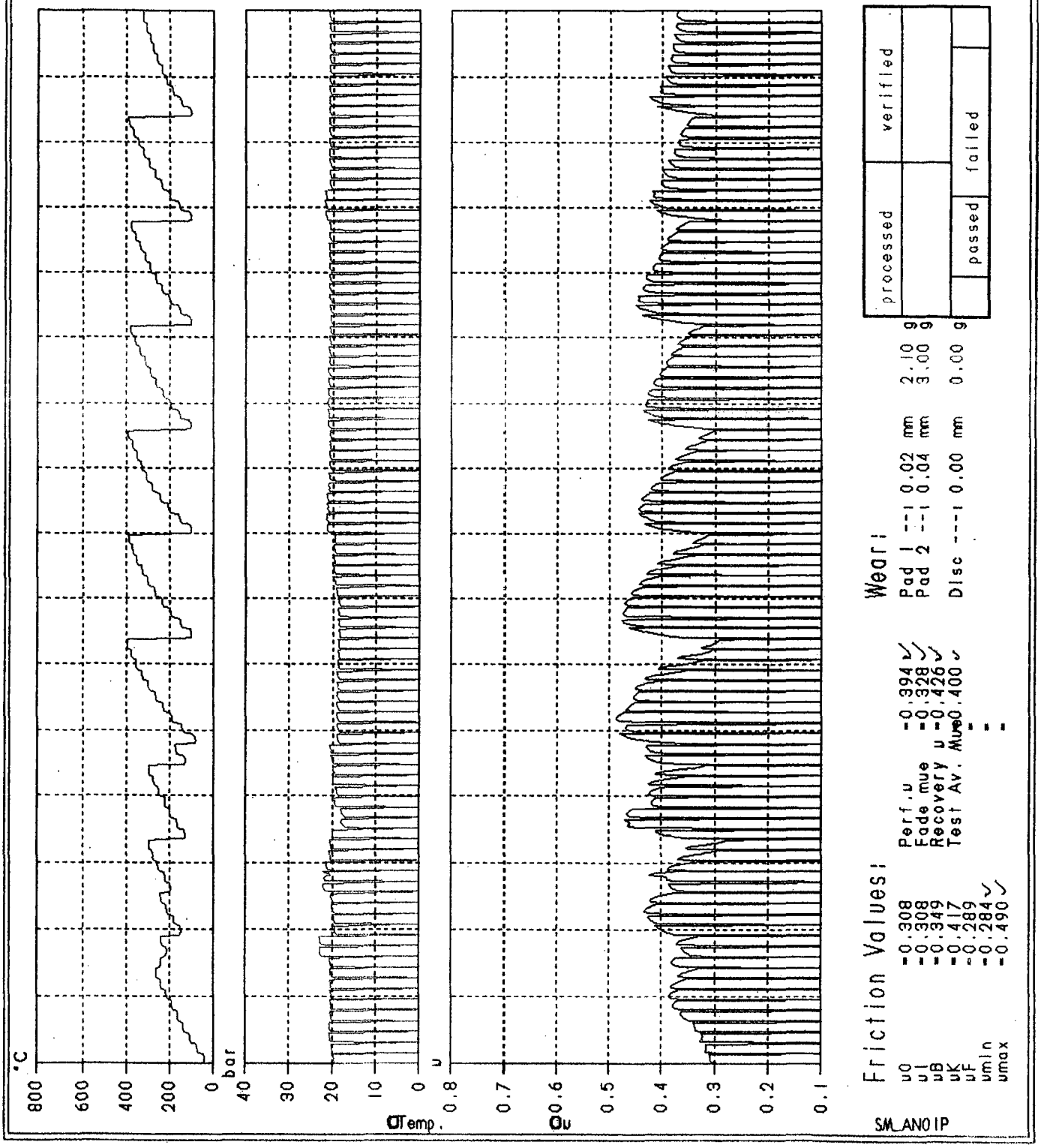

Wear:

Pad 1 --: 0.02 mm 2.10 g
Pad 2 --: 0.04 mm 3.00 g
Disc ---: 0.00 mm 0.00 g

Friction Values:

u0	=0.308	Perf.u	=0.394 ✓
u1	=0.308	Fade mue	=0.328 ✓
uB	=0.349	Recovery u	=0.426 ✓
uK	=0.417	Test Av. Mue	0.400 ✓
uF	=0.289		=
umin	=0.284 ✓		=
umax	=0.490 ✓		

SML_AN01P

ALLIED NIPPON LTD.

(A joint venture with Japan Brake Ind. Co.)

TEST PROTOCOL
FRICTION TEST

A17

Test program	STANDARD TEST
Program no.	0051
Protocol no.	IIT (26)
Operator	VIJAY
Tester	OWI18
Test Date	14.01.2009
WVA no.	20731 00
Index	ADB130 FM 29.1
Batch	SAMPLE
Customer	
Customer no.	ADB-0130

Comment:
STANDARD TEST

Technical Data:

Caliper	SLIDING
Disc dia	215mm
Disc thickness	10.5mm
Disc no.	0
Test no.	8913
Frict. Radius	95.5mm
Pad Area	29.1 cm²
Test Pressure	20.0 Bar

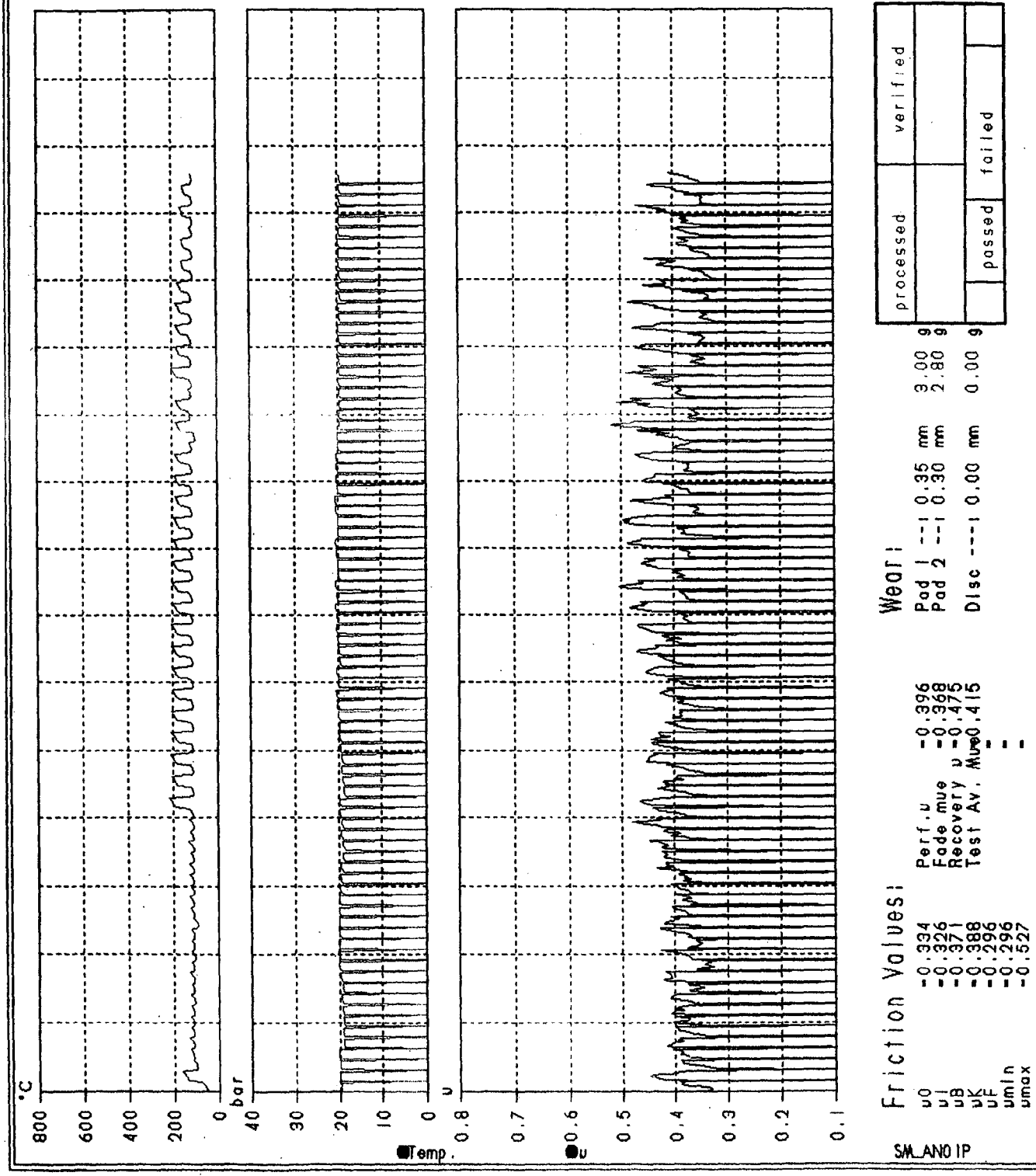

ALLIED NIPPON LTD.

(A joint venture with Japan Brake Ind. Co.)

TEST PROTOCOL
FRICTION TEST

A18

Test program	STANDARD TEST
Program no.	0051
Protocol no.	IIT (25)
Operator	VIJAY
Tester	OWI18
Test Date	14.01.2009
WVA no.	20731 00
Index	ADB130 FM 29.1
Batch	SAMPLE
Customer	
Customer no.	ADB-0130
Comment	STANDARD TEST

Technical Data:

Caliper	SLIDING
Disc dia	215mm
Disc thickness	10.5mm
Disc no.	0
Test no.	8912
Frict. Radius	95.5mm
Pad Area	29.1 cm²
Test Pressure	20.0 Bar

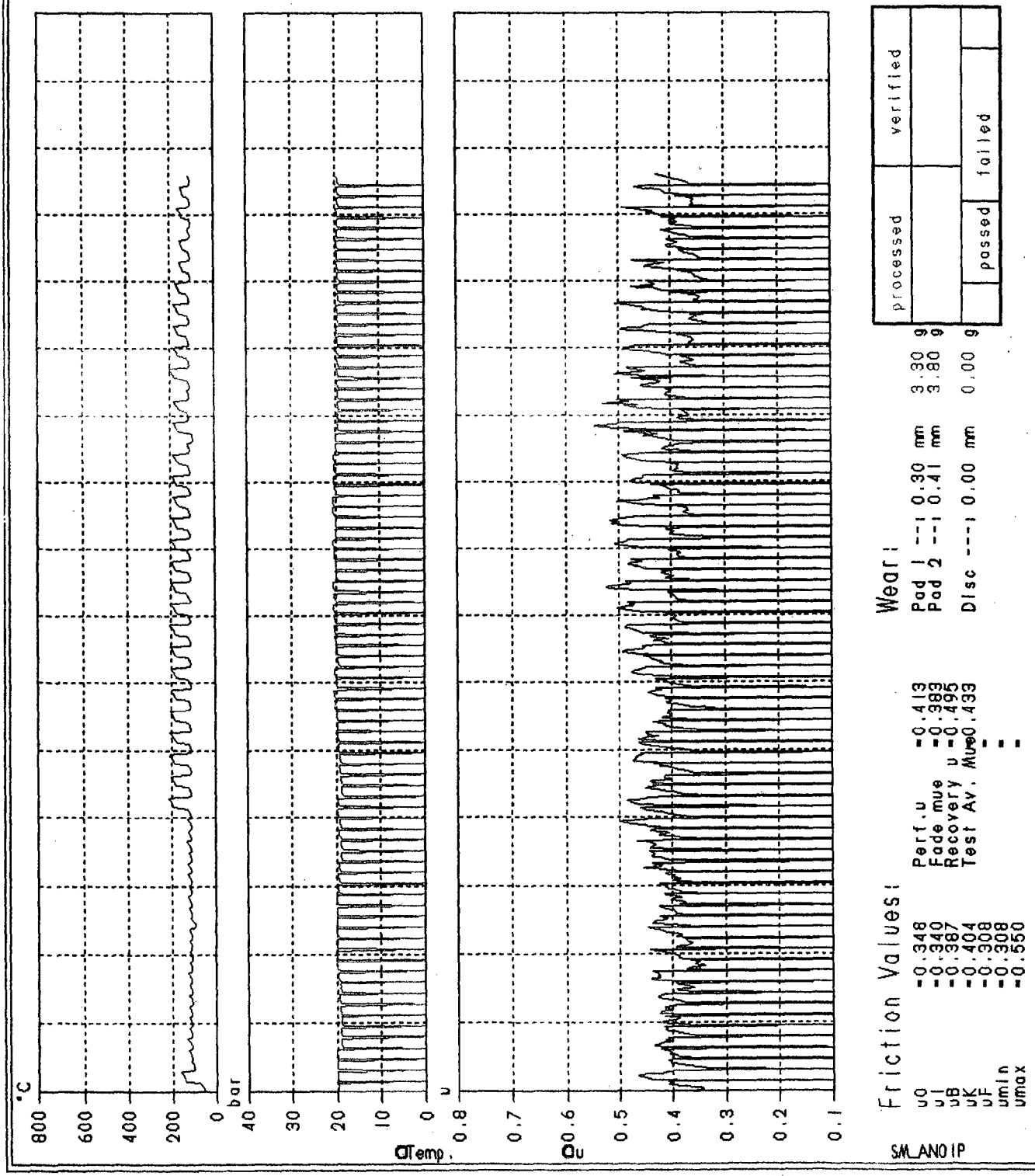

ALLIED NIPPON LTD.

(A joint venture with Japan Brake Ind. Co.)

TEST PROTOCOL
FRICTION TEST

A19

Test program	STANDARD TEST
Program no.	0051
Protocol no.	IIT (24)
Operator	VIJAY
Tester	OWI18
Test Date	14.01.2009
WVA no.	20731 00
Index	ADB130 FM 29.1
Batch	SAMPLE
Customer	
Customer no.	ADB-0130

Comment:
STANDARD TEST

Technical Data:

Caliper	SLIDING
Disc dia	215mm
Disc thickness	10.5mm
Disc no.	0
Test no.	8911
Frict. Radius	95.5mm
Pad Area	29.1cm²
Test Pressure	20.0 Bar

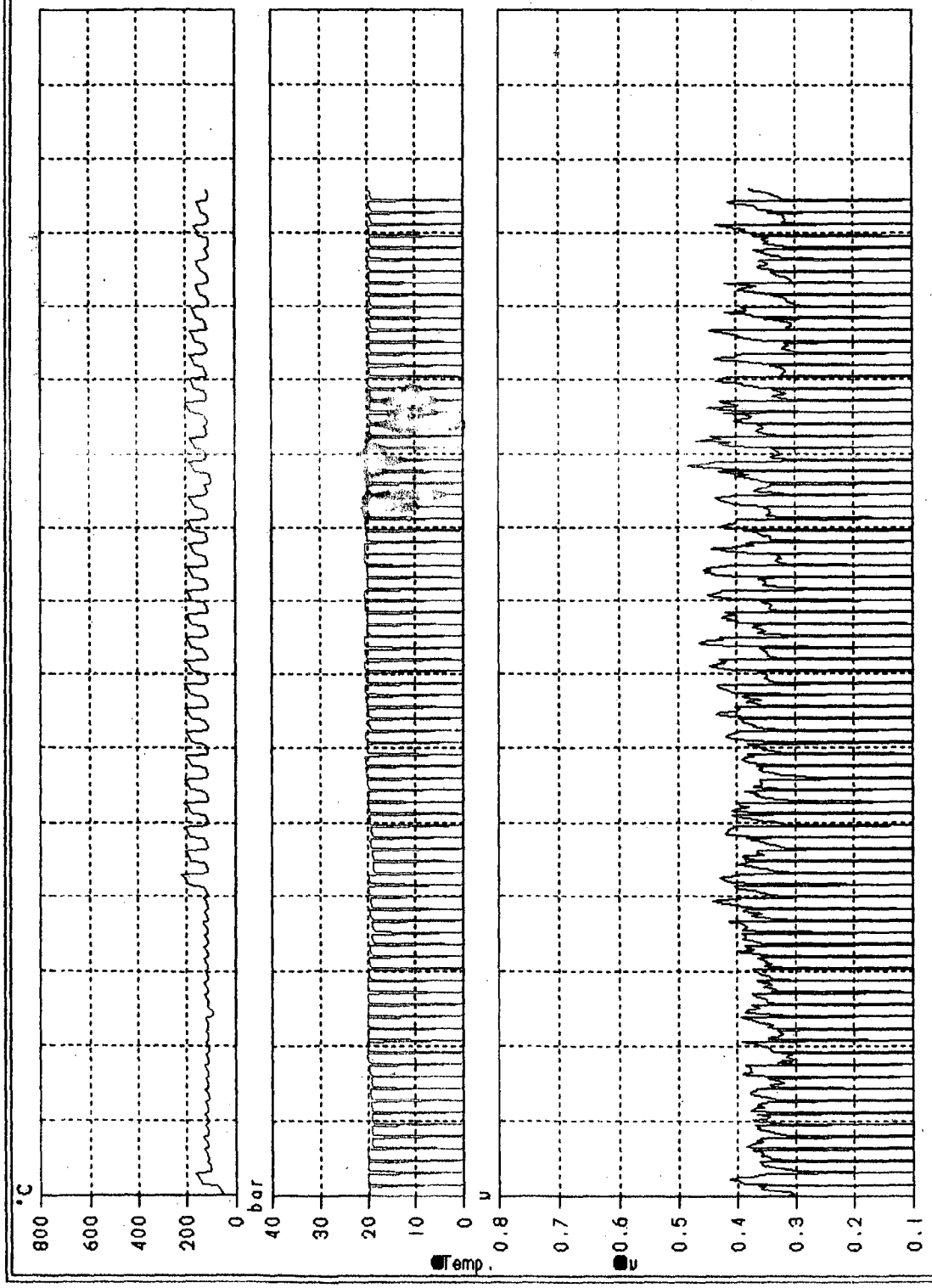

	processed	verified
passed		failed

Wear:

Pad 1	0.31 mm	3.00 g
Pad 2	0.35 mm	3.20 g
Disc	0.00 mm	0.00 g

Friction Values:

u0	-0.308	Perf.u	-0.365
u1	-0.301	Fade mue	-0.339
uB	-0.342	Recovery u	-0.438
uK	-0.358	Test Av. Mue	0.383
uF	-0.273		
umin	-0.273		
umax	-0.486		

SM_AN01P

ALLIED NIPPON LTD.

(A joint venture with Japan Brake Ind. Co.)

TEST PROTOCOL
FRICTION TEST

A20

Test program	STANDARD TEST
Program no.	0051
Protocol no.	IIT (23)
Operator	VIJAY
Tester	OWI18
Test Date	14.01.2009
WVA no.	20731 00
Index	ADB130 FM 29.1
Batch	SAMPLE
Customer	
Customer no.	ADB-0130

Comment:
STANDARD TEST

Technical Data:

Caliper	SLIDING
Disc dia	215mm
Disc thickness	10.5mm
Disc no.	0
Test no.	8910
Frict. Radius	95.5mm
Pad Area	29.1 cm²
Test Pressure	20.0 Bar

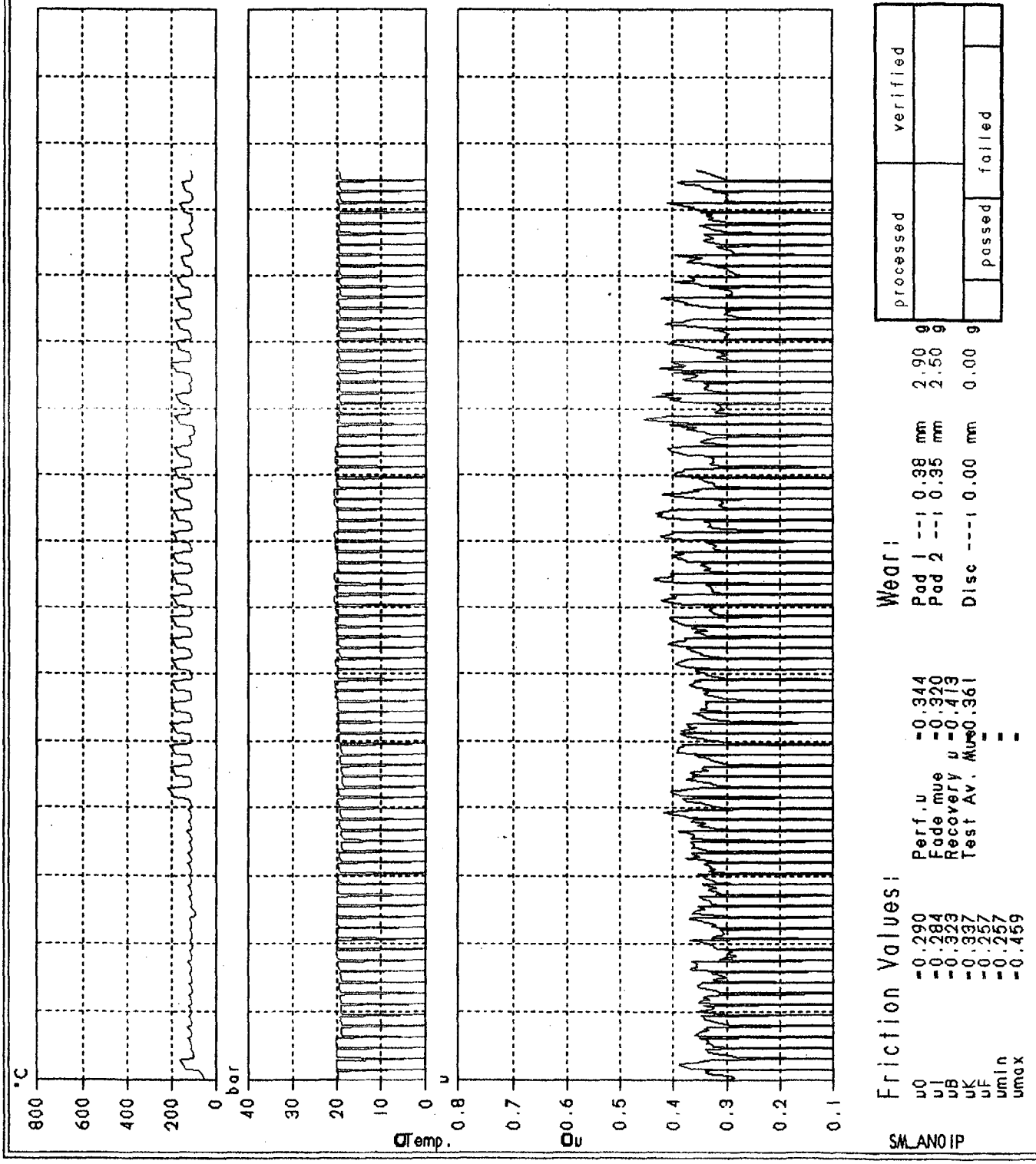

ALLIED NIPPON LTD.

(A joint venture with Japan Brake Ind. Co.)

TEST PROTOCOL
FRICTION TEST

A21

Test program ---: STANDARD TEST
Program no. ----: 0051
Protocol no. ---: IIT (21)
Operator -------: VIJAY
Tester ---------: OWI18
Test Date ------: 14.01.2009
WVA no. --------: 20731 00
Index ----------: ADB130 FM 29.1
Batch ----------: SAMPLE
Customer -------:
Customer no. ---: ADB-0130
Comment:
STANDARD TEST

Technical Data:

Caliper -------: SLIDING
Disc dia ------: 215mm
Disc thickness : 10.5mm
Disc no. ------: 0
Test no. ------: 8909
Frict. Radius -: 95.5mm
Pad Area ------: 29.1 cm²
Test Pressure--: 20.0 Bar

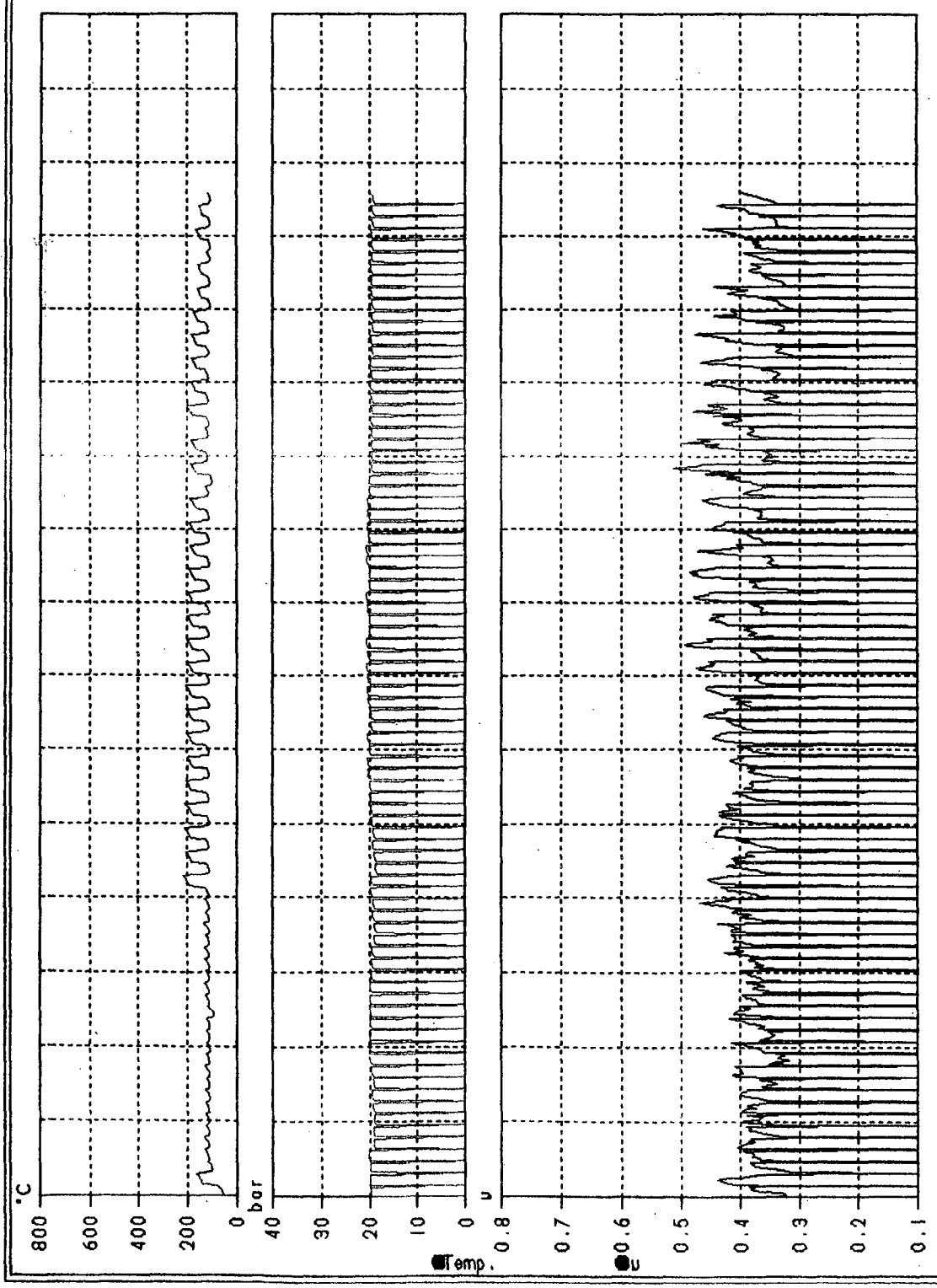

processed | verified
passed | failed

Wear:
Pad 1 --: 0.40 mm 6.30 g
Pad 2 --: 0.43 mm 8.90 g
Disc ---: 0.00 mm 0.00 g

Friction Values:

u0	-0.327	Perf.u	-0.388
u1	-0.320	Fade mue	-0.360
uB	-0.363	Recovery u	-0.465
uK	-0.380	Test Av. Mue	0.407
uF	-0.290		
umin	-0.290		
umax	-0.517		

SM_AN01P

Annexure- II

Sub-scale dynamometer test for brake pads of AN32 aircraft

(Page B1 to B24)

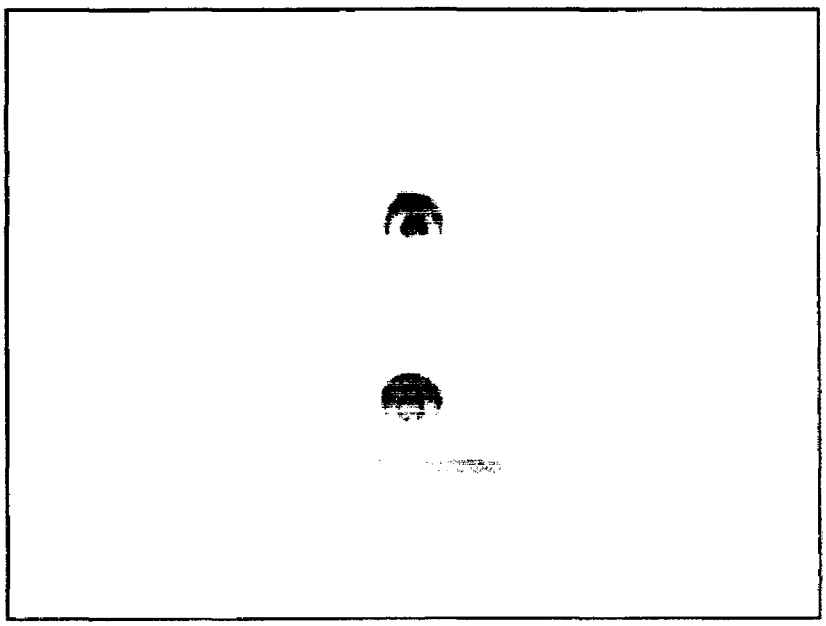

DEVELOPED BRAKE PAD FOR AN-32 AIRCRAFT

HINDUSTAN AERONAUTICS LIMITED - BANGALORE

FOUNDRY AND FORGE DIVISION

B1

FRICTION TEST CONSOLIDATED REPORT

Date	9/22/2009	
Time	1:32:54 PM	
Project Name	IIT-ROORKEE	
Part No	RR-AL-23-1	
Batch Number	AL-23-1	
Brake Speed	1000	RPM
Brake Pressure	19.46	kg/sq.cm
Brake Force	160	kgf
File Name	AL-23-1_9_22_2009_1_32_54 PM	

	Kinetic Energy (kgfm)	RD rev.	RD time (sec)	Coefficient of friction	Mean Torque (kgfm)	Peak Torque (kgfm)	Mean Drag (kgf)	Peak Drag (kgf)	Pad1-Temp (DegC)	Pad2-Temp (DegC)
Max	17300	64	7.7	0.36	41	69	228	384	122	0
Min	17300	49	5.9	0.3	34	49	191	271	38	0
Avg	17300	54	6.5	0.34	39	60	216	334	80	0

WEAR REPORT

PAD No	THICKNESS in mm			WEIGHT IN grams		
	Initial	Final	Wear	Initial	Final	Wear
1	10.74	10.19	0.55	2377	2370	7
2	10.67	9.99	0.68	2376	2370	6

Total Number of Cycles completed: 50

DISPOSITION :

PRODUCTION/DEVELOPMENT : As reported.

24/9/09

HINDUSTAN AERONAUTICS LIMITED - BANGALORE

FOUNDRY AND FORGE DIVISION

B2

FRICTION TEST FINAL REPORT

Date	9/22/2009	
Time	1:32:54 PM	
Project Name	IIT-ROORKEE	
Part No	RR-AL-23-1	
Batch Number	AL-23-1	
Brake Speed	1000	RPM
Brake Pressure	19.46	kg/sq.cm
Brake Force	160	Kgf
File Name	AL-23-1_9_22_2009_1_32_54 PM	

Sl NO	Kinetic Energy (kgfm)	RD rev.	RD time (sec)	Coefficient of friction	Mean Torque (kgfm)	Peak Torque (kgfm)	Mean Drag (kgf)	Peak Drag (kgf)	Pad1-Temp (DegC)	Pad2-Temp (DegC)
1	17300	61	7.4	0.31	36	55	198	307	38	0
2	17300	64	7.6	0.30	34	49	191	271	39	0
3	17300	62	7.5	0.30	35	52	195	290	40	0
4	17300	63	7.6	0.31	35	51	196	285	41	0
5	17300	64	7.7	0.30	35	55	194	304	43	0
6	17300	61	7.4	0.31	36	55	199	305	45	0
7	17300	57	6.9	0.33	38	55	209	306	46	0
8	17300	55	6.7	0.33	38	54	210	301	48	0
9	17300	57	6.8	0.34	39	61	215	339	49	0
10	17300	58	6.9	0.33	38	53	210	293	51	0
11	17300	57	6.9	0.33	38	54	212	300	52	0
12	17300	54	6.5	0.35	40	62	222	342	53	0
13	17300	56	6.7	0.34	39	56	215	312	55	0
14	17300	55	6.6	0.35	40	58	220	325	57	0
15	17300	57	6.9	0.33	38	60	212	335	59	0
16	17300	56	6.7	0.33	38	58	211	323	60	0
17	17300	56	6.8	0.33	37	69	208	384	63	0
18	17300	55	6.6	0.34	39	52	215	289	65	0
19	17300	56	6.7	0.33	38	63	212	352	66	0
20	17300	57	6.8	0.33	38	59	208	329	69	0
21	17300	55	6.6	0.34	39	63	216	351	71	0
22	17300	53	6.4	0.35	40	61	220	339	73	0
23	17300	54	6.5	0.33	38	52	211	291	75	0
24	17300	52	6.3	0.35	40	62	221	344	77	0
25	17300	53	6.4	0.35	39	59	218	330	79	0
26	17300	53	6.3	0.35	40	59	222	326	81	0
27	17300	52	6.3	0.35	40	59	220	326	83	0
28	17300	52	6.2	0.35	40	60	222	331	86	0
29	17300	51	6.1	0.35	40	62	222	347	88	0
30	17300	52	6.2	0.34	39	56	217	314	90	0
31	17300	52	6.2	0.35	39	58	219	325	92	0
32	17300	50	6.0	0.36	41	57	228	317	94	0
33	17300	51	6.2	0.35	40	65	223	362	96	0
34	17300	53	6.4	0.34	39	63	215	348	98	0
35	17300	53	6.3	0.35	39	64	218	358	98	0
36	17300	50	6.0	0.36	41	64	226	357	100	0
37	17300	51	6.1	0.36	40	67	225	370	103	0
38	17300	49	5.9	0.36	40	63	224	351	105	0
39	17300	52	6.3	0.35	39	69	217	383	107	0
40	17300	50	6.0	0.36	41	67	228	374	108	0
41	17300	51	6.1	0.36	40	68	224	375	109	0
42	17300	52	6.3	0.35	40	62	220	342	111	0
43	17300	49	5.9	0.36	41	67	226	372	112	0
44	17300	52	6.3	0.36	41	60	226	335	114	0
45	17300	52	6.2	0.35	40	61	221	341	115	0
46	17300	52	6.2	0.35	40	67	220	371	117	0
47	17300	50	6.1	0.35	40	65	222	362	118	0
48	17300	49	5.9	0.36	41	66	228	367	119	0
49	17300	52	6.2	0.35	40	61	221	339	121	0
50	17300	52	6.3	0.35	39	65	217	359	122	0

HINDUSTAN AERONAUTICS LIMITED - BANGALORE

FOUNDRY AND FORGE DIVISION

B3

FRICTION TEST CONSOLIDATED REPORT

Date	9/23/2009	
Time	7:09:55 AM	
Project Name	IIT-ROORKEE	
Part No	RR-AL-24-1	
Batch Number	AL-24-1	
Brake Speed	1000	RPM
Brake Pressure	19.86	kg/sq.cm
Brake Force	160	kgf
File Name	AL-24-1_9_23_2009_7_09_55 AM	

	Kinetic Energy (kgfm)	RD rev.	RD time (sec)	Coefficient of friction	Mean Torque (kgfm)	Peak Torque (kgfm)	Mean Drag (kgf)	Peak Drag (kgf)	Pad1-Temp (DegC)	Pad2-Temp (DegC)
Max	17300	60	7.2	0.35	40	76	221	422	135	0
Min	17300	51	6.2	0.31	36	50	199	278	35	0
Avg	17300	56	6.7	0.33	38	60	210	333	86	0

WEAR REPORT

PAD No	THICKNESS in mm			WEIGHT IN grams		
	Initial	Final	Wear	Initial	Final	Wear
1	10.54	9.44	1.1	2374	2365	9
2	11.61	9	2.61	2385	2364	21

Total Number of Cycles completed: 50

DISPOSITION :

PRODUCTION/DEVELOPMENT : As reported

24/9/09.

HINDUSTAN AERONAUTICS LIMITED - BANGALORE

FOUNDRY AND FORGE DIVISION

B4

FRICTION TEST FINAL REPORT

Date	9/23/2009	
Time	7:09:55 AM	
Project Name	IIT-ROORKEE	
Part No	RR-AL-24-1	
Batch Number	AL-24-1	
Brake Speed	1000	RPM
Brake Pressure	19.86	kg/sq.cm
Brake Force	160	Kgf
File Name	AL-24-1_9_23_2009_7_09_55 AM	

Sl NO	Kinetic Energy (kgfm)	RD rev.	RD time (sec)	Coefficient of friction	Mean Torque (kgfm)	Peak Torque (kgfm)	Mean Drag (kgf)	Peak Drag (kgf)	Pad1-Temp (DegC)	Pad2-Temp (DegC)
1	17300	60	7.2	0.31	36	54	199	301	35	0
2	17300	59	7.1	0.31	36	55	202	306	36	0
3	17300	58	7.0	0.31	36	52	202	289	36	0
4	17300	59	7.1	0.32	37	50	204	278	37	0
5	17300	58	6.9	0.32	37	56	207	309	38	0
6	17300	57	6.9	0.32	38	57	208	319	40	0
7	17300	57	6.9	0.32	37	60	208	336	41	0
8	17300	59	7.1	0.32	37	52	204	287	44	0
9	17300	58	7.0	0.32	37	59	208	328	46	0
10	17300	56	6.7	0.33	38	63	211	351	48	0
11	17300	56	6.8	0.33	38	57	209	318	50	0
12	17300	56	6.7	0.33	38	51	211	285	53	0
13	17300	56	6.7	0.33	38	59	212	327	55	0
14	17300	55	6.7	0.33	38	55	210	305	58	0
15	17300	54	6.4	0.33	38	59	213	329	60	0
16	17300	54	6.5	0.33	38	58	214	320	63	0
17	17300	55	6.6	0.33	38	61	210	338	65	0
18	17300	55	6.6	0.33	38	57	214	317	68	0
19	17300	55	6.6	0.32	37	57	205	315	71	0
20	17300	58	7.0	0.31	36	52	202	289	73	0
21	17300	55	6.6	0.32	38	65	209	359	76	0
22	17300	57	6.8	0.32	37	54	206	300	79	0
23	17300	56	6.7	0.32	38	58	208	321	81	0
24	17300	55	6.6	0.33	38	57	214	316	84	0
25	17300	53	6.4	0.33	39	58	215	322	87	0
26	17300	56	6.7	0.33	38	66	210	368	89	0
27	17300	57	6.9	0.32	37	58	205	321	92	0
28	17300	54	6.5	0.33	38	57	210	315	95	0
29	17300	56	6.7	0.33	38	58	211	320	97	0
30	17300	53	6.4	0.34	40	64	221	356	100	0
31	17300	54	6.5	0.34	39	66	217	367	102	0
32	17300	53	6.4	0.35	40	66	221	369	103	0
33	17300	57	6.9	0.32	37	59	208	330	106	0
34	17300	55	6.6	0.34	39	75	215	418	108	0
35	17300	55	6.6	0.34	39	60	215	331	110	0
36	17300	56	6.7	0.33	38	58	211	325	113	0
37	17300	58	6.9	0.33	38	61	209	338	115	0
38	17300	56	6.8	0.33	38	66	210	364	116	0
39	17300	53	6.4	0.33	38	76	210	422	119	0
40	17300	51	6.2	0.34	39	69	218	382	121	0
41	17300	56	6.7	0.33	38	61	213	337	123	0
42	17300	57	6.8	0.33	38	57	211	316	124	0
43	17300	58	7.0	0.32	37	60	205	333	124	0
44	17300	57	6.9	0.33	38	66	211	367	125	0
45	17300	56	6.8	0.33	38	73	212	404	126	0
46	17300	54	6.5	0.33	39	60	214	332	128	0
47	17300	56	6.8	0.33	38	58	210	323	130	0
48	17300	57	6.9	0.33	38	63	209	352	132	0
49	17300	58	7.0	0.32	37	61	207	341	133	0
50	17300	58	6.9	0.33	38	66	209	368	135	0

F - 50

HINDUSTAN AERONAUTICS LIMITED - BANGALORE

FOUNDRY AND FORGE DIVISION

B5

FRICTION TEST CONSOLIDATED REPORT

Date	9/23/2009	
Time	1:45:22 PM	
Project Name	IIT-ROORKEE	
Part No	RR-AL-25-1	
Batch Number	AL-25-1	
Brake Speed	1000	RPM
Brake Pressure	18.68	kg/sq.cm
Brake Force	160	kgf
File Name	AL-25-1_9_23_2009_1_45_22 PM	

	Kinetic Energy (kgfm)	RD rev.	RD time (sec)	Coefficient of friction	Mean Torque (kgfm)	Peak Torque (kgfm)	Mean Drag (kgf)	Peak Drag (kgf)	Pad1-Temp (DegC)	Pad2-Temp (DegC)
Max	17300	59	7.1	0.38	42	74	231	411	132	0
Min	17300	50	6.1	0.33	37	54	203	301	41	0
Avg	17300	53	6.4	0.36	39	62	219	346	83	0

WEAR REPORT

PAD No	THICKNESS in mm			WEIGHT IN grams		
	Initial	Final	Wear	Initial	Final	Wear
1	10.46	10.04	0.42	2379	2370	9
2	11.26	1.74	0.52	2372	2364	8

Total Number of Cycles completed: 50

DISPOSITION : As reported

PRODUCTION/DEVELOPMENT : 24/9/09

Development file.

HINDUSTAN AERONAUTICS LIMITED - BANGALORE

B8

FOUNDRY AND FORGE DIVISION

FRICTION TEST FINAL REPORT

Date	**12/22/2008**	
Time	**10:05:17 AM**	
Project Name	**AL BRAKE PAD**	
Part No	**RR 21**	
Batch Number	**RR 21**	
Brake Speed	**835**	**RPM**
Brake Pressure	**11.9**	**kg/sq.cm**
Brake Force	**100**	**Kgf**
File Name	**RR 21_12_22_2008_10_05_17 AM**	

Sl NO	Kinetic Energy (kgfm)	RD rev.	RD time (sec)	Coefficient of friction	Mean Torque (kgfm)	Peak Torque (kgfm)	Mean Drag (kgf)	Peak Drag (kgf)	Pad1-Temp (DegC)	Pad2-Temp (DegC)
1	12000	89	12.7	0.28	20	38	109	210	0	116
2	12000	91	13.1	0.28	20	34	111	190	0	111
3	12000	89	12.7	0.29	21	38	114	210	0	108
4	12000	87	12.5	0.30	21	32	116	176	0	104
5	12000	87	12.5	0.29	21	31	115	170	0	102
6	12000	86	12.4	0.30	21	30	115	169	0	99
7	12000	85	12.2	0.30	21	35	118	195	0	97
8	12000	86	12.3	0.30	21	31	116	172	0	95
9	12000	85	12.2	0.30	21	30	117	168	0	94
10	12000	81	11.6	0.31	21	33	119	185	0	93
11	12000	83	12.0	0.31	22	33	120	181	0	91
12	12000	81	11.7	0.31	22	31	121	175	0	91
13	12000	80	11.6	0.32	22	41	124	229	0	91
14	12000	81	11.7	0.32	22	33	123	183	0	90
15	12000	83	11.9	0.32	22	42	123	234	0	89
16	12000	82	11.8	0.31	22	35	123	193	0	89
17	12000	85	12.2	0.31	21	31	119	171	0	89
18	12000	83	12.0	0.31	22	34	120	186	0	89
19	12000	81	11.6	0.31	22	31	121	173	0	89
20	12000	84	12.1	0.30	21	34	118	186	0	89
21	12000	82	11.8	0.31	22	30	122	164	0	89
22	12000	83	11.9	0.31	22	35	121	193	0	89
23	12000	82	11.7	0.32	22	32	123	176	0	89
24	12000	80	11.5	0.32	23	33	125	183	0	89
25	12000	78	11.2	0.33	23	34	129	189	0	89
26	12000	79	11.3	0.33	23	31	126	171	0	89
27	12000	78	11.3	0.33	23	49	127	274	0	89
28	12000	80	11.5	0.32	23	33	125	183	0	90
29	12000	78	11.3	0.33	23	47	128	261	0	90
30	12000	78	11.2	0.33	23	34	128	190	0	91
31	12000	79	11.4	0.33	23	34	128	187	0	91
32	12000	76	10.9	0.34	24	40	133	223	0	91
33	12000	76	10.9	0.34	24	31	133	174	0	91
34	12000	73	10.5	0.35	24	36	136	198	0	92
35	12000	73	10.5	0.35	25	37	137	207	0	92
36	12000	74	10.6	0.35	24	32	134	178	0	92
37	12000	75	10.8	0.35	24	31	133	173	0	92
38	12000	75	10.7	0.35	24	35	134	193	0	92
39	12000	77	11.0	0.34	24	36	131	199	0	93
40	12000	77	11.0	0.34	23	32	130	177	0	93
41	12000	74	10.7	0.34	23	32	130	176	0	94
42	12000	75	10.7	0.34	23	32	131	178	0	94
43	12000	76	11.0	0.34	24	32	132	177	0	94
44	12000	76	10.9	0.34	24	32	132	177	0	95
45	12000	76	11.0	0.34	24	36	131	202	0	95
46	12000	79	11.3	0.33	23	37	128	203	0	95
47	12000	78	11.2	0.34	23	32	129	179	0	96
48	12000	78	11.3	0.33	23	32	128	180	0	96
49	12000	79	11.3	0.33	23	33	127	181	0	96
50	12000	77	11.1	0.34	23	34	129	187	0	96

HINDUSTAN AERONAUTICS LIMITED - BANGALORE

FOUNDRY AND FORGE DIVISION

B9

FRICTION TEST CONSOLIDATED REPORT

Date	9/10/2008	
Time	12:09:10 PM	
Project Name	ROORKEE	
Part No	ALLUMINIUM PAD	
Batch Number	PM08RK33-2	
Brake Speed	835	RPM
Brake Pressure	10.97	kg/sq.cm
Brake Force	100	kgf
File Name	PM08RK33-2_9_10_2008_12_09_10 PM	

	Kinetic Energy	RD rev.	RD time	Coefficient	Mean Torque	Peak Torque	Mean Drag	Peak Drag	Pad1-Temp	Pad2-Temp
	(kgfm)		(sec)	of friction	(kgfm)	(kgfm)	(kgf)	(kgf)	(DegC)	(DegC)
Max	12000	77	11.1	0.41	26	63	146	348	133	117
Min	12000	60	8.6	0.33	22	37	120	203	47	52
Avg	12000	64	9.2	0.39	25	44	139	247	96	83

WEAR REPORT

PAD	THICKNESS in mm			WEIGHT IN grams		
No	Initial	Final	Wear	Initial	Final	Wear
1	10.32	9.53	0.79	2400	2393	7
2	9.77	9.14	0.63	2395	2388	7

Total Number of Cycles completed: 50

DISPOSITION :

PRODUCTION/DEVELOPMENT :

HINDUSTAN AERONAUTICS LIMITED - BANGALORE

B10

FOUNDRY AND FORGE DIVISION

FRICTION TEST FINAL REPORT

Date	9/10/2008	
Time	12:09:10 PM	
Project Name	ROORKEE	
Part No	ALLUMINIUM PAD	
Batch Number	PM08RK33-2	
Brake Speed	835	RPM
Brake Pressure	10.97	kg/sq.cm
Brake Force	100	Kgf
File Name	PM08RK33-2_9_10_2008_12_09_10 PM	

Sl NO	Kinetic Energy (kgfm)	RD rev.	RD time (sec)	Coefficient of friction	Mean Torque (kgfm)	Peak Torque (kgfm)	Mean Drag (kgf)	Peak Drag (kgf)	Pad1-Temp (DegC)	Pad2-Temp (DegC)
1	12000	77	11.1	0.33	22	37	120	203	47	52
2	12000	74	10.6	0.34	22	41	124	227	49	52
3	12000	73	10.5	0.34	23	38	125	210	52	53
4	12000	69	9.9	0.36	23	37	131	205	55	53
5	12000	71	10.2	0.35	23	37	127	206	58	54
6	12000	69	9.9	0.36	24	39	131	217	60	55
7	12000	65	9.4	0.38	25	38	137	211	61	56
8	12000	65	9.4	0.38	25	42	138	233	64	57
9	12000	65	9.3	0.38	25	42	138	234	66	58
10	12000	64	9.2	0.39	25	43	139	240	69	59
11	12000	63	9.0	0.40	26	39	142	216	71	61
12	12000	61	8.8	0.40	26	41	142	225	75	62
13	12000	62	8.9	0.40	26	40	142	221	77	63
14	12000	62	8.9	0.40	26	45	142	247	79	65
15	12000	63	9.0	0.40	25	39	141	218	80	66
16	12000	63	9.1	0.39	25	47	140	262	83	68
17	12000	63	9.1	0.39	25	44	139	245	85	69
18	12000	63	9.1	0.39	25	47	140	261	86	70
19	12000	63	9.0	0.40	25	59	141	326	89	72
20	12000	61	8.7	0.41	26	63	146	348	91	74
21	12000	61	8.8	0.40	26	49	144	272	94	75
22	12000	63	9.0	0.40	25	46	141	258	95	77
23	12000	61	8.7	0.40	26	49	144	273	96	78
24	12000	61	8.8	0.40	26	43	143	239	97	80
25	12000	61	8.8	0.40	26	46	143	255	99	82
26	12000	62	8.9	0.40	25	41	142	229	100	83
27	12000	60	8.6	0.41	26	50	145	278	102	85
28	12000	63	9.0	0.40	26	51	142	284	103	87
29	12000	62	8.9	0.41	26	46	144	255	105	88
30	12000	61	8.8	0.41	26	46	144	255	107	90
31	12000	61	8.8	0.41	26	49	143	270	108	91
32	12000	63	9.0	0.40	25	46	141	253	110	92
33	12000	62	8.9	0.41	26	50	143	280	111	94
34	12000	63	9.0	0.40	25	45	142	247	113	96
35	12000	62	8.9	0.40	25	39	140	217	114	97
36	12000	64	9.1	0.40	25	52	140	291	116	98
37	12000	63	9.1	0.40	25	50	141	276	117	100
38	12000	63	9.0	0.40	25	42	141	235	119	102
39	12000	63	9.1	0.40	25	41	141	230	120	104
40	12000	63	9.1	0.40	25	47	141	263	121	105
41	12000	64	9.2	0.39	25	45	139	253	123	106
42	12000	63	9.1	0.40	25	40	140	222	124	107
43	12000	63	9.1	0.40	25	40	140	224	125	108
44	12000	66	9.4	0.39	25	39	138	216	125	110
45	12000	66	9.5	0.38	24	42	136	231	127	111
46	12000	64	9.2	0.40	25	45	140	252	129	112
47	12000	64	9.3	0.39	25	49	139	271	130	114
48	12000	65	9.4	0.39	25	42	138	232	131	115
49	12000	64	9.1	0.39	25	50	139	280	132	117
50	12000	65	9.3	0.40	25	46	140	258	133	117

F A/--25

HINDUSTAN AERONAUTICS LIMITED - BANGALORE

FOUNDRY AND FORGE DIVISION

. B11

FRICTION TEST CONSOLIDATED REPORT

Date	12/24/2008	
Time	10:29:19 AM	
Project Name	AL BRAKE PAD	
Part No	RR 24	
Batch Number	RR 24	
Brake Speed	835	RPM
Brake Pressure	12.1	kg/sq.cm
Brake Force	100	kgf
File Name	RR 24_12_24_2008_10_29_19 AM	

	Kinetic Energy (kgfm)	RD rev.	RD time (sec)	Coefficient of friction	Mean Torque (kgfm)	Peak Torque (kgfm)	Mean Drag (kgf)	Peak Drag (kgf)	Pad1-Temp (DegC)	Pad2-Temp (DegC)
Max	12000	93	13.4	0.31	22	56	121	314	0	103
Min	12000	82	11.8	0.27	19	32	107	180	0	52
Avg	12000	85	12.2	0.3	21	43	118	239	0	79

WEAR REPORT

PAD No	THICKNESS in mm			WEIGHT IN grams		
	Initial	Final	Wear	Initial	Final	Wear
1	9.32	8.97	0.35	2359	2356	3
2	8.75	8.37	0.38	2354	2350	4

Total Number of Cycles completed: 50

DISPOSITION :

PRODUCTION/DEVELOPMENT :

HINDUSTAN AERONAUTICS LIMITED - BANGALORE

B12

FOUNDRY AND FORGE DIVISION

FRICTION TEST FINAL REPORT

Date	**12/24/2008**	
Time	**10:29:19 AM**	
Project Name	**AL BRAKE PAD**	
Part No	**RR 24**	
Batch Number	**RR 24**	
Brake Speed	**835**	**RPM**
Brake Pressure	**12.1**	**kg/sq.cm**
Brake Force	**100**	**Kgf**
File Name	**RR 24_12_24_2008_10_29_19 AM**	

Sl NO	Kinetic Energy (kgfm)	RD rev.	RD time (sec)	Coefficient of friction	Mean Torque (kgfm)	Peak Torque (kgfm)	Mean Drag (kgf)	Peak Drag (kgf)	Pad1-Temp (DegC)	Pad2-Temp (DegC)
1	12000	83	11.9	0.29	21	49	117	271	0	52
2	12000	93	13.4	0.27	19	41	107	227	0	53
3	12000	91	13.0	0.28	20	32	110	180	0	53
4	12000	91	13.0	0.28	20	38	112	210	0	53
5	12000	89	12.7	0.28	20	33	113	183	0	54
6	12000	85	12.3	0.29	21	39	116	215	0	55
7	12000	86	12.4	0.29	21	37	116	204	0	56
8	12000	86	12.4	0.30	21	55	118	305	0	58
9	12000	86	12.3	0.30	21	40	118	224	0	59
10	12000	87	12.5	0.29	21	40	116	223	0	61
11	12000	88	12.6	0.29	21	46	116	255	0	62
12	12000	87	12.6	0.29	21	43	116	241	0	63
13	12000	87	12.5	0.29	21	53	115	296	0	64
14	12000	86	12.4	0.30	21	34	117	188	0	66
15	12000	86	12.4	0.30	21	50	117	279	0	67
16	12000	85	12.2	0.30	21	44	118	244	0	69
17	12000	84	12.0	0.30	22	36	120	198	0	70
18	12000	83	11.9	0.30	22	37	120	203	0	71
19	12000	84	12.1	0.30	22	49	120	271	0	72
20	12000	83	11.9	0.30	22	36	120	199	0	74
21	12000	84	12.0	0.30	21	40	119	220	0	75
22	12000	83	11.9	0.31	22	46	121	254	0	77
23	12000	83	11.9	0.30	22	45	120	249	0	78
24	12000	83	12.0	0.30	22	44	120	244	0	79
25	12000	84	12.0	0.31	22	51	120	285	0	80
26	12000	83	11.9	0.31	22	47	120	262	0	81
27	12000	83	11.9	0.31	22	50	120	280	0	82
28	12000	83	11.9	0.31	22	38	120	211	0	84
29	12000	82	11.8	0.31	22	56	120	314	0	84
30	12000	83	11.9	0.30	21	51	119	281	0	86
31	12000	84	12.0	0.31	22	35	120	195	0	87
32	12000	83	11.9	0.31	22	48	120	267	0	87
33	12000	84	12.1	0.31	22	51	120	284	0	89
34	12000	83	11.9	0.31	22	46	120	258	0	90
35	12000	83	11.9	0.31	22	46	121	258	0	91
36	12000	83	11.9	0.31	22	37	120	208	0	92
37	12000	83	12.0	0.31	22	38	120	211	0	92
38	12000	84	12.0	0.31	21	34	119	192	0	94
39	12000	84	12.0	0.31	21	45	119	252	0	94
40	12000	84	12.0	0.30	21	38	119	211	0	95
41	12000	83	11.9	0.31	22	39	120	217	0	96
42	12000	83	12.0	0.31	21	40	119	221	0	97
43	12000	83	12.0	0.31	21	54	119	300	0	98
44	12000	83	11.9	0.31	21	39	119	217	0	99
45	12000	85	12.2	0.30	21	38	117	209	0	99
46	12000	85	12.3	0.30	21	38	118	213	0	101
47	12000	84	12.1	0.30	21	56	118	308	0	100
48	12000	84	12.1	0.30	21	39	118	219	0	102
49	12000	86	12.3	0.30	21	56	117	311	0	102
50	12000	84	12.1	0.30	21	35	118	195	0	103

HINDUSTAN AERONAUTICS LIMITED - BANGALORE

B13

FOUNDRY AND FORGE DIVISION

FRICTION TEST CONSOLIDATED REPORT

Date	12/20/2008	
Time	12:45:47 PM	
Project Name	AL BRAKE PAD	
Part No	RR 25	
Batch Number	RR 25	
Brake Speed	835	RPM
Brake Pressure	11.53	kg/sq.cm
Brake Force	100	kgf
File Name	AL 08 DR 20-(25)_12_20_2008_12_45_47 PM	

	Kinetic Energy	RD rev.	RD time	Coefficient	Mean Torque	Peak Torque	Mean Drag	Peak Drag	Pad1-Temp	Pad2-Temp
	(kgfm)		(sec)	of friction	(kgfm)	(kgfm)	(kgf)	(kgf)	(DegC)	(DegC)
Max	12000	109	15.7	0.31	21	46	116	258	0	84
Min	12000	86	12.4	0.25	17	27	93	147	0	47
Avg	12000	94	13.4	0.29	19	32	108	178	0	64

WEAR REPORT

PAD	THICKNESS in mm			WEIGHT IN grams		
No	Initial	Final	Wear	Initial	Final	Wear
1	7.7	7.58	0.12	2352	2349	3
2	7.58	7.33	0.25	2350	2347	3

Total Number of Cycles completed: 50

DISPOSITION :

PRODUCTION/DEVELOPMENT :

HINDUSTAN AERONAUTICS LIMITED - BANGALORE

B14

FOUNDRY AND FORGE DIVISION

FRICTION TEST FINAL REPORT

Date	**12/20/2008**	
Time	**12:45:47 PM**	
Project Name	**AL BRAKE PAD**	
Part No	**RR 25**	
Batch Number	**RR 25**	
Brake Speed	**835**	**RPM**
Brake Pressure	**11.53**	**kg/sq.cm**
Brake Force	**100**	**Kgf**
File Name	**AL 08 DR 20-(25)_12_20_2008_12_45_47 PM**	

Sl NO	Kinetic Energy (kgfm)	RD rev.	RD time (sec)	Coefficient of friction	Mean Torque (kgfm)	Peak Torque (kgfm)	Mean Drag (kgf)	Peak Drag (kgf)	Pad1-Temp (DegC)	Pad2-Temp (DegC)
1	12000	109	15.7	0.25	17	29	93	160	0	47
2	12000	108	15.5	0.25	17	27	94	147	0	47
3	12000	105	15.1	0.26	17	28	97	157	0	48
4	12000	102	14.6	0.27	18	27	100	151	0	48
5	12000	100	14.4	0.27	18	34	101	191	0	49
6	12000	99	14.3	0.27	18	38	102	212	0	49
7	12000	98	14.0	0.28	19	30	104	165	0	50
8	12000	98	14.0	0.27	19	29	103	161	0	50
9	12000	98	14.1	0.28	19	31	104	170	0	51
10	12000	97	13.9	0.28	19	31	105	172	0	52
11	12000	96	13.8	0.28	19	32	106	176	0	52
12	12000	95	13.6	0.29	19	30	107	167	0	53
13	12000	95	13.7	0.28	19	33	106	184	0	54
14	12000	94	13.5	0.29	19	30	108	169	0	55
15	12000	95	13.7	0.28	19	30	105	165	0	55
16	12000	94	13.5	0.29	19	32	106	179	0	57
17	12000	95	13.7	0.29	19	38	107	210	0	57
18	12000	94	13.6	0.28	19	30	106	165	0	59
19	12000	95	13.6	0.29	19	30	108	167	0	59
20	12000	95	13.7	0.28	19	29	106	160	0	60
21	12000	95	13.6	0.29	19	35	107	195	0	61
22	12000	93	13.4	0.28	19	31	106	172	0	61
23	12000	93	13.4	0.29	20	33	109	183	0	63
24	12000	94	13.6	0.29	19	30	107	168	0	64
25	12000	94	13.5	0.29	19	29	108	162	0	64
26	12000	91	13.1	0.30	20	34	112	188	0	65
27	12000	91	13.1	0.30	20	31	111	175	0	66
28	12000	92	13.2	0.30	20	31	111	172	0	66
29	12000	89	12.9	0.30	20	31	114	175	0	67
30	12000	86	12.4	0.30	20	31	114	170	0	68
31	12000	87	12.5	0.31	21	46	116	258	0	69
32	12000	88	12.6	0.31	20	35	114	194	0	69
33	12000	91	13.0	0.30	20	32	112	179	0	70
34	12000	91	13.0	0.30	20	31	112	170	0	72
35	12000	91	13.0	0.30	20	32	112	176	0	72
36	12000	90	13.0	0.30	20	33	113	185	0	73
37	12000	90	13.0	0.30	20	32	112	180	0	74
38	12000	88	12.6	0.31	21	34	114	186	0	74
39	12000	89	12.8	0.31	21	33	114	181	0	75
40	12000	90	12.9	0.30	20	35	113	195	0	76
41	12000	90	12.9	0.30	20	35	113	197	0	77
42	12000	90	12.9	0.30	20	33	113	184	0	78
43	12000	90	13.0	0.30	20	35	111	193	0	78
44	12000	90	12.9	0.30	20	33	113	181	0	79
45	12000	92	13.2	0.30	20	31	111	172	0	80
46	12000	89	12.8	0.30	20	34	113	188	0	81
47	12000	90	13.0	0.30	20	31	113	172	0	81
48	12000	90	12.9	0.30	20	32	113	176	0	82
49	12000	90	12.9	0.31	20	32	113	177	0	83
50	12000	90	13.0	0.30	20	34	112	187	0	84

HINDUSTAN AERONAUTICS LIMITED - BANGALORE

B15

FOUNDRY AND FORGE DIVISION

FRICTION TEST CONSOLIDATED REPORT

Date	12/24/2008	
Time	8:03:57 AM	
Project Name	AL BRAKE PAD	
Part No	RR 22	
Batch Number	RR 22	
Brake Speed	835	RPM
Brake Pressure	12.83	kg/sq.cm
Brake Force	100	kgf
File Name	RR 22_12_24_2008_8_03_57 AM	

	Kinetic Energy	RD rev.	RD time	Coefficient	Mean Torque	Peak Torque	Mean Drag	Peak Drag	Pad1-Temp	Pad2-Temp
	(kgfm)		(sec)	of friction	(kgfm)	(kgfm)	(kgf)	(kgf)	(DegC)	(DegC)
Max	12000	90	13	0.3	23	67	126	370	0	82
Min	12000	79	11.4	0.26	20	35	110	192	0	33
Avg	12000	84	12.1	0.28	21	46	118	258	0	56

WEAR REPORT

PAD	THICKNESS in mm			WEIGHT IN grams		
No	Initial	Final	Wear	Initial	Final	Wear
1	7.79	6.69	1.1	2348	2341	7
2	8.01	7	1.01	2358	2348	10

Total Number of Cycles completed: 50

DISPOSITION :

PRODUCTION/DEVELOPMENT :

HINDUSTAN AERONAUTICS LIMITED - BANGALORE

B16

FOUNDRY AND FORGE DIVISION

FRICTION TEST FINAL REPORT

Date	**12/24/2008**	
Time	**8:03:57 AM**	
Project Name	**AL BRAKE PAD**	
Part No	**RR 22**	
Batch Number	**RR 22**	
Brake Speed	**835**	**RPM**
Brake Pressure	**12.83**	**kg/sq.cm**
Brake Force	**100**	**Kgf**
File Name	**RR 22_12_24_2008_8_03_57 AM**	

Sl NO	Kinetic Energy (kgfm)	RD rev.	RD time (sec)	Coefficient of friction	Mean Torque (kgfm)	Peak Torque (kgfm)	Mean Drag (kgf)	Peak Drag (kgf)	Pad1-Temp (DegC)	Pad2-Temp (DegC)
1	12000	89	12.8	0.27	20	55	114	307	0	33
2	12000	85	12.2	0.28	21	42	119	233	0	33
3	12000	84	12.1	0.28	22	47	121	262	0	33
4	12000	84	12.0	0.29	22	51	121	286	0	34
5	12000	80	11.5	0.29	22	51	123	285	0	35
6	12000	79	11.4	0.30	23	55	126	303	0	35
7	12000	82	11.8	0.29	22	57	124	314	0	36
8	12000	81	11.7	0.30	23	41	125	227	0	37
9	12000	81	11.7	0.30	22	53	125	294	0	38
10	12000	82	11.8	0.29	22	57	124	314	0	39
11	12000	80	11.5	0.30	23	42	126	232	0	40
12	12000	81	11.7	0.30	22	58	125	322	0	41
13	12000	81	11.6	0.30	23	67	126	370	0	42
14	12000	81	11.6	0.30	23	52	125	289	0	43
15	12000	82	11.7	0.30	22	41	124	229	0	44
16	12000	81	11.6	0.29	22	40	124	220	0	45
17	12000	82	11.8	0.29	22	41	122	229	0	47
18	12000	81	11.6	0.29	22	38	124	213	0	48
19	12000	80	11.5	0.29	22	43	124	239	0	49
20	12000	80	11.6	0.29	22	44	123	246	0	50
21	12000	81	11.7	0.29	22	52	122	289	0	52
22	12000	84	12.0	0.28	22	40	120	222	0	53
23	12000	81	11.7	0.29	22	56	121	309	0	54
24	12000	83	11.9	0.29	22	44	120	246	0	55
25	12000	84	12.0	0.28	21	40	119	222	0	55
26	12000	84	12.0	0.28	21	40	118	221	0	57
27	12000	82	11.8	0.28	21	39	119	219	0	58
28	12000	85	12.2	0.28	21	38	117	212	0	60
29	12000	83	12.0	0.28	21	44	119	243	0	60
30	12000	82	11.8	0.28	21	48	118	269	0	62
31	12000	86	12.3	0.28	21	43	116	241	0	63
32	12000	87	12.5	0.27	21	44	114	245	0	64
33	12000	88	12.6	0.27	20	37	113	204	0	66
34	12000	88	12.6	0.27	20	35	113	192	0	67
35	12000	88	12.7	0.27	20	48	113	266	0	67
36	12000	86	12.4	0.27	20	40	111	223	0	68
37	12000	89	12.8	0.27	20	50	111	278	0	69
38	12000	89	12.7	0.27	20	61	111	339	0	70
39	12000	90	13.0	0.27	20	60	112	331	0	72
40	12000	88	12.7	0.27	20	38	111	213	0	72
41	12000	90	12.9	0.26	20	47	110	261	0	73
42	12000	89	12.8	0.27	20	43	111	240	0	74
43	12000	87	12.5	0.27	20	37	111	205	0	75
44	12000	88	12.7	0.27	20	47	113	260	0	77
45	12000	87	12.5	0.27	20	36	113	202	0	78
46	12000	88	12.6	0.27	20	42	114	235	0	78
47	12000	86	12.4	0.28	21	42	117	235	0	79
48	12000	85	12.3	0.29	21	42	118	232	0	80
49	12000	89	12.8	0.27	20	55	112	307	0	81
50	12000	90	12.9	0.27	20	57	113	319	0	82

HINDUSTAN AERONAUTICS LIMITED - BANGALORE

FOUNDRY AND FORGE DIVISION

B17

FRICTION TEST CONSOLIDATED REPORT

Date	9/2/2008	
Time	1:46:37 PM	
Project Name	ROORKEE	
Part No	RK11	
Batch Number	PM08RK33	
Brake Speed	687	RPM
Brake Pressure	7.5	kg/sq.cm
Brake Force	70	kgf
File Name	PM08RK33_9_2_2008_1_46_37 PM	

	Kinetic Energy (kgfm)	RD rev.	RD time (sec)	Coefficient of friction	Mean Torque (kgfm)	Peak Torque (kgfm)	Mean Drag (kgf)	Peak Drag (kgf)	Pad1-Temp (DegC)	Pad2-Temp (DegC)
Max	8000	70	12.3	0.4	17	40	97	223	129	117
Min	8000	64	11.2	0.36	16	25	87	140	81	97
Avg	8000	67	11.7	0.38	17	29	92	164	105	106

WEAR REPORT

PAD	THICKNESS in mm			WEIGHT IN grams		
No	Initial	Final	Wear	Initial	Final	Wear
1	11.24	10.89	0.35	2399	2396	3
2	10.53	10.34	0.19	2403	2400	3

Total Number of Cycles completed: 50

DISPOSITION :

PRODUCTION/DEVELOPMENT :

HINDUSTAN AERONAUTICS LIMITED - BANGALORE

B18

FOUNDRY AND FORGE DIVISION

FRICTION TEST FINAL REPORT

Date	**9/2/2008**	
Time	**1:46:37 PM**	
Project Name	**ROORKEE**	
Part No	**RK11**	
Batch Number	**PM08RK33**	
Brake Speed	**687**	**RPM**
Brake Pressure	**7.5**	**kg/sq.cm**
Brake Force	**70**	**Kgf**
File Name	**PM08RK33_9_2_2008_1_46_37 PM**	

Sl NO	Kinetic Energy (kgfm)	RD rev.	RD time (sec)	Coefficient of friction	Mean Torque (kgfm)	Peak Torque (kgfm)	Mean Drag (kgf)	Peak Drag (kgf)	Pad1-Temp (DegC)	Pad2-Temp (DegC)
1	8000	70	12.3	0.36	16	39	87	215	81	113
2	8000	66	11.5	0.39	17	26	94	145	81	112
3	8000	66	11.5	0.38	16	27	92	152	83	110
4	8000	65	11.4	0.39	17	27	95	150	84	108
5	8000	66	11.6	0.39	17	27	93	148	84	106
6	8000	64	11.2	0.40	17	30	97	169	86	104
7	8000	66	11.5	0.39	17	29	94	159	86	102
8	8000	64	11.2	0.40	17	28	96	153	87	101
9	8000	65	11.3	0.39	17	25	94	140	87	100
10	8000	65	11.4	0.39	17	27	94	151	88	100
11	8000	65	11.4	0.39	17	27	94	150	89	98
12	8000	66	11.5	0.39	17	28	94	156	89	97
13	8000	66	11.5	0.39	17	27	94	150	89	97
14	8000	65	11.4	0.39	17	27	95	151	89	97
15	8000	65	11.3	0.39	17	27	95	151	90	97
16	8000	66	11.5	0.39	17	29	94	162	91	97
17	8000	65	11.3	0.39	17	30	95	166	91	98
18	8000	66	11.6	0.39	17	30	93	167	93	98
19	8000	66	11.5	0.39	17	31	94	172	95	98
20	8000	69	12.1	0.37	16	26	90	144	97	99
21	8000	67	11.7	0.38	17	26	92	145	98	99
22	8000	68	11.8	0.38	17	28	92	156	100	99
23	8000	67	11.7	0.38	17	33	92	183	101	100
24	8000	67	11.7	0.38	17	27	93	151	103	101
25	8000	67	11.6	0.38	17	28	93	157	105	102
26	8000	66	11.6	0.38	16	27	92	152	106	103
27	8000	66	11.6	0.38	17	29	93	164	108	103
28	8000	67	11.7	0.38	16	29	92	162	110	104
29	8000	65	11.4	0.38	17	26	93	146	110	105
30	8000	67	11.7	0.38	17	30	92	169	112	106
31	8000	68	11.8	0.37	16	28	91	157	112	106
32	8000	68	11.8	0.37	16	31	91	170	113	107
33	8000	67	11.7	0.38	17	30	92	168	114	108
34	8000	68	11.8	0.38	16	28	91	155	115	109
35	8000	68	11.9	0.37	16	29	91	160	116	109
36	8000	67	11.7	0.38	17	29	93	159	117	111
37	8000	69	12.0	0.37	16	26	90	147	118	111
38	8000	68	11.9	0.37	16	31	91	173	119	111
39	8000	69	12.0	0.37	16	34	90	191	120	111
40	8000	68	11.9	0.37	16	33	91	181	122	112
41	8000	68	11.9	0.38	16	30	91	168	123	113
42	8000	69	12.0	0.37	16	30	91	165	124	113
43	8000	68	11.9	0.38	16	36	91	199	125	114
44	8000	67	11.7	0.39	17	35	93	197	126	114
45	8000	69	12.0	0.37	16	33	90	184	127	114
46	8000	69	12.0	0.38	16	30	91	169	128	115
47	8000	69	12.1	0.38	16	27	90	150	128	116
48	8000	68	11.9	0.38	16	31	91	172	129	116
49	8000	69	12.1	0.37	16	40	90	223	129	116
50	8000	68	11.8	0.38	16	31	92	170	129	117

Sample 5 - Tested at 17300 Kgfm Energy

HINDUSTAN AERONAUTICS LIMITED - BANGALORE

B19

FOUNDRY AND FORGE DIVISION

FRICTION TEST CONSOLIDATED REPORT

Date	2/20/2009	
Time	8:13:05 AM	
Project Name	AL BRAKE PAD	
Part No	RR 22	
Batch Number	RR 22 A	
Brake Speed	1000	RPM
Brake Pressure	18	kg/sq.cm
Brake Force	160	kgf
File Name	RR 22 A_2_20_2009_8_13_05 AM	

	Kinetic Energy (kgfm)	RD rev.	RD time (sec)	Coefficient of friction	Mean Torque (kgfm)	Peak Torque (kgfm)	Mean Drag (kgf)	Peak Drag (kgf)	Pad1-Temp (DegC)	Pad2-Temp (DegC)
Max	17300	71	8.5	0.42	44	104	244	580	100	142
Min	17300	58	7	0.34	36	56	198	309	58	84
Avg	17300	63	7.6	0.39	41	72	228	398	79	114

WEAR REPORT

PAD	THICKNESS in mm			WEIGHT IN grams		
No	Initial	Final	Wear	Initial	Final	Wear
1	10.23	8.76	1.47	2364	2352	12
2	10.35	7.91	2.44	2379	2352	27

Total Number of Cycles completed: 50

DISPOSITION :

PRODUCTION/DEVELOPMENT : As reported. 24/9/09

V.N. ANIL KUMAR
CM (Brakepads)

Remark :- Pad no 2 is broken during removal of Pad from the friction test Holder after Testing.

HINDUSTAN AERONAUTICS LIMITED - BANGALORE

B20

FOUNDRY AND FORGE DIVISION

FRICTION TEST FINAL REPORT

Date	2/20/2009	
Time	8:13:05 AM	
Project Name	AL BRAKE PAD	
Part No	RR 22	
Batch Number	RR 22 A	
Brake Speed	1000	RPM
Brake Pressure	18	kg/sq.cm
Brake Force	160	Kgf
File Name	RR 22 A_2_20_2009_8_13_05 AM	

V.N. ANIL KUMAR
CM (Brakepads)

Sl NO	Kinetic Energy (kgfm)	RD rev.	RD time (sec)	Coefficient of friction	Mean Torque (kgfm)	Peak Torque (kgfm)	Mean Drag (kgf)	Peak Drag (kgf)	Pad1-Temp (DegC)	Pad2-Temp (DegC)
1	17300	70	8.3	0.34	36	56	198	309	59	91
2	17300	69	8.3	0.36	37	60	208	332	58	89
3	17300	67	8.0	0.37	38	57	213	319	58	86
4	17300	61	7.4	0.39	40	57	224	319	58	86
5	17300	63	7.6	0.39	40	60	225	333	58	85
6	17300	61	7.4	0.40	42	60	231	333	58	84
7	17300	61	7.3	0.40	42	59	233	326	59	85
8	17300	60	7.2	0.41	42	61	235	338	59	85
9	17300	59	7.1	0.41	43	62	238	347	60	87
10	17300	58	7.0	0.42	44	66	243	364	62	88
11	17300	59	7.1	0.41	43	63	239	350	63	90
12	17300	59	7.0	0.42	43	68	241	378	64	92
13	17300	60	7.2	0.41	43	60	237	335	65	94
14	17300	59	7.1	0.42	43	66	241	369	67	96
15	17300	58	7.0	0.41	43	95	237	529	68	97
16	17300	59	7.1	0.41	42	63	236	352	69	100
17	17300	58	7.0	0.42	44	104	244	580	71	102
18	17300	59	7.1	0.42	43	87	241	484	72	104
19	17300	58	7.0	0.42	43	70	240	391	73	106
20	17300	59	7.1	0.42	43	67	242	373	75	108
21	17300	60	7.2	0.41	43	68	240	377	77	110
22	17300	59	7.1	0.41	43	82	238	457	77	111
23	17300	59	7.1	0.42	44	68	244	379	79	113
24	17300	61	7.3	0.41	43	73	238	407	80	115
25	17300	62	7.4	0.41	42	76	236	422	82	117
26	17300	63	7.5	0.40	42	68	232	380	83	119
27	17300	60	7.3	0.41	43	73	238	406	84	121
28	17300	62	7.5	0.40	42	73	234	405	84	122
29	17300	61	7.3	0.40	42	70	234	387	85	123
30	17300	63	7.5	0.40	42	72	232	397	87	124
31	17300	63	7.5	0.40	42	67	233	372	87	125
32	17300	63	7.6	0.40	42	70	232	388	88	126
33	17300	62	7.5	0.39	41	76	228	422	89	128
34	17300	63	7.5	0.40	42	86	234	480	90	129
35	17300	65	7.8	0.39	41	69	225	381	90	130
36	17300	65	7.8	0.39	40	97	225	541	90	131
37	17300	67	8.1	0.37	39	80	218	443	91	132
38	17300	65	7.9	0.38	40	75	221	418	92	134
39	17300	64	7.7	0.38	40	89	222	496	92	135
40	17300	67	8.0	0.38	39	80	219	443	94	136
41	17300	68	8.1	0.37	39	67	217	370	95	136
42	17300	67	8.0	0.38	39	90	219	503	95	137
43	17300	67	8.1	0.37	39	73	216	403	96	137
44	17300	67	8.0	0.38	39	68	219	378	97	137
45	17300	69	8.3	0.37	38	72	213	400	98	139
46	17300	70	8.4	0.36	38	71	211	392	98	139
47	17300	71	8.5	0.36	37	73	208	403	99	140
48	17300	69	8.3	0.36	38	74	209	409	99	141
49	17300	70	8.4	0.36	38	70	210	389	100	141
50	17300	70	8.4	0.36	38	69	210	381	100	142

HAL

HINDUSTAN AERONAUTICS LIMITED - BANGALORE

FOUNDRY AND FORGE DIVISION

B21

FRICTION TEST CONSOLIDATED REPORT

Date	12/20/2008	
Time	2:18:51 PM	
Project Name	AL BRAKE PAD	
Part No	RR 23	
Batch Number	RR 23	
Brake Speed	835	RPM
Brake Pressure	11.3	kg/sq.cm
Brake Force	100	kgf
File Name	RR 23_12_20_2008_2_18_51 PM	

	Kinetic Energy (kgfm)	RD rev.	RD time (sec)	Coefficient of friction	Mean Torque (kgfm)	Peak Torque (kgfm)	Mean Drag (kgf)	Peak Drag (kgf)	Pad1-Temp (DegC)	Pad2-Temp (DegC)
Max	12000	112	16.2	0.3	20	40	109	220	0	116
Min	12000	92	13.3	0.25	16	26	90	142	0	87
Avg	12000	102	14.7	0.27	18	29	99	162	0	99

WEAR REPORT

PAD	THICKNESS in mm			WEIGHT IN grams		
No	Initial	Final	Wear	Initial	Final	Wear
1	9.04	7.28	1.76	2368	2349	19
2	9.1	7.8	1.3	2368	2336	32

Total Number of Cycles completed: 50

DISPOSITION :

PRODUCTION/DEVELOPMENT :

HINDUSTAN AERONAUTICS LIMITED - BANGALORE

B22

FOUNDRY AND FORGE DIVISION

FRICTION TEST FINAL REPORT

Date	**12/20/2008**	
Time	**2:18:51 PM**	
Project Name	**AL BRAKE PAD**	
Part No	**RR 23**	
Batch Number	**RR 23**	
Brake Speed	**835**	**RPM**
Brake Pressure	**11.3**	**kg/sq.cm**
Brake Force	**100**	**Kgf**
File Name	**RR 23_12_20_2008_2_18_51 PM**	

Sl NO	Kinetic Energy (kgfm)	RD rev.	RD time (sec)	Coefficient of friction	Mean Torque (kgfm)	Peak Torque (kgfm)	Mean Drag (kgf)	Peak Drag (kgf)	Pad1-Temp (DegC)	Pad2-Temp (DegC)
1	12000	102	14.7	0.26	17	26	95	142	0	111
2	12000	100	14.4	0.27	18	26	99	142	0	108
3	12000	100	14.3	0.27	18	27	100	148	0	104
4	12000	94	13.6	0.28	19	29	104	159	0	100
5	12000	95	13.6	0.29	19	28	105	156	0	97
6	12000	94	13.4	0.30	19	28	107	157	0	95
7	12000	93	13.3	0.30	19	28	108	155	0	93
8	12000	93	13.3	0.30	20	27	109	148	0	91
9	12000	96	13.7	0.29	19	27	106	148	0	90
10	12000	95	13.7	0.29	19	29	106	159	0	89
11	12000	97	13.9	0.29	19	26	104	145	0	88
12	12000	95	13.7	0.29	19	26	107	147	0	88
13	12000	94	13.5	0.30	19	27	108	148	0	87
14	12000	93	13.3	0.30	19	28	108	157	0	87
15	12000	92	13.3	0.30	19	31	108	174	0	88
16	12000	94	13.4	0.29	19	26	106	143	0	88
17	12000	93	13.4	0.29	19	28	107	158	0	89
18	12000	97	13.9	0.28	19	29	103	159	0	88
19	12000	99	14.2	0.28	18	27	102	150	0	89
20	12000	101	14.5	0.28	18	26	101	143	0	90
21	12000	101	14.5	0.27	18	27	100	150	0	90
22	12000	102	14.6	0.27	18	28	100	154	0	91
23	12000	103	14.7	0.27	18	29	99	160	0	91
24	12000	101	14.5	0.27	18	29	98	164	0	92
25	12000	106	15.2	0.26	17	29	96	159	0	93
26	12000	106	15.3	0.26	17	31	95	170	0	94
27	12000	105	15.0	0.27	17	30	97	168	0	95
28	12000	105	15.0	0.27	17	31	97	175	0	96
29	12000	108	15.5	0.26	17	32	95	178	0	97
30	12000	105	15.0	0.26	17	31	96	172	0	97
31	12000	105	15.1	0.26	17	27	96	152	0	98
32	12000	105	15.1	0.27	17	29	97	160	0	100
33	12000	107	15.4	0.26	17	32	94	179	0	100
34	12000	108	15.6	0.26	17	27	94	148	0	102
35	12000	107	15.4	0.26	17	30	94	167	0	102
36	12000	108	15.5	0.26	17	28	95	156	0	104
37	12000	107	15.4	0.26	17	31	95	171	0	104
38	12000	107	15.4	0.26	17	34	95	188	0	105
39	12000	107	15.3	0.26	17	33	95	183	0	106
40	12000	106	15.2	0.26	17	31	94	174	0	107
41	12000	108	15.6	0.26	17	31	94	174	0	108
42	12000	109	15.6	0.26	17	31	94	170	0	109
43	12000	109	15.6	0.26	17	28	94	158	0	109
44	12000	109	15.7	0.26	17	32	93	176	0	110
45	12000	110	15.8	0.25	17	27	93	153	0	112
46	12000	111	16.0	0.25	16	29	92	164	0	112
47	12000	111	15.9	0.25	17	32	92	179	0	113
48	12000	111	16.0	0.25	16	33	91	181	0	114
49	12000	109	15.7	0.25	17	40	92	220	0	115
50	12000	112	16.2	0.25	16	32	90	175	0	116

AL

HINDUSTAN AERONAUTICS LIMITED - BANGALORE

B23

FOUNDRY AND FORGE DIVISION

FRICTION TEST CONSOLIDATED REPORT

Date	12/20/2008	
Time	11:10:07 AM	
Project Name	AL BRAKE PAD	
Part No	RR 17	
Batch Number	AL 08 DR 20	
Brake Speed	835	RPM
Brake Pressure	11.71	kg/sq.cm
Brake Force	100	kgf
File Name	AL 08 DR 20_12_20_2008_11_10_07 AM	

	Kinetic Energy (kgfm)	RD rev.	RD time (sec)	Coefficient of friction	Mean Torque (kgfm)	Peak Torque (kgfm)	Mean Drag (kgf)	Peak Drag (kgf)	Pad1-Temp (DegC)	Pad2-Temp (DegC)
ax	37141	129	16.5	0.32	44	62	247	344	0	84
in	12000	87	10.3	0.23	16	31	89	170	0	44
/g	13508	105	14.7	0.26	19	37	107	206	0	64

WEAR REPORT

	THICKNESS in mm			WEIGHT IN grams		
	Initial	Final	Wear	Initial	Final	Wear
	7.25	7.02	0.23	2347.5	2344	3.5
	7.05			2348		

Total Number of Cycles completed: 50

DISPOSITION :

PRODUCTION/DEVELOPMENT :

HINDUSTAN AERONAUTICS LIMITED - BANGALORE

B24

FOUNDRY AND FORGE DIVISION

FRICTION TEST FINAL REPORT

Date	12/20/2008	
Time	11:10:07 AM	
Project Name	AL BRAKE PAD	
Part No	RR 17	
Batch Number	RR 17	
Brake Speed	835	RPM
Brake Pressure	11.71	kg/sq.cm
Brake Force	100	Kgf
File Name	AL 08 DR 20_12_20_2008_11_10_07 AM	

Sl No	Kinetic Energy (kgfm)	RD rev.	RD time (sec)	Coefficient of friction	Mean Torque (kgfm)	Peak Torque (kgfm)	Mean Drag (kgf)
1	12000	87	12.5	0.30	20	46	114
2	37141	126	10.3	0.31	44	59	243
3	37141	128	10.5	0.32	44	61	247
4	37141	129	10.5	0.31	44	62	246
5	12000	99	14.3	0.27	18	44	103
6	12000	98	14.1	0.27	19	34	103
7	12000	97	14.0	0.27	19	37	104
8	12000	96	13.8	0.27	19	33	104
9	12000	98	14.0	0.27	19	33	104
10	12000	96	13.8	0.28	19	33	106
11	12000	98	14.1	0.27	19	32	104
12	12000	99	14.2	0.27	18	32	103
13	12000	103	14.8	0.26	18	35	98
14	12000	104	14.9	0.26	18	35	98
15	12000	104	14.9	0.26	18	33	98
16	12000	100	14.4	0.27	18	32	101
17	12000	100	14.3	0.27	18	33	102
18	12000	99	14.3	0.27	18	33	101
19	12000	101	14.5	0.27	18	32	101
20	12000	101	14.5	0.27	18	36	101
21	12000	102	14.6	0.26	18	36	100
22	12000	99	14.3	0.27	18	34	101
23	12000	102	14.6	0.26	18	38	98
24	12000	105	15.1	0.25	17	45	97
25	12000	110	15.7	0.24	17	38	93
26	12000	113	16.2	0.24	16	49	90
27	12000	112	16.2	0.23	16	44	89
28	12000	115	16.5	0.23	16	36	89
29	12000	111	15.9	0.24	16	39	90
30	12000	115	16.5	0.23	16	36	89
31	12000	110	15.8	0.24	17	31	92
32	12000	110	15.8	0.24	17	31	92
33	12000	107	15.3	0.25	17	33	95
34	12000	107	15.4	0.25	17	36	95
35	12000	110	15.8	0.24	17	34	93
36	12000	106	15.3	0.25	17	33	96
37	12000	106	15.3	0.25	17	36	96
38	12000	104	15.0	0.26	18	38	97
39	12000	105	15.1	0.26	17	35	97
40	12000	106	15.2	0.25	17	35	96
41	12000	104	14.9	0.26	18	33	98
42	12000	105	15.1	0.26	17	37	97
43	12000	106	15.3	0.25	17	32	96
44	12000	107	15.4	0.25	17	32	94
45	12000	105	15.2	0.25	17	32	96
46	12000	104	14.9	0.26	18	37	98
47	12000	107	15.3	0.25	17	36	95
48	12000	105	15.1	0.25	17	37	95
49	12000	107	15.3	0.25	17	39	95
50	12000	105	15.1	0.26	17	31	96

C1

PHASE-WISE DEVELOPMENT & OPTIMIZATION OF FRICTION MATERIAL CHEMISTRY BASED ON LABORATORY LEVEL TESTS

Designation	Constituents (wt.%)						Density (gm/cc)		Hardness (BHN)	
	Al	SiC	Graphite	Sb_2S_3	$BaSo_4$	Others	Green	Forged		
FA101	80.0	20.0	-	-	-	-	2.54	2.78	67	1st Phase
FA102	78.0	22.0	-	-	-	-	2.65	2.82	69	
FA103	75.0	25.0	-	-	-	-	2.41	2.56	72	
FA104	74.8	18.2	4.0	1.0	2.0	-	2.40	2.62	65	2nd Phase
FA105	70.0	20.0	5.0	1.0	2.0	Ceramic wool-2.0	2.56	2.75	64	3rd Phase
FA106	70.0	20.0	5.0	1.0	2.0	Coconut fiber-2.0	2.49	2.70	66	
FA107	70.0	20.0	5.0	2.0	3.0	-	2.46	2.67	64	O1-Optimized from 2nd Phase
FA108	71.5	18.0	6.5	1.5	2.5	-	2.39	2.61	57	
FA109	78.0	15.0	4.0	2.0	1.0	-	2.41	2.46	52	
FA110	76.0	15.0	6.0	2.0	1.0	-	2.26	2.39	56	
FA111	74.0	15.0	4.0	2.0	4.0	-	2.41	2.71	70	
FA112	83.0	15.0	6.0	2.0	4.0	-	2.39	2.68	65	
FA113	81.0	15.0	8.0	2.0	4.0		2.54	2.73	67	
FA114	79.0	10.0	4.0	2.0	4.0	-	2.62	2.75	69	

LA

Designation	Constituents (wt.%)						Density (gm/cc)		Hardness (BHN)	
	Al	SiC	Graphite	Sb_2S_3	$BaSo_4$	Others	Green	Forged		
FAl15	81.0	7.0	6.0	2.0	4.0	-	2.61	2.87	65	O2-Optimized from 2nd Phase with low SiC
FAl16	76.0	10.0	8.0	2.0	4.0	-	2.52	2.80	66	
FAl17	80.0	10.0	4.0	2.0	4.0	-	2.37	2.80	66	
FAl18	78.0	10.0	6.0	2.0	4.0	-	2.62	2.89	69	
FAl19	77.0	10.0	7.0	2.0	4.0	-	2.51	2.82	64	
FAl20	74.0	10.0	8.0	2.0	4.0	Zn-2.0	2.45	2.80	69	
FAl21	75.0	8.45	9.54	2.0	3.0	Zn-2.0	2.67	2.90	67	
FAl22	75.0	-	9.54	2.0	3.0	Zn-2.0	2.48	2.71	70	O3-Optimized from O2 with Zn
FAl23 (heavy)	75.0	8.45	11.54	2.0	3.0	-	2.39	2.86	70	
FAl24 (light)	75.0	6.45	9.54	2.0	3.0	Zn-4.0	2.45	2.80	67	
FAl25	77.0	8.45	7.54	2.0	3.0	Zn-2.0	2.58	2.89	65	
FAl26	77.5	7.50	8.0	2.0	3.0	Zn-2.0	2.57	2.84	66	
FAl27	75.5	7.50	8.0	2.0	3.0	Zn-4.0	2.57	2.85	70	
FAl28	77.0	8.50	9.5	2.0	3.0	--	2.69	3.00	75	
FAl29	75.0	6.45	9.54	2.0	3.0	Zn-3.0	2.60	2.80	70	
FAl30	77.0	8.45	7.54	2.0	3.0	Zn-3.0	2.50	2.89	70	
Back plate	70	30	-	-	-	-	-	-	85	